

AD-A077 384

ENVIRONMENTAL RESEARCH INST OF MICHIGAN ANN ARBOR IN--ETC F/6 17/5
STATISTICAL ANALYSIS OF TERRAIN BACKGROUND MEASUREMENTS DATA.(U)
MAR 77 R SPELLICY , J BEARD , J R MAXWELL N00123-76-C-0708
ERIM-120500-12-F NL

UNCLASSIFIED

1 OF 4
ADA
077 584



LEVEL IV

12
B.S.

Final Report

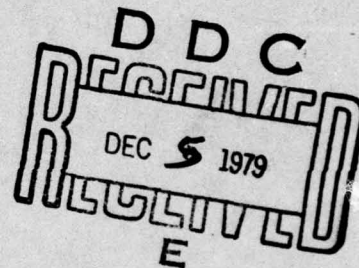
**STATISTICAL ANALYSIS OF TERRAIN
BACKGROUND MEASUREMENTS DATA**

AD A 077584

Infrared and Optics Division

MARCH 1977

Approved for Public Release:
Distribution Unlimited



Optical Signatures Program
Naval Weapons Center
China Lake, California

DDC FILE COPY

**ENVIRONMENTAL
RESEARCH INSTITUTE OF MICHIGAN**

FORMERLY WILLOW RUN LABORATORIES, THE UNIVERSITY OF MICHIGAN
BOX 618 • ANN ARBOR • MICHIGAN 48107

79 12 4 092

Notices

Sponsorship The work reported herein was conducted by the Environmental Research Institute of Michigan (formerly the Willow Run Laboratory of The University of Michigan) for the Naval Weapons Center, China Lake, California under Contract Number N00123-76-C-0708. The Project Managers were Dr. Lowell Wilkins and Mr. Ted Smith.

Disclaimer The views and conclusions contained in this document are those of the authors and should not be interpreted as necessarily representing the official policies, either expressed or implied, of the Department of Defense or of the U. S. Government.

DISCLAIMER NOTICE

**THIS DOCUMENT IS BEST QUALITY
PRACTICABLE. THE COPY FURNISHED
TO DDC CONTAINED A SIGNIFICANT
NUMBER OF PAGES WHICH DO NOT
REPRODUCE LEGIBLY.**

UNCLASSIFIED

SECURITY CLASSIFICATION OF THIS PAGE (When Data Entered)

REPORT DOCUMENTATION PAGE		READ INSTRUCTIONS BEFORE COMPLETING FORM
1. REPORT NUMBER 120500-12-F	2. GOVT ACCESSION NO.	3. RECIPIENT'S CATALOG NUMBER
4. TITLE (and Subtitle) Statistical Analysis of Terrain Background Measurements Data		5. TYPE OF REPORT & PERIOD COVERED Final Report
7. AUTHOR(s) R. Spellicy, J. Beard, J. R. Maxwell		6. PERFORMING ORG. REPORT NUMBER ERIM-120500-12-F
9. PERFORMING ORGANIZATION NAME AND ADDRESS Infrared and Optics Division Environmental Research Institute of Michigan P O Box 618, Ann Arbor, MI 48107		8. CONTRACT OR GRANT NUMBER (s) N00123-76-C-0708
11. CONTROLLING OFFICE NAME AND ADDRESS Dr. Lowell Wilkins, Code 51403 (713 939-3814) Naval Weapons Center China Lake, California 93555		10. PROGRAM ELEMENT, PROJECT, TASK AREA & WORK UNIT NUMBERS 12 294
14. MONITORING AGENCY NAME AND ADDRESS (if different from Controlling Office) Receiving Officer Naval Weapons Center China Lake, CA 93555		12. REPORT DATE March 1977
16. DISTRIBUTION STATEMENT (of this Report) Approved for Public Release: Distribution Unlimited		13. NUMBER OF PAGES 307
17. DISTRIBUTION STATEMENT (of the abstract entered in Block 20, if different from Report)		15. SECURITY CLASS. (of this report) Unclassified
18. SUPPLEMENTARY NOTES		15a. DECLASSIFICATION/DOWNGRADING SCHEDULE
19. KEY WORDS (Continue on reverse side if necessary and identify by block number) Terrain backgrounds data, statistical analysis, multispectral data		
20. ABSTRACT (Continue on reverse side if necessary and identify by block number) Several terrain background scenes were selected and statistics derived from calibrated multispectral airborne scanner data. Conventional statistical parameters - means, standard deviations, histograms, spectral correlations, and power spectra - are reported for the 1.0-1.4 μm , 1.5-1.8 μm , 2.0 - 2.6 μm , 4.5-5.5 μm , and 9.3-11.7 μm spectral bands. In addition, a program has been initiated to develop equivalent elliptical area/intensity statistics for these background scenes which more adequately describe		

DD FORM 1 JAN 73 1473 EDITION OF 1 NOV 65 IS OBSOLETE

UNCLASSIFIED

SECURITY CLASSIFICATION OF THIS PAGE (When Data Entered)

micrometers

408 259

503

UNCLASSIFIED

SECURITY CLASSIFICATION OF THIS PAGE (When Data Entered)

the infrequent occurrence of small areas of high intensity which cause seekers and trackers false alarm problems. Area/intensity statistics are reported for two of the scenes.

UNCLASSIFIED

SECURITY CLASSIFICATION OF THIS PAGE (When Data Entered)

TABLE OF CONTENTS

1.	Introduction and Summary	7
2.	The Multispectral Scanner	11
3.	Procedures and Selected Examples	23
3.1	Preprocessing of Scanner Data	23
3.2	Statistics Definitions	27
3.2.1	Point Statistics: Means and Standard Deviations	27
3.2.2	Correlative and Area Statistics	32
3.3	Modeling the Background Scene	50
4.	Discussion of Results	57
5.	Summary and Recommendations	61
Appendix I: Details of Calibration and Field-of-View		
Averaging Procedures		I-1
Appendix II: Complete Compilation of Statistical Data		II-2

Accession For	
NTIS GRA&I	<input checked="" type="checkbox"/>
DDC TAB	<input type="checkbox"/>
Unannounced	<input type="checkbox"/>
Justification	
By _____	
Distribution/	
Availability Codes	
Dist	Avail and/or special
A	22

LIST OF FIGURES

2.1	Airborne Multispectral Scanner Operation	12
2.2	Optical Schematic of ERIM Experimental Multispectral Scanner, M-7	14
2.3	ERIM Experimental Multispectral Scanner System	16
2.4	Scanner Voltage Output Versus Time	18
2.5	ERIM M-5 Multispectral Scanner	21
3.1	Schematic Representation of the Procedures used for Field-of-View Averaging	26
3.2	Subarea Histograms for the 9.3 - 11.7 μm Channel of Flint-1 .	30
3.3	Total Area Histogram for the 9.3 - 11.7 μm Channel of Flint-1	31
3.4	Equivalent Elliptical Areas for the 9.3 - 11.7 μm Channel of Flint-1 with a 1.5 σ Threshold	36
3.5	Equivalent Elliptical Areas for the 9.3 - 11.7 μm Channel of Flint-1 with a 2.0 σ Threshold	37
3.6	Equivalent Elliptical Areas for the 9.3 - 11.7 μm Channel of Flint-1 with a 2.5 σ Threshold	38
3.7	Equivalent Elliptical Areas for the 9.3 - 11.7 μm Channel of Flint-1 with a 3.0 σ Threshold	39
3.8	In-Track One Dimensional Averaged Wiener Spectrum for the 9.3 - 11.7 μm Channel of Flint-1	47
3.9	Cross-Track One-Dimensional Averaged Wiener Spectrum for the 9.3 - 11.7 μm Channel of Flint-1	48
3.10	Two-Dimensional Wiener Spectrum for the 9.3 - 11.7 μm Channel of Flint-1	49
3.11	Artificial Color Image of the 9.3 - 11.7 μm Channel of Flint-1	51
3.12	Artificial Color Representation of the Pseudo-Image Generated From the 9.3 - 11.7 μm Channel of Flint-1	51

LIST OF TABLES

2.1	M7 Scanner Performance Characteristics	19
2.2	Detector Configurations for ERIM M7 Scanner	20
3.1	Sub-Area and Total Area Means and Standards Deviations for Flint-1	29
3.2	Correlation Coefficients for the Reflective IR Channels in Sub-Area 2 of Flint-1	34
3.3	Area Distribution for Recognized Regions in the 9.3 - 11.7 μ m Channel of Flint-1 with a 1 σ Threshold	41
3.4	Perimeter Distributions for Recognized Regions in the 9.3 - 11.7 μ m Channel of Flint-1 with 1 σ Threshold	42
3.5	Shape Factor Distributions for Recognized Regions in the 9.3 - 11.7 μ m Channel of Flint-1 with a 1 σ Threshold	43
3.6	Area Distributions for Recognized Regions in the Real and Pseudo-Image of the 9.3 - 11.7 μ m Channel of Flint-1	53
3.7	Area Distributions for Recognized Regions in the Real and Pseudo-Images of the 9.3 - 11.7 μ m Channels of Flint-1	54
3.8	Area Distributions for Recognized Regions in the Real and Pseudo-Images of the 9.3 - 11.7 μ m Channels of Flint-1	55
3.9	Area Distributions for Recognized Regions in the Real and Pseudo-Images of the 9.3 - 11.7 μ m Channels of Flint-1	56
4.1	Total Area Data Summary	58-59

INTRODUCTION AND SUMMARY

There is a need for both target and background data for the design of sensors to detect and track targets against sky, cloud, and terrain backgrounds. The objective of this backgrounds analysis program is to develop backgrounds data useful to systems designers. The first phase of the program, which has been completed [Reference 1], was to survey the available backgrounds data and compile an index - bibliography of pertinent information. In general there is considerable data on terrain backgrounds but much less on sky and cloud backgrounds. Data is especially lacking for two-dimensional high spatial resolution data on clouds in the spectral bands of interest. In this second phase of the program we have selected a variety of terrain backgrounds for which high spatial resolution multispectral data are available. A variety of statistical measures have been derived from these data and are presented in this technical report. These include the conventional statistical parameters of means, standard deviations, histograms, Wiener (power) spectra, and spectral correlations as well as new area/intensity statistics which are particularly relevant in view of recent advances in sensor and processor technology. Additional efforts to assess the utility of the various background statistical measures will be reported in future technical reports.

Conventional background statistics have in the past been adequate since in many instances there is a high contrast between the target and background. In such instances, the highest intensity background points determine the highest threshold setting necessary to eliminate all false alarms and the histograms provide estimates of how the detection probability and false alarm rate vary with threshold setting. However, today there is a need for higher order background statistics because of the increased sophistication of background rejection techniques employed

[1] J. Beard, J. Braithwaite, R. Turner, Infrared Background Survey and Analysis, Environmental Research Institute of Michigan, Ann Arbor, June 1976.

with large detector arrays and imaging or scanning sensors. Although the power spectrum is a background statistic which does vary with the spatial distribution of radiances in the scene, it is clearly an inadequate background descriptor for most of today's problems. Small areas of high radiance produce most of the false alarms in today's sensors, and the power spectrum does not distinguish between scenes with many low intensity areas and those with a few high intensity areas. This is a well known fact and a result which is evident from the background modeling work of R. Clark Jones and the early working group on infrared backgrounds, WGIRB [Reference 2].

Hence, in addition to the conventional statistics on terrain backgrounds, we have also developed area/intensity statistics as a statistical measure that is more directly useful to the sensor designer in estimating detection probabilities and false alarm rates with today's sensor and processor technology. The statistics developed are the probabilities that regions (of various sizes, shapes, and orientations) will occur in the scene above a specified radiance threshold. The region descriptors are area, major and minor axes, and the angular orientation for an elliptical area that is equivalent, in geometric area and ratio of second moments, to each contiguous region above the radiance threshold. For most scenes the number of regions and their areas decrease as the threshold is raised, while the number of small regions above any preset threshold varies from one scene to the next. These area/intensity statistics are analogous to the more familiar pulse length statistics for one-dimensional records.

The statistical parameters for the occurrence of areas and intensities in the various background scenes are not only directly useful for estimating sensor performance but may also be useful in simulating whole classes of backgrounds. The equivalent ellipses at each threshold can be positioned to simulate the actual scene from which they were

[2] R. Clark Jones, Dr., The Study of IR Backgrounds by the Wiener Spectrum Method, Polaroid Corporation, Cambridge, Massachusetts, December 1959.

derived, or repositioned at random to simulate many scenes having the same area/intensity statistics. Such simulations of backgrounds do reproduce many of the spatial characteristics of the original scene as is shown by example in this report.

Seven scenes were selected for analysis in this program representing a wide range of backgrounds; two residential scenes (Flint-1 and Baltimore), an industrial scene (Flint-2), a mountainous structured terrain (Mill Creek, OK), a natural busy terrain of trees and hills with numerous shadows (Black Hills, S. D.) and two mountainous unstructured terrains (Pisgah Crater, CA and Mono Lake, CA). These were collected with the ERIM airborne multispectral scanner system with a nominal 5 to 10 foot spatial resolution in spectral bands including 1.0-1.4 μm , 1.5-1.8 μm , 2.0-2.6 μm , 4.5-5.5 μm , and 9.3-11.7 μm . Conventional statistics including means, standard deviations, histograms, and spectral correlations are reported here and calibrated data tapes are available to qualified users for additional statistical analysis and simulation. In addition to these statistics, Wiener (power) spectra and area/intensity statistics are reported for two spectral bands of Flint-1 and Mill Creek. An actual simulation of the Flint-1 scene in the 9.3-11.7 μm spectral band has also been created with equivalent ellipses and is compared with the true background scene.

The remainder of this report is broken down into four sections: Section 2 presents the ERIM calibrated multispectral airborne scanner system; Section 3, the procedures used for calibration and statistical analysis with selected examples; Section 4, a brief discussion of the results of the analysis; and Section 5, a summary with recommendations. The complete data and statistics package is contained in Appendix II.

THE MULTISPECTRAL SCANNER*

Two multispectral scanner systems have been in use at ERIM since 1968. The newer M-7 scanner was used at the time the Flint, Baltimore, and Mill Creek data was generated while its predecessor the M-5 scanner was used in gathering the Pisgah Crater, Black Hills, and Mono Lake data. These two scanners are similar so that only the M-7 will be discussed in detail with the difference between the two systems elaborated on at the end of this section.

The M-7 scanner, covering a wavelength range from 0.33 to 14.0 micrometers, can operate in up to 19 different bands of the ultraviolet, visible, and infrared regions. Of these bands, 12 can be selected for tape recording at any one time on a 14-track analog tape machine. More recently a digital recording system has been added. As many as five separate radiation reference sources may be recorded sequentially along with the ground video once each scan line. The total system, including boresight cameras, is usually operated in a Douglas C-47 aircraft.

The simplified diagrams of Figure 2.1 illustrate a typical line scanner and its method of airborne use. As shown in the optical schematic at the top of the figure, the scanner basically consists of an optical telescope with its narrow field of view redirected by a rotating flat mirror. This mirror causes the system to scan in a plane perpendicular to the longitudinal axis of the aircraft. A radiation detector in the focal plane of the telescope converts the focused beam of radiation to an electrical signal. The optical system's field-of-view (ground resolution element) first scans laterally across the aircraft ground track through an opening in the bottom of the aircraft. Then before making the next ground scan, it scans radiation references (not shown) which are internal to the scanner. By the time the next scan begins, the aircraft has moved forward, thus subsequent line scans build upon one another to produce a continuous strip image of the terrain beneath the aircraft.

* The ERIM Airborne Multispectral Data Collection is described in the ERIM 190901-1-F report prepared by Philip G. Hasell, Jr. under contract NAS 9-9304. The multispectral scanner as described in that report, is presented here in order to familiarize the reader with the multispectral scanner system used to collect the data which is being processed on this program.

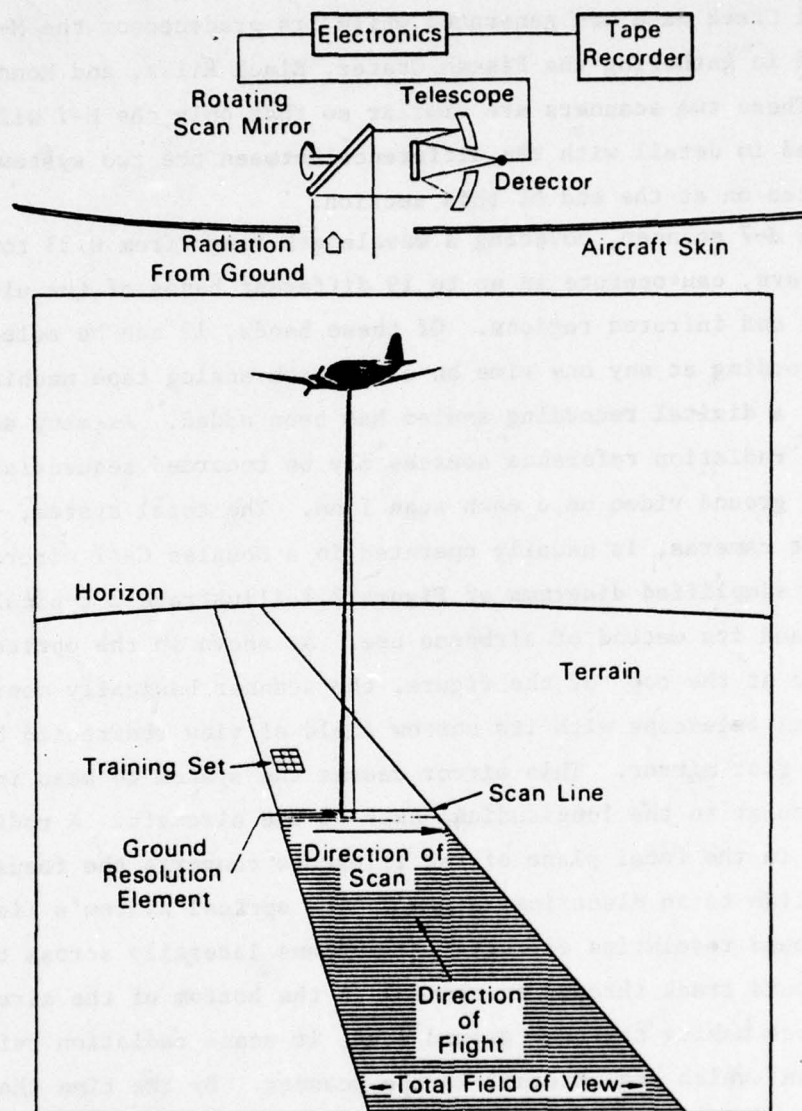


FIGURE 2.1 AIRBORNE MULTISPECTRAL SCANNER OPERATION

The multispectral scanner evolved from this single-channel scanner concept. This evolution required replacement of the single detector element with a system of beamsplitters, dispersing optics, and spectral filters. Figure 2.2 shows the optical configuration of the current M-7 multispectral scanner. A key feature in this design is its flexibility for accepting different radiation reference sources and new detector assemblies. Weight and space savings were sacrificed to provide this flexibility, which allows increased opportunities for adaptation to a diverse number of data gathering modes. Such flexibility is an important attribute for a general-purpose experimental system.

The radiation intercepted by the 5-inch-diameter collecting aperture is directed into the Dall-Kirkham telescope, which has a 3-inch-diameter secondary mirror. The incoming radiation prevented from entering the telescope by this secondary mirror is directed upward by a folding mirror to Detector Position 1. This 3-inch-diameter collecting aperture operates over the broad band of 0.3 to 14.0 μm . To provide thermal data at this position, a focusing lens designed for the 8.0-14.0 μm band is used in combination with a cooled HgCdTe detector. A dichroic mirror mounted ahead of this lens diverts ultraviolet and visible radiation onto a photomultiplier detector which is filtered so the energy it receives for recording is restricted to a narrow pre-selected band.

The radiation collected by the effective 4-inch aperture of the Dall-Kirkham telescope is folded into a dichroic mirror which reflects radiation below 1.0 μm but transmits that of longer wavelengths. The radiation thus transmitted is focused onto three separately filtered indium arsenide detector elements in Position 2 by lens achromatized for the 1.0 to 2.6 μm region. This dichroic and lens can be readily changed for different detector configurations.

Radiation at wavelengths shorter than 1.0 μm is focused onto the entrance slit of a prism spectrometer at Detector Position 3. The spectrometer divides and directs visible and near-infrared radiation

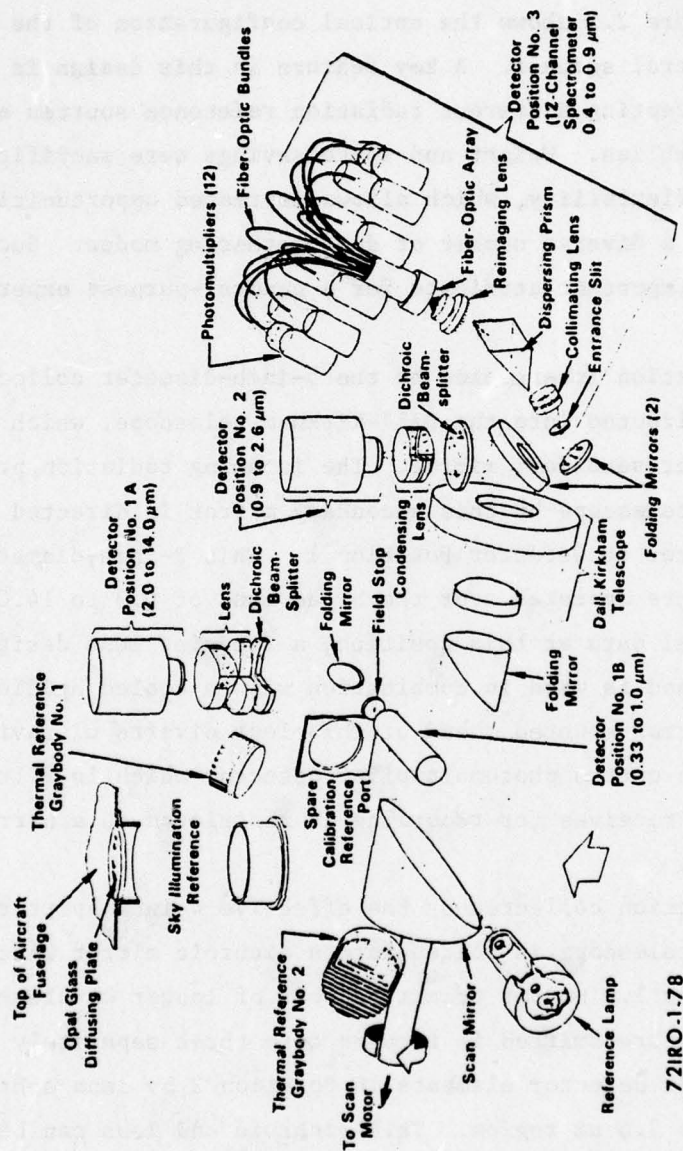


FIGURE 2.2 OPTICAL SCHEMATIC OF ERIM EXPERIMENTAL MULTISPECTRAL SCANNER, M7

through a fiber-optic image slicer to as many as twelve photomultiplier tubes. (In the current configuration the radiation goes to nine separate photomultipliers.)

The radiation reference sources are positioned in line with the scan mirror, so that each source is "seen" and registered sequentially once each scan line. Currently, five reference sources are being used: an NBS lamp packaged to simulate a point source; one ambient and two temperature-controlled graybody thermal references that fill the collecting aperture; and a sky illumination reference consisting of an opal glass diffusing plate mounted in the top of the aircraft. Through electronic control of the lamp and graybodies and by means of attenuating optical filters for the sky illumination, the radiation from all but the ambient temperature reference sources is under operator control. During data collection, all internal sources are monitored and recorded manually by the operator. To assure their validity as references, these sources are calibrated periodically against external standards in the laboratory.

The complete airborne scanner system is diagrammed in Figure 2.3. Terrain radiation enters the scanner at the bottom left; radiation detectors in the scanner assembly register this input along with that of the reference sources. The electrical signals comprising detector video outputs are amplified in preamplifiers before being transmitted to the operator console where the operator monitors them and adjusts amplifier gain to the proper level for tape recording. To confirm satisfactory recording, he is also able to monitor signals reproduced from the tape record. The system linearly transforms input radiation to voltage analogs which are recorded on the magnetic tape. The scanner system can generate video signals in up to nineteen different spectral bands over a wavelength range extending from 0.33 to 14.0 μm . Any twelve of these bands may be tape recorded at any one time on a 14-track analog tape machine; the other two tape recorder tracks are used for housekeeping purposes.

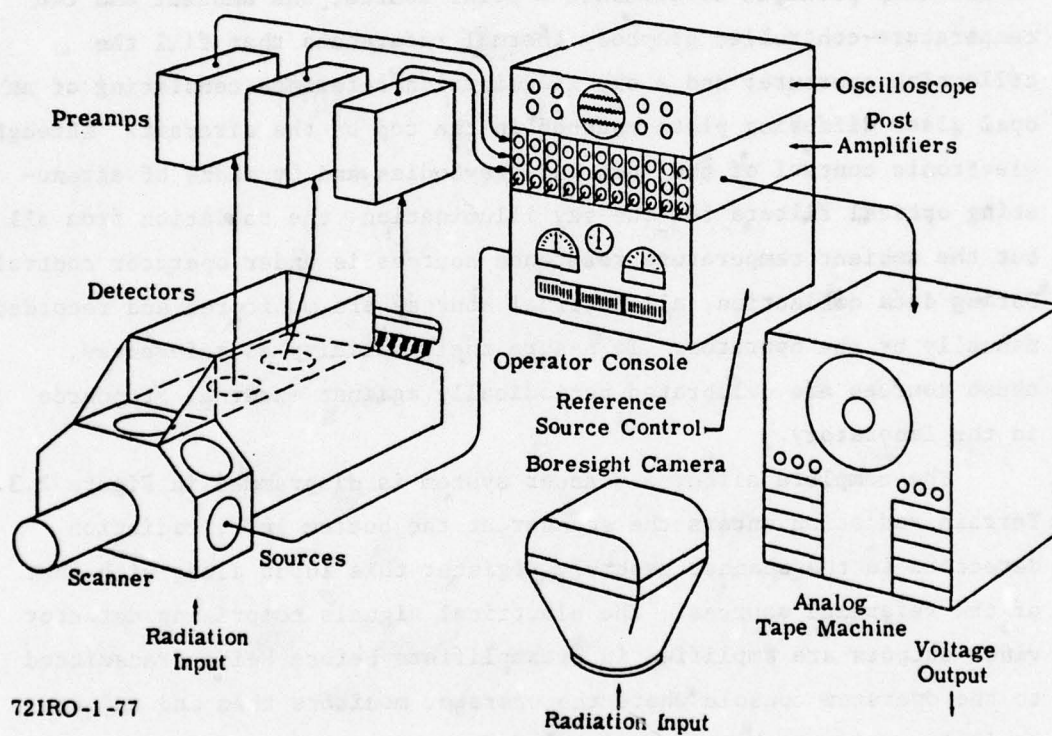


FIGURE 2.3 ERIM EXPERIMENTAL MULTISPECTRAL SCANNER SYSTEM

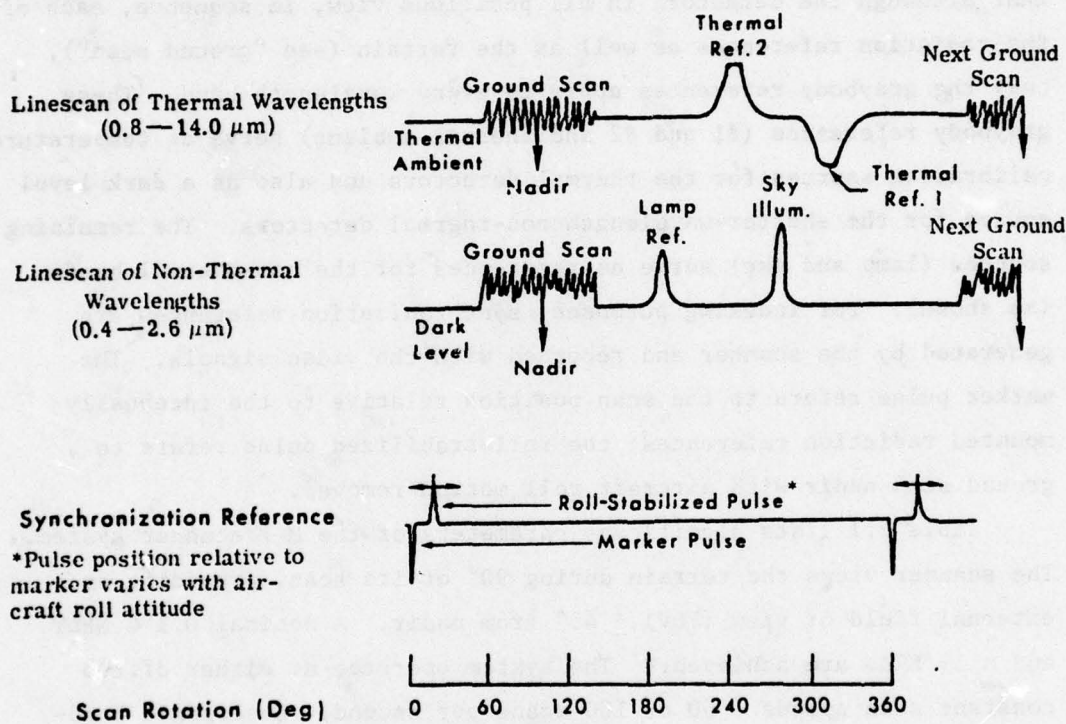
The airborne system (Figure 2.3) also includes an array of bore-sight cameras utilizing various film-filter combinations. These aerial cameras produce film records often useful in the subsequent analysis of the scanner data.

Electrical voltage representations of single line scans for the thermal and non-thermal wavelength bands are shown in Figure 2.4. Note that although the detectors in all positions view, in sequence, each of the radiation references as well as the terrain (see "ground scan"), only the graybody references apply to every wavelength band. These graybody references (#1 and #2 and thermal ambient) serve as temperature calibration sources for the thermal detectors and also as a dark level source for the shorter-wavelength non-thermal detectors. The remaining sources (lamp and sky) serve as references for the non-thermal bands (as shown). For indexing purposes, synchronization references are generated by the scanner and recorded with the video signals. The marker pulse refers to the scan position relative to the internally mounted radiation references; the roll-stabilized pulse refers to ground scan nadir with aircraft roll motion removed.

Table 2.1 lists significant parameters of the M-7 scanner system. The scanner views the terrain during 90° of its scan, providing an external field of view (FOV) $\pm 45^\circ$ from nadir. A nominal 0.1°C NEAT and a 1% NEAP are achieved.* The system operates at either of two constant scan speeds - 60 or 100 scans per second. Electronic bandwidth is tape-recorder-limited to a range of dc to 90 kHz. Table 2.2 identifies those detector assemblies currently in use with the system. Where there is a choice of detectors, the first-listed unit is the one commonly used.

The M-5 scanner, shown schematically in Figure 2.5, is a double-ended scanner using a double "axe-blade" scanning mirror to direct radiation to the two ends. In most respects it is the same as the M-7 except that the data collected from the two ends of the scanner

*NEAT = Noise Equivalent change in Temperature
NEAP = Noise Equivalent change in reflection



721RO-1-79

FIGURE 2.4 SCANNER VOLTAGE OUTPUT VERSUS TIME

TABLE 2.1

M7 SCANNER PERFORMANCE CHARACTERISTICS

12 Spectral Bands in UV, Visible and IR Regions

90° External FOV ($\pm 45^\circ$ from nadir)

2 mrad Maximum Spatial Resolution

0.1°C Nominal Thermal Resolution

1% Nominal Reflectance Resolution

Five Radiation Reference Ports

5-inch Diameter Collector Optics

Scan Rate of 60 or 100 scans/sec

DC to 90 kHz Electronic Bandwidth

Roll-Stabilized Imagery

TABLE 2.2

DETECTOR CONFIGURATIONS FOR ERIM M-5 AND M-7 SCANNER SYSTEMS

Detector Position 1† (0.3 μ m-15.0 μ m)				Detector Position 2† (1.1 μ m-14 μ m)*				Detector Position 3† (0.4 μ m-1.1 μ m)*			
Position 1A (2.0 μ m-14 μ m)*				Position 1B (0.3 μ m-0.7 μ m)*							
Detector	Band (μ m)	IFOV (mrad)		Detector	Band (μ m)	IFOV (mrad)		Detector	Band (μ m)	IFOV (mrad)	
HgCdTe 1-3	2.0-11.8**	3.1 \times 3.1		UVPM 1-3	† 3.0 \times 3.0			PM9-1	0.83-1.15	2.5 \times 2.5	
	or								0.72-0.94	2.5 \times 2.5	
HgCdTe 1-2	2.0-15.0**	6.6 \times 6.6							0.65-0.80	2.5 \times 2.5	
	or								0.60-0.70	2.5 \times 2.5	
HgCdTe 2-2	2.0** -10.9	21 \times 28		InSb 3-6	2.0-2.6	2.0 \times 4.0			0.55-0.64	2.5 \times 2.5	
	9.4-12.1	21 \times 21			1.0-1.4	2.0 \times 4.0			0.52-0.59	2.5 \times 2.5	
	or				or				0.49-0.55	2.5 \times 2.5	
HgCdTe 3-1	2.0** -9.1	20 \times 20		InAs 3-6	2.0-2.6	2.0 \times 4.0			0.45-0.51	2.5 \times 2.5	
	8.7-10.7	20 \times 20			1.3-1.8	2.0 \times 4.0			0.40-0.47	2.5 \times 2.5	
	9.9-14.0	20 \times 20			1.0-1.4	2.0 \times 4.0		PM12-1	0.67-0.94	2 \times 2	
	or				or				0.62-0.70	2 \times 2	
HgCdTe 1-5	2.0-12.0**	3.3 \times 3.3		HgCdTe 2-3	2.0-2.6	2.6 \times 2.6			0.58-0.64	2 \times 2	
					1.0-1.8	2.6 \times 2.6			0.55-0.60	2 \times 2	
					or				0.52-0.57	2 \times 2	
				InAs 1-2	1.0-2.6	3.0 \times 3.0			0.50-0.54	2 \times 2	
					or				0.48-0.52	2 \times 2	
				HgCdTe 1-2	2.0-15.0	4.0 \times 4.0			0.46-0.49	2 \times 2	
									0.41-0.48	2 \times 2	

Notes: *Bandpass established by replaceable dichroic mirror.

**Bandpass established by external optical filter.

†Any band between 0.3 μ m and 0.7 μ m may be selected by external optical filter.

‡Any one of the detectors shown may be installed in the position shown. Any 12 channels of a given configuration may be selected for FM recording on magnetic tape.

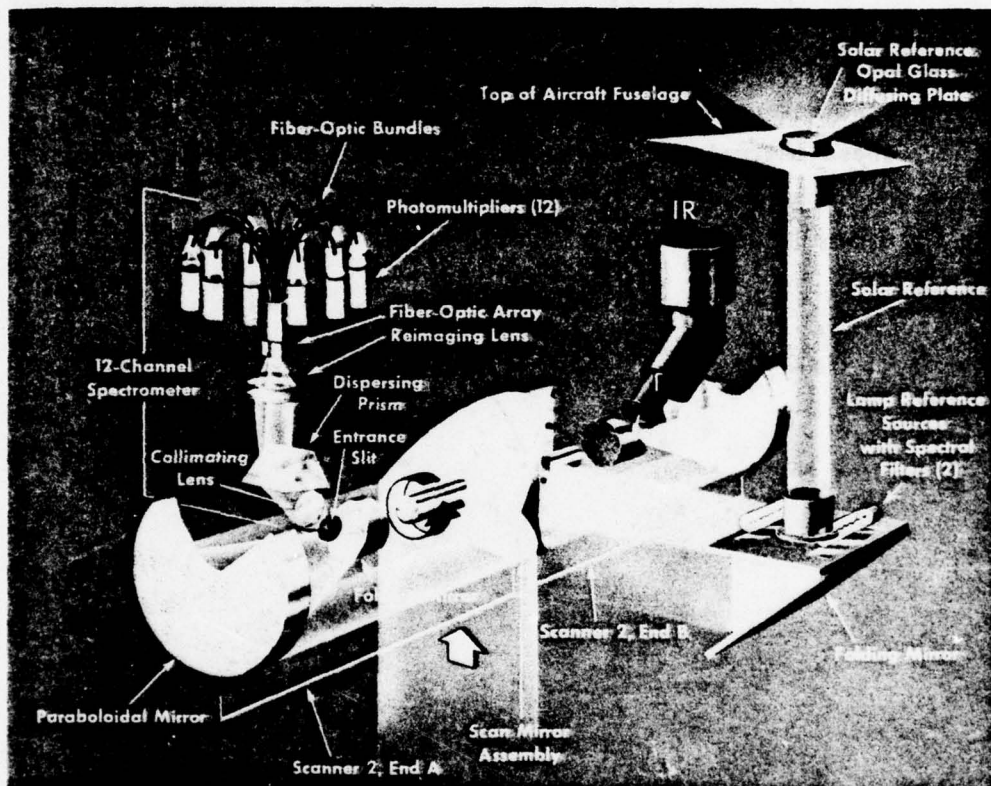


FIGURE 2.5 ERIM M-5 MULTISPECTRAL SCANNER

are 90° out of phase. Two M-5 scanners in the aircraft were used to collect data. Essentially the same detector assemblies were used with the M-5 as are used with the M-7 system. One M-5 scanner was used to collect multispectral data in the visible and near infrared. Calibration lamps were added in the scanner housing which did not restrict the field-of-view below the aircraft. Another M-5 scanner was used to collect thermal data, and "hot" and "cold" graybody thermal references were added at the scanner aperture so the thermal IR channels could be calibrated. These thermal plates extended into the field-of-view of the scanner below the aircraft so that the video was limited to approximately $\pm 20^\circ$ from nadir.

PROCEDURES AND SELECTED EXAMPLES

The multispectral scanner data selected for terrain backgrounds statistical analysis on this program were recorded on analog magnetic tape, and these analog tapes were converted to high density digital tapes. The general pre-processing procedure used to create calibrated data tapes is discussed in Section 3.1 with a detailed discussion of the procedures used for each scene being presented in Appendix I. The statistical measures derived from the data are described in Section 3.2; point statistics in Section 3.2.1 and correlative statistics in Section 3.2.2. Three types of correlative statistics are discussed. These include spectral correlations between pairs of bands; area/intensity statistics and the development of the equivalent elliptical area concept; and one- and two-dimensional Wiener (power) spectra. In Section 3.3 an example is shown in which the original background scene is actually replaced by the equivalent elliptical areas and most of the spatial information is preserved.

Examples of each type of statistical data are presented in Section 3, with the complete summary of terrain backgrounds statistical data included as Appendix II.

3.1 PREPROCESSING OF SCANNER DATA

Output from the ERIM scanners was converted to high-density-digital tapes in which each data value is recorded as an 8-bit integer ranging in value from 0 to 255. Each channel (wavelength band) is recorded on a separate tape channel and the amplifier gains adjusted so that all data values fall in the 0 - 255 range. On this tape the scan lines for a single M-7 scanner channel or reflective IR M-5 scanner channel consists of 790 data points of which the first 646 are scene elements (pixels) covering the range -45° to $+45^{\circ}$ with respect to nadir while the remaining 144 points are calibration values, 24 data points

for each of 6 calculation sources. For the thermal M-5 scanner channels the scanner elements cover pixels 162 to 484 with pixels 1 - 161 and 485 - 646 being used for the graybody thermal sources.

Before the scanner data may be used to generate scene statistics some pre-processing is required:

- 1) The high density digital tapes must be converted to computer compatible tapes:
- 2) Each channel must be calibrated in temperature or radiance using the calibration data at the end of each scan line;
- 3) Averaging was employed to reduce oversampling and to equalize any differences in the fields-of-view of the various detectors; and
- 4) A set of calibrated, formatted tapes must be generated.

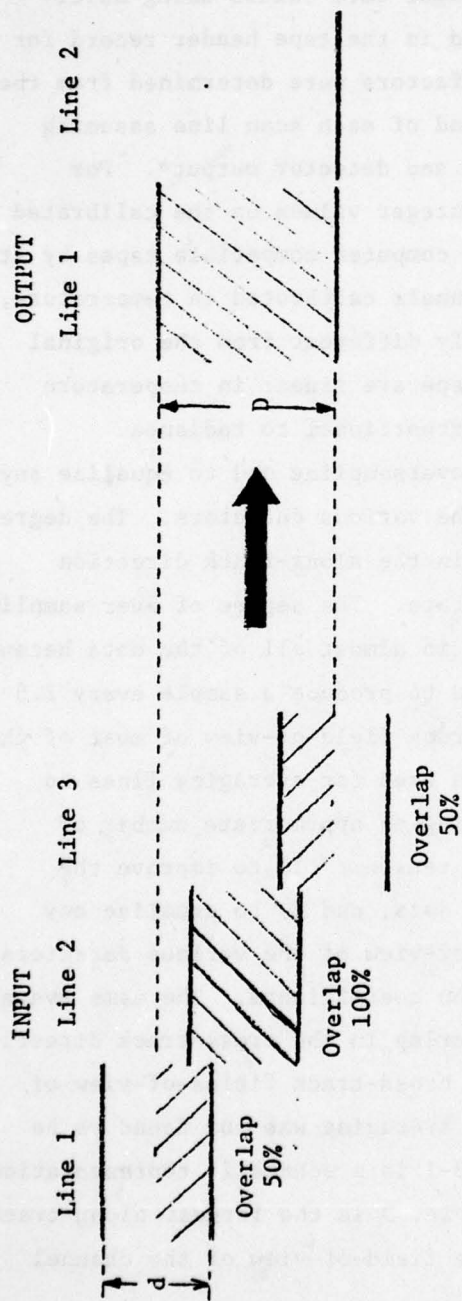
The first of these processes, conversion of high density tapes to computer compatible tapes, has been accomplished using the conversion facilities at Bendix Aerospace Systems Division in Ann Arbor and the MIDAS computer system at ERIM. The result of this conversion process was a low density (800 BPI) tape for each of the scenes desired. Using these tapes, the remainder of the pre-processing (2,3, and 4) was performed using a computer code written for the University of Michigan's AMDAHL computer system. It is the set of calibrated tapes generated from this code that are used for all image processing.

The data values appearing on the calibrated tapes are themselves integers, ranging from 0 to 255, but these integers have been modified so that a linear relationship exists between them and the apparent scene radiance or temperature. The data in the near IR channels was converted to equivalent radiance in $\text{uw/cm}^2 \cdot \text{sr} \cdot \mu\text{m}$). The equivalent radiance is the value of the spectral radiance at the center wavelength of the filter produced by a 2850 K NBS lamp source filling the sensor aperture and giving the same detector response. The data in the thermal IR channels was converted to apparent temperature in degrees Kelvin. The apparent temperature is the temperature of a blackbody filling the sensor aperture producing the same detector response.

A table of apparent temperatures and their corresponding band radiances is included as Table I-1 in Appendix I. The radiance (or temperature) is recovered from the integer data values using multiplicative and additive factors recorded in the tape header record for each channel. These "mult" and "add" factors were determined from the calibration sources appearing at the end of each scan line assuming a linear relationship between radiance and detector output*. For channels calibrated in radiance, the integer values on the calibrated tape differ from those on the original computer compatible tapes by at most a zero level correction. For channels calibrated in temperature, however, the new integers are distinctly different from the original values since those on the calibrated tape are linear in temperature while those on the original tape are proportional to radiance.

Averaging was employed to reduce oversampling and to equalize any differences in the fields-of-view of the various detectors. The degree of oversampling was generally largest in the along-track direction because of the constant (60/sec) scan rate. The degree of oversampling in the cross-track direction was small in almost all of the data because a 3.8×10^5 /sec. sampling rate was used to produce a sample every 2.5 mr to correspond to the 2.5 mr cross-track field-of-view of most of the detectors. The technique that has been used for averaging lines to reduce oversampling, rather than dropping an appropriate number of alternate lines, was developed for two reasons: 1) to improve the signal-to-noise ratio in the resulting data, and 2) to equalize any differences in the along-track fields-of-view of the various detectors for calculating the spectral correlation coefficients. The same averaging technique can be used to reduce any overlap in the cross-track direction and to equalize any differences in the cross-track fields-of-view of the various detectors, but cross-track averaging was not found to be necessary in any of the data. Figure 3-1 is a schematic representation of the procedure used*. In this example, D is the largest along-track field-of-view of the channels and d the field-of-view of the channel

* See Appendix I for a detailed description of the procedures used.



$$\text{Output Line 1} = \{0.5 (\text{Input Line 1}) + 1.0 (\text{Input Line 2}) + 0.5 (\text{Input Line 3})\} / 2.0$$

FIGURE 3-1 SCHEMATIC REPRESENTATION OF THE PROCEDURES USED FOR FIELD-OF-VIEW AVERAGING

being averaged. The averaging was done by summing the radiances of the scan line times their overlap with the desired output line and dividing by the sum of the overlap factors. If the scan lines for the largest field-of-view were themselves overlapped, non-overlapped fields-of-view were generated by taking as output lines those with fields-of-view D each of which was displaced by D as in the right side of Figure 3-1. Overlap factors were then determined in an identical manner between the original scan lines with field-of-view D and this set of non-overlapped output lines.

After calibration and field-of-view averaging, a new data tape was generated. To be compatible with existing data processing systems, this tape was written in ERIM-7094 format which consists of 36-bit words each of which contain 4 data values. The individual scan lines were written with the channels interleaved with 646 9-bit data points per channel per scan line. The "mult" and "add" factors required for calibration of the data were written in the tape header record along with necessary format information. These tapes could then be used directly as input to new or existing statistics generation programs.

3.2 STATISTICS DEFINITIONS

Several sets of statistics have been generated for each of the chosen scenes. These may be broken down into two groups:

- 1) Point statistics: Those defined by individual data points in a single channel; and
- 2) Correlative and area statistics: Those requiring calculation of correlation effects for a scene either in a single channel or between channels.

3.2.1 POINT STATISTICS: MEANS AND STANDARD DEVIATIONS

The point statistics generated were the mean and standard deviation for each channel and a histogram of the data value distributions of these channels. To determine the degree of homogeneity that existed, the total scene was broken down into sub-areas and the point statistics

generated for these sub-areas as well as for the total area. In practice, the sub-area statistics were generated first and the total area statistics derived from them.

The mean value for sub-area η in Channel J ($\overline{x(J)_\eta}$) was evaluated using

$$\overline{x(J)_\eta} = \frac{1}{N_\eta} \sum_{i=1}^{N_\eta} x(J)_i \quad (1)$$

where $x(J)_i$ is the data value of pixel i in Channel J and N_η is the total number of data points in the sub-area. Using the same notation the standard deviation, $\sigma(J)_\eta$, is given by

$$\sigma^2(J)_\eta = \left(\frac{N_\eta}{N_\eta - 1} \right) \left\{ \frac{1}{N_\eta} \sum_{i=1}^{N_\eta} x^2(J)_i - \overline{x(J)_\eta}^2 \right\} \quad (2)$$

The corresponding total scene values in Channel J are then related to those of the sub-areas through the following relations

$$\overline{x(J)} = \frac{1}{N} \sum_{\eta} N_\eta \overline{x(J)_\eta}$$

and

$$\sigma^2(J) = \left(\frac{N}{N - 1} \right) \left\{ \frac{1}{N} \sum_{\eta} N_\eta \left[\left(\frac{N_\eta - 1}{N_\eta} \right) \sigma^2(J)_\eta + \overline{x(J)_\eta}^2 \right] - \overline{x(J)}^2 \right\} \quad (3)$$

where N is the number of points in the total scene. Typical examples of these statistics, generated from the Flint-1 data, are given in Table 3-1. In this scene the sub-areas had on the order of 77,000 data points while the total scene had approximately 464,000 points.

At the same time that these statistics were generated, the number of data points having each of the possible data values (0 to 255) was tabulated and this tabulation used to generate histograms for the scene. Representative sub-areas and total area histograms for the 9.3 to 11.7 μm channel of Flint-1 are shown in Figures 3-2 and 3-3 respectively.

TABLE 3-1. SUB-AREA AND TOTAL AREA MEANS AND STANDARD DEVIATIONS FOR FLINT-1

All entries have units of $\mu\text{w}/(\text{cm}^2\cdot\text{sr}\cdot\mu\text{m})$ except for the 9.3-11.7 μm band which is in degrees Kelvin.

	SUB-AREA 1	SUB-AREA 2	SUB-AREA 3	SUB-AREA 4	SUB-AREA 5	SUB-AREA 6	TOTAL
<u>1.0 - 1.4 μm</u>							
Mean	1280	1278	1306	1191	1312	1231	1273
Std. Dev.	347	355	424	344	355	355	364
<u>1.5 - 1.8 μm</u>							
Mean	230	180	164	192	159	125	173
Std. Dev.	77	74	82	80	80	73	83
<u>2.0 - 2.6 μm</u>							
Mean	41	38	34	36	35	30	36
Std. Dev.	11	11	11	10	9	8	10
<u>9.3 - 11.7 μm</u>							
Mean	295	295	294	295	294	293	294
Std. Dev.	2.7	3.5	2.6	3.3	3.1	2.7	3.1

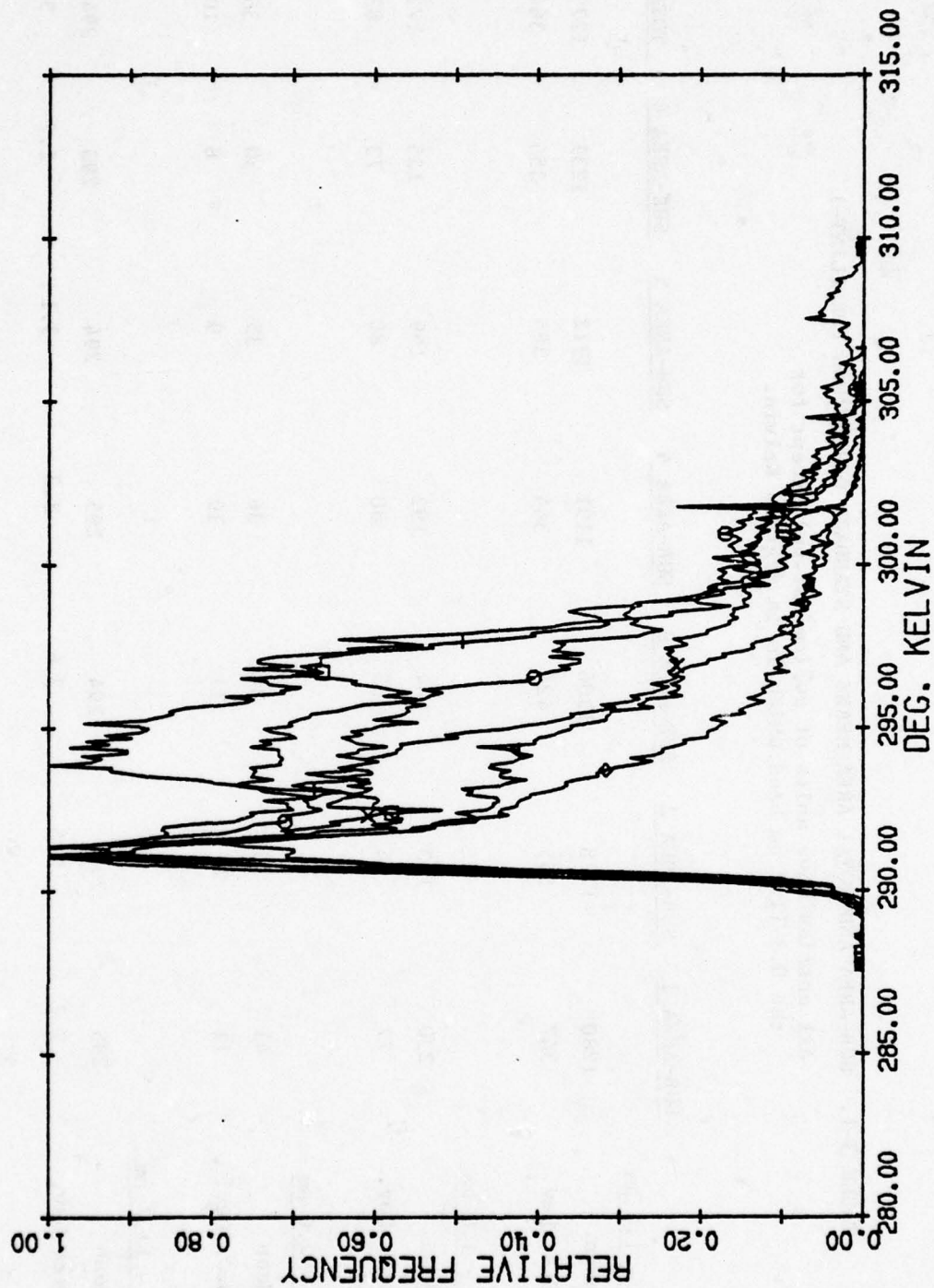


FIGURE 3-2 SUBAREA HISTOGRAMS FOR THE 9.3 - 11.7 μ m CHANNEL OF FLINT-1

AREA: FLINT 1
 LAMBDA= 9.3 TO 11.7 μ m
 SUBAREAS

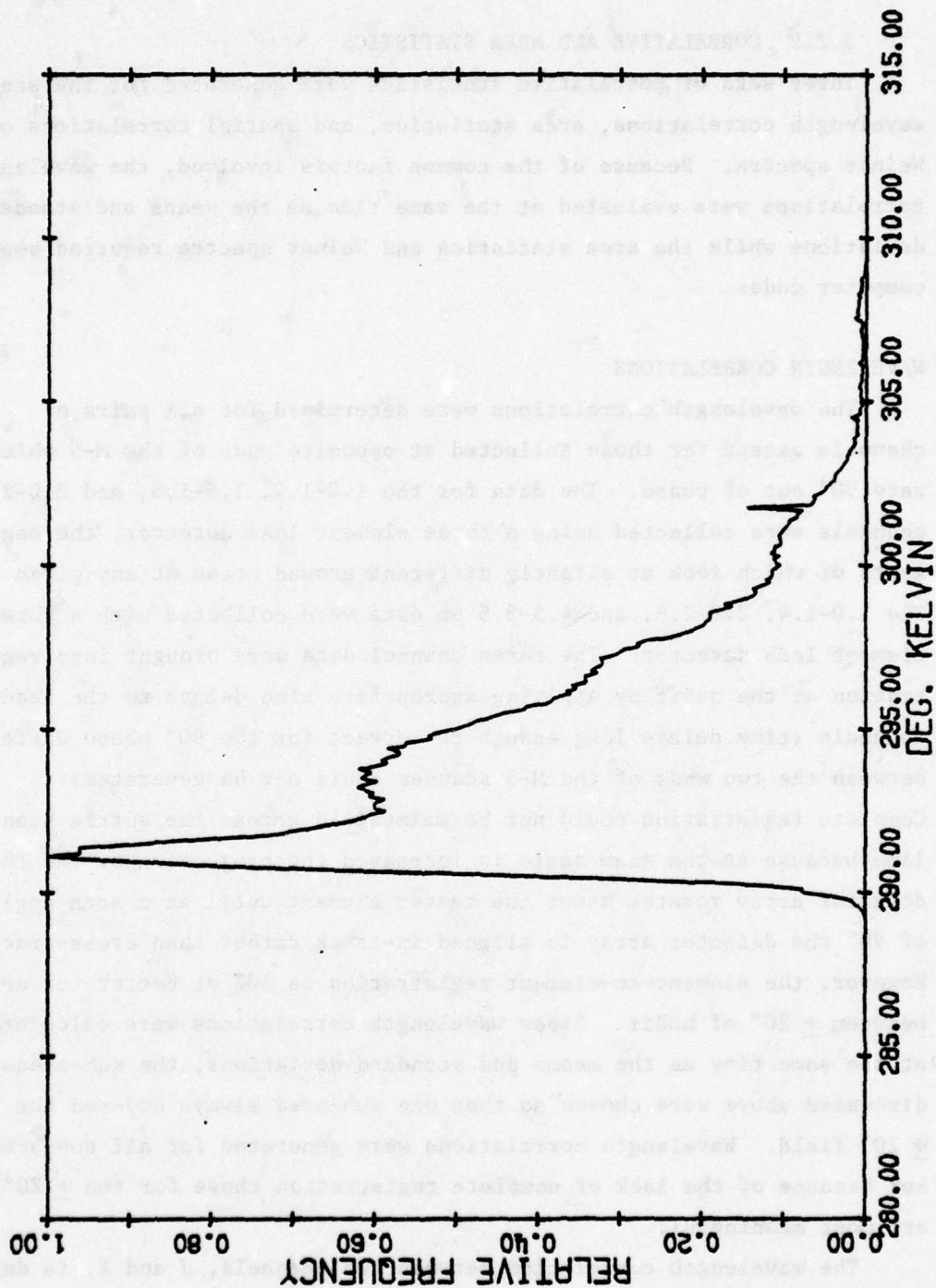


FIGURE 3-3 TOTAL AREA HISTOGRAM FOR THE 9.3 - 11.7 μ m CHANNEL OF FLINT-1

AREA: FLINT 1
 LAMBDA= 9.3 TO 11.7 μ m
 TOTAL AREA

MEAN = 294.43
 ST.DEV.= 3.14

3.2.2 CORRELATIVE AND AREA STATISTICS

Three sets of correlative statistics were generated for the scenes: wavelength correlations, area statistics, and spatial correlations or Wiener spectra. Because of the common factors involved, the wavelength correlations were evaluated at the same time as the means and standard deviations while the area statistics and Wiener spectra required separate computer codes.

WAVELENGTH CORRELATIONS

The wavelength correlations were determined for all pairs of channels except for those collected at opposite ends of the M-5 which were 90° out of phase. The data for the 1.0-1.4, 1.5-1.8, and 2.0-2.6 μm channels were collected using a three element InAs detector, the segments of which look at slightly different ground areas at any given time. The 1.0-1.4, 2.0-2.6, and 4.5-5.5 μm data were collected with a three-element InSb detector. The three channel data were brought into registration at the nadir by applying appropriate time delays to the leading channels (time delays long enough to correct for the 90° phase difference between the two ends of the M-5 scanner could not be generated). Complete registration could not be maintained across the entire scan line because as the scan angle is increased the projection of the three detector array rotates about the center element until at a scan angle of 90° the detector array is aligned in-track rather than cross-track. However, the element-to-element registration is 50% or better for angles between $\pm 20^\circ$ of nadir. Since wavelength correlations were calculated at the same time as the means and standard deviations, the sub-areas discussed above were chosen so that one sub-area always covered the $\pm 20^\circ$ field. Wavelength correlations were generated for all sub-areas but because of the lack of complete registration those for the $\pm 20^\circ$ are most meaningful.

The wavelength correlation between two channels, J and K, is defined in terms of a correlation coefficient which is the ratio of the covariance of the two channels to the product of their standard deviations:

$$\text{COR}(J,K) = \frac{\text{COV}(J,K)}{\sigma(J)\sigma(K)} \quad (4)$$

where $\text{COR}(J,K)$ is the correlation coefficient for the two channels, $\sigma(J)$ and $\sigma(K)$ their standard deviations, and $\text{COV}(J,K)$, the J-K element of the covariance matrix for a given sub-area, is defined as

$$\text{COV}(J,K)_n = \frac{N_n}{N_n - 1} \left\{ \frac{1}{N_n} \sum_{i=1}^{N_n} x(J)_i x(K)_i - \overline{x(J)}_n \overline{x(K)}_n \right\} \quad (5)$$

where all symbols are the same as those of Equations 1 and 2. The reason for the simultaneous evaluation of Equations 2 and 5 is obvious: the square of the standard deviation $\sigma^2(J)$ is the autocovariance or the covariance of a given channel with itself $\text{COV}(J,J)$.

An example of the correlation coefficients for the infrared channels of Flint-1 are given in Table 3-2.

AREA/INTENSITY STATISTICS

Since means, standard deviations, and histograms do not give any information about the positions of data values in the scene or possible clustering of these values, area statistics have been generated by determining contiguous regions of the scene for which the enclosed points had values greater than some prescribed threshold [Reference 3]. Once these regions had been defined, their geometric centroids, areas, and second moments were determined and these parameters used to define a set of equivalent elliptical areas. The output from this procedure was, for each threshold level, a tabulation of centroids, tilt angles and semi-major and minor axes defining the equivalent ellipses.

The semi-major and semi-minor axes of the equivalent ellipses were taken coincident with the principal axes of the regions they represented. If I_x^c and I_y^c are the second moments of a region about the centroid and I_{xy}^c its product of inertia, the angle of rotation of the principal axes relative to a fixed x-y coordinate system is given by

- [3] W. G. Burge, W. L. Brown, A study of Waterfowl Habitat in North Dakota Using Remote Sensing Techniques, Report No. 2771-7-F, Willow Run Laboratories, University of Michigan, Ann Arbor, July 1970.

TABLE 3-2
CORRELATION COEFFICIENTS FOR THE TOTAL AREA OF FLINT-1

Spectral Correlation	1.0-1.4 μm	1.5-1.8 μm	2.0-2.6 μm	9.3-11.7 μm
1.0- 1.4 μm	1.000			
1.5- 1.8 μm	0.392	1.000		
2.0- 2.6 μm	0.303	0.603	1.000	
9.3-11.7 μm	-0.455	0.048	0.177	1.000

$$\alpha = \frac{1}{2} \tan^{-1} \left\{ \frac{2I_{xy}^c}{I_y^c - I_x^c} \right\} \quad (6)$$

where α is in radians. The second moments of the region about the principal axes are then given by

$$I_{x'} = \left(\frac{I_x^c + I_y^c}{2} \right) + \left(\frac{I_x^c - I_y^c}{2} \right) \cos 2\alpha - I_{xy}^c \sin 2\alpha$$

and (7)

$$I_{y'} = \left(\frac{I_x^c + I_y^c}{2} \right) - \left(\frac{I_x^c - I_y^c}{2} \right) \cos 2\alpha + I_{xy}^c \sin 2\alpha$$

Since the area and the second moments of an arbitrary region cannot be simultaneously matched using an ellipse, equality was demanded between the geometric areas and the ratios of the principal moments. If the semi-major and semi-minor axes of the ellipse are defined as a and b respectively and the a -axis is aligned with the larger of the principal axes of the region, these equalities give

$$a^2 = \frac{A}{\pi} \sqrt{\frac{I_1}{I_2}}$$

and (8)

$$b^2 = \frac{A}{\pi} \sqrt{\frac{I_2}{I_1}}$$

where A is the area of the region and I_1 and I_2 are the moments given by Equation 7 with $I_1 > I_2$. If $I_{y'}$ of Equation 7 is the larger of the moments, the a -axis of the ellipse is oriented at an angle α with respect to the fixed x -axis; if $I_{x'}$ is larger, the a -axis is at an angle $\alpha + \pi/2$. An example of the equivalent elliptical areas generated for the 9.3 - 11.7 μm channel of Flint-1 is shown in Figures 3-4 through 3-7. Each of these figures represents the areas found for data values

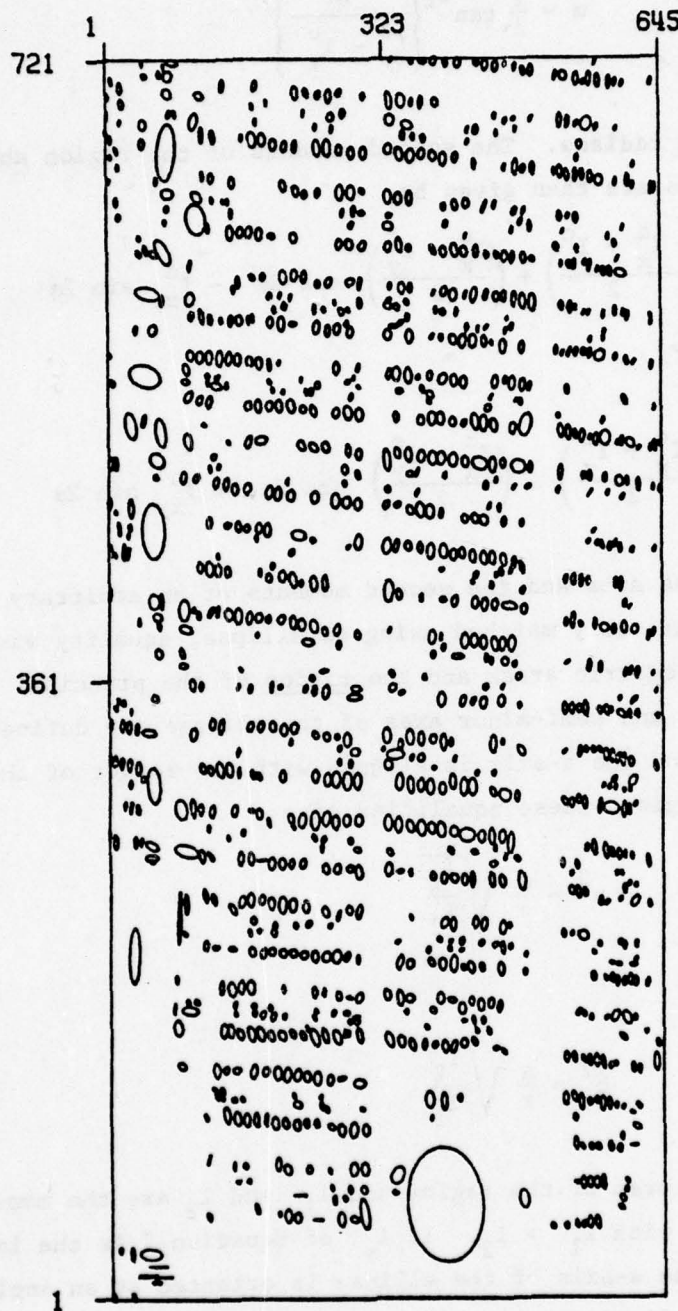


FIGURE 3-4 EQUIVALENT ELLIPTICAL AREAS
FOR THE 9.3 - 11.7 μm CHANNEL
OF FLINT-1 WITH A 1.5σ THRESHOLD

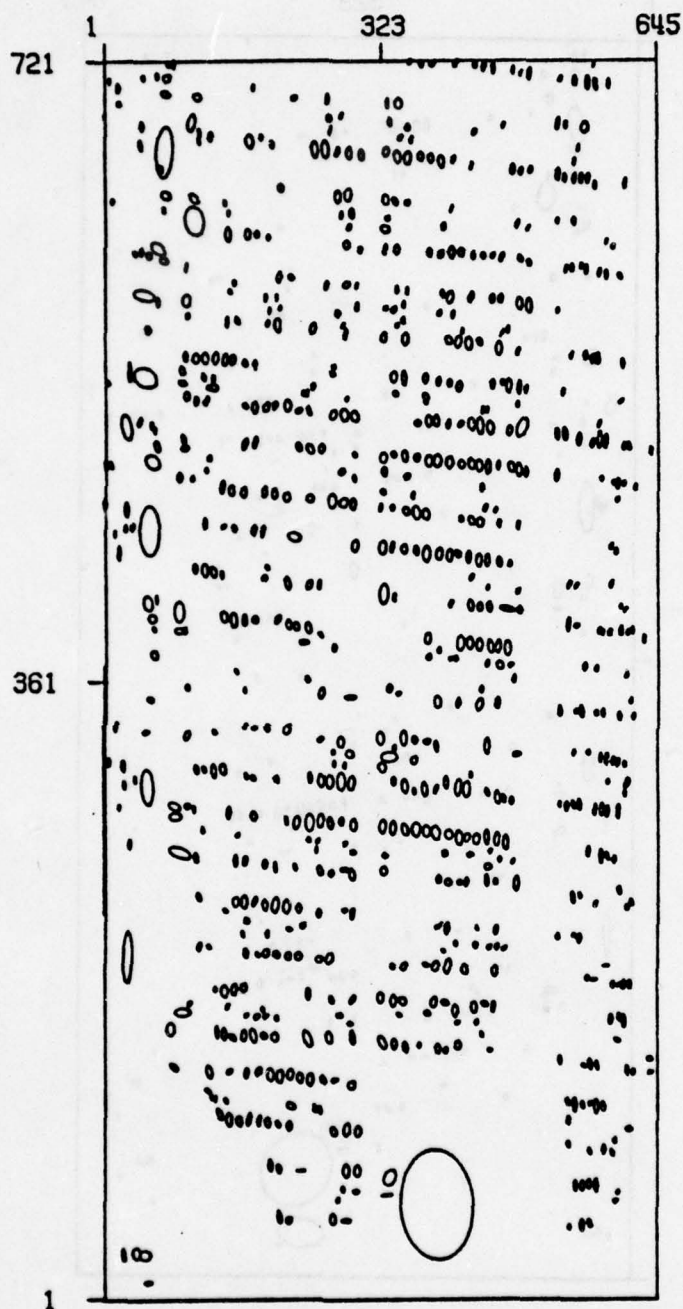


FIGURE 3-5 EQUIVALENT ELLIPTICAL AREAS FOR
THE 9.3 - 11.7 μm CHANNEL OF
FLINT-1 WITH A 2.0σ THRESHOLD

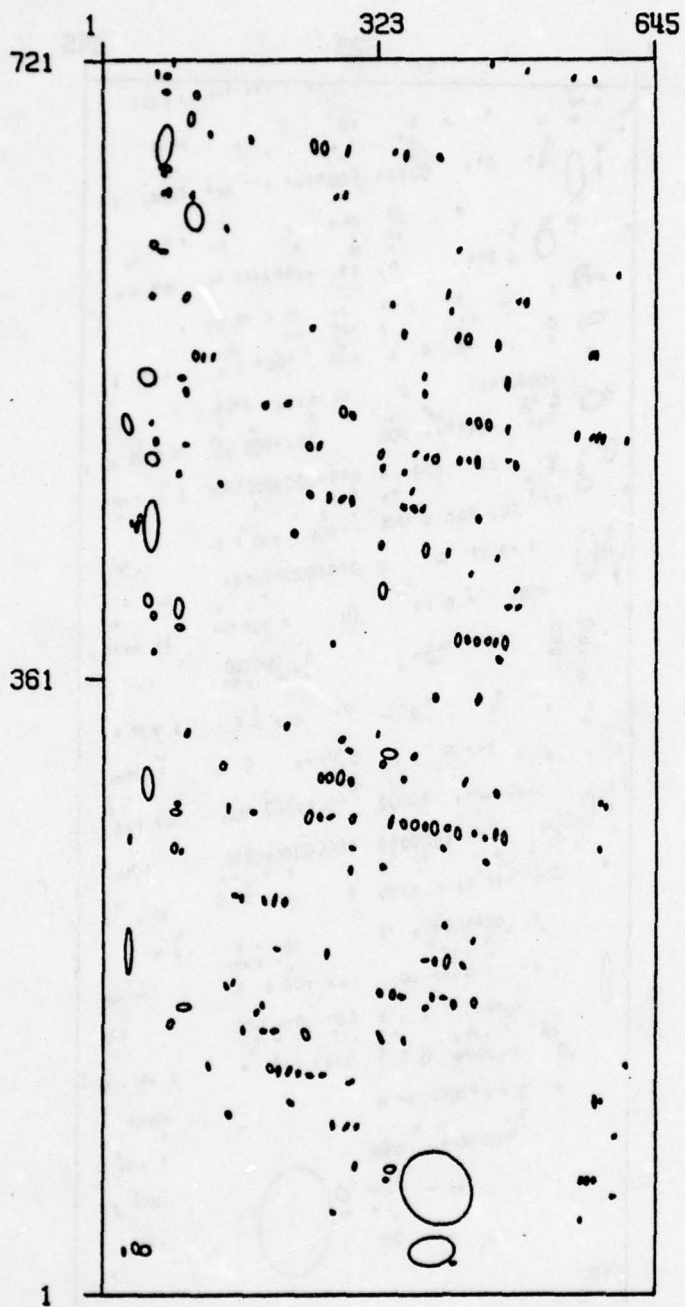


FIGURE 3-6 EQUIVALENT ELLIPTICAL AREAS FOR
THE 9.3 - 11.7 μm CHANNEL OF
FLINT-1 WITH A 2.5σ THRESHOLD

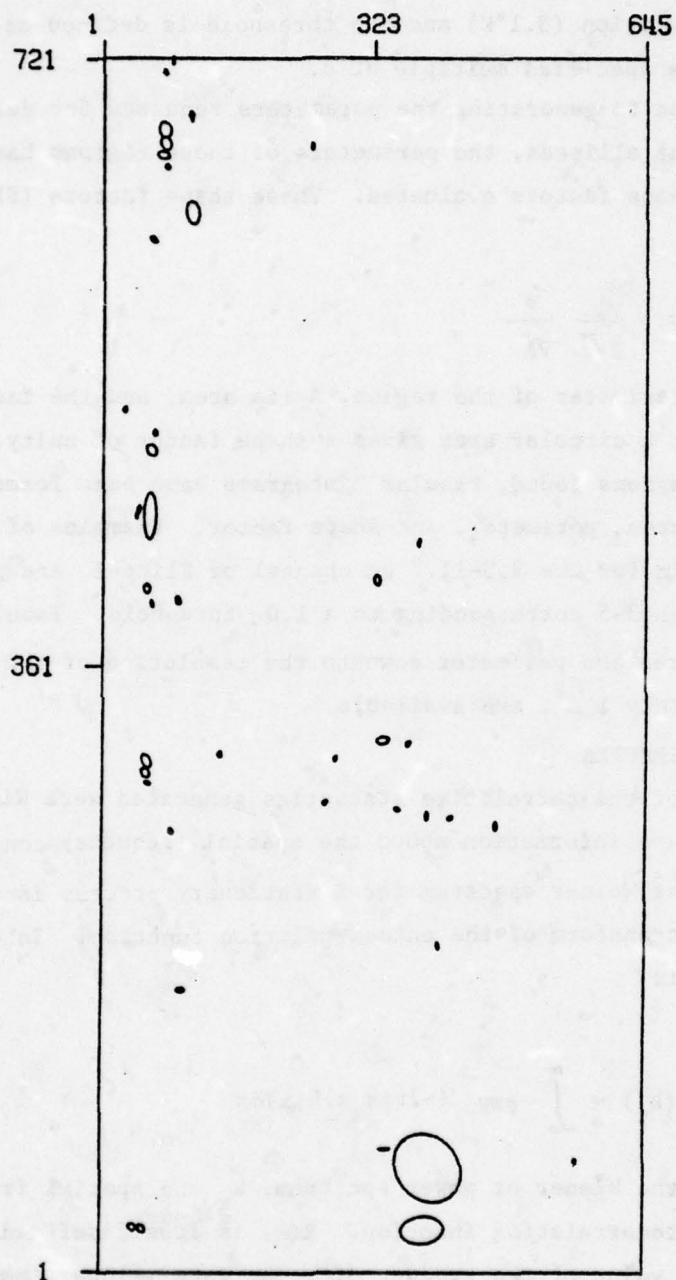


FIGURE 3-7 EQUIVALENT ELLIPTICAL AREAS FOR
THE 9.3 - 11.7 μm CHANNEL OF
FLINT-1 WITH A 3.0σ THRESHOLD

exceeding the specified threshold (1.5σ , 2.0σ , 2.5σ , 3.0σ) where σ is the standard deviation (3.1°K) and the threshold is defined as the mean (294°K) plus the specified multiple of σ .

In addition to generating the parameters required for definition of the equivalent ellipses, the perimeters of these regions have been tabulated and shape factors evaluated. These shape factors (SF) were defined as

$$SF = \frac{1}{2\sqrt{\pi}} \frac{P}{\sqrt{A}} \quad (9)$$

where P is the perimeter of the region, A its area, and the factor $1/2\sqrt{\pi}$ included so that a circular area gives a shape factor of unity.

For all regions found, tabular histograms have been formed sorting the regions by area, perimeter, and shape factor. Examples of these histograms, again for the $9.3\text{--}11.7 \mu\text{m}$ channel of Flint-1, are given in Table 3-3 through 3-5 corresponding to a 1.0σ threshold. Tabulations with increments in area and perimeter down to the resolution of the scanner data, approximately 1 m^2 , are available.

WIENER (POWER) SPECTRA

The last of the correlative statistics generated were Wiener spectra which gave information about the spatial frequency content of the images. The Wiener spectrum for a stationary process is defined as the Fourier transform of the autocorrelation function. In one dimension this is

$$S(k_x) = \int_{-\infty}^{\infty} \exp(-2\pi i k_x x) R(x) dx \quad (10)$$

where $S(k_x)$ is the Wiener or power spectrum, k_x the spatial frequency and $R(x)$ the autocorrelation function. $R(x)$ is itself defined as the expectation value of the product of scene data values times the corresponding values for the scene when displaced by x :

$$R(x) = E \{f(X)f(X + x)\} \quad (11)$$

TABLE 3-3

AREA DISTRIBUTION FOR RECOGNIZED REGIONS
IN THE 9.3-11.7 μm CHANNEL OF FLINT-1 WITH A 1σ THRESHOLD

SQUARE METERS		FREQUENCY
0.0 TO	100.0	2047
100.0 TO	200.0	78
200.0 TO	500.0	26
500.0 TO	1000.0	8
1000.0 TO	1500.0	2
1500.0 TO	2000.0	0
2000.0 TO	2500.0	0
2500.0 TO	3000.0	0
3000.0 TO	4000.0	1
4000.0 TO	5000.0	0
5000.0 TO	6000.0	0
6000.0 TO	8000.0	1
8000.0 TO	10000.0	0
10000.0 TO	15000.0	0
15000.0 TO	20000.0	0
20000.0 TO	40000.0	0
40000.0 TO	80000.0	0
80000.0 TO	160000.0	0
OVER 160000.0		0

TABLE 3-4

PERIMETER DISTRIBUTIONS FOR RECOGNIZED REGIONS
IN THE 9.3-11.7 μm CHANNEL OF FLINT-1 WITH A 1σ THRESHOLD

METERS	FEET	FREQUENCY
0 TO 50	0 TO 164	1991
50 TO 100	164 TO 328	128
100 TO 150	328 TO 492	16
150 TO 200	492 TO 656	15
200 TO 250	656 TO 820	5
250 TO 300	820 TO 984	3
300 TO 350	984 TO 1148	1
350 TO 400	1148 TO 1312	1
400 TO 500	1312 TO 1640	1
500 TO 600	1640 TO 1968	0
600 TO 700	1968 TO 2296	0
700 TO 800	2296 TO 2624	0
800 TO 900	2624 TO 2952	1
900 TO 1000	2952 TO 3280	1
1000 TO 1200	3280 TO 3937	0
1200 TO 1400	3937 TO 4593	0
1400 TO 1600	4593 TO 5249	0
1600 TO 2000	5249 TO 6561	0
OVER 2000	OVER 6561	0

TABLE 3-5

SHAPE FACTOR DISTRIBUTIONS FOR RECOGNIZED REGIONS
IN THE 9.3-11.7 μm CHANNEL OF FLINT-1 WITH A 1σ THRESHOLD

SHAPE FACTOR	FREQUENCY
0.0 TO 1.0	11
1.0 TO 1.1	2
1.1 TO 1.2	447
1.2 TO 1.3	303
1.3 TO 1.4	513
1.4 TO 1.5	280
1.5 TO 1.6	227
1.6 TO 1.7	133
1.7 TO 1.8	59
1.8 TO 1.9	50
1.9 TO 2.0	34
2.0 TO 2.2	43
2.2 TO 2.4	21
2.4 TO 2.6	9
2.6 TO 2.8	7
2.8 TO 3.0	5
3.0 TO 3.5	15
3.5 TO 4.0	3
OVER 4.0	1

where E represents the expectation value of the argument. The Wiener spectrum may be evaluated without first determining the autocorrelation function if the integral

$$\int_{-\infty}^{\infty} |xR(x)| dx \quad (12)$$

is bounded, which is usually the case for non-periodic data with zero mean. In this case it may be shown that [Reference 4]

$$S(k_x) = \lim_{(x_2 - x_1) \rightarrow \infty} \left| \int_{x_1}^{x_2} f(x) \exp(-2\pi i k_x x) dx \right|^2 \quad (13)$$

so that the Wiener spectrum is, in the limit, the modulus squared of the Fourier transform of the scene. Written in terms of the discrete Fourier transform, this equation becomes

$$S(j) = \frac{\Delta x}{(N-1)} \left| \sum_{\ell=0}^{N-1} f(\ell) \exp(-2\pi i j \ell / N) \right|^2 \quad (14)$$

where N is the total number of points being transformed, i is the square root of -1 , and the spatial frequency k_x , evaluated only at integer values of j , is given by

$$k_x = \frac{j}{N\Delta x} \quad (15)$$

where Δx is the displacement between successive data points.

It may be seen from Equation 14 that the Wiener spectrum $S(j)$ is symmetric about $j = N/2$ since

$$\exp(-2\pi i (N-j)\ell/N) = \exp(+2\pi i j\ell/N) \quad (16)$$

[4] A. Papoulis, Probability, Random Variables, and Stochastic Processes, McGraw-Hill Book Company, New York, 1965.

Hence

$$S(N - j) = S(j) \quad \text{for } j = 1, 2, \dots, N/2 \quad (17)$$

and only the first half of the Wiener spectrum needs to be evaluated. The calculated frequency range is then

$$\frac{1}{N\Delta x} \leq k_x \leq \frac{1}{2\Delta x} \quad (18)$$

The two dimensional Wiener spectrum is defined in an analogous manner except that two transforms are required, one for each dimension:

$$S(j, \ell) = \left(\frac{\Delta x}{N-1} \right) \left(\frac{\Delta y}{M-1} \right) \left| \sum_{n=0}^{N-1} \exp(-2\pi i j n / N) * \sum_{m=0}^{M-1} \exp(-2\pi i \ell m / M) f(n, m) \right|^2 \quad (19)$$

where the spatial frequencies in the two dimensions are given in terms of the integers j and ℓ by

$$k_x = \frac{j}{N\Delta x} \quad \text{and} \quad k_y = \frac{\ell}{M\Delta y} \quad (20)$$

One dimensional Wiener spectra were evaluated both cross-track (along scan line) and in-track (parallel to the aircraft flight paths). These are average spectra since Equation 14 was used to transform individual "lines" of data and the transforms have been averaged over a number of "lines". Since the Fourier transform algorithms were substantially less expensive if the number of points transformed was a power of 2, only 512 points were used for both the cross-track and in-track "lines" of data. The middle 512 scan lines were averaged to obtain the cross-track Wiener spectra; 25 along-track lines equally spaced across the image were averaged to obtain the in-track Wiener spectra. Examples of in-track and

cross-track Wiener spectra for the 9.3-11.7 μm channel of Flint-1 are shown in Figures 3-8 and 3-9. The units of power density are $(\text{K})^2/\text{cycle}$ per meter for the 9.3-11.7 μm band and $(\mu\text{W}/\text{cm}^2 \cdot \text{sr} \cdot \mu\text{m})^2/\text{cycle}$ per meter for the 1.0-1.4, 1.5-1.8 and 2.0-2.6 μm bands.

Representative two-dimensional Wiener spectra were evaluated only for the Flint-1 scene. Figure 3-10 shows a plot of the two-dimensional spectrum for the 9.3-11.7 μm channel. The units of power density for the two-dimensional Wiener spectrum are $(\text{K})^2/(\text{cycle per meter})^2$. As for the one-dimensional spectra, the two-dimensional spectra were evaluated using 512 data points in each of the dimensions. The utility of the two-dimensional Wiener spectra to the system designer has not been firmly established so that only limited two-dimensional Wiener spectra processing has been performed to date.

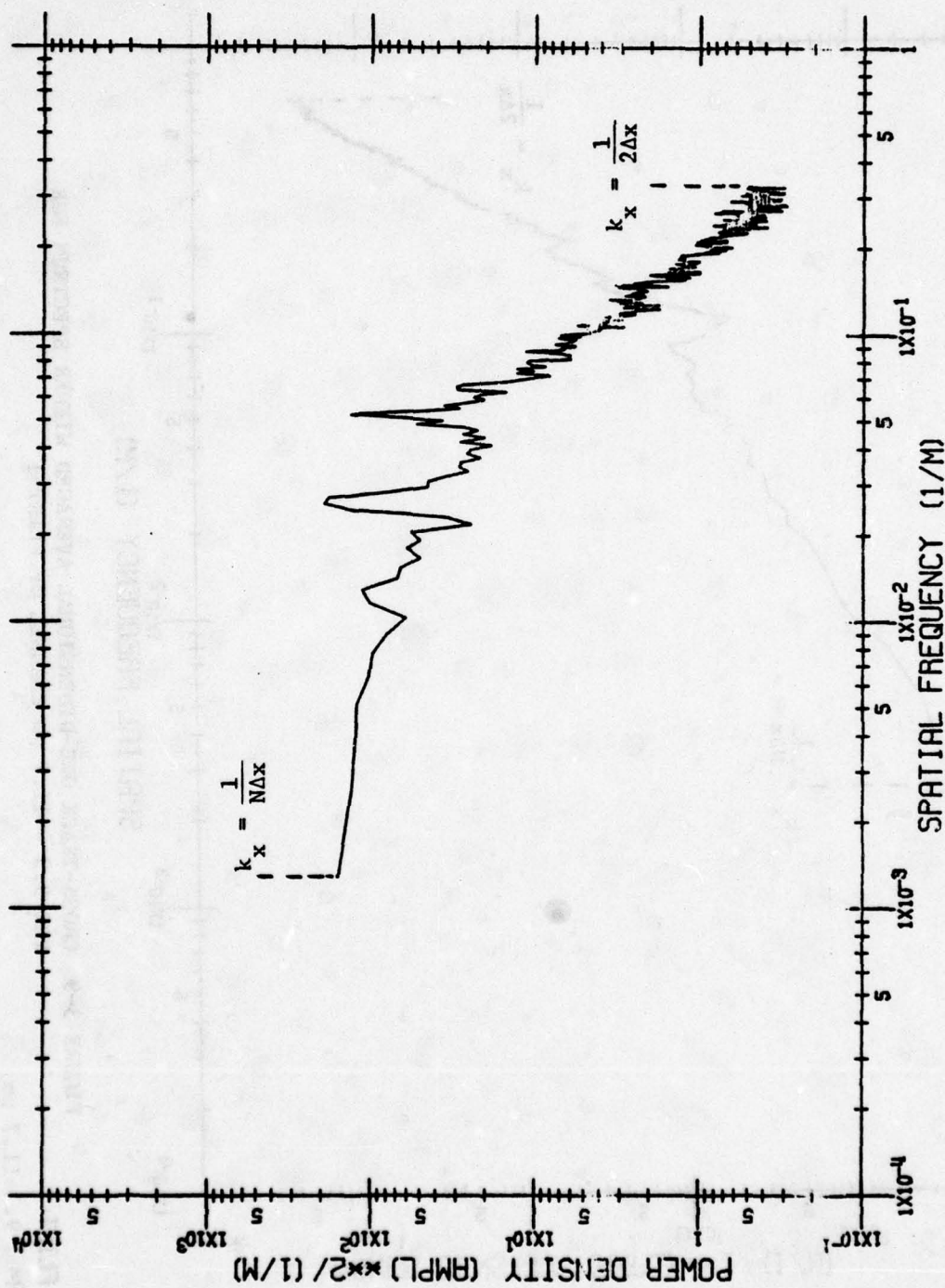


FIGURE 3-8 IN-TRACK ONE-DIMENSIONAL AVERAGED WIENER SPECTRUM FOR THE
9.3 - 11.7 μm CHANNEL OF FLINT-1

AREA: FLINT 1
 LAMBDA= 9.3-11.7 μm
 INTRACK

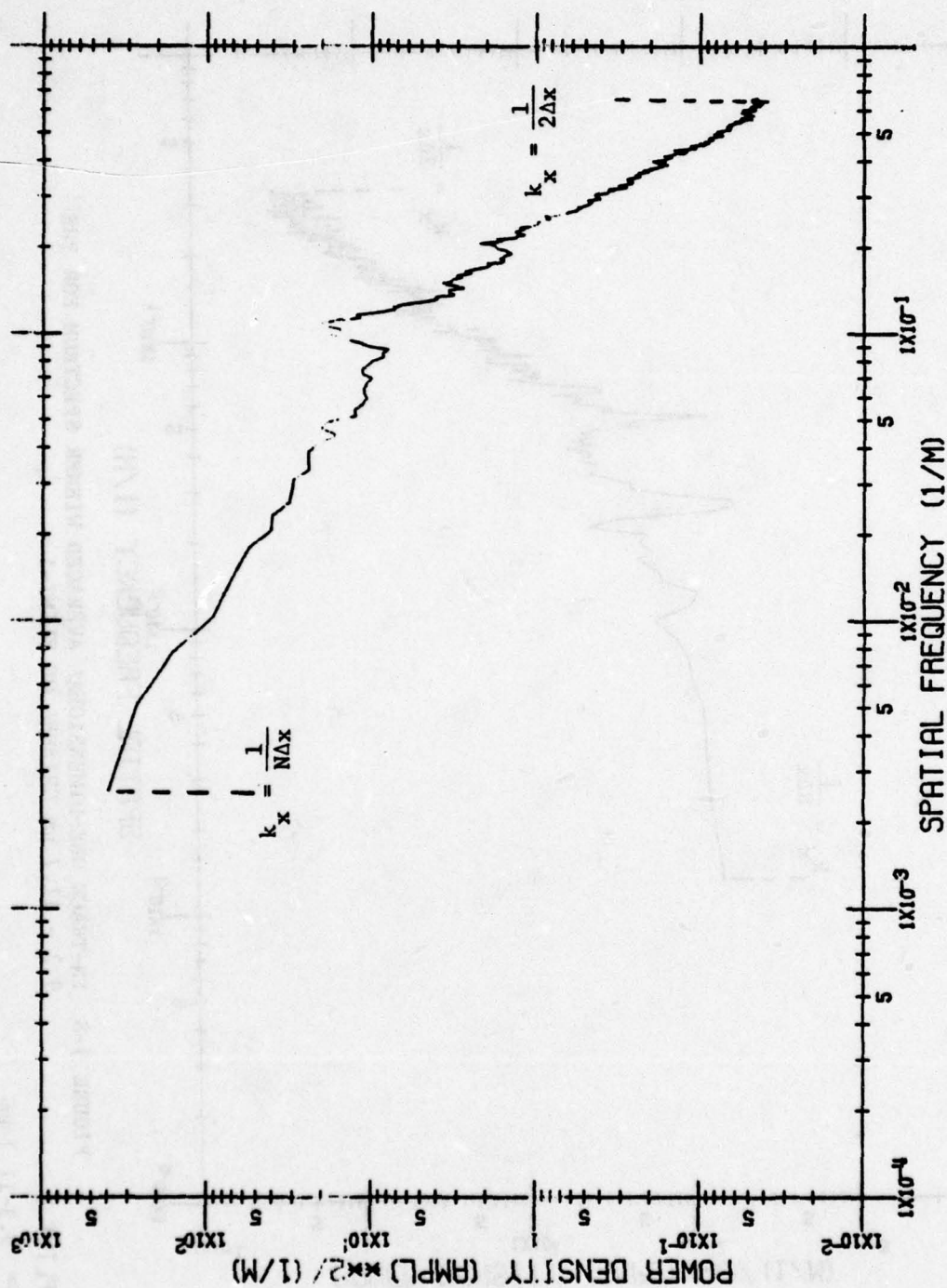


FIGURE 3-9 CROSS-TRACK ONE-DIMENSIONAL AVERAGED WIENER SPECTRUM FOR
THE 9.3 - 11.7 μm CHANNEL OF FLINT-1

AREA: FLINT 1
 LAMBDA= 9.3-11.7 μm
 CROSSTRACK

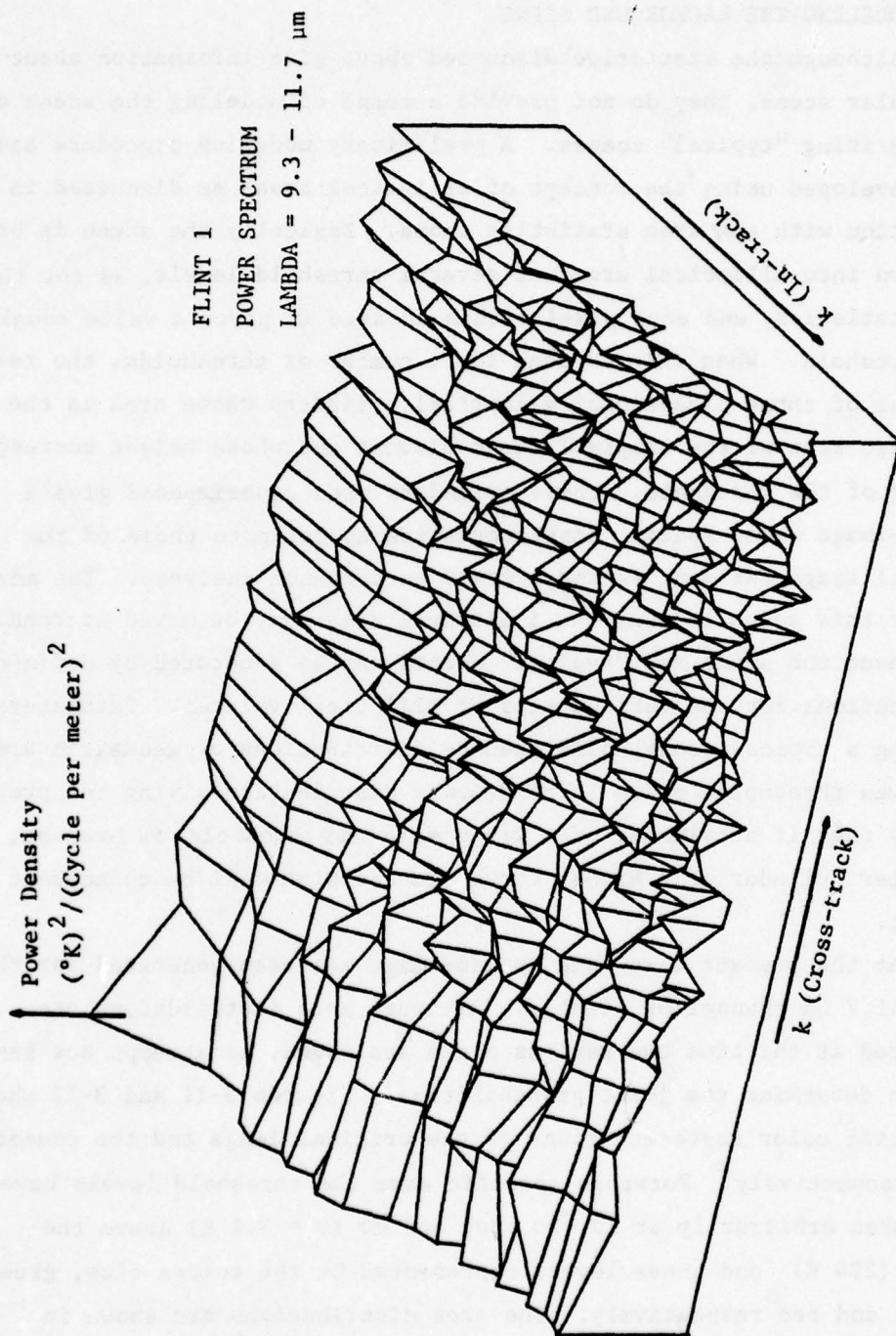


FIGURE 3-10 TWO-DIMENSIONAL WIENER SPECTRUM FOR THE 9.3 - 11.7 μm CHANNEL OF FLINT-1

3.3 MODELING THE BACKGROUND SCENE

Although the statistics discussed above give information about the particular scene, they do not provide a means of modeling the scene or of generating "typical" scenes. A preliminary modeling procedure has been developed using the concept of elliptical areas as discussed in connection with the area statistics above. Basically the scene is broken down into elliptical areas at several threshold levels, as for the area statistics, and each pixel within an area is given a value equal to the threshold. When this is done for a number of thresholds, the result is a set of three-dimensional elliptical cylinders whose area is the geometric area of the original scene element and whose height corresponds to that of the threshold. These cylinders when superimposed give a pseudo-image whose spatial characteristics approximate those of the original image for many sensor systems performance analyses. The advantage of this scene is that the individual areas may be moved at random throughout the scene and "typical" scenes may be generated by defining distributions for the various sets of elliptical volumes. Parameters defining a typical scene could then be distributions of geometric areas for given thresholds and a joint density distribution giving the probability that if a cylinder of a given size and threshold is present, a smaller cylinder of a higher threshold and size will be coincident with it.

At the present time, one pseudo-image has been generated for the 9.3 - 11.7 μm channel of Flint-1. Although area distributions are generated at the time the various areas are found, no attempt has been made to determine the joint probabilities. Figures 3-11 and 3-12 show artificial color representations of the original image and the pseudo-image respectively. For this specific case the threshold levels have been taken arbitrarily at 1σ , 2σ , 3σ , and 4σ ($\sigma = 3.1 \text{ K}$) above the mean (294 K) and these levels represented by the colors blue, green, yellow, and red respectively. The area distributions are shown in Tables 3-6 through 3-9.



Blue = 288 - 304°K Yellow = 304 - 307°K
 Green = 301 - 304°K Red = 307 - 310°K
 Brown = <288°K

FIGURE 3-11. ARTIFICIAL COLOR IMAGE OF THE
 9.3 - 11.7 μ m CHANNEL OF FLINT-1.

FIGURE 3-12. ARTIFICIAL COLOR REPRESENTATION
 OF THE PSEUDO-IMAGE GENERATED FROM THE
 9.3 - 11.7 μ m CHANNEL OF FLINT-1.

TABLE 3-6

AREA DISTRIBUTIONS FOR RECOGNIZED REGIONS IN THE
REAL AND PSEUDO-IMAGES OF THE 9.3-11.7 μ m CHANNEL OF FLINT-1.

THRESHOLD LEVEL = 1 σ

SQUARE METERS		FREQUENCY
0.0 TO	100.0	2047
100.0 TO	200.0	78
200.0 TO	500.0	26
500.0 TO	1000.0	8
1000.0 TO	1500.0	2
1500.0 TO	2000.0	0
2000.0 TO	2500.0	0
2500.0 TO	3000.0	0
3000.0 TO	4000.0	1
4000.0 TO	5000.0	0
5000.0 TO	6000.0	0
6000.0 TO	8000.0	1
8000.0 TO	10000.0	0
10000.0 TO	15000.0	0
15000.0 TO	20000.0	0
20000.0 TO	40000.0	0
40000.0 TO	80000.0	0
80000.0 TO	160000.0	0
OVER 160000.0		0
TOTAL NUMBER OF REGIONS		= 2163

TABLE 3-7

AREA DISTRIBUTIONS FOR RECOGNIZED REGIONS IN THE
REAL AND PSEUDO-IMAGES OF THE 9.3-11.7 μm CHANNELS OF FLINT-1.

THRESHOLD LEVEL = 2σ .

SQUARE METERS		FREQUENCY
0.0 TO	100.0	1110
100.0 TO	200.0	10
200.0 TO	500.0	4
500.0 TO	1000.0	2
1000.0 TO	1500.0	0
1500.0 TO	2000.0	0
2000.0 TO	2500.0	0
2500.0 TO	3000.0	0
3000.0 TO	4000.0	0
4000.0 TO	5000.0	0
5000.0 TO	6000.0	1
6000.0 TO	8000.0	0
8000.0 TO	10000.0	0
10000.0 TO	15000.0	0
15000.0 TO	20000.0	0
20000.0 TO	40000.0	0
40000.0 TO	80000.0	0
80000.0 TO	160000.0	0
OVER	160000.0	0
TOTAL NUMBER OF REGIONS		= 1127

TABLE 3-8

AREA DISTRIBUTIONS FOR RECOGNIZED REGIONS IN THE
REAL AND PSEUDO-IMAGES OF THE 9.3-11.7 μm CHANNEL OF FLINT-1.

THRESHOLD LEVEL = 3σ .

SQUARE METERS		FREQUENCY
0.0 TO	100.0	97
100.0 TO	200.0	1
200.0 TO	500.0	2
500.0 TO	1000.0	1
1000.0 TO	1500.0	0
1500.0 TO	2000.0	0
2000.0 TO	2500.0	0
2500.0 TO	3000.0	0
3000.0 TO	4000.0	1
4000.0 TO	5000.0	0
5000.0 TO	6000.0	0
6000.0 TO	8000.0	0
8000.0 TO	10000.0	0
10000.0 TO	15000.0	0
15000.0 TO	20000.0	0
20000.0 TO	40000.0	0
40000.0 TO	80000.0	0
80000.0 TO	160000.0	0
OVER 160000.0		0
TOTAL NUMBER OF REGIONS =		102

TABLE 3-9

AREA DISTRIBUTIONS FOR RECOGNIZED REGIONS IN THE
REAL AND PSEUDO-IMAGES OF THE 9.3-11.7 μm CHANNEL OF FLINT-1.

THRESHOLD LEVEL = 4σ .

SQUARE METERS		FREQUENCY
0.0 TO	100.0	6
100.0 TO	200.0	1
200.0 TO	500.0	0
500.0 TO	1000.0	1
1000.0 TO	1500.0	0
1500.0 TO	2000.0	1
2000.0 TO	2500.0	0
2500.0 TO	3000.0	0
3000.0 TO	4000.0	0
4000.0 TO	5000.0	0
5000.0 TO	6000.0	0
6000.0 TO	8000.0	0
8000.0 TO	10000.0	0
10000.0 TO	15000.0	0
15000.0 TO	20000.0	0
20000.0 TO	40000.0	0
40000.0 TO	80000.0	0
80000.0 TO	160000.0	0
OVER	160000.0	0
TOTAL NUMBER OF REGIONS		= 9

DISCUSSION OF RESULTS

The complete summary of statistical measures for the chosen background scenes are included as Appendix II of this report. Means, standard deviations, and spectral correlation coefficients are tabulated, and histograms for sub-areas of the scene as well as for the total scene are presented.

Some of the more obvious features follow expected patterns. For example, the mean values of radiances in the reflective near IR channels vary widely, due in part to the different background reflectivities in the different areas and in part to variation in solar elevation angles at the time the data were collected (giving some large shadowed areas). The Mill Creek data were collected early in the morning and the radiance levels are low and shadows clearly evident. The standard deviations are proportionately larger for this scene because of these shadows. In the thermal channel, 9.3-11.7 μm , the standard deviation about the mean temperature is smaller in the Mill Creek data than in other scenes as is expected early in the morning. The spectral correlation coefficients between pairs of near IR channel data are high in the Mill Creek data and low in the Baltimore data. This is indicative of a wide variety of materials in the Baltimore scene, some with reflectivities that increase and others that decrease with wavelength, and of the large shadowed areas and/or the predominance of materials in the Mill Creek scene that have the same relative spectral reflectance characteristics. The spectral correlations between the reflective and thermal IR channels are low as expected. A summary of these total area statistics is shown in Table 4-1.

The histogram data reveal the very non-Gaussian characteristics of most of the terrain backgrounds data. Especially notable is the wide distribution of the Mill Creek data with its large areas of shadow. Histograms derived from the multispectral scanner data of Mill Creek should vary dramatically during the diurnal cycle because of the topography

TABLE 4-1. TOTAL AREA DATA SUMMARY

Mean \pm standard deviation for reflective IR channels in $\mu\text{W}/\text{cm}^2 \cdot \text{sr} \cdot \mu\text{m}$ and in Kelvin for the thermal IR channel.

Spectral Band	FLINT-1		FLINT-2		BALTIMORE		MILL CREEK	
	1132 AM, Sept 18 Residential		1155, Sept 18 Industrial		1137, May 11 Residential		0733, June 30 Mountains	
1.0- 1.4 μm	1273 \pm 364		790 \pm 305		2133 \pm 778		112 \pm 62	
1.5- 1.8 μm	173 \pm 83		240 \pm 78		—		36 \pm 20	
2.0- 2.6 μm	36 \pm 10		39 \pm 14		78 \pm 44		4.2 \pm 2.9	
9.3-11.7 μm	294 \pm 3.1		297 \pm 3.2		299 \pm 5.9		298 \pm .97	
Spectral Correlations								
1.0-1.4, 1.5-1.8	0.392		0.718		—		0.835	
1.0-1.4, 2.0-2.6	0.303		0.489		0.084		0.869	
1.0-1.4, 9.3-11.7	-0.455		-0.437		—		0.052	
1.5-1.8, 2.0-2.6	0.603		0.634		—		0.880	
1.5-1.8, 9.3-11.7	0.048		-0.180		—		0.256	
2.0-2.6, 9.3-11.7	0.177		-0.036		—		0.245	

TABLE 4-1. TOTAL AREA DATA SUMMARY (Continued)

Spectral Band	BLACK HILLS-1	BLACK HILLS-2	PISGAH CRATER	MONO LAKE
	1340, July 22 Forested Mountains	1340, July 22 Forested Mountains	0822, Oct 30 Mountains	0952, Sept 23 Mountains
1.0- 1.4 μm	1799 \pm 618	1603 \pm 464	—	2053 \pm 334
1.5- 1.8 μm	—	447 \pm 155	—	—
2.0- 2.6 μm	106 \pm 55	91 \pm 39	—	95 \pm 17
4.5- 5.5 μm	295 \pm 2.3	—	—	286 \pm 1.3
8.0-13.5 μm	294 \pm 2.4	—	—	289 \pm 1.6
11.3-13.5 μm			290 \pm 2.9	
8.0-10.9 μm			289 \pm 2.5*	
9.4-12.1 μm			289 \pm 2.5*	
Spectral Correlations				
1.0-1.4, 1.5-1.8	—	0.743	—	—
1.0-1.4, 2.0-2.6	0.505	0.518	—	0.892
1.5-1.8, 2.0-2.6	—	0.908	—	—
1.0-1.4, 4.5-5.5	-0.166	—	—	0.833
2.0-2.6, 4.5-5.5	0.498	—	—	0.814
8.0-10.9, 9.4-12.1	—	—	0.811*	—

*Sub-area 2 data only

and this factor must be accounted for when using these backgrounds data for sensor performance estimates under conditions other than those for which the data were collected. The histograms for the various sub-areas of the Baltimore and Mill Creek scenes show the largest inhomogeneity of the background scenes analyzed.

The one-dimensional power spectra for the 1.0-1.4 and 9.3-11.7 μm data of Flint-1 and Mill Creek do not show any particularly unique or distinguishing characteristics, nor do the two-dimensional power spectra for the Flint-1 data. However, there are very pronounced differences in the spatial characteristics of these background scenes which may be important to the performance of a sensor in detecting or tracking a target against these backgrounds. The area/intensity statistics, that is the occurrence of equivalent elliptical areas representing contiguous regions of the background above a threshold, for Flint-1 and Mill Creek are quite distinctive. Especially noticeable in the thermal infrared are the warm roofs of houses, many of which exceed two standard deviations above the mean.

The area/intensity statistics do preserve many of the characteristics of background scenes that may cause false alarms in many sensor systems. The equivalent elliptical areas above each threshold setting, 1σ , 2σ , 3σ , and 4σ above the mean, can in most instances be identified with the specific spatial features they represent in the original image. A simulation of the actual scene with these equivalent elliptical areas was shown in Section 3. The utility of the area/intensity statistics will depend on whether or not the simulated scene adequately represents the actual scene for sensor performance estimates, and whether or not sensor performances depends specifically on the placement of these equivalent ellipses within the scene. This subject will be the basis for future terrain background statistical analyses.

SUMMARY AND RECOMMENDATIONS

Several terrain backgrounds were selected and statistics were derived for these backgrounds from calibrated multispectral scanner data. Conventional statistical parameters - means, standard deviations, histograms, spectral correlations, and power spectra - are reported. In addition a program has been initiated for developing statistical parameters of terrain backgrounds particularly relevant to the sensor designer's problem of detecting and tracking targets with low probability of false alarm or false track. These statistical parameters are the equivalent elliptical area/intensity statistics that have been reported.

It is intuitively obvious that these area/intensity statistics are approximations of what sensor system designers need to estimate systems performance characteristics. It is now necessary 1) to demonstrate that these statistics are adequate, i.e. that the performance of sensors against the actual background and against the simulated background is essentially the same and that the salient spatial features of the background have been preserved, and 2) to demonstrate that terrain backgrounds can be classified in some way, e.g. residential, industrial, mountainous, etc., so that the statistics can be inferred without recourse to actual measurement. Future backgrounds efforts should be directed to demonstrating the utility of the area/intensity statistics for terrain backgrounds and to expanding these efforts to include sky and cloud backgrounds.

PRECEDING PAGE BLANK-NOT FILMED

APPENDIX I

DETAILS OF CALIBRATION AND FIELD-OF-VIEW
AVERAGING PROCEDURES

APPENDIX I

DETAILS OF CALIBRATION AND FIELD-OF-VIEW
EQUALIZATION PROCEDURES

CALIBRATION OF SCANNER DATA

As discussed in Section 3.1, output from the ERIM scanners is in the form of digital tapes in which the data values are represented by integers ranging in value from 0 to 255. At the end of each scan line a set of calibration sources is scanned and the integers observed for these sources are used to calibrate the data in apparent radiance or temperature. The resulting calibrated tape also represents the data as integers but these integers are adjusted so that they are linear in radiance or temperature and a set of multiplicative and additive factors are used to convert these integer values to the appropriate units.

The calibration sources scanned once per scan line are: controllable temperature "hot" and "cold" plates; an ambient temperature plate; a visible-near-IR lamp; an ultraviolet lamp; and a sun sensor. The visible-reflective IR channels (approximately 0.4 μm to 3.0 μm) are generally calibrated in radiance using the visible-near-IR lamp as a radiance standard and the "ambient" plate as a dark level reference. If a linear relationship is assumed between radiance and detector output, the apparent radiance of the target (the radiance observed at the scanner aperture) is given by

$$L_T^a = \left(\frac{V_T - V_A}{V_L - V_A} \right) (L_L - L_A) + L_A \quad (\text{I-1})$$

where

V_T = The integer value observed for the target

V_A = The integer value observed for the ambient plate

V_L = The integer value observed for the lamp

L_{ℓ} = The radiance of the lamp at the center of the bandpass of the channel to be calibrated

L_A = The ambient radiance at the center of the bandpass of the channel to be calibrated

and L_T^a is the apparent radiance of the target which is related to the actual target radiance L_T as

$$L_T^a = L_T \tau_P + L_P \quad (I-2)$$

where τ_P is transmission of the intervening path and L_P the radiance of this path.

The lamp radiance L_{ℓ} in Equation I-1 is obtained from a calibration of the visible-near-IR lamp using an NBS standard lamp while the ambient radiance L_A is taken as the radiance of the ambient temperature plate with emissivity ϵ_A given by

$$L_A = \epsilon_A L_A^{BB} + (1 - \epsilon_A) L_A^{BB} \quad (I-3)$$

where the first term is the plate emittance and the second term the surrounding radiance reflected from this plate. Since the ambient temperature plate and its surroundings are at the same temperature, this equation simply gives L_A equal to L_A^{BB} or the radiance of a black-body at ambient temperature.

Equation I-1 is then written in terms of a "mult" and an "add" factor as

$$L_T^a = V_T \cdot \text{MULT} + \text{ADD} \quad (I-4)$$

where

$$\text{MULT} = W$$

$$\text{ADD} = L_A^{BB} - W V_A$$

and

$$W = (L_{\ell} - L_A^{BB}) / (V_{\ell} - V_A) \quad (I-5)$$

The computer program used for calibration initially averages the integer values (bin values) of the calibration sources for all scan lines in the image and outputs a mean and a standard deviation for them. If the standard deviations are small compared to the mean values the program allows for an "average" calibration in which the mean bin values of V_ℓ and V_A are used in Equations I-4 and I-5. In this case the integer data values on the calibrated tape are the same as those in the original tape; only "mult" and "add" factors are evaluated by the calibration procedure. However, if the standard deviations are not small compared to the means, indicating a drift in the system, a "line-by-line" calibration is required. For this type of calibration values of V_ℓ and V_A are taken from the calibration sources at the end of each scan line and these values used to determine "mult" and "add" factors from Equation I-5. These factors are then used to modify the integer data values of a given scan line so that only one "mult" and "add" factor is required for the total image. The single "mult" and "add" factors used are those determined from the mean V_ℓ , V_A values and the modified integer data value is taken as

$$V_T' = \frac{V_T \cdot \overline{MULT} + \overline{ADD} - \overline{ADD}}{\overline{MULT}} \quad (I-6)$$

where the average factors are \overline{MULT} and \overline{ADD} , those determined for each line are $MULT$ and ADD , and V_T' is the modified integer data value.

The long wavelength IR channels ($\lambda > 3.0 \mu\text{m}$) are calibrated in temperature and require a somewhat more involved calibration procedure. Since the detector output is proportional to radiance and not temperature, the first step in the process is to relate bin value (integer data value) to radiance, as in the reflective IR channels, using the "cold" plate as a dark level reference, the "hot" plate as a radiance standard, and the "ambient" plate to correct for ambient radiation levels. If a linear relationship is again assumed between detector output and radiance the apparent target radiance is given by an equation identical to I-1 except that the ambient radiance (L_A) and bin value (V_A) are replaced

by those for the "cold" plate (L_C , V_C) and the lamp radiance (L_ℓ) and bin value (V_ℓ) are replaced by those for the "hot" plate (L_H , V_H):

$$L_T^a = L_C + \left(\frac{V_T - V_C}{V_H - V_C} \right) (L_H - L_C) \quad (I-7)$$

In this case however the "hot" plate radiance is given by

$$L_H = \epsilon_H L_H^{BB} + (1 - \epsilon_H) L_A^{BB} \quad (I-8)$$

where ϵ_H is the emissivity of the "hot" plate, L_H^{BB} the radiance of a blackbody at the same temperature as the "hot" plate, and L_A^{BB} the ambient blackbody radiance. Similarly, the "cold" plate radiance is given by

$$L_C = \epsilon_C L_C^{BB} + (1 - \epsilon_C) L_A^{BB} \quad (I-9)$$

In both of these expressions the first term is the radiance emitted by the plate while the second term is the ambient radiance reflected by the plate.

Substitution of Equations I-8 and I-9 into I-7 and taking the plate emissivities equal gives

$$L_T^a = \left[\epsilon L_C^{BB} + (1 - \epsilon) L_A^{BB} \right] + \left(\frac{V_S - V_C}{V_H - V_C} \right) \left[\epsilon (L_H^{BB} - L_C^{BB}) \right] \quad (I-10)$$

This equation could be used for calibration but the ambient radiance L_A^{BB} would have to be calculated from ambient temperature measurements. This may be avoided by again assuming linearity of the detectors and taking

$$L_A^{BB} = L_C + \left(\frac{V_A - V_C}{V_H - V_C} \right) (L_H - L_C) \quad (I-11)$$

as for L_T^a in Equation I-7. Substituting Equations I-8 and I-9 into this expression it is found that many of the terms cancel and the ambient

radiance is given by

$$L_A^{BB} = L_C^{BB} + \left(\frac{V_A - V_C}{V_H - V_C} \right) (L_H^{BB} - L_C^{BB}) \quad (I-12)$$

where all radiances are now blackbody radiances evaluated at the plate temperatures. Making a final substitution of Equation I-12 into Equation I-10 and rearranging terms gives

$$L_T^a = L_C^{BB} + W [(1 - \epsilon)V_A - V_C] + \epsilon W V_T \quad (I-13)$$

where

$$W = \left(\frac{L_H^{BB} - L_C^{BB}}{V_H - V_C} \right) \quad (I-14)$$

Equation I-13 then relates the data bin values (V_T) to radiance and a second transformation is required to convert these values to temperature.

The computations required to convert radiance to temperature have been minimized by noting that the radiance values are bounded; the minimum value being given by $V_T = 0$ and the maximum by $V_T = 255$. Using this fact a table of temperature versus radiance is constructed, as shown in Table I-1, by integrating the Planck function over the bandpass of the channel to be calibrated choosing a range of temperatures sufficient to cover the entire radiance range. The temperature increments in this table are taken small enough ($\sim 1^\circ\text{C}$) so that interpolation may be used to form an array of temperature versus data bin value $T(V_T)$ for all possible bin values. It is this array which is then used to directly convert the uncalibrated data values to temperature.

Unlike the radiance data, the integer values appearing in the calibrated images for the thermal channels are never the same as those of the original image since the calibrated values are now proportional to temperature not radiance. This new set of integer data values is scaled from 0 to 255 using

TABLE I-1a. TABLE OF BLACKBODY RADIANCE vs TEMPERATURE IN THE 4.5 - 5.5 μ m BAND

TEMPERATURE (DEG K)	RADIANCE (μ W/CM ² /STR)	TEMPERATURE (DEG K)	RADIANCE (μ W/CM ² /STR)	TEMPERATURE (DEG K)	RADIANCE (μ W/CM ² /STR)
245.	3.1552E+01	272.	9.9325E+01	299.	2.5496E+02
246.	3.3067E+01	273.	1.0310E+02	300.	2.6318E+02
247.	2.4601E+01	274.	1.0718E+02	301.	2.7160E+02
248.	3.5277E+01	275.	1.1120E+02	302.	2.8023E+02
249.	3.7976E+01	276.	1.1535E+02	303.	2.8908E+02
250.	3.9701E+01	277.	1.1969E+02	304.	2.9815E+02
251.	4.1572E+01	278.	1.2430E+02	305.	3.0744E+02
252.	4.3473E+01	279.	1.2903E+02	306.	3.1696E+02
253.	4.5405E+01	280.	1.3380E+02	307.	3.2671E+02
254.	4.7400E+01	281.	1.3872E+02	308.	3.3670E+02
255.	4.9410E+01	282.	1.4378E+02	309.	3.4692E+02
256.	5.1409E+01	283.	1.4894E+02	310.	3.5739E+02
257.	5.3405E+01	284.	1.5434E+02	311.	3.6816E+02
258.	5.5400E+01	285.	1.5985E+02	312.	3.7906E+02
259.	5.7386E+01	286.	1.6552E+02	313.	3.9028E+02
260.	5.9381E+01	287.	1.7135E+02	314.	4.0175E+02
261.	6.1381E+01	288.	1.7734E+02	315.	4.1340E+02
262.	6.3388E+01	289.	1.8349E+02	316.	4.2545E+02
263.	6.5395E+01	290.	1.8982E+02	317.	4.3777E+02
264.	6.7403E+01	291.	1.9632E+02	318.	4.5032E+02
265.	6.9410E+01	292.	2.0300E+02	319.	4.6315E+02
266.	7.1420E+01	293.	2.0985E+02	320.	4.7625E+02
267.	7.3436E+01	294.	2.1689E+02	321.	4.8966E+02
268.	7.5451E+01	295.	2.2412E+02	322.	5.0335E+02
269.	7.7466E+01	296.	2.3154E+02	323.	5.1733E+02
270.	7.9481E+01	297.	2.3915E+02	324.	5.3162E+02
271.	8.1496E+01	298.	2.4696E+02	325.	5.4621E+02

TABLE I-1b. TABLE OF BLACKBODY RADIANCE VS TEMPERATURE IN THE 9.3 - 11.7 μ m BAND

TEMPERATURE (DEG K)	RADIANCE (μ W/CM ² /STR)	TEMPERATURE (DEG K)	RADIANCE (μ W/CM ² /STR)	TEMPERATURE (DEG K)	RADIANCE (μ W/CM ² /STR)
245.	8.2666E+02	272.	1.4466E+03	299.	2.2937E+03
246.	8.4578E+02	273.	1.4738E+03	300.	2.3294E+03
247.	8.6518E+02	274.	1.5013E+03	301.	2.3658E+03
248.	8.8487E+02	275.	1.5292E+03	302.	2.4023E+03
249.	9.0484E+02	276.	1.5574E+03	303.	2.4392E+03
250.	9.2511E+02	277.	1.5859E+03	304.	2.4764E+03
251.	9.4567E+02	278.	1.6147E+03	305.	2.5139E+03
252.	9.6652E+02	279.	1.6438E+03	306.	2.5517E+03
253.	9.8766E+02	280.	1.6733E+03	307.	2.5899E+03
254.	1.0091E+03	281.	1.7030E+03	308.	2.6284E+03
255.	1.0308E+03	282.	1.7331E+03	309.	2.6672E+03
256.	1.0529E+03	283.	1.7635E+03	310.	2.7064E+03
257.	1.0752E+03	284.	1.7942E+03	311.	2.7459E+03
258.	1.0978E+03	285.	1.8253E+03	312.	2.7857E+03
259.	1.1207E+03	286.	1.8566E+03	313.	2.8254E+03
260.	1.1440E+03	287.	1.8883E+03	314.	2.8663E+03
261.	1.1675E+03	288.	1.9203E+03	315.	2.9070E+03
262.	1.1913E+03	289.	1.9526E+03	316.	2.9482E+03
263.	1.2155E+03	290.	1.9853E+03	317.	2.9894E+03
264.	1.2399E+03	291.	2.0182E+03	318.	3.0314E+03
265.	1.2647E+03	292.	2.0515E+03	319.	3.0734E+03
266.	1.2897E+03	293.	2.0852E+03	320.	3.1150E+03
267.	1.3151E+03	294.	2.1191E+03	321.	3.1586E+03
268.	1.3408E+03	295.	2.1534E+03	322.	3.2017E+03
269.	1.3667E+03	296.	2.1879E+03	323.	3.2450E+03
270.	1.3930E+03	297.	2.2229E+03	324.	3.2888E+03
271.	1.4196E+03	298.	2.2581E+03	325.	3.3328E+03

TABLE I-1c. TABLE OF BLACKBODY RADIANCE vs TEMPERATURE IN THE 8.0-13.5 μ m BAND

TEMPERATURE (DEG K)	RADIANCE (μ W/CM ² /STR)	TEMPERATURE (DEG K)	RADIANCE (μ W/CM ² /STR)	TEMPERATURE (DEG K)	RADIANCE (μ W/CM ² /STR)
245.	1.8275E+03	272.	3.1775E+03	299.	5.0315E+03
246.	1.8691E+03	273.	3.2369E+03	300.	5.1103E+03
247.	1.9113E+03	274.	3.2970E+03	301.	5.1899E+03
248.	1.9541E+03	275.	3.3578E+03	302.	5.2702E+03
249.	1.9975E+03	276.	3.4194E+03	303.	5.3512E+03
250.	2.0416E+03	277.	3.4816E+03	304.	5.4330E+03
251.	2.0864E+03	278.	3.5445E+03	305.	5.5155E+03
252.	2.1317E+03	279.	3.6081E+03	306.	5.5987E+03
253.	2.1777E+03	280.	3.6725E+03	307.	5.6827E+03
254.	2.2244E+03	281.	3.7375E+03	308.	5.7675E+03
255.	2.2717E+03	282.	3.8033E+03	309.	5.8529E+03
256.	2.3196E+03	283.	3.8697E+03	310.	5.9391E+03
257.	2.3682E+03	284.	3.9369E+03	311.	6.0261E+03
258.	2.4175E+03	285.	4.0049E+03	312.	6.1138E+03
259.	2.4675E+03	286.	4.0734E+03	313.	6.2023E+03
260.	2.5179E+03	287.	4.1428E+03	314.	6.2915E+03
261.	2.5692E+03	288.	4.2128E+03	315.	6.3814E+03
262.	2.6211E+03	289.	4.2836E+03	316.	6.4721E+03
263.	2.6737E+03	290.	4.3551E+03	317.	6.5636E+03
264.	2.7269E+03	291.	4.4274E+03	318.	6.6557E+03
265.	2.7809E+03	292.	4.5003E+03	319.	6.7487E+03
266.	2.8355E+03	293.	4.5740E+03	320.	6.8424E+03
267.	2.8908E+03	294.	4.6484E+03	321.	6.9368E+03
268.	2.9467E+03	295.	4.7236E+03	322.	7.0320E+03
269.	3.0034E+03	296.	4.7995E+03	323.	7.1279E+03
270.	3.0607E+03	297.	4.8761E+03	324.	7.2246E+03
271.	3.1188E+03	298.	4.9534E+03	325.	7.3220E+03

$$N = \frac{T(V_T) - T(0)}{T(255) - T(0)} \quad 255 \quad (I-15)$$

where T is the temperature versus bin value array with $T(V_T)$ equal to the temperature corresponding to bin value V_T . The "mult" and "add" factors for the thermal channels are then taken as

$$\text{MULT} = \frac{T(255) - T(0)}{255} \quad (I-16)$$

$$\text{ADD} = T(0)$$

The calibration program allows for "average" or "line-by-line" calibration of the thermal channels as it did for the reflective IR channels. Because of the amount of computation required to set up the temperature versus bin value array, only one such array is generated using the scene average values of V_C , V_A , and V_H in Equation I-13. If an "average" calibration is used this array directly relates data bin values (V_T) to temperature and Equation I-15 is used directly. However, if a "line-by-line" calibration is required the data bin values must be modified so that I-13, using scene average values of V_C , V_A , and V_H , gives the correct radiance. The modification of the data bin values is done in the same way as for the reflective IR channels using Equation I-6. In this case the "mult" factors are given by ϵW or $\epsilon \bar{W}$ and the "add" factors by the first two terms of Equation I-13 or

$$\text{ADD} = L_C^{BB} + W [(1 - \epsilon) V_A - V_C]$$

$$\bar{\text{ADD}} = L_C^{BB} + \bar{W} [(1 - \epsilon) \bar{V}_A - \bar{V}_C]$$

To avoid round-off errors the values determined from I-6 are not rounded to the nearest integer but taken as floating point numbers and interpolation in the $T(V_T)$ array is used to determine the temperature. This temperature is then used in place of $T(V_T)$ in Equation I-15 to evaluate the calibrated integer value.

In a typical data set both thermal and reflective IR channels are present so that both of the above procedures are used in generating a calibrated image tape.

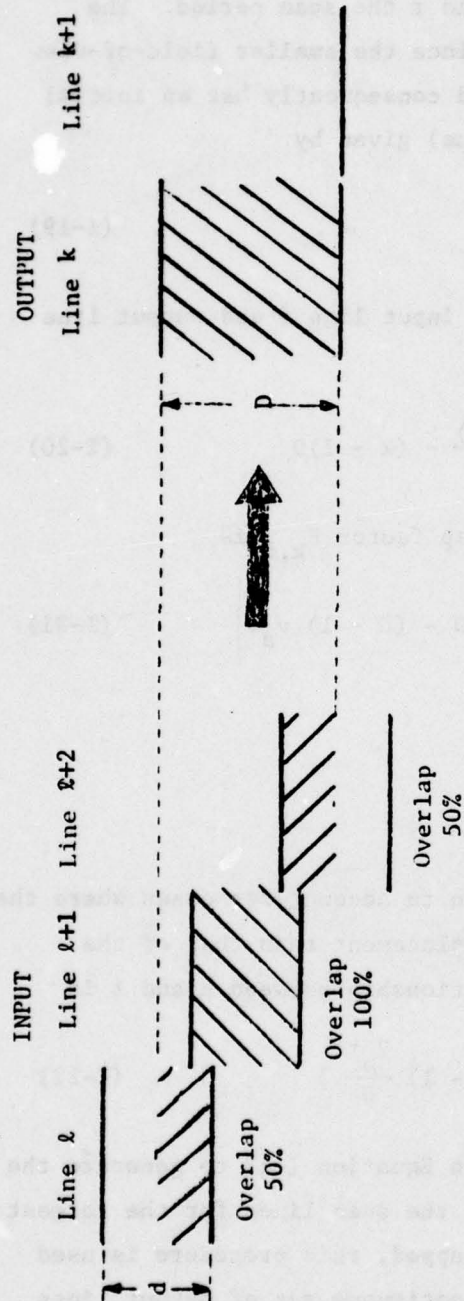
CORRECTIONS FOR OVERLAP AND UNEQUAL FIELDS-OF-VIEW

Since the detectors used in the various channels (wavelength regions) vary in size and consequently in instantaneous field-of-view, direct comparisons of the channels is not possible unless the fields-of-view are normalized in some fashion. A second, although less critical, problem is that depending on the aircraft altitude, scan lines and/or pixels may be highly overlapped resulting in oversampling of the scene. Both of these problems were corrected at the time the data was calibrated by averaging the scan lines (and/or pixels) of the smaller field-of-view channels and generating an equivalent scan line (and/or pixel) with a field-of-view equal to the largest field-of-view. This procedure must be carried out separately for scan lines and pixels within a scan line since the fields-of-view and the data taking rates are different in these two dimensions. In the following discussion only scan line averaging will be discussed since pixel averaging is completely analogous.

As outlined in Section 3.1, the averaging procedure consists of setting up a set of contiguous output lines with a field-of-view equal to the largest field-of-view (D) and then combining the smaller field-of-view (d) scan lines to generate equivalent lines with fields-of-view D. As shown in Figure I-1, the combining of scan lines is accomplished using a weighted average given by

$$V_k = \frac{\sum_{\ell} F_{k,\ell} V_{\ell}}{\sum_{\ell} F_{k,\ell}} \quad (I-17)$$

where V_k is the k^{th} output line data value for a given pixel, V_{ℓ} the ℓ^{th} input line data value for the same pixel, and $F_{k,\ell}$ the overlap between input line ℓ and output line k . Since the overlap will be non-zero only for a small number of lines about the output line, $F_{k,\ell}$ need only be calculated for a few values of ℓ . A general expression for the overlap was determined by considering the displacements of the scan lines from the beginning of the scene. The displacement to the bottom of input scan line ℓ is given by



$$\text{Output Line } k = \{0.5 (\text{Input Line } l) + 1.0 (\text{Input Line } l+1) + 0.5 (\text{Input Line } l+2)\} / 2.0$$

FIGURE I-1 SCHEMATIC REPRESENTATION OF THE PROCEDURES USED FOR SCAN LINE AVERAGING

$$(\ell - 1) v_a \tau + \frac{(D + d)}{2} \quad (I-18)$$

where v_a is the aircraft ground velocity and τ the scan period. The second term in this equation is included since the smaller field-of-view (d) is concentric with D in scan line 1 and consequently has an initial displacement (to the bottom of the scan line) given by

$$D - \frac{(D - d)}{2} = \frac{(D + d)}{2} \quad (I-19)$$

As shown in Figure I-2 the overlap between input line ℓ and output line k is then given by

$$\gamma = (\ell - 1)v_a \tau + \frac{(D + d)}{2} - (k - 1)D \quad (I-20)$$

so that the percent overlap (γ/d) or overlap factor $F_{k,\ell}$ is

$$F_{k,\ell} = \frac{1}{2} \left[1 + \frac{D}{d} \right] - \frac{1}{d} \left| (k - 1)D - (\ell - 1)v_a \tau \right| \quad (I-21)$$

with the constraints

$$F_{k,\ell} \rightarrow 1 \text{ if } F_{k,\ell} \geq 1$$

$$F_{k,\ell} \rightarrow 0 \text{ if } F_{k,\ell} \leq 0$$

The absolute value appears in this equation to account for cases where the bottom of the input line has a greater displacement than that of the output line. It may be seen that the relationship between k and ℓ is

$$(k - 1) = \text{Integer value of } \left[(\ell - 1) \frac{v_a \tau}{D} \right] \quad (I-22)$$

These overlap factors are then used in Equation I-17 to generate the equivalent output lines. Since in general the scan lines for the largest field-of-view channel are themselves overlapped, this procedure is used to average these lines as well so that a contiguous set of output lines is obtained in all channels. In this case, the same equations are used but d is equal to D .

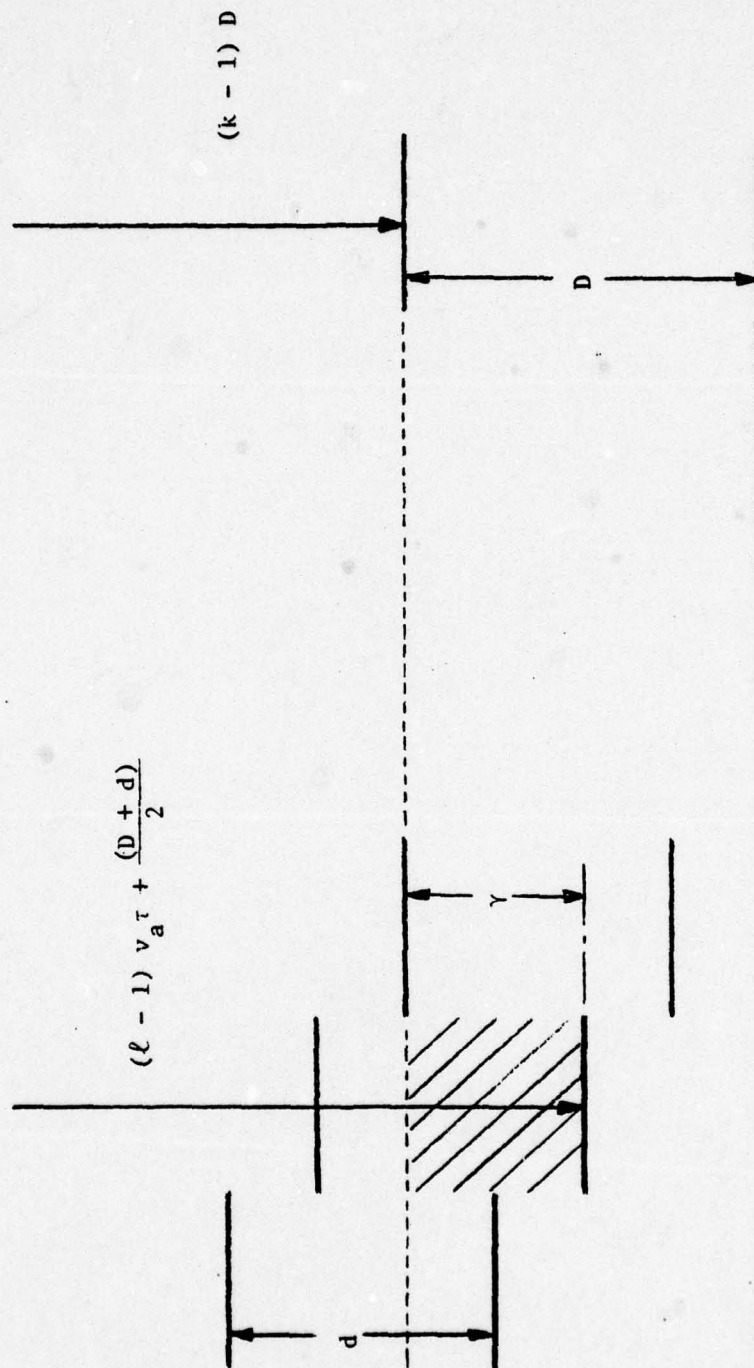


FIGURE I-2 SCHEMATIC OF DISPLACEMENTS USED TO DERIVE THE OVERLAP FACTORS F_k, ℓ

PRECEDING PAGE BLANK-NOT FILMED

APPENDIX II

COMPLETE COMPILATION OF STATISTICAL DATA

APPENDIX II

COMPLETE COMPILATION OF STATISTICAL DATA

DISCUSSION OF FORMATS, SPECIFIC PROCEDURES, ANOMALIES AND LIMITATIONS

This appendix presents the statistics generated for all of the chosen scenes. It is broken down into two major sections, the first of which presents the mean values, standard deviations, spectral correlations, and histograms for each of the scenes, while the second section presents the area/intensity statistics and Wiener spectra computed for Flint-1 and Mill Creek. It is important to emphasize that the data presented here are only descriptive of the specific scenes for the specific conditions under which the imagery was collected and that generalizations to other background scenes, other background types or other conditions cannot be made without further data analysis and modeling. The primary purpose of this presentation is to familiarize the potential user of the data with what is and what can be made available to assist in systems analysis.

In the first section of this appendix, the statistics for each scene are preceded by (1) maps showing the regions covered, (2) line-scan images for each of the wavelength bands generated from the scanner data, and (3) a visual image showing the subareas defined for statistics generation. The histograms for the subareas, total area, and calibration sources of each scene are presented in graphical form but tabulations of the data used to generate these plots are available at ERIM for quantitative analysis. Histograms of the calibration sources have been included for two reasons:

- (1) To indicate the range of possible data values so saturation problems may be identified, and
- (2) To indicate the distribution of calibration source values and hence the possible uncertainty associated with the radiance or temperature calibrations.

Histograms of the calibration sources are not presented for the 9.3-11.7 μm Baltimore data, the 1.0-1.4 and 2.0-2.6 μm Black Hills-1 data,

and the 1.0-1.4 and 2.0-2.6 μm Mono Lake data. Only the position of the calibration signal used is shown. The Baltimore data were processed before the calibration histogram capability was developed, and the Black Hills-1 and Mono Lake calibration histograms are not shown because the calibration was inferred from other data as discussed later.

Each of the calibration source histograms is presented with dual abscissa units: the recorded integer data value (bin number) and the calibrated radiance or temperature. Since the data is collected as positive 8-bit integers, this data is constrained to the range 0 to 255 with negative data points being given the value zero and points with values greater than 255 being given the value 255. Consequently, if the wings of a given data distribution show the presence of scene elements with calibrated data values corresponding to a bin value of zero or 255, it must be assumed that these points are saturated and that the actual scene contained values outside the 0 - 255 range. Cases where 255 saturation are in evidence are in the Flint-2 2.0-2.6 μm channel, the Mill Creek 1.5-1.8 and 2.0-2.6 μm channels, the Black Hills-1 2.0-2.6 μm channel, and the Black Hills-2 1.5-1.8 μm channel. Zero saturations were found in the Baltimore 9.3-11.7 μm channel.

The histograms of the calibration sources cannot be used to directly infer the influence of system noise on the distribution of scene data values. This is the case since in many instances the spread of calibration source values is due to a cyclical variation or a drift of the source throughout the scene which is corrected for using the line-by-line calibration procedures discussed in Section 3. No attempt has been made at the present time to determine the degree to which these line-by-line procedures completely removed these cyclical or drift variations during calibration.

A few comments regarding the data appearing in the first section of this appendix are in order:

- (1) Each of the histograms for the subareas and total area are independently normalized by assigning a relative frequency of unity to the data value appearing most frequently in the

scene. As a result, if 255 saturations occur and a large enough number of points have this value, the histogram may never reach unity except for the spike appearing at 255. This is in evidence in the histogram of the 2.0-2.6 μm channel of Flint-2 data.

- (2) In addition to the digital saturations discussed earlier, some of the data histograms show an anomalously large number of data points at the high end of the distribution which are not digitally saturated. In the cases where this has been identified, it was found to be due to analog saturation in the aircraft recording system, and hence is not indicative of the true scene distribution. Cases where this has been observed are the Flint-1 9.3-11.7 μm channel around data value 308K, the Black Hills-1 4.5-5.5 μm channel near data value 307K, and the Black Hills-2 2.0-2.6 μm channel near data value 280 $\mu\text{W}/\text{cm}^2 \cdot \text{sr} \cdot \mu\text{m}$).
- (3) In the 9.3-11.7 μm channels of Flint-1, Flint-2, and Mill Creek, as well as the 11.3-13.5, 8.0-10.9, and 9.4-12.1 μm channels of Pisgah Crater, some spikes appear in the data histograms. These are the results of the analog-to-digital conversion process in which certain data values are digitized as the next higher or lower integer value. This digitization error is not important as it is an error in magnitude of only a few tenths degree Kelvin. These are not seen in the imagery since these data values appear randomly throughout the scene but they do appear in the histograms.

As discussed elsewhere in this report^{*}, the computer code developed for data calibration was equipped to do three different types of calibration:

^{*}See Section 3 and Appendix I.

- (1) An average calibration in which the average bin values of the calibration sources for the whole scene are used;
- (2) A line-by-line dark level correction in which the dark level value of each scan line is used in conjunction with average values for the other calibration sources; and
- (3) A line-by-line calibration in which the bin values of all calibration sources taken from the individual scan lines are used.

In general, an average calibration was used when the calibration sources were reasonably constant throughout the scene so that their average bin values had small standard deviations, while a line-by-line procedure was used when the calibration sources showed cyclical variations or drifts. Of the two possible line-by-line procedures, a dark level correction (2) was used if only the dark level varied, while a complete line-by-line calibration (3) was used if any or all of the other calibration sources showed variation. However, in its present form, the computer code is constrained to use the same type of calibration on all channels calibrated in radiance and a separate type for all channels calibrated in temperature. Consequently, if any of the radiance (or temperature) channels required a line-by-line calibration, the remainder of the radiance (or temperature) channels had to be similarly calibrated.

To assist in determining the calibration procedure required for each scene, three types of data displays have been used:

- (1) Histograms of the calibration sources for the total scene to determine mean values and standard deviations (Figure II-1);
- (2) "A"-scope traces of several full scan lines to determine line-to-line variations and to see if variations in the video portion of the scan followed those in the calibration sources (Figure II-2); and,
- (3) Time history traces of the calibration sources to observe source drifts or cyclical variations (Figure II-3).

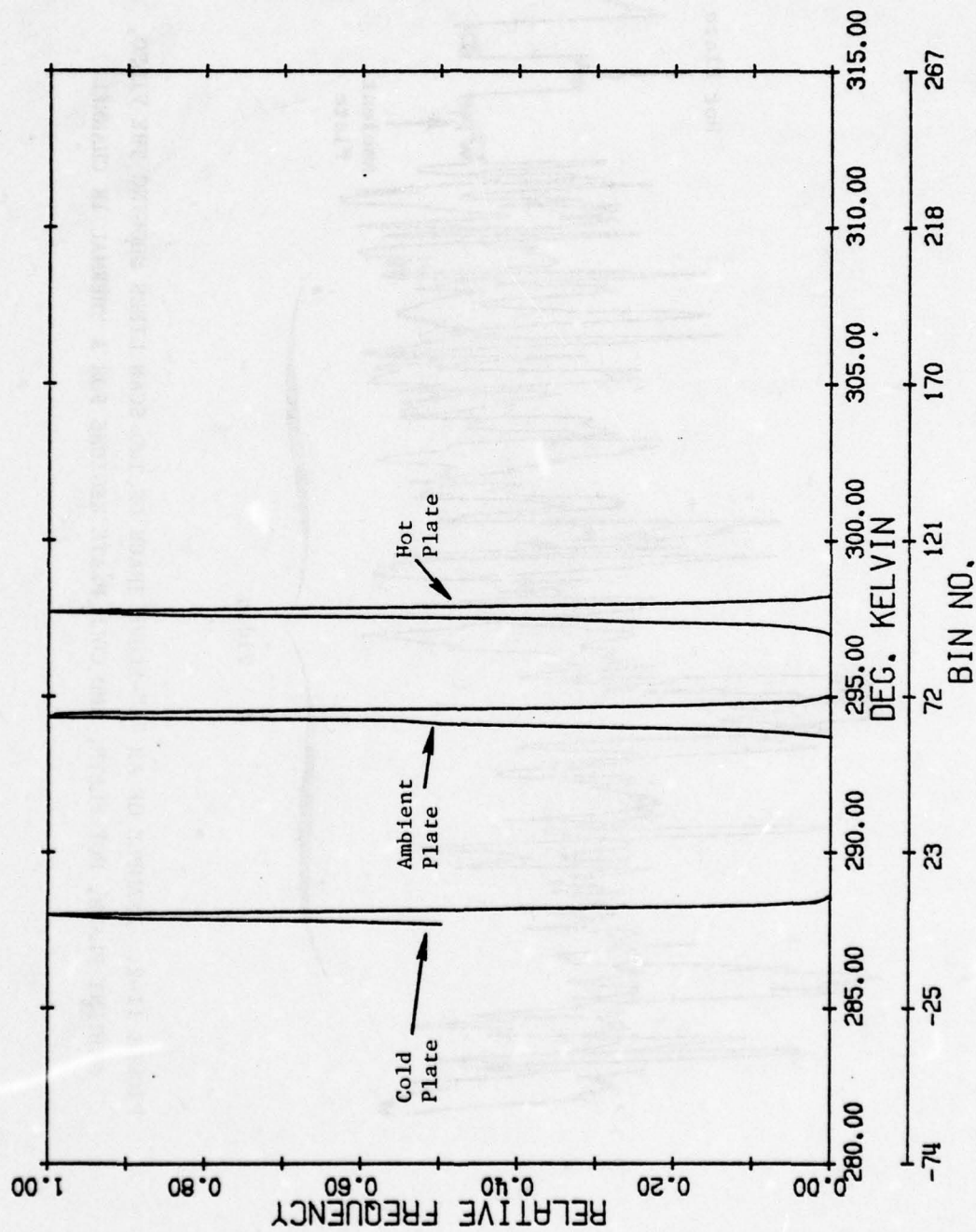


FIGURE II-1. EXAMPLE OF CALIBRATION SOURCE HISTOGRAMS FOR A THERMAL IR CHANNEL SHOWING THE COLD, AMBIENT, AND HOT PLATE DISTRIBUTIONS

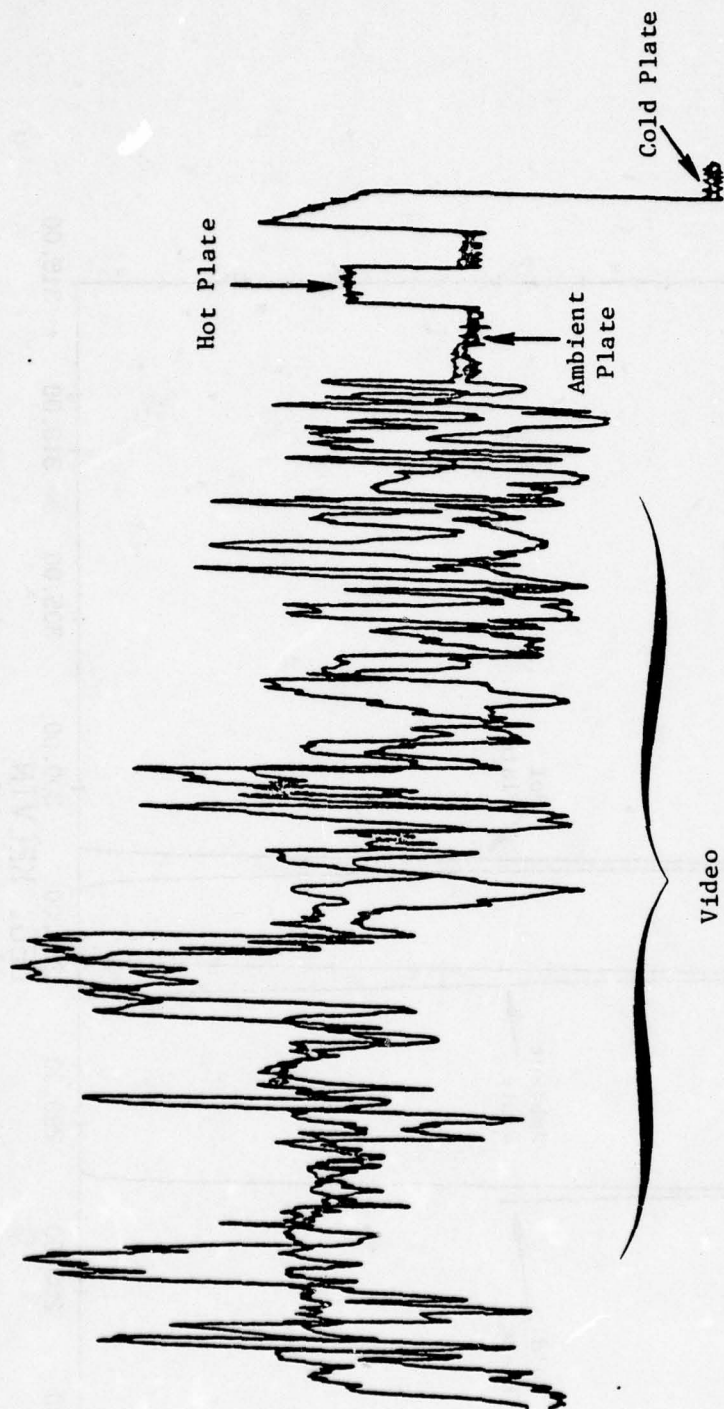


FIGURE II-2. EXAMPLE OF AN "A"-SCOPE TRACE OF TWO SCAN LINES SHOWING THE VIDEO, AMBIENT PLATE, HOT PLATE, AND COLD PLATE REGIONS FOR A THERMAL IR CHANNEL.

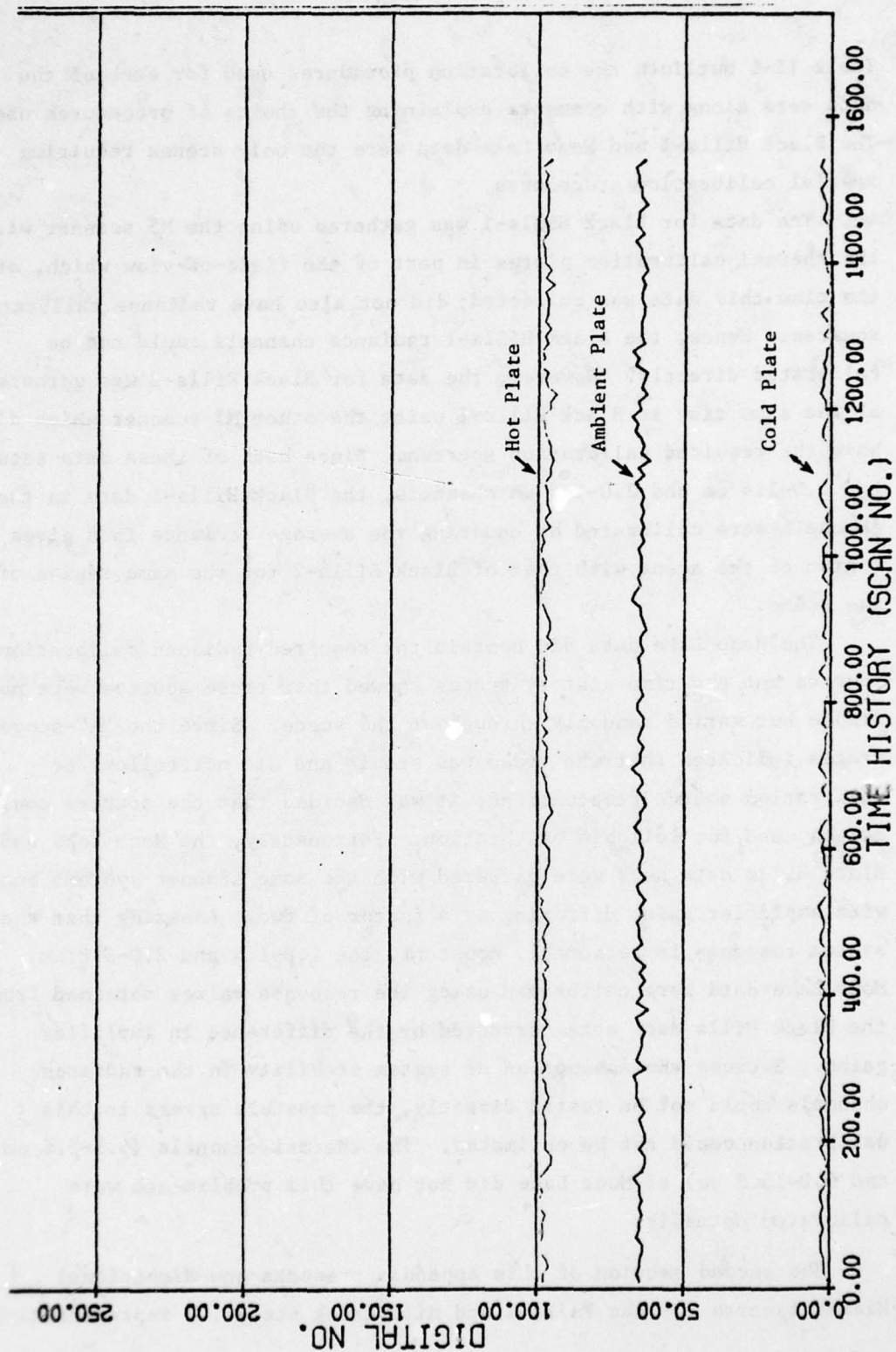


FIGURE 11-3. EXAMPLES OF TIME HISTORY TRACES OF THE COLD, AMBIENT, AND HOT PLATE DATA VALUES FOR A THERMAL IR CHANNEL

Table II-1 outlines the calibration procedures used for each of the data sets along with comments explaining the choice of procedures used. The Black Hills-1 and Mono Lake data were the only scenes requiring special calibration procedures.

The data for Black Hills-1 was gathered using the M5 scanner with the thermal calibration plates in part of the field-of-view which, at the time this data was collected, did not also have radiance calibration sources. Hence, the Black Hills-1 radiance channels could not be calibrated directly. However, the data for Black Hills-2 was gathered at the same time as Black Hills-1 using the other M5 scanner which did have the required calibration sources. Since both of these data sets had 1.0-1.4 μm and 2.0-2.6 μm channels, the Black Hills-1 data in these channels were calibrated by equating the average radiance in a given region of the scene with that of Black Hills-2 for the same region of the scene.

The Mono Lake data did contain the required radiance calibration sources but the time history traces showed that these sources were not stable but varied randomly throughout the scene. Since the "A"-scope traces indicated that the video was stable and did not follow the calibration source fluctuations, it was decided that the sources could not be used for reliable calibration. Fortunately, the Mono Lake and Black Hills data sets were gathered with the same scanner systems but with amplifier gains differing by a factor of two. Assuming that the system response is reasonably constant, the 1.0-1.4 and 2.0-2.6 μm Mono Lake data were calibrated using the response values obtained from the Black Hills data sets corrected by the difference in amplifier gains. Because the assumption of system stability in the radiance channels could not be tested directly, the possible errors in this calibration could not be estimated. The thermal channels (4.5-5.6 μm and 8.0-13.5 μm) of Mono Lake did not have this problem and were calibrated normally.

The second section of this appendix presents one-dimensional Wiener spectra for the Flint-1 and Mill Creek scenes, a representative

TABLE II-1. CALIBRATION PROCEDURES USED FOR THE VARIOUS BACKGROUND SCENES

Scene (Scanner)	Calibration Used Radiance Channels Temperature Channels	Comments
Flint-1 (M7)	Line-by-line Average	Line-by-line required because of cyclical variations in the 2.0-2.6 μ m channel calibration sources.
Flint-2 (M7)	Line-by-line Average	Line-by-line required because of cyclical variations in the 1.5-1.8 μ m and 2.0-2.6 μ m channel calibration sources.
Baltimore (M7)	Average Average	Thermal 9.3 - 11.7 μ m channel run separately, consequently not in registration with radiance channels.
Mill Creek (M7)	Average Average	---
Black Hills-2 (M5)	(See Text) Line-by-line	No lamp present for calibration of radiance channels. These were calibrated using corresponding channels in Black Hills-2. Thermal channel calibration sources had cyclical variation requiring line-by-line calibration. The 8-13.5 μ m channel is not spatially registered with the 1-1.4, 2-2.6, and 4.5-5.5 μ m channels.
Black Hills-2 (M5)	Average ---	---
Pisgah Crater (M5)	--- Average	No field-of-view averaging was used. The 11.3-13.5 μ m channel is not spatially registered with the 8-10.9 and 9.4-12.1 μ m.
Mono Lake (M5)	(See Text) Average	Radiance channel calibration sources very noisy. Calibration done using Black Hills-2 data since both sets collected with same scanner and equipment. The 8-13.5 μ m channel is not spatially registered with the 1-1.4, 2-2.6, and 4.5-5.5 μ m channels.

two-dimensional Wiener spectrum for the 9.3-11.7 μm band of Flint-1, and area/intensity statistics for the 1.0-1.4 μm and 9.3-11.7 μm bands of Flint-1 and Mill Creek.

Included with the one-dimensional Wiener spectra for Flint-1 are spectra of the dark level (ambient or cold calibration source) since these plots indicate that the feature at 0.5 cycles/meter is not a scene feature but a spatial frequency generated by the scanner itself. The area/intensity statistics are presented in two forms: plots of the equivalent elliptical areas for each threshold and tabulations of these areas as sorted by geometric area, perimeter, and shape factor. These latter tabulations are broken down into coarse increments, only to cover a large enough range to be generally applicable; these increments are not indicative of the resolution of the system and tabulations with much finer increments may be generated as required.

Calibrated data tapes for each of the scenes presented have been prepared and are available for additional processing as the need for additional statistics becomes apparent.

MEAN VALUES, STANDARD DEVIATIONS, SPECTRAL
CORRELATIONS, AND HISTOGRAMS FOR THE SUB-
AREAS AND TOTAL AREAS OF THE CHOSEN BACK-
GROUND SCENES

FLINT-1*

Scene Type	Residential
Date of Flight	18 September 1971
Time of Flight	1132 - 1133
Altitude (Ft)	1000
No. of Sub-Areas	6
No. of Data Points	514,065

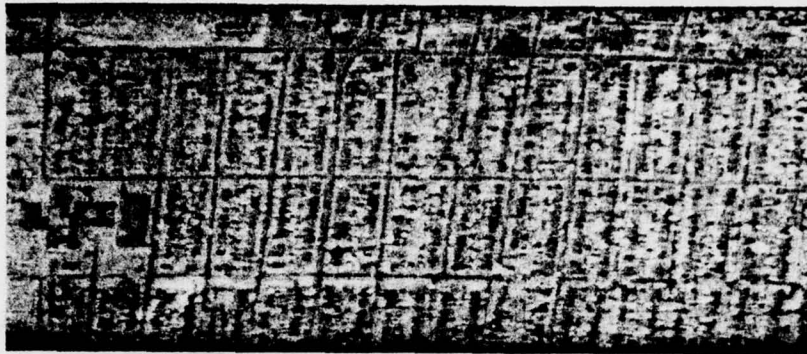
Channels	2	3	4	5
Wavelength (μm)	1.0-1.4	1.5-1.8	2.0-2.6	9.3-11.7
Resolution (mr)				
In-Track	5.0	5.0	5.0	5.0
Cross-Track	2.5	2.5	2.5	2.9
Nadir Pixel Dimensions (m)				
In-Track	1.524	1.524	1.524	1.524
Cross-Track	0.762	0.762	0.762	0.884
Nadir Ground Sample Distance (m)				
In-Track	1.524	1.524	1.524	1.524
Cross-Track	0.762	0.762	0.762	0.762

Line Averaging used on ALL channels.

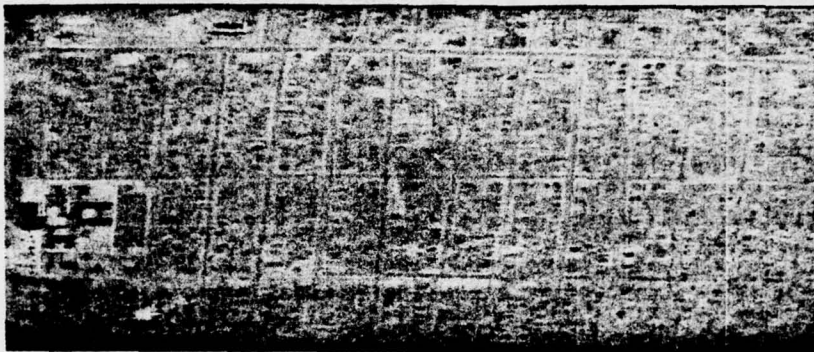
*These data were obtained with the M-7 scanner. All data are in spatial registration.



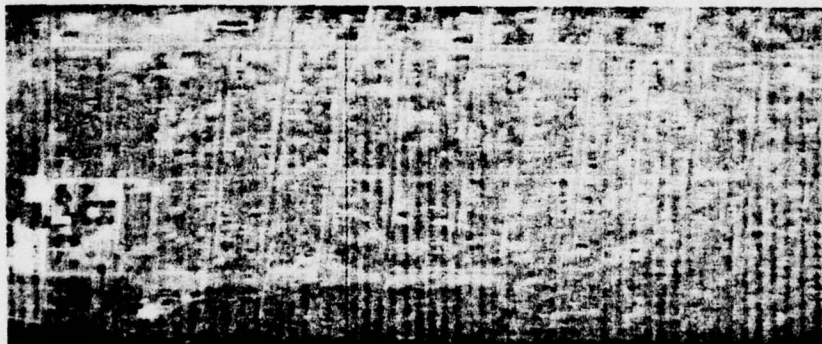
MAP OF THE FLINT AREA SHOWING THE REGION COVERED IN THE FLINT-1 RUN ABOUT FLIGHT LINE 28



1.0 - 1.4 μm



1.5 - 1.8 μm



2.0 - 2.6 μm



9.3 - 11.7 μm

LINE SCAN IMAGES PRODUCED FROM THE VARIOUS INFRARED CHANNEL OF FLINT-1



Pixel 1

Pixel 161

Pixel 484

Pixel 645

Line 10

Line 403

Line 806

SUB-AREAS DEFINED FOR STATISTICS GENERATION IN THE FLINT-1 IMAGE. Uneven areas were chosen so that Areas 2 and 5 covered the $\pm 20^\circ$ range suitable for correlation. Approximate scene dimensions are 3985 ft (1215 m) by 1612 ft (491 m). Each sub-area as well as the total area have been histogrammed. Histogram plots and their respective sub-areas are identified with the following key:

▣ Sub-area 1

+ Sub-area 4

○ Sub-area 2

× Sub-area 5

▲ Sub-area 3

◆ Sub-area 6

FLINT-1

SUB-AREA 1

CORRELATION	2	3	4	5
2	1.000			
3	0.493	1.000		
4	0.316	0.614	1.000	
5	0.468	0.020	0.132	1.000

CHANNELS	2	3	4	5
MEAN	1.2804E+03	2.3001E+02	4.1237E+01	2.9495E+02
ST. DEV.	3.4702E+02	7.7473E+01	1.0691E+01	2.6918E+00
TOTAL PIS.	63040.	63040.	63040.	63040.

FLINT-1

SUB-AREA 2

CORRELATION	2	3	4	5
2	1.000			
3	0.521	1.000		
4	0.313	0.715	1.000	
5	-0.482	-0.004	0.167	1.000

CHANNELS	2	3	4	5
MEAN	1.2757E+03	1.7978E+02	3.7621E+01	2.9495E+02
ST. DEV.	3.5471E+02	7.4411E+01	1.0746E+01	3.5245E+00
TOTAL PTS.	127262.	127262.	127262.	127262.

FLINT-1

SUB-AREA 3

CORRELATION	2	3	4	5
2	1.000			
3	0.724	1.000		
4	0.552	0.758	1.000	
5	-0.288	0.011	0.112	1.000

CHANNELS	2	3	4	5
MEAN	1.3056E+03	1.6356E+02	3.4348E+01	2.9379E+02
ST. DEV.	4.2441E+02	8.1826E+01	1.1244E+01	2.6476E+00
TOTAL PTS.	63828.	63828.	63828.	63828.

FLINT-1

SUB-AREA 4

CORRELATION	2	3	4	5
2	1.000			
3	0.266	1.000		
4	0.236	0.440	1.000	
5	-0.520	0.012	0.116	1.000

CHANNELS	2	3	4	5
MEAN	1.1905E+03	1.9209E+02	3.6268E+01	2.9499E+02
ST. DEV.	3.4131E+02	7.9889E+01	9.6634E+00	3.2649E+00
TOTAL PTS.	64480.	64480.	64480.	64480.

FLINT-1

SUB-AREA 5

CORRELATION	2	3	4	5
2	1.000			
3	0.228	1.000		
4	0.191	0.406	1.000	
5	-0.525	-0.017	0.149	1.000

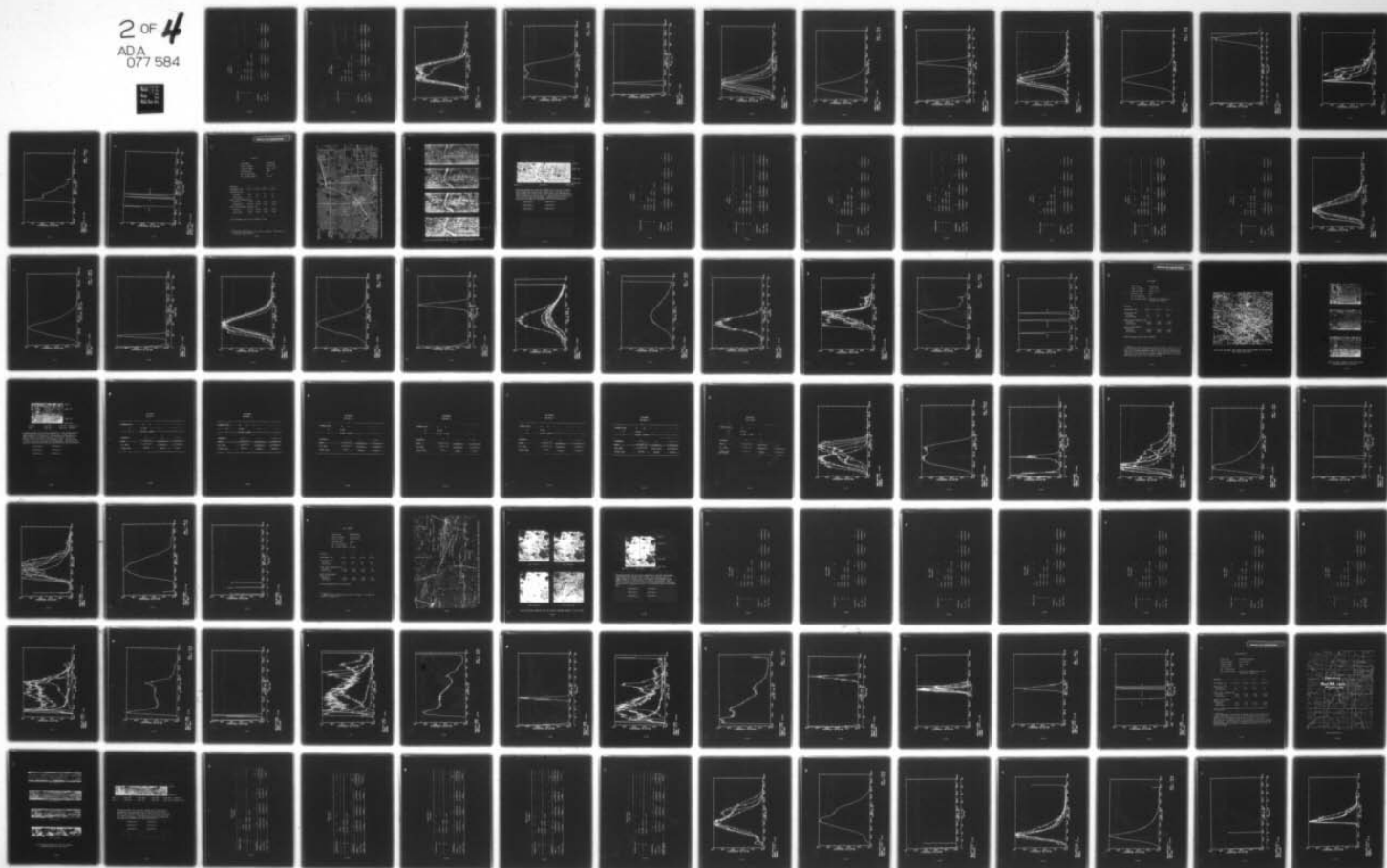
CHANNFIS	2	3	4	5
MEAN	1.3120F+03	1.5884E+02	3.5162F+01	2.9422E+02
ST. DEV.	3.5515F+02	7.9948E+01	8.9344E+00	3.0812E+00
TOTAL PTS.	130169.	130169.	130169.	130169.

AD-A077 584

ENVIRONMENTAL RESEARCH INST OF MICHIGAN ANN ARBOR IN--ETC F/G 17/5
STATISTICAL ANALYSIS OF TERRAIN BACKGROUND MEASUREMENTS DATA.(U)
MAR 77 R SPELICY, J BEARD, J R MAXWELL N00123-76-C-0708
ERIM-120500-12-F NL

UNCLASSIFIED

2 OF 4
ADA
077 584



FLINT-1

SUB-AREA 6

CORRELATION	2	3	4	5
2	1.000			
3	0.353	1.000		
4	0.295	0.373	1.000	
5	-0.440	-0.043	0.084	1.000

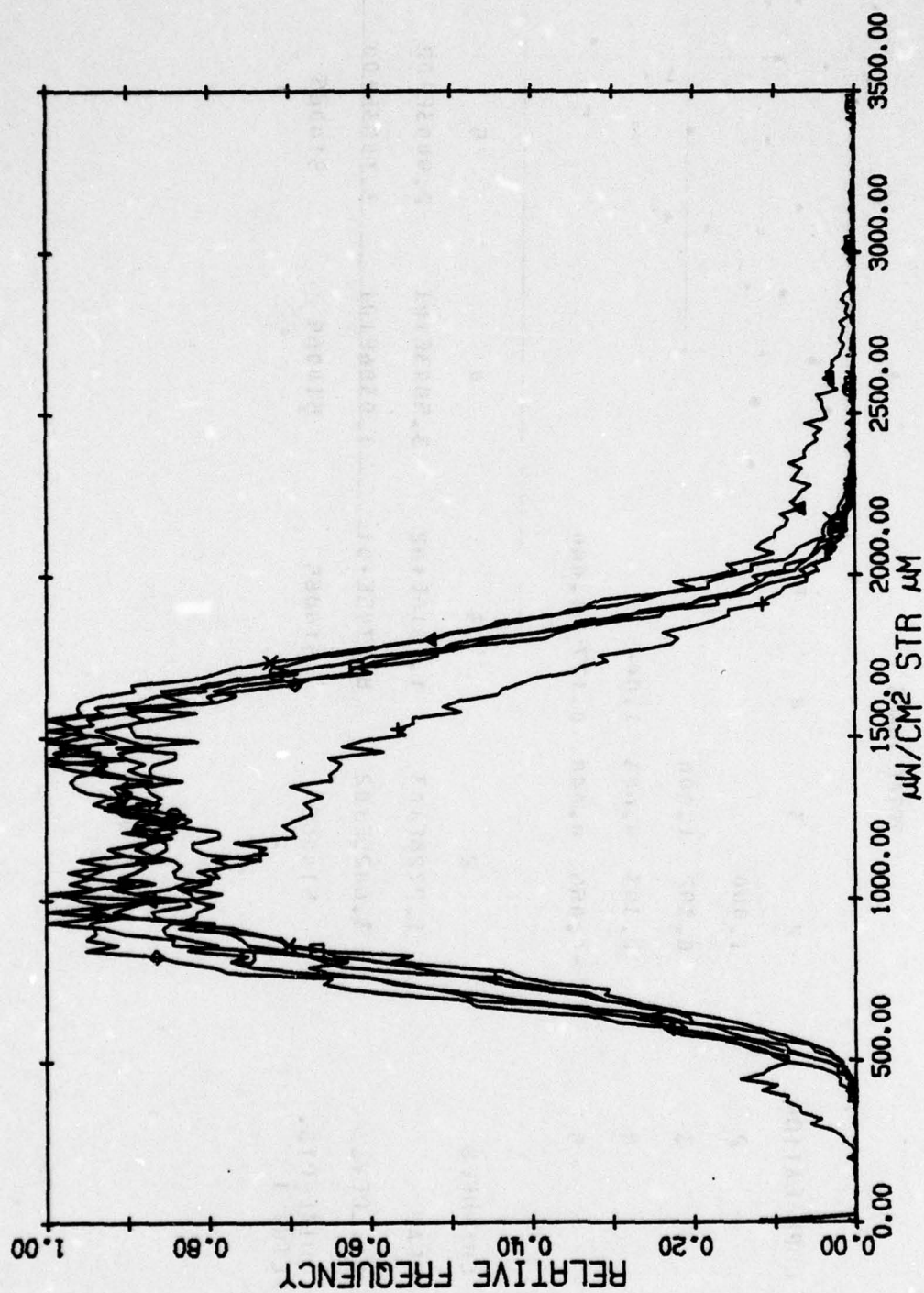
CHANNELS	2	3	4	5
MEAN	1.2313E+03	1.2457E+02	2.9571E+01	2.9338E+02
ST. DEV.	3.5484E+02	7.2868E+01	7.8701E+00	2.7294E+00
TOTAL PIS.	65286.	65286.	65286.	65286.

FLINT-1

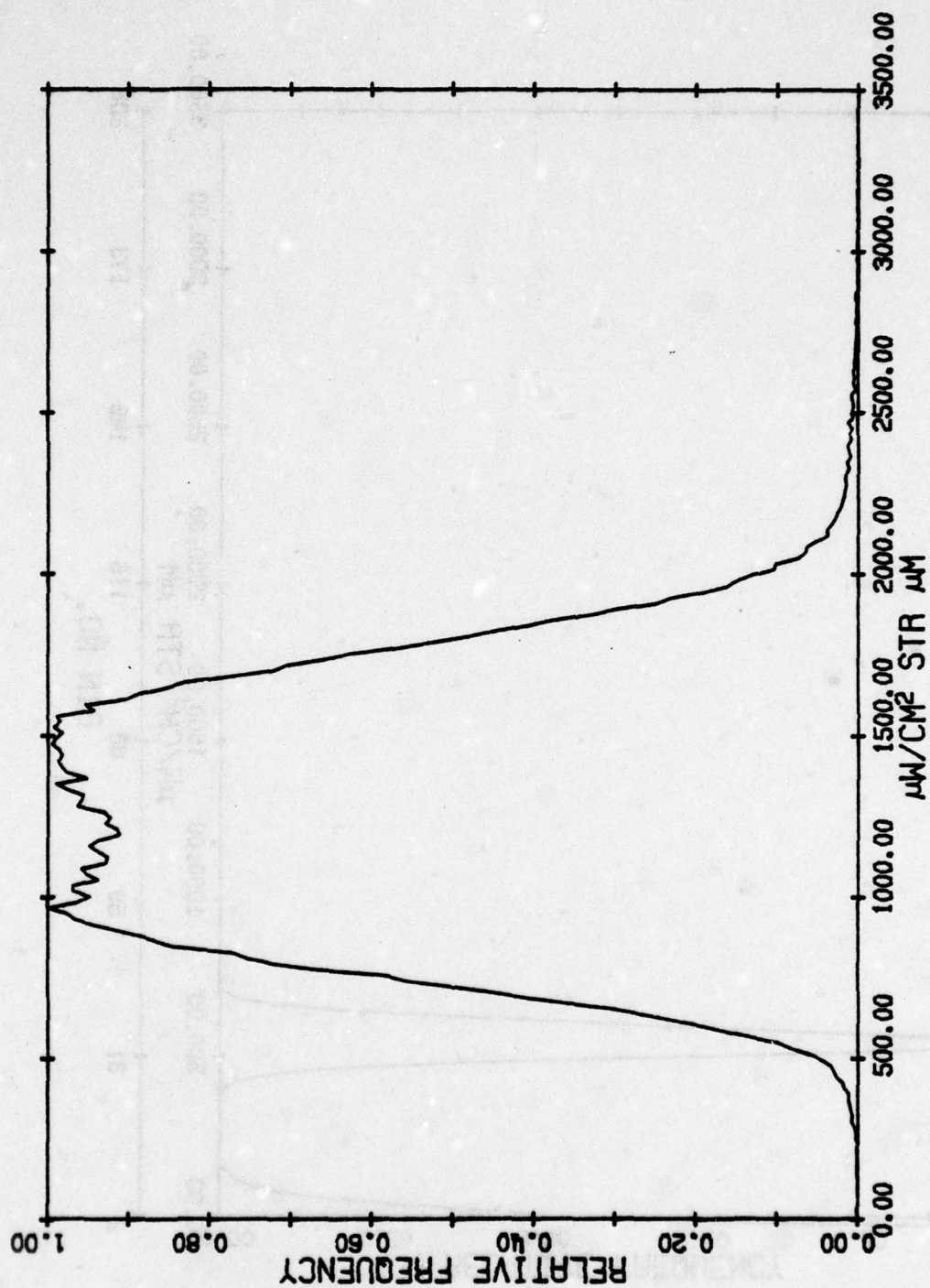
TOTAL IMAGE

CORRELATION	2	3	4	5
2	1.000			
3	0.392	1.000		
4	0.303	0.603	1.000	
5	-0.455	0.048	0.177	1.000

CHANNELS	2	3	4	5
MEAN	1.2728E+03	1.7316E+02	3.5843E+01	2.9443E+02
ST. DEV.	3.6425E+02	8.2745E+01	1.0386E+01	3.1403E+00
TOTAL PTS. FLINT 1	514065	514065	514065	514065

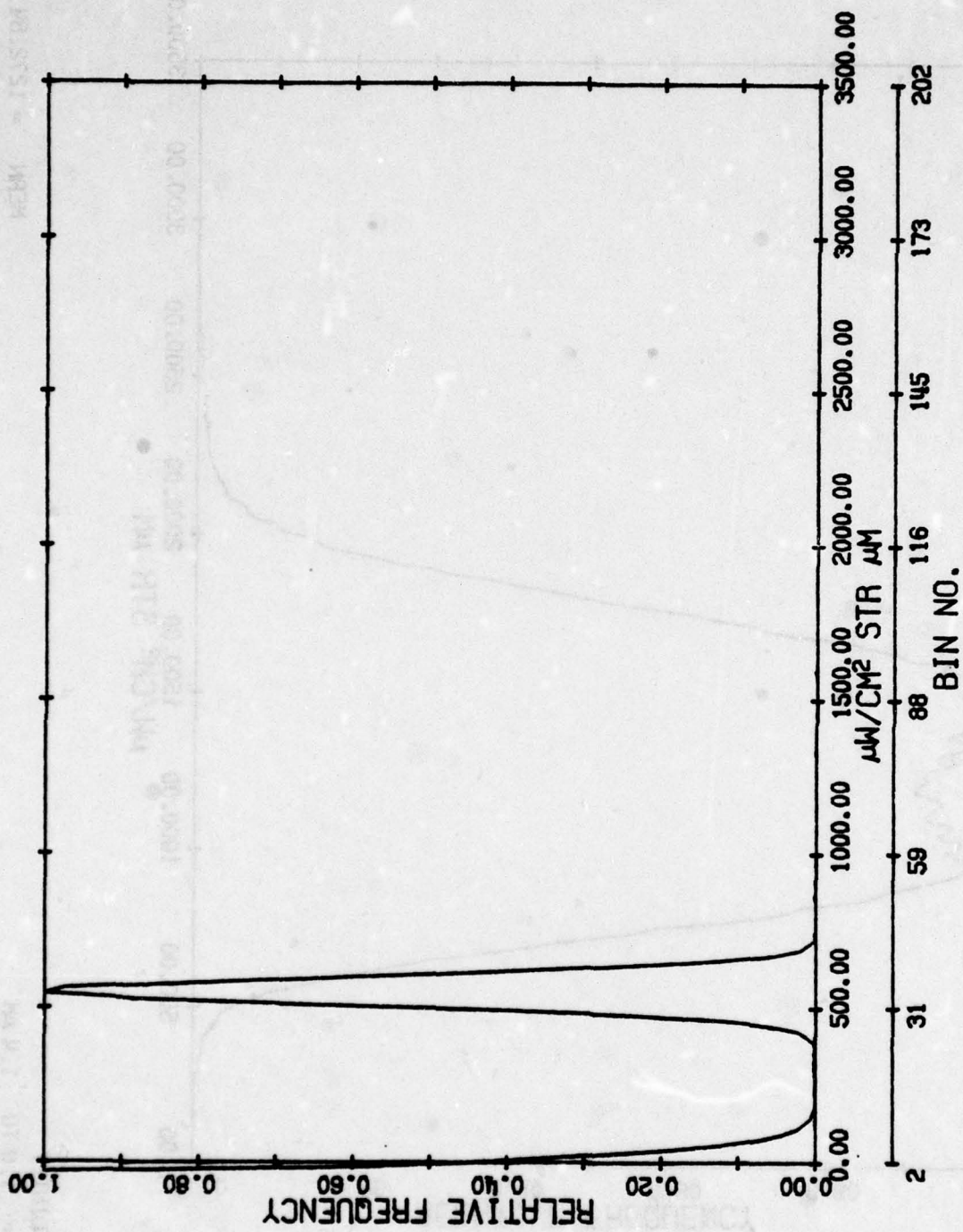


AREA: FLINT 1
LAMBDA= 1.0 TO 1.4 μM
SUBAREAS

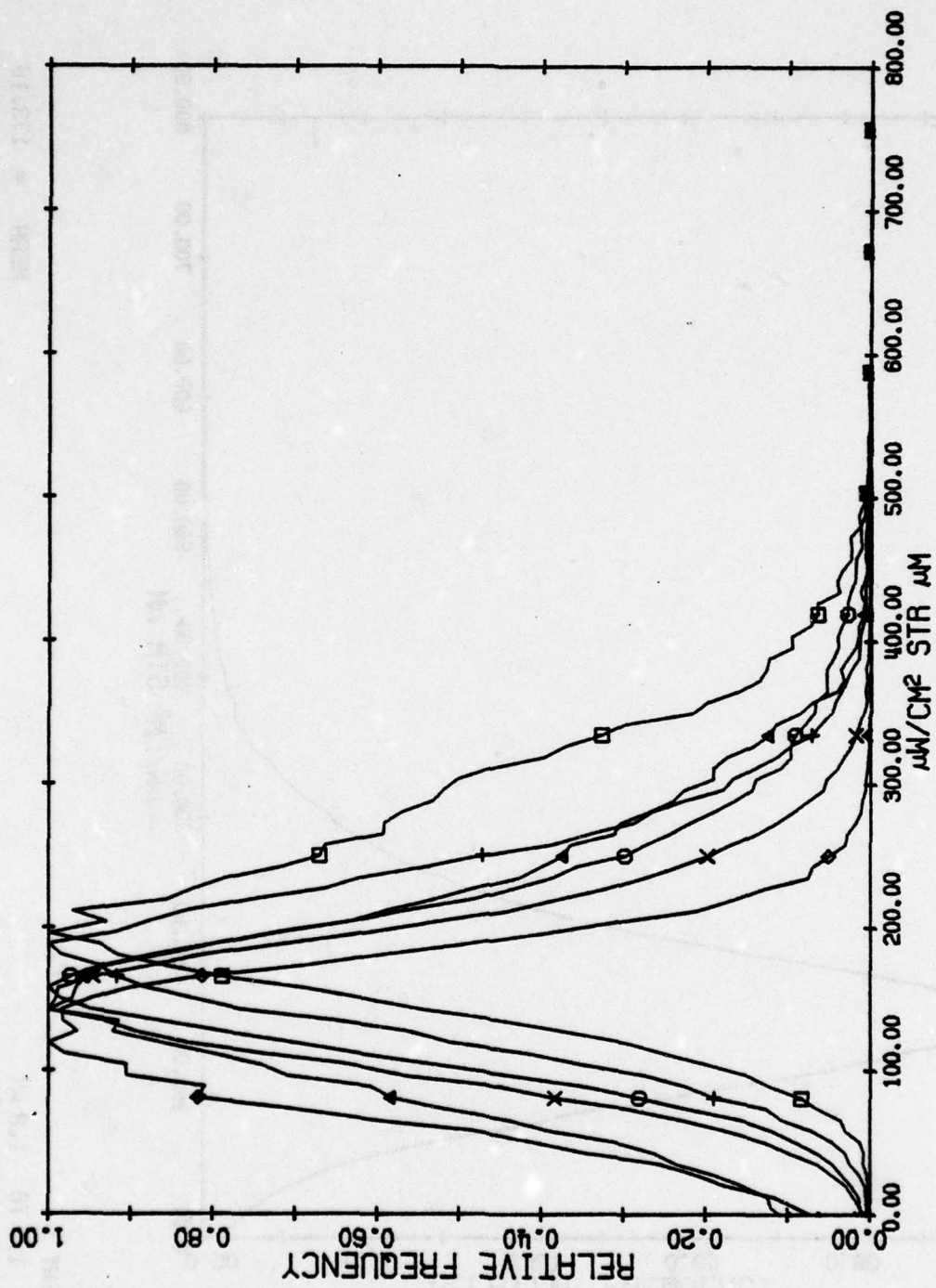


MEAN = 1272.84
ST. DEV. = 364.25

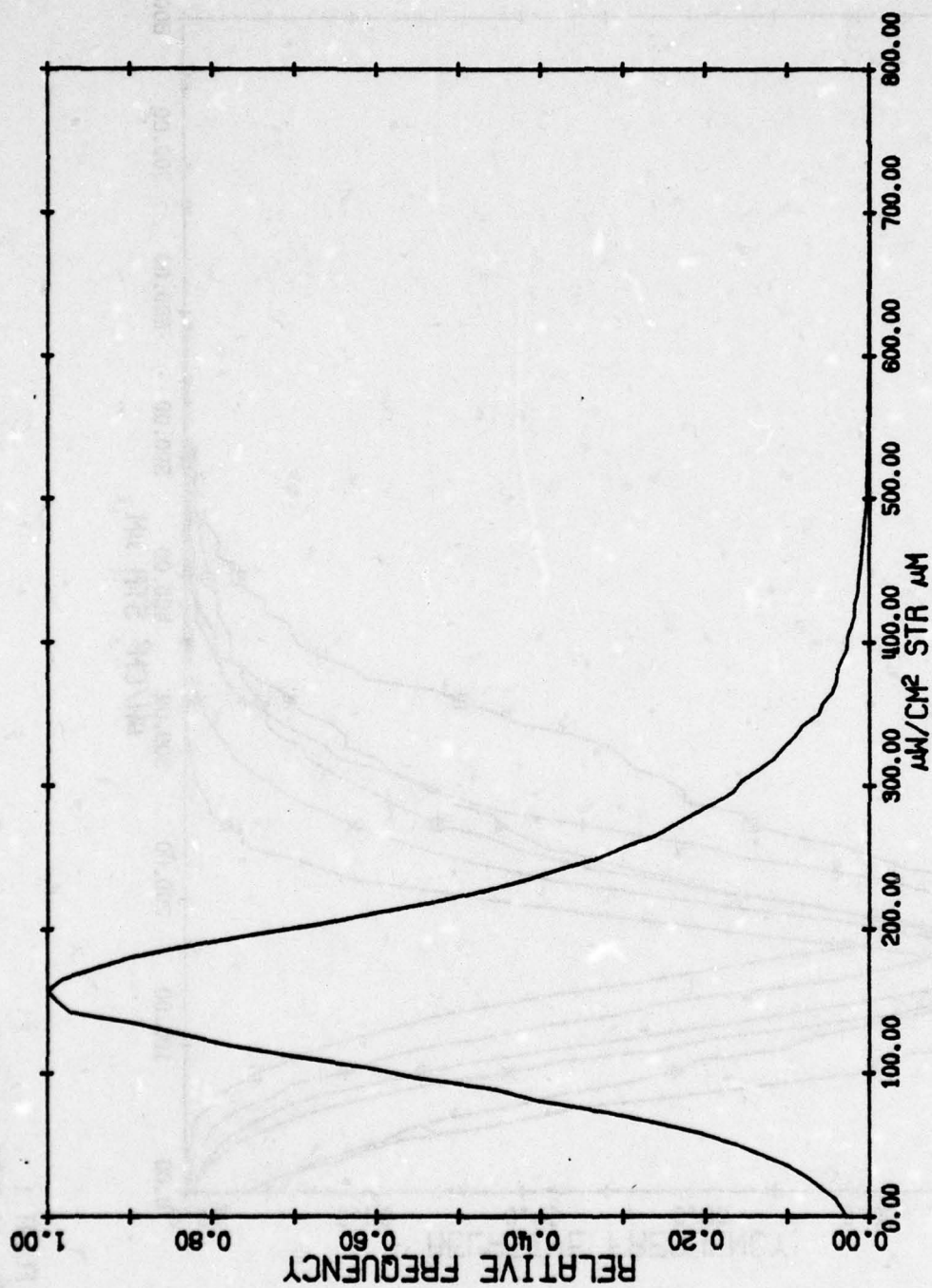
AREA: FLINT 1
LAMBDA= 1.0 TO 1.4 μM
TOTAL AREA



AREA: FLINT 1
 WAVELENGTH= 1.0 TO 1.4 μm
 CALIB. PLATES

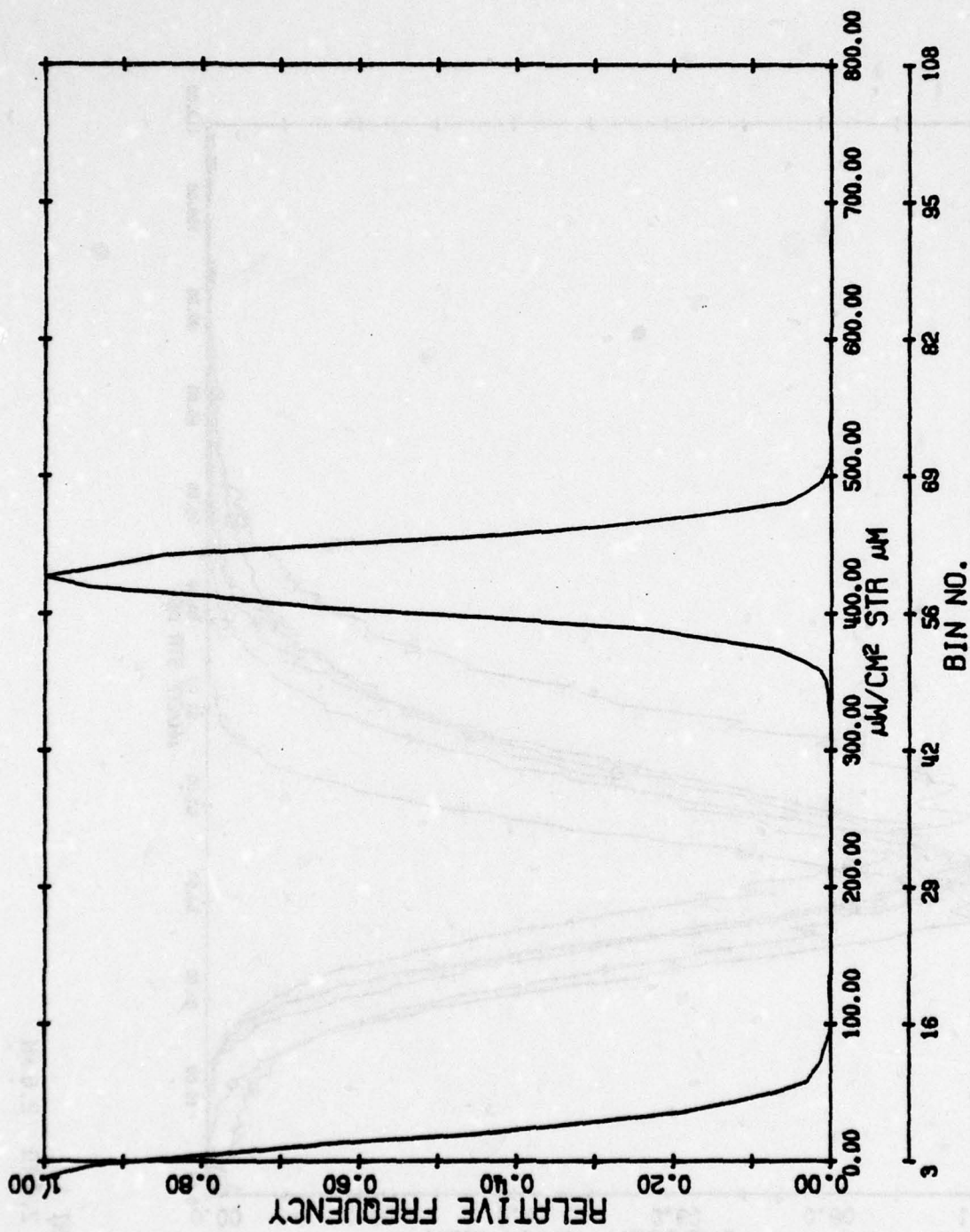


AREA: FLINT 1
 LAMBDA= 1.5 TO 1.8 μm
 SUBAREAS

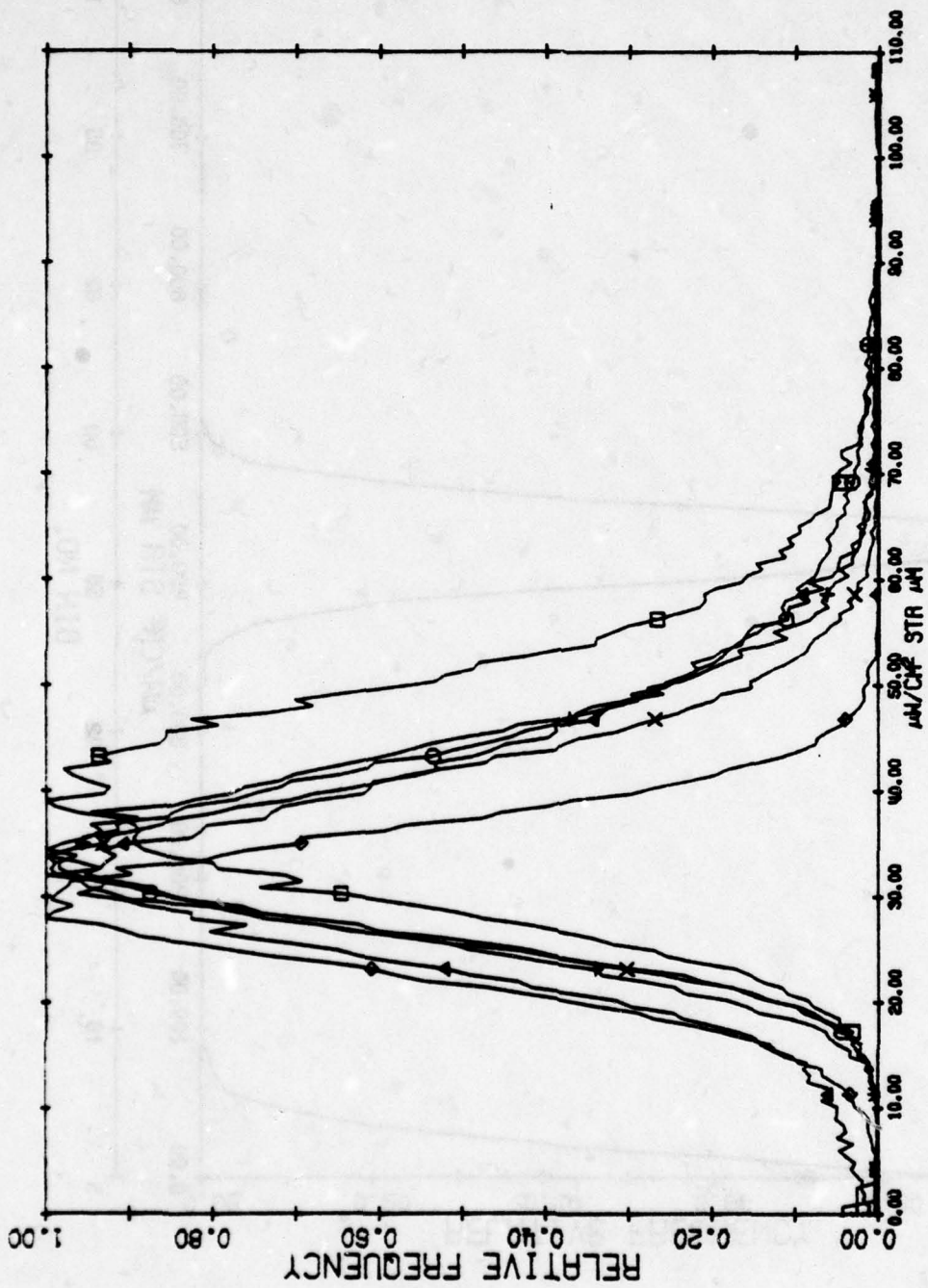


AREA: FLINT 1
WAVELENGTH= 1.5 TO 1.8 μm
TOTAL AREA

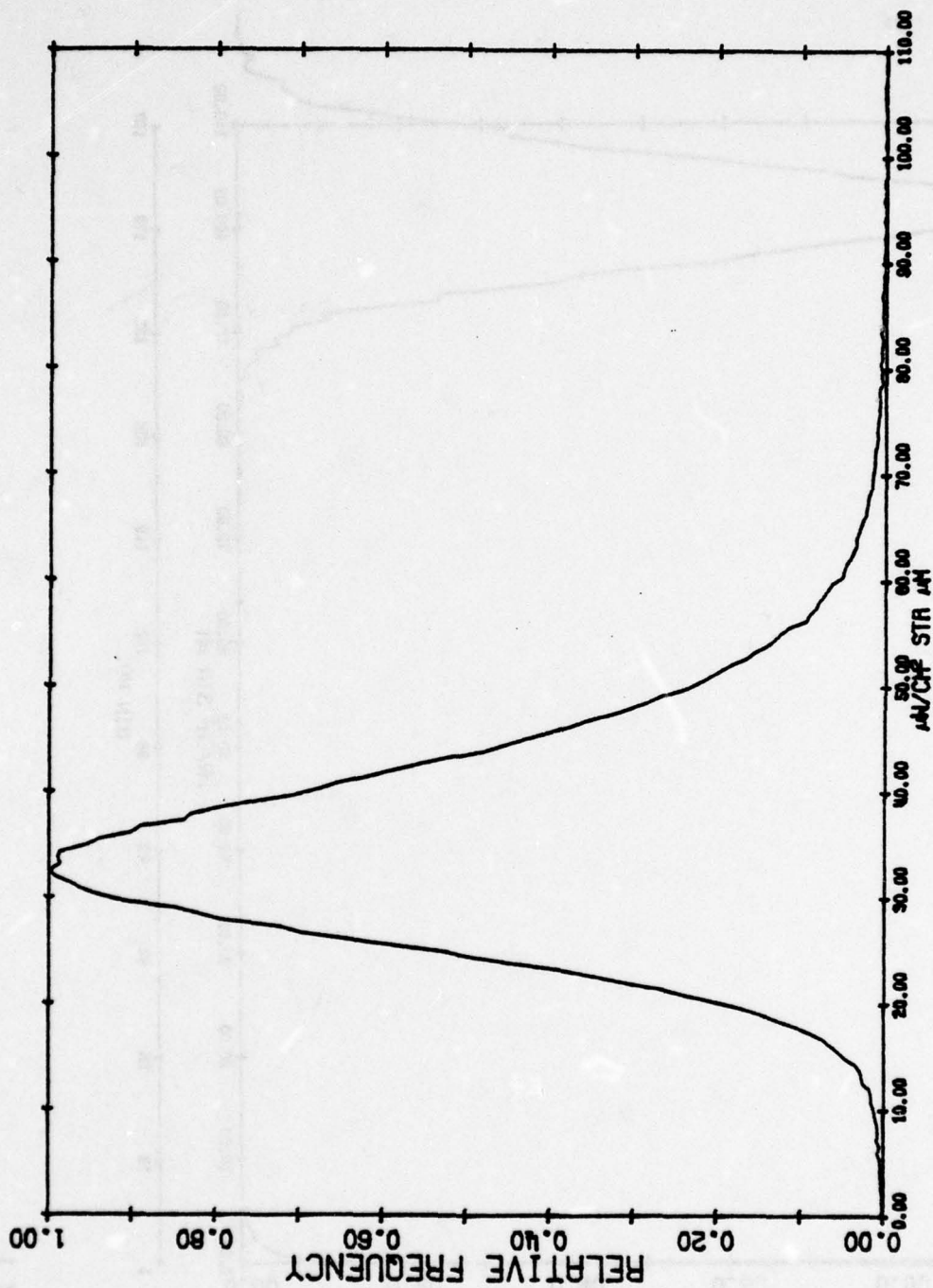
MEAN = 173.16
ST. DEV. = 82.74



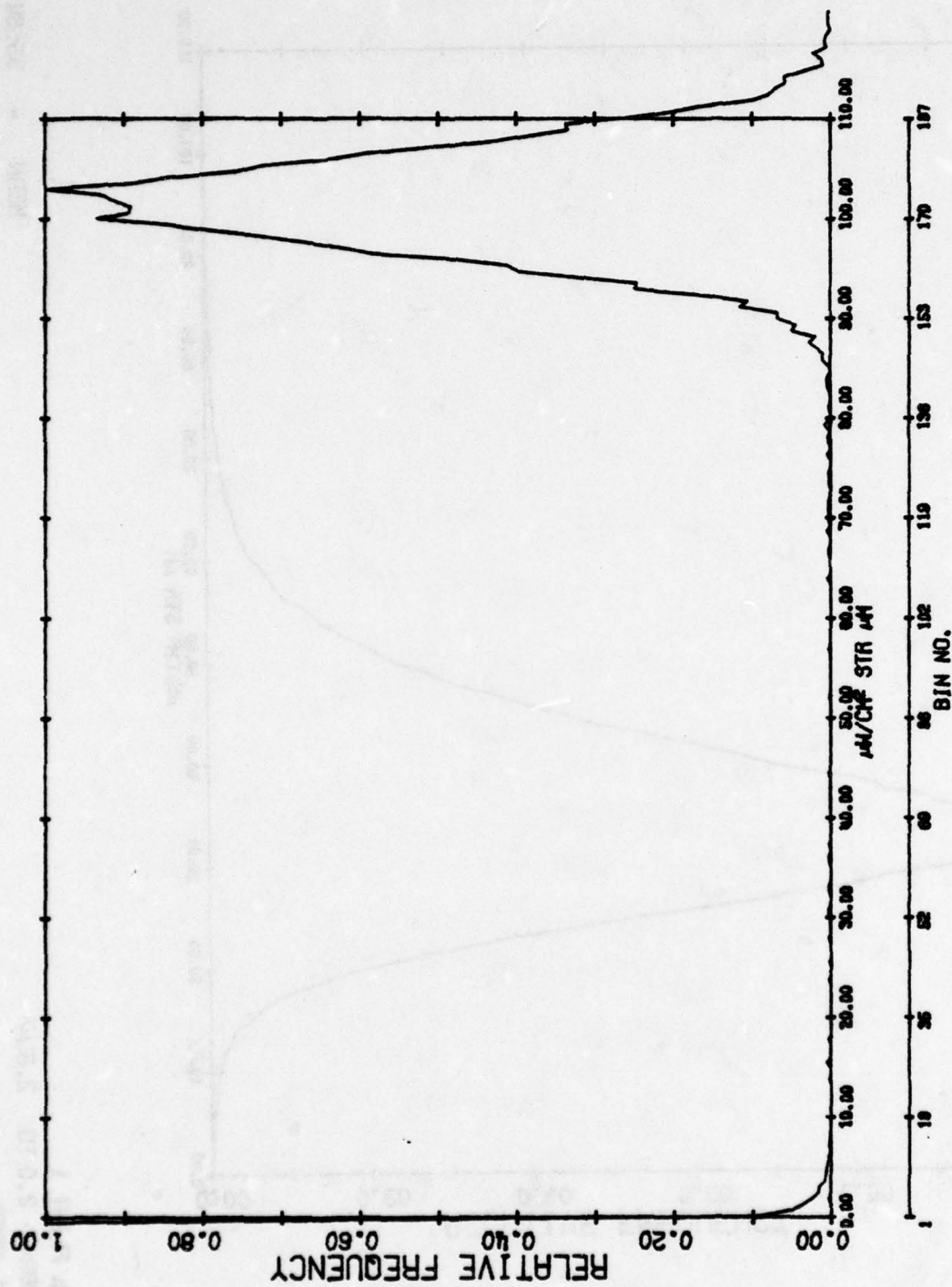
AREA: FLINT 1
 WAVELENGTH 1.5 TO 1.8 μm
 CALIB. PLATES



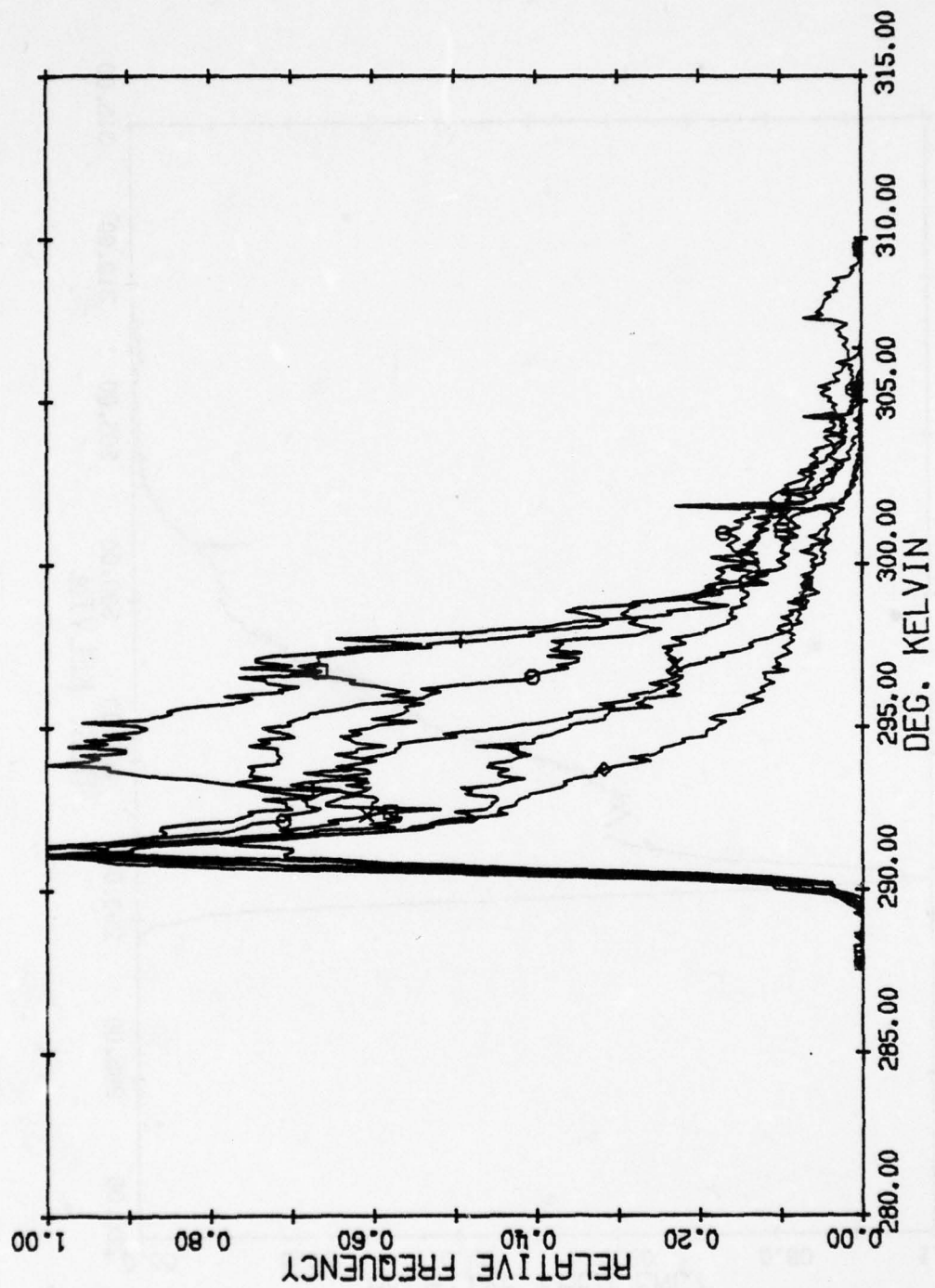
AREA: FLINT 1
WAVELENGTH= 2.0 TO 2.6 μm
SUBAREAS



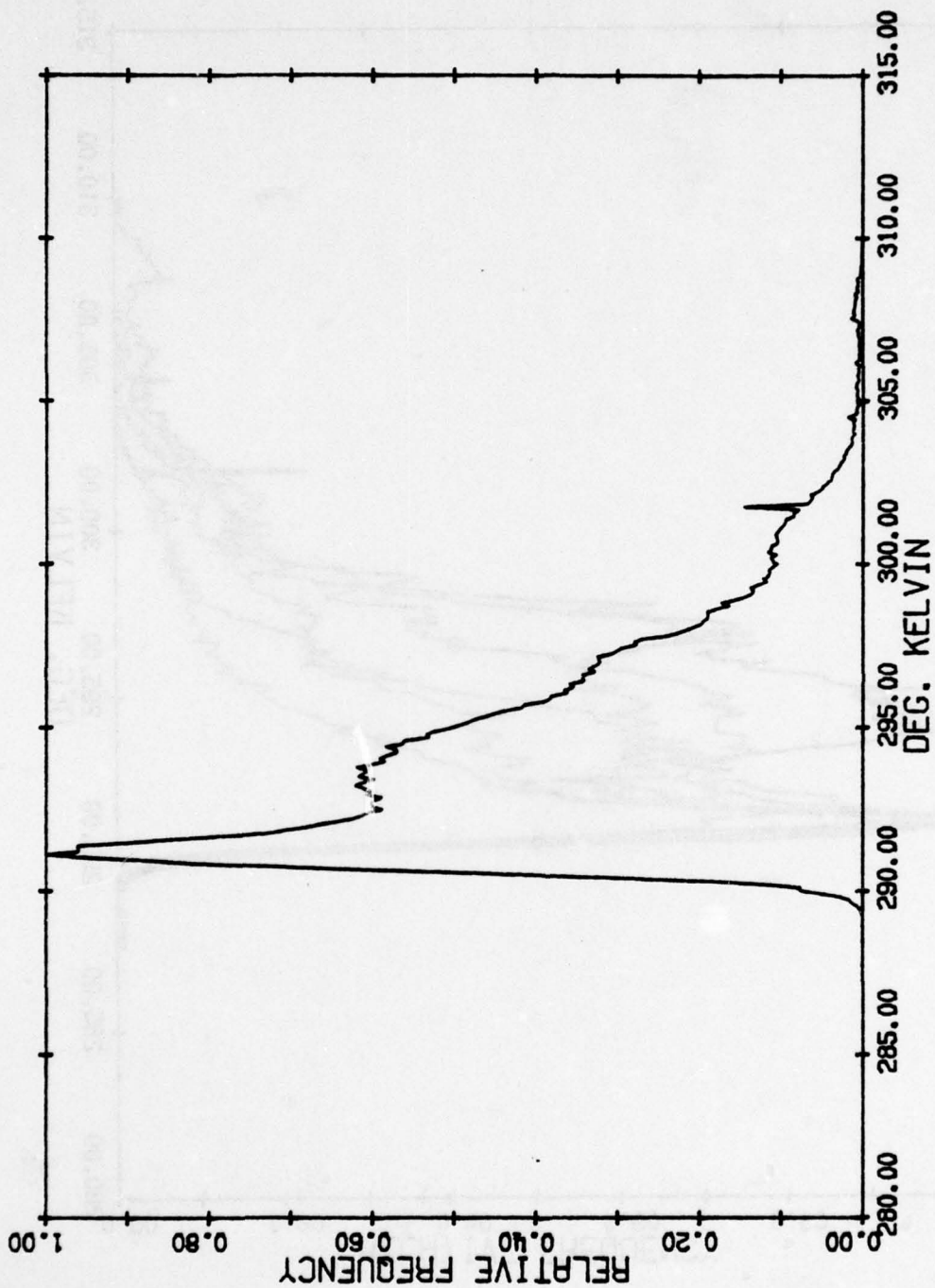
AREA: FLINT 1
 LAMBDA= 2.0 TO 2.6 nm
 TOTAL AREA
 MEAN = 35.84
 ST.DEV. = 10.39



AREA: FLJNT 1
 WAVELENGTH 2.0 TO 2.6 μm
 CALIB. PLATES

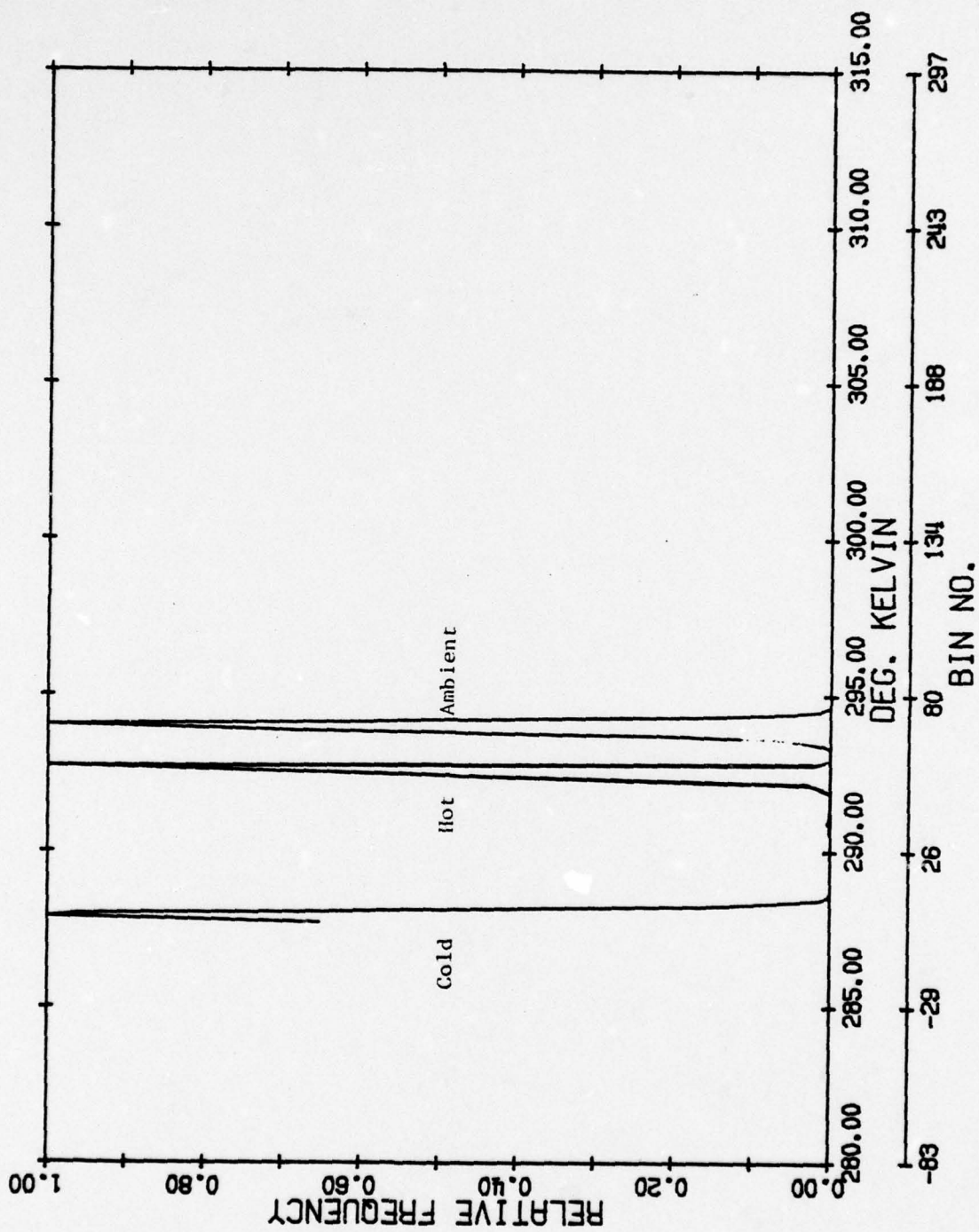


AREA: FLINT 1
LAMBDA= 9.3 TO 11.7 μ M



AREA: FLINT 1
LAMBDA= 9.3 TO 11.7 μ M
TOTAL AREA

MEAN = 294.43
ST.DEV.= 3.14



AREA: FLINT 1
 LAMBDA= 9.3 TO 11.7 μ M
 CALIB. PLATES

FLINT-2*

Scene Type	Industrial
Date of Flight	18 Sep 1971
Time of Flight	1155 - 1157
Altitude (Ft.)	1000
No. of Sub-Areas	6
No. of Data Points	572,115

Channels	2	3	4	5
Wavelength (μm)	1.0-1.4	1.5-1.8	2.0-2.6	9.3-11.7
Resolution (mr)				
In-Track	5.0	5.0	5.0	5.0
Cross-Track	2.5	2.5	2.5	2.9
Nadir Pixel Dimensions (m)				
In-Track	1.524	1.524	1.524	1.524
Cross-Track	0.762	0.762	0.762	0.884
Nadir Ground Sample Distance (m)				
In-Track	1.524	1.524	1.524	1.524
Cross-Track	0.762	0.762	0.762	0.762

Line averaging used on all channels of data

* These data were obtained with the M-7 scanner. All data are on spatial registration.



MAP OF THE FLINT AREA SHOWING THE REGION COVERED IN THE FLINT-2 RUN ABOUT FLIGHT LINE 31



1.0 - 1.4 μm



1.5 - 1.8 μm



2.0 - 2.6 μm



9.3 - 11.7 μm

LINE SCAN IMAGES PRODUCED FROM THE VARIOUS INFRARED CHANNELS OF FLINT-2



Line 10

Line 484

Line 896

Pixel 1

Pixel 161

Pixel 484

Pixel 645

SUB-AREAS DEFINED FOR STATISTICS GENERATION IN THE FLINT-2 IMAGE. Uneven areas were chosen so that Areas 2 and 5 covered the $\pm 20^\circ$ range suitable for correlation. Approximate scene dimensions are 4435 ft (1352 m) by 1612 ft (491 m). Each sub-area as well as the total area have been histogrammed. Histogram plots and their respective sub-areas are identified with the following key:

- | | |
|--------------|--------------|
| ▣ Sub-area 1 | + Sub-area 4 |
| ○ Sub-area 2 | × Sub-area 5 |
| △ Sub-area 3 | ◇ Sub-area 6 |

FLINT-2
SUB-AREA 1

CORRELATION	2	3	4	5
2	1.000			
3	0.771	1.000		
4	0.620	0.682	1.000	
5	-0.244	-0.041	0.057	1.000

CHANNELS	2	3	4	5
MEAN	7.6551F+02	2.4053E+02	3.4190E+01	2.9738E+02
ST. DEV.	2.9745F+02	8.2458F+01	1.4956F+01	3.0840E+00
TOTAL PTS.	70240.	70240.	70240.	70240.

FLINT-2

SUB-AREA 2

CORRELATION	2	3	4	5
2	1.000			
3	0.797	1.000		
4	0.562	0.654	1.000	
5	-0.429	-0.254	-0.104	1.000

II-44

CHANNELS	2	3	4	5
MEAN	7.4670E+02	2.3931E+02	3.8759E+01	2.9747E+02
ST. DEV.	3.0490E+02	8.0797E+01	1.3607E+01	3.1748E+00
TOTAL PTS.	141797.	141797.	141797.	141797.

FLINT-2

SUB-AREA 3

CORRELATION	2	3	4	5
2	1.000			
3	0.602	1.000		
4	0.249	0.554	1.000	
5	-0.507	-0.129	0.092	1.000

CHANNELS	2	3	4	5
MEAN	8.8222E+02	2.2722E+02	3.5325E+01	2.9565E+02
ST. DEV.	3.0389E+02	6.3982E+01	1.1400E+01	3.5800E+00
TOTAL PTS.	71118.	71118.	71118.	71118.

FLINT-2

SUB-AREA 4

CORRELATION	2	3	4	5
2	1.000			
3	0.618	1.000		
4	0.378	0.549	1.000	
5	-0.550	-0.219	-0.039	1.000

CHANNELS	2	3	4	5
MEAN	8.9297E+02	2.5540E+02	4.1351F+01	2.9645E+02
ST. DEV.	2.8731F+02	7.1670E+01	1.3339E+01	2.6239F+00
TOTAL PTS.	71680.	71680.	71680.	71680.

FLINT-2
SUB-AREA 5

CORRELATION	2	3	4	5
2	1.000			
3	0.784	1.000		
4	0.586	0.648	1.000	
5	-0.391	-0.286	-0.163	1.000

CHANNELS	2	3	4	5
MEAN	7.1104E+02	2.3130E+02	3.9399E+01	2.9773E+02
ST. DEV.	2.9382E+02	7.8817E+01	1.4050E+01	3.1146E+00
TOTAL PTS.	144704.	144704.	144704.	144704.

FLINT-2

SUB-AREA 6

CORRELATION	2	3	4	5
2	1.000			
3	0.652	1.000		
4	0.434	0.617	1.000	
5	-0.311	0.071	0.146	1.000

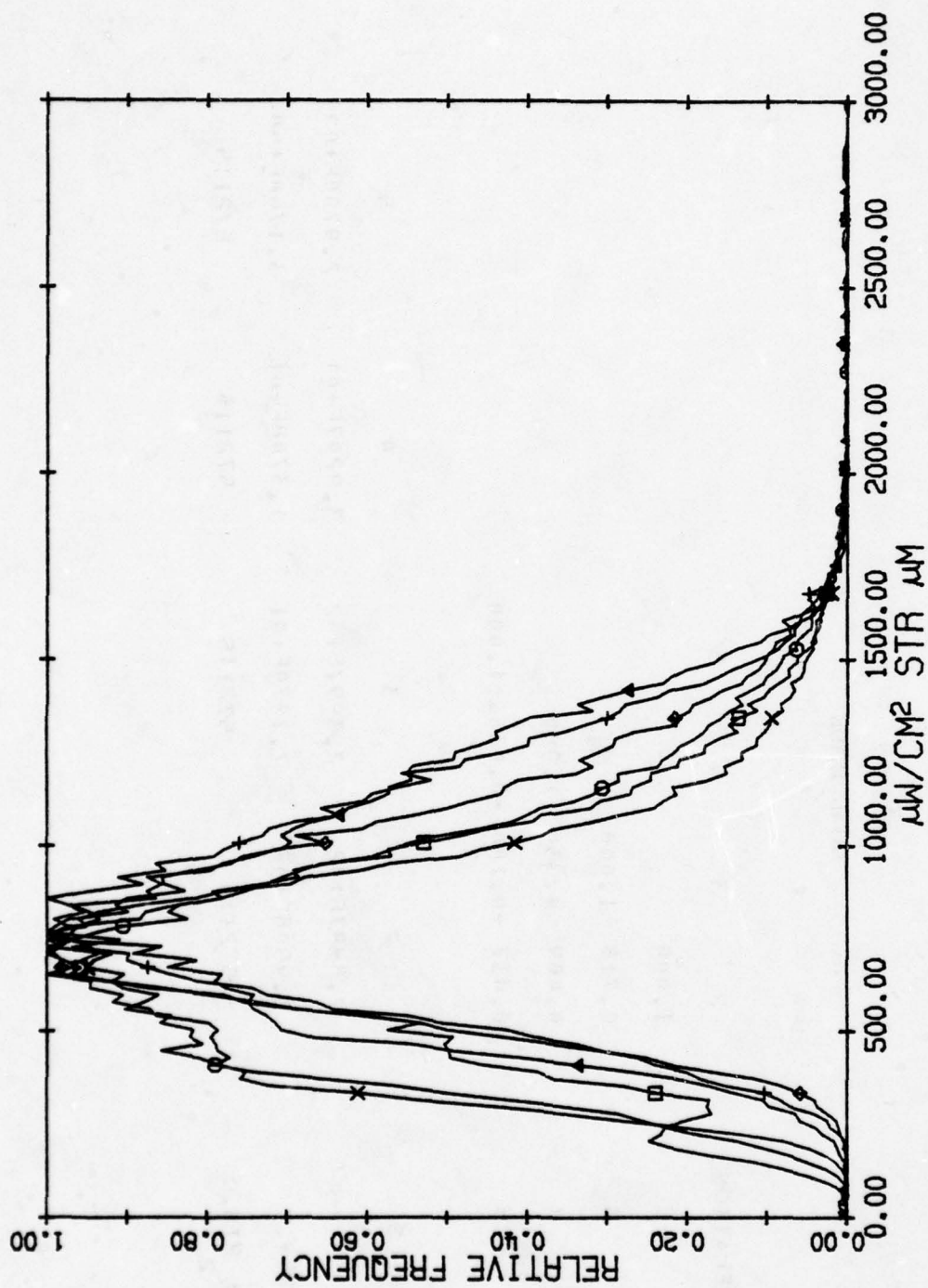
CHANNELS	2	3	4	5
MEAN	8.6346E+02	2.5525E+02	4.2684E+01	2.9611E+02
ST. DEV.	2.8527E+02	7.8829E+01	1.3500E+01	2.7154E+00
TOTAL PTS.	72576.	72576.	72576.	72576.

FLINT-2

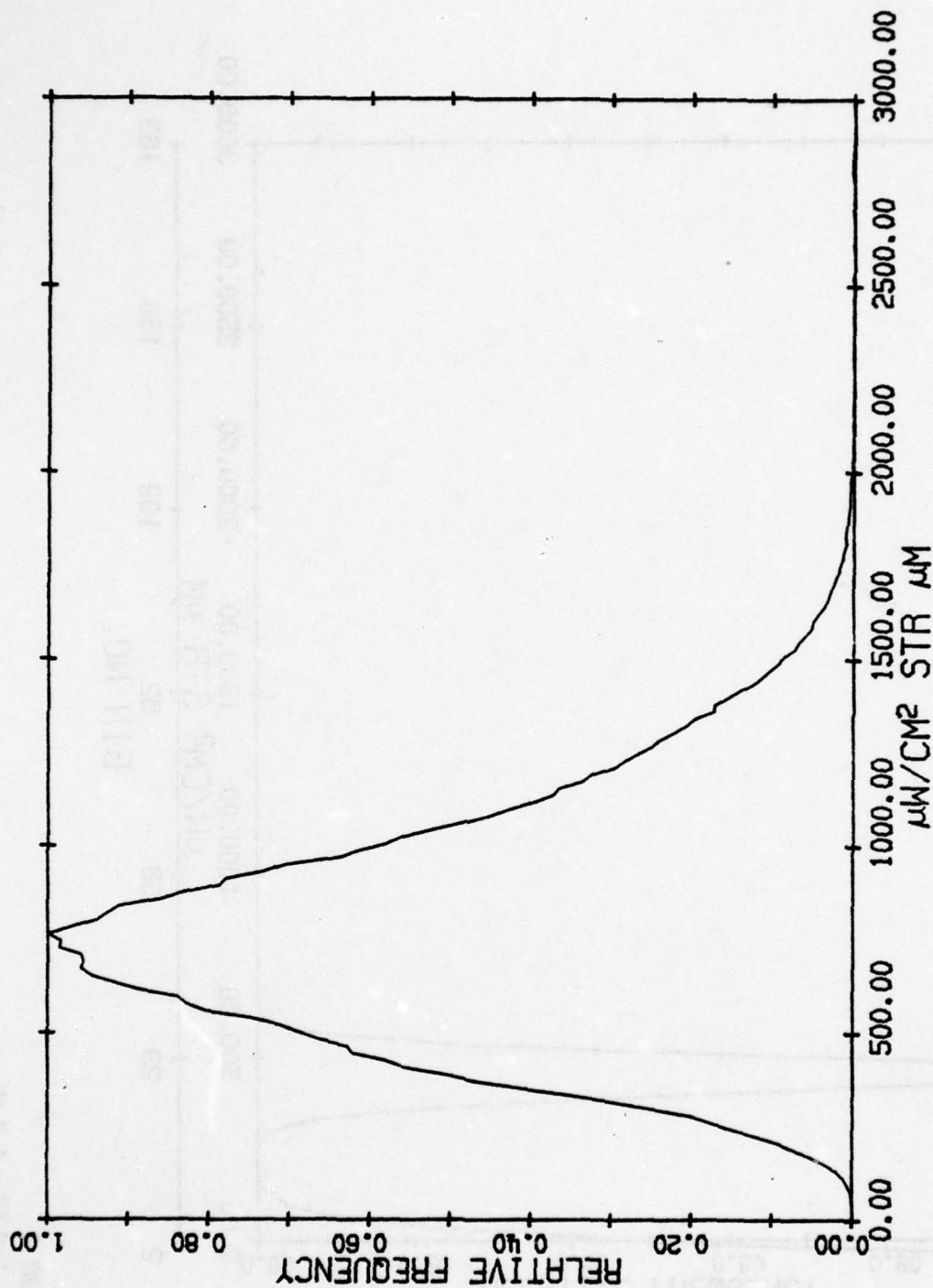
TOTAL IMAGE

CORRELATION	2	3	4	5
2	1.000			
3	0.718	1.000		
4	0.489	0.634	1.000	
5	-0.437	-0.180	-0.036	1.000

CHANNELS	2	3	4	5
MEAN	7.8997E+02	2.3097E+02	3.9247E+01	2.9700E+02
ST. DEV.	3.0508E+02	7.7870E+01	-1.3748E+01	3.1768E+00
TOTAL PTS. FLINT 2	572115	572115	572115	572115

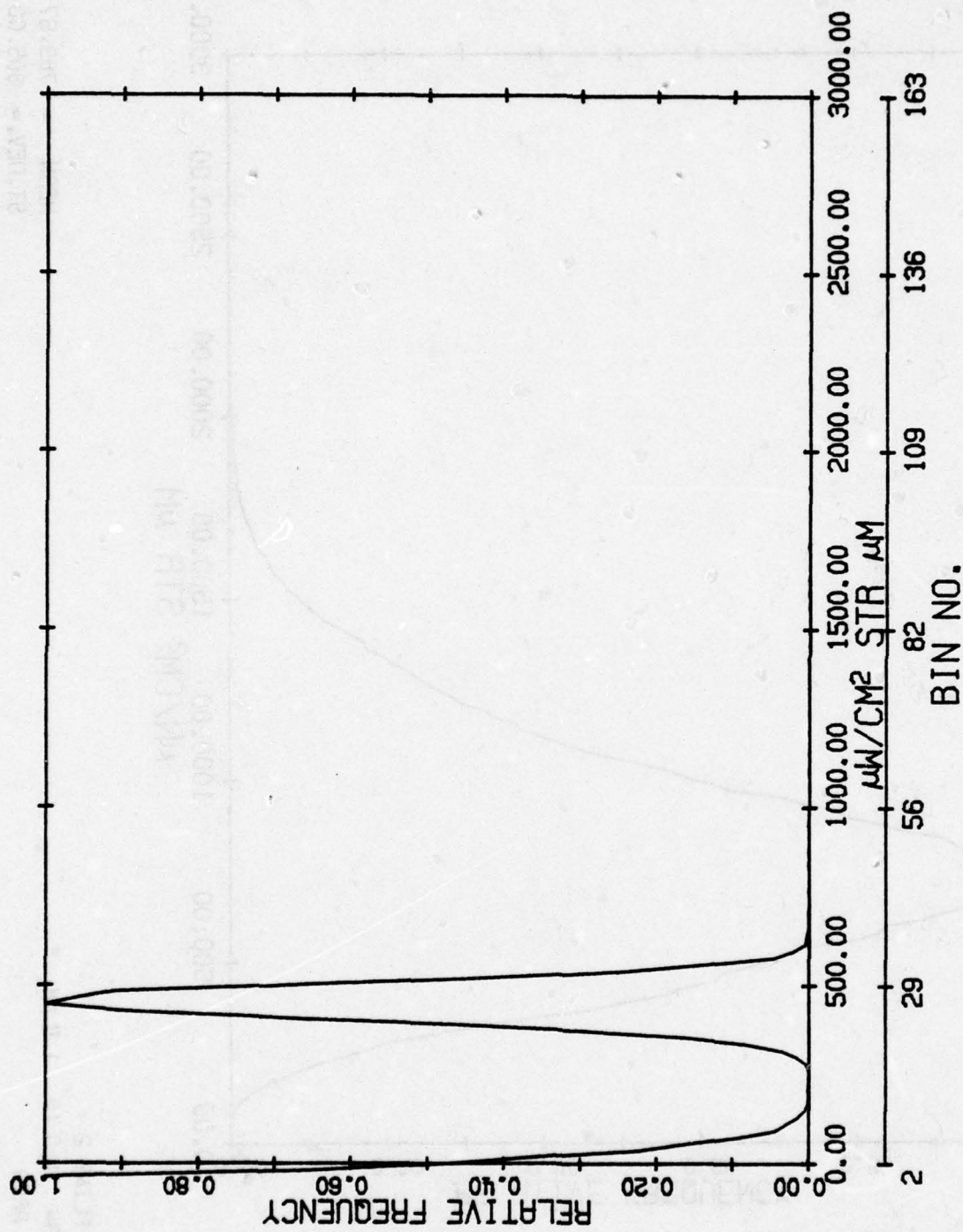


AREA: FLINT 2
 LAMBDA= 1.0 TO 1.4 μm
 SUBAREAS

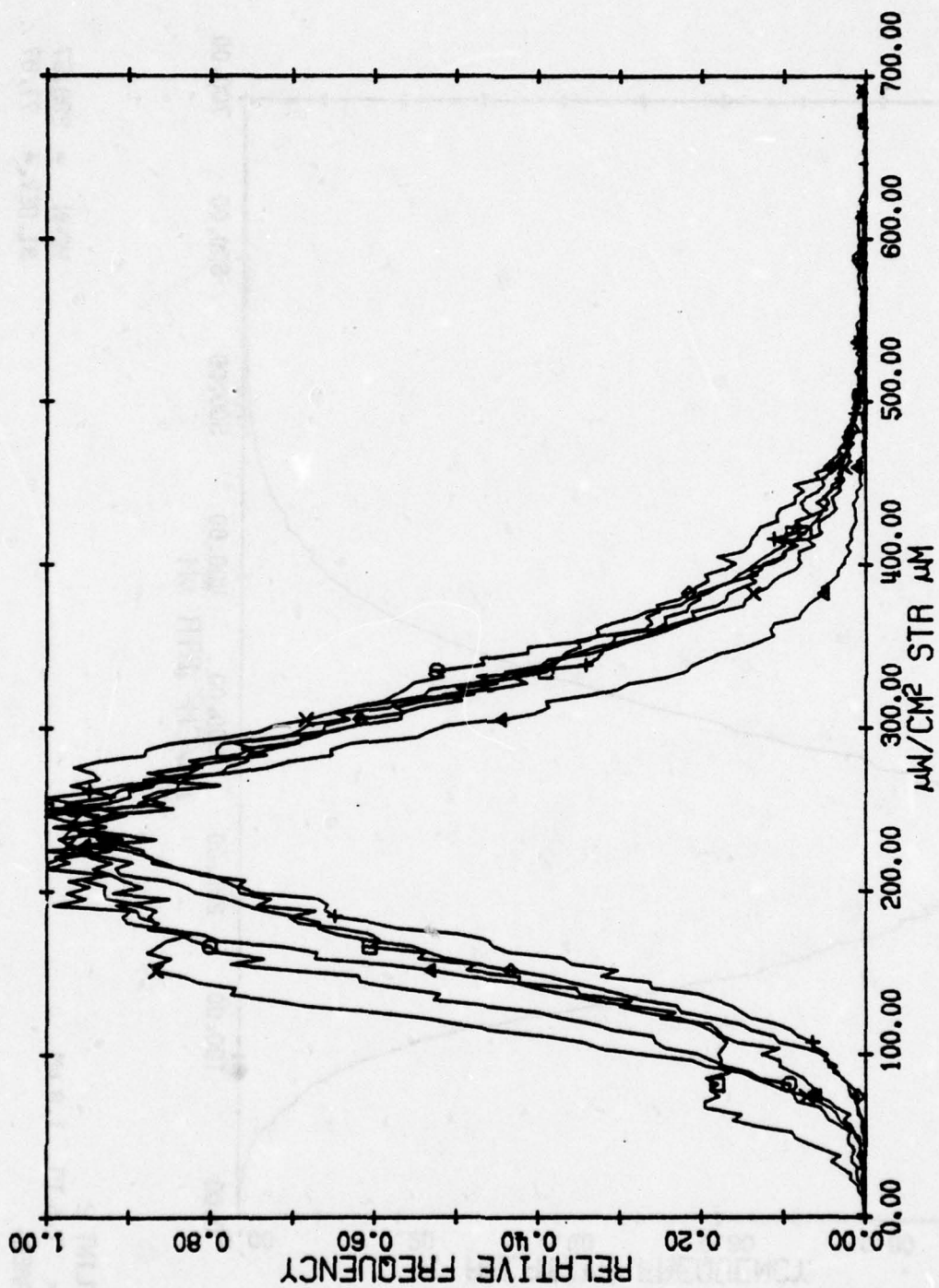


AREA: FLINT 2
 LAMBDA= 1.0 TO 1.4 μM
 TOTAL AREA

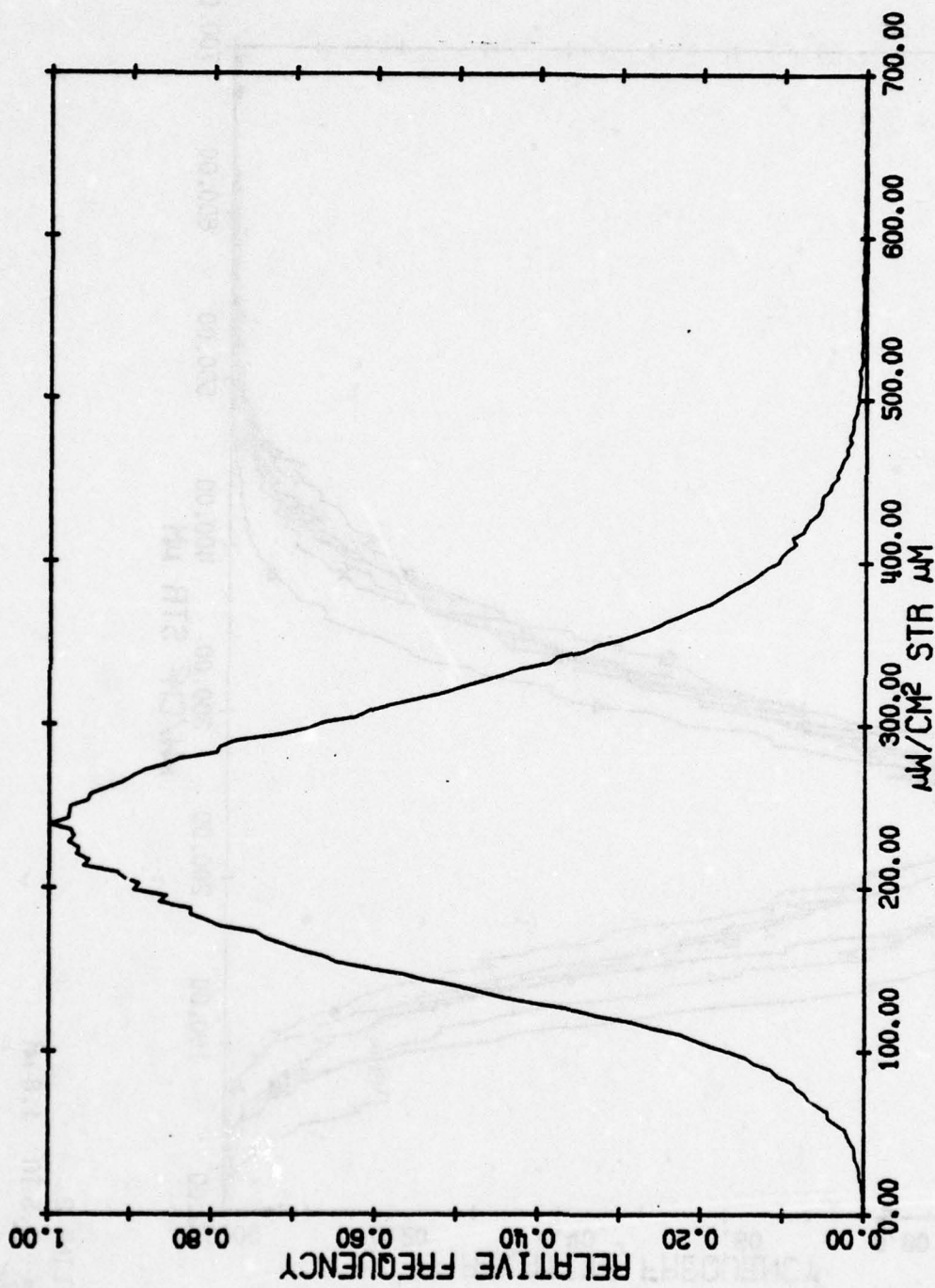
MEAN = 789.97
 ST.DEV.= 305.08



AREA: FLINT 2
 WAVELENGTH= 1.0 TO 1.4 μm
 CALIB. PLATES

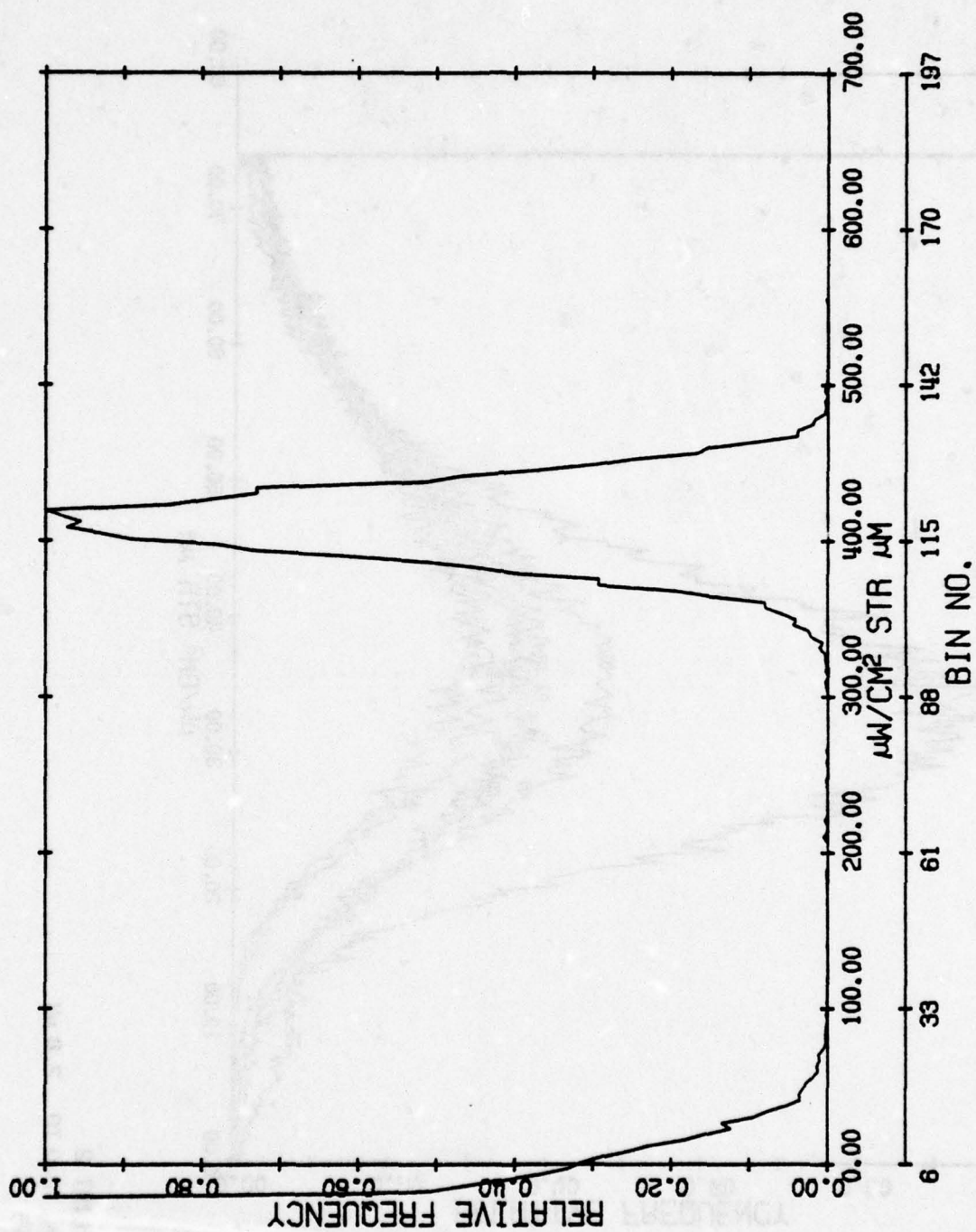


AREA: FLINT 2
WAVELENGTH 1.5 TO 1.8 μm
SUBAREAS

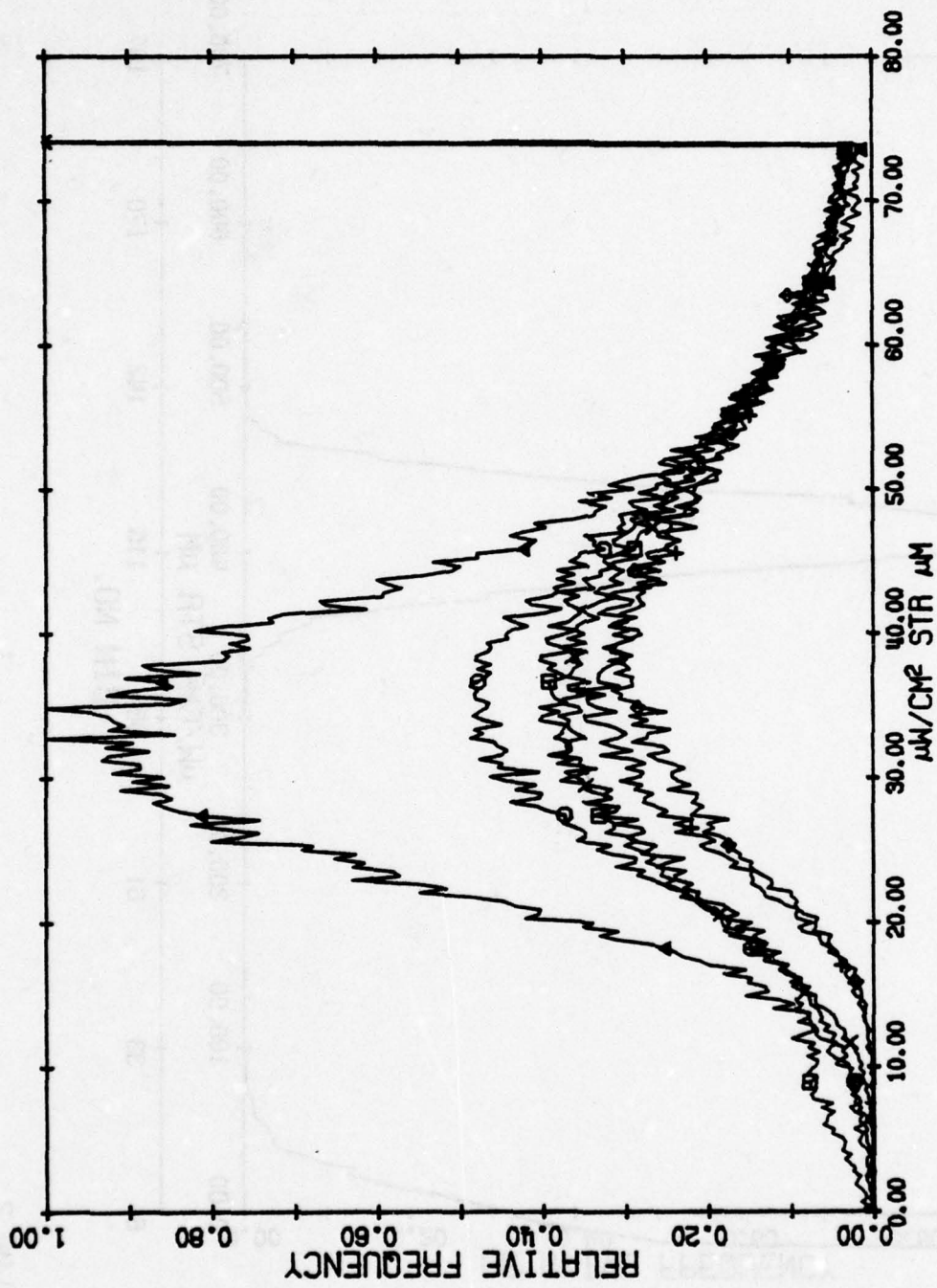


AREA: FLINT 2
WAVELENGTH: 1.5 TO 1.8 μm
TOTAL AREA

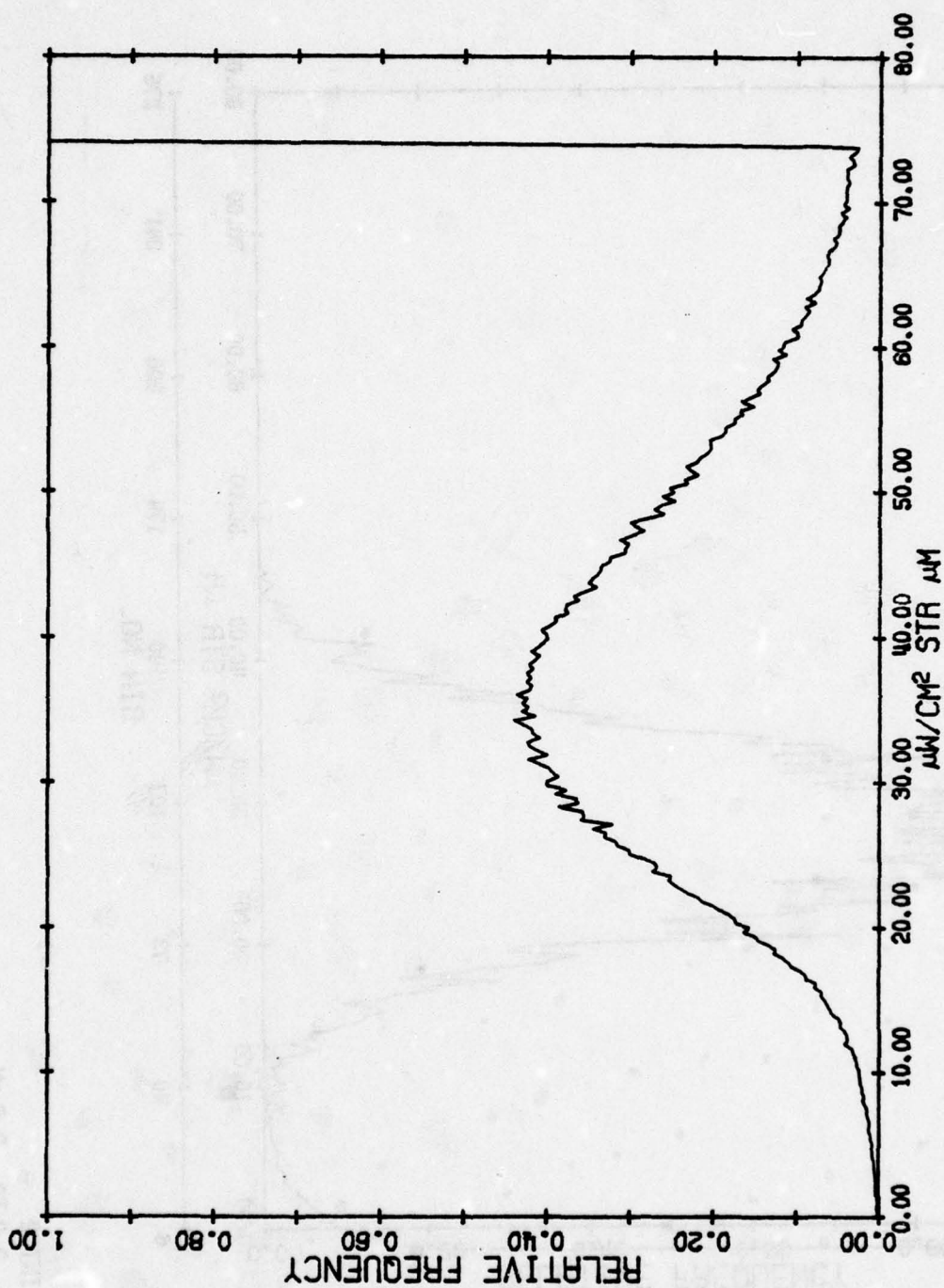
MEAN = 239.87
ST.DEV. = 77.87



AREA: FLINT 2
LAMBDA= 1.5 TO 1.8 μM
CALIB. PLATES

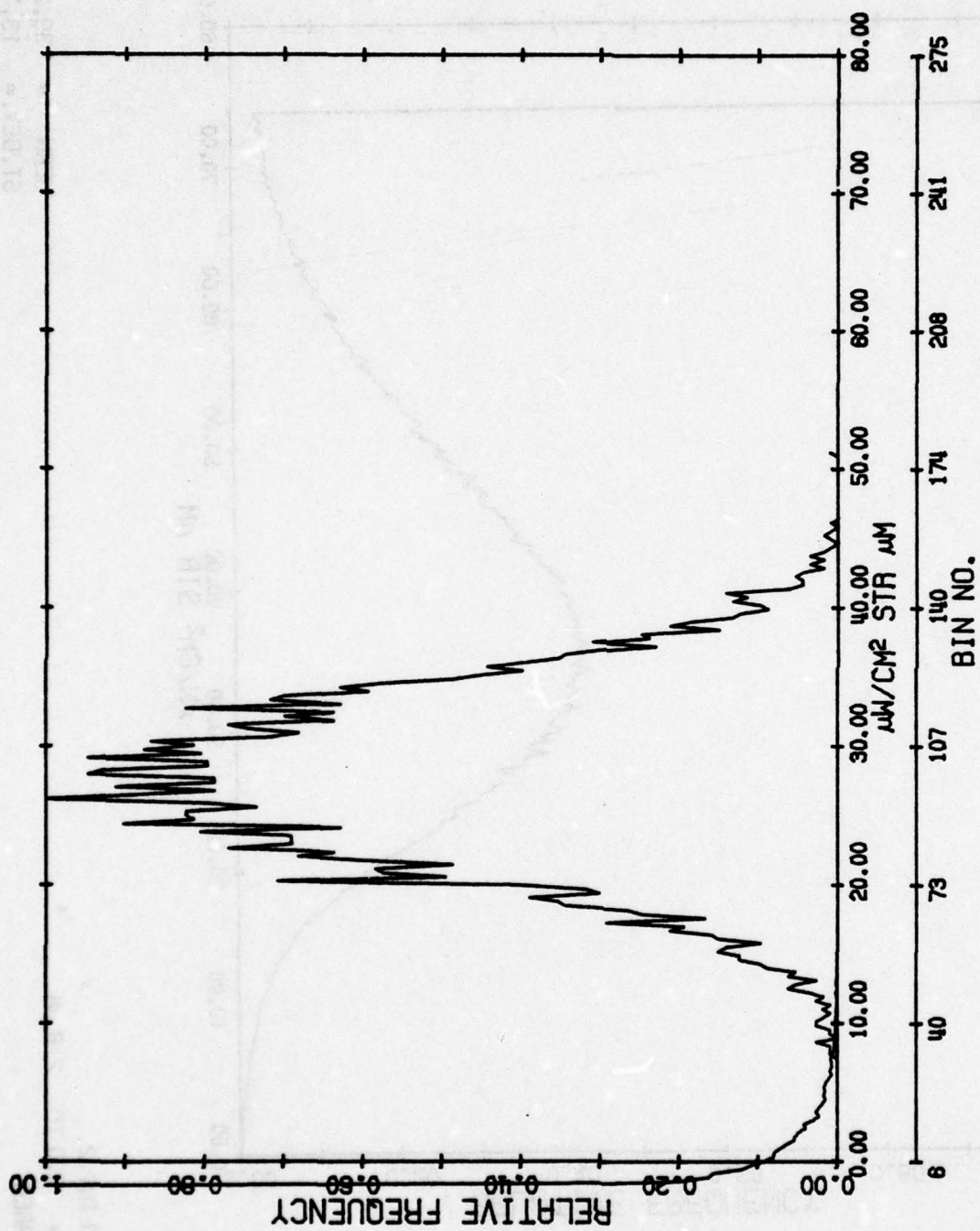


AREA: FLINT 2
WAVELENGTH= 2.0 TO 2.6 μm
SUBPLOTS

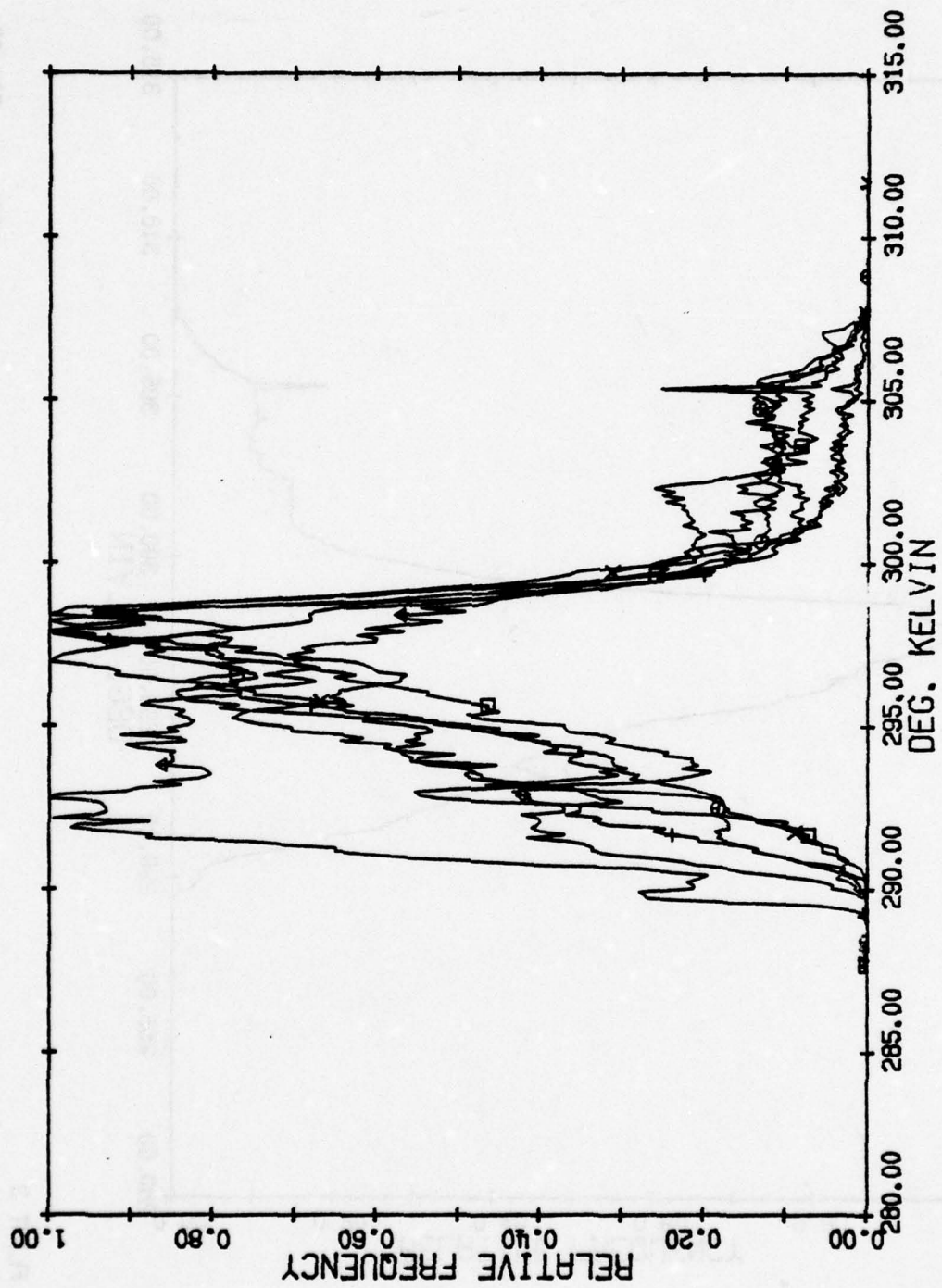


AREA: FLINT 2
WAVELENGTH= 2.0 TO 2.6 μm
TOTAL AREA

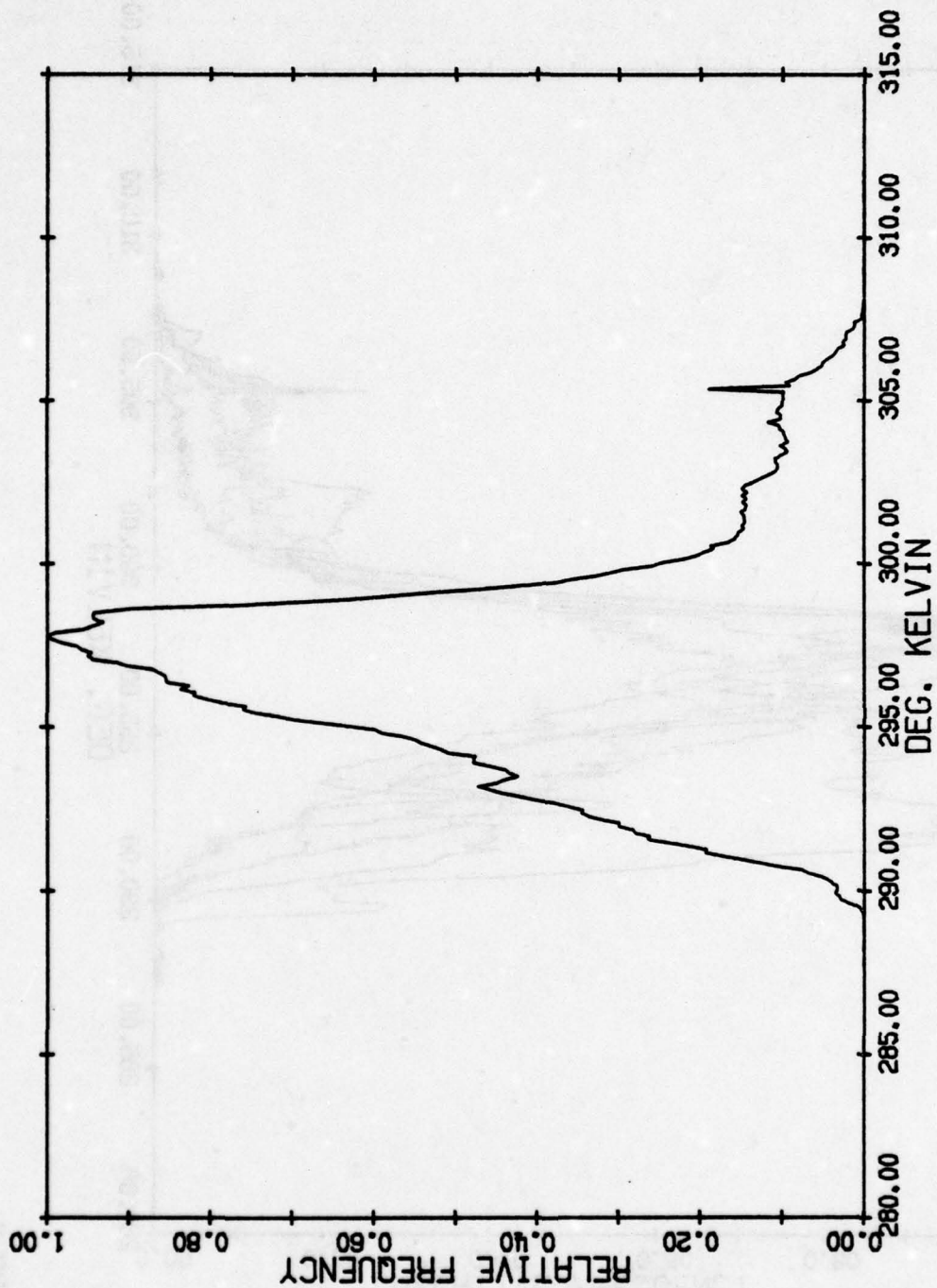
MEAN = 39.25
ST. DEV. = 13.75



AREA: FLINT 2
 LAMBDA= 2.0 TO 2.6 μm
 CALIB.PLATES

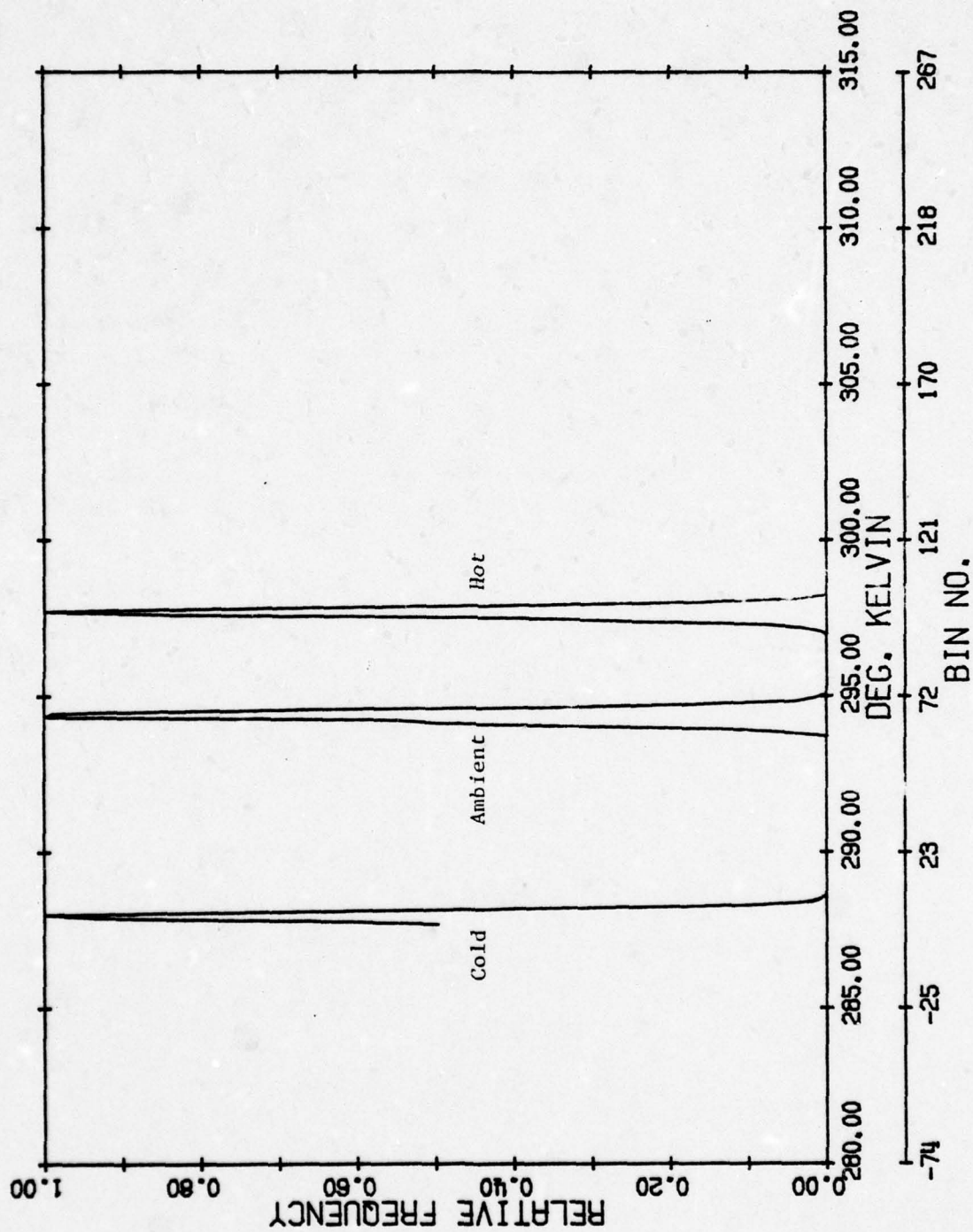


AREA: FLINT 2
LAMBDA= 9.3 TO 11.7 μ M
SUBAREAS



AREA: FLINT 2
WAVELENGTH= 9.3 TO 11.7 μ M
TOTAL AREA

MEAN = 297.00
ST.DEV.= 3.18



AREA: FLINT 2
 LAMBDA= 9.3 TO 11.7 μ M
 CALIB. PLATES

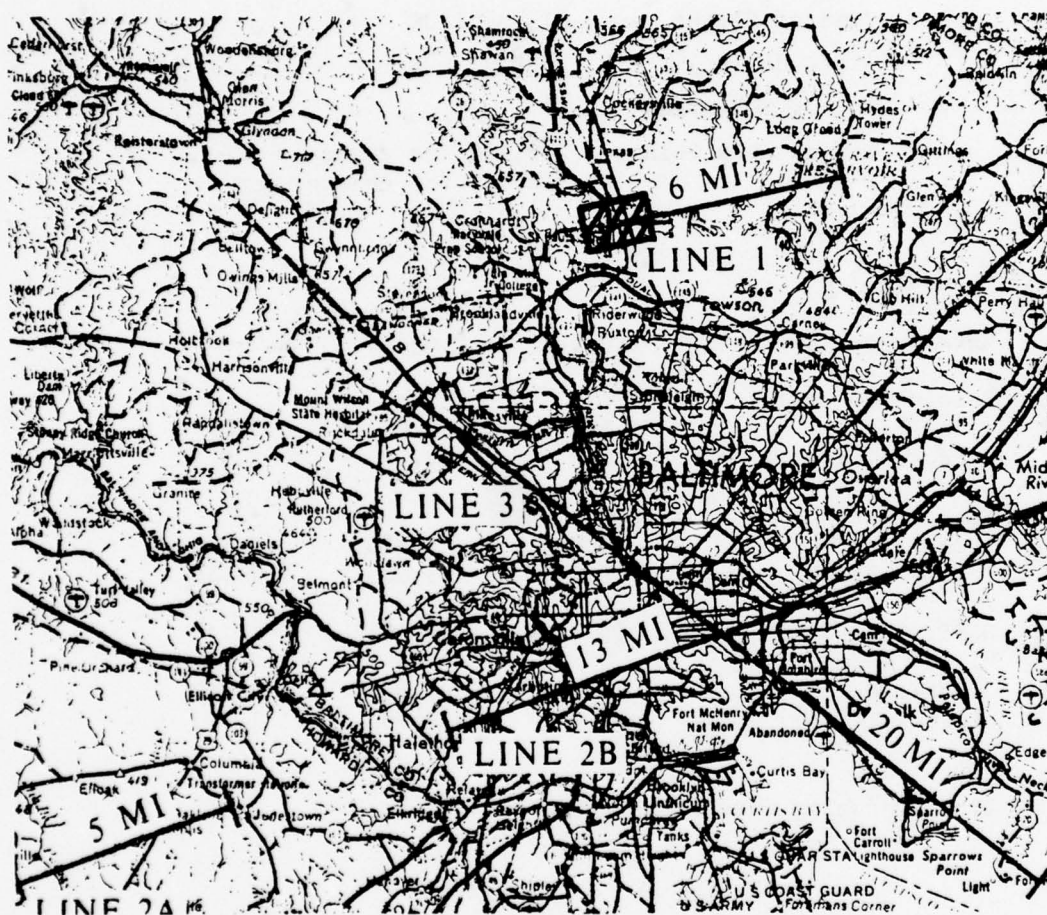
BALTIMORE*

Scene Type	Residential
Date of Flight	11 May 1972
Time of Flight	1137 - 1139
Altitude (Ft)	2500
No. of Sub-Areas	6
No. of Data Points	269,610 for channels 2,4 322,500 for channel 5

Channels	2	4	5
Wavelength (μm)	1.0-1.4	2.0-2.6	9.3-11.7
Resolution (mr)			
In-Track	5.0	5.0	5.0
Cross-Track	2.5	2.5	2.9
Nadir Pixel Dimensions (m)			
In-Track	3.810	3.810	3.810
Cross-Track	1.905	1.905	2.210
Nadir Ground Sample Distance (m)			
In-Track	3.810	3.810	3.810
Cross-Track	1.905	1.905	1.905

Line Averaging used for ALL channels.

*These data were obtained with the M-7 scanner. The 1.0-1.4 and 2.0-2.6 μm data are in spatial registration, but the 9.3-11.7 μm data were processed separately and are not in spatial registration with the 1.0-1.4 and 2.0-2.6 μm data. Hence, spectral correlation coefficients have not been determined between the 9.3-11.7 μm data and either the 1.0-1.4 μm or 2.0-2.6 μm data.



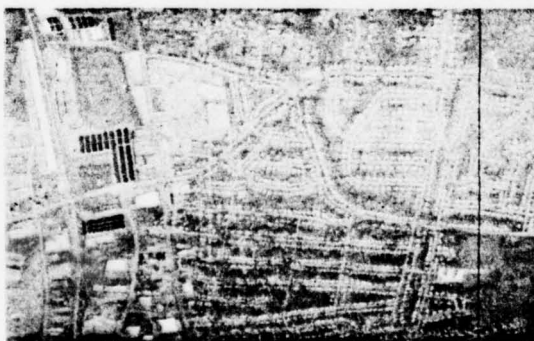
MAP OF THE BALTIMORE AREA SHOWING THE REGION COVERED IN THE BALTIMORE
RUN ABOUT FLIGHT LINE 1



1.0 - 1.4 μm

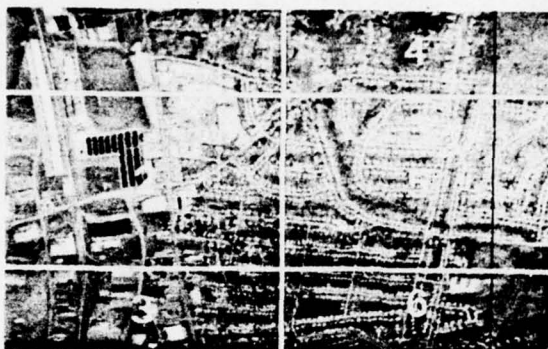


2.0 - 2.6 μm



9.3 - 11.7 μm

LINE SCAN IMAGES PRODUCED FROM THE VARIOUS
INFRARED CHANNELS OF BALTIMORE



Pixel 1

Pixel 161

Pixel 484

Pixel 645

Line 10

Line 213

Line 427 - Channels 2, 4

Line 1

Line 250

Line 500 - Channel 5

SUB-AREAS DEFINED FOR STATISTICS GENERATION IN THE BALTIMORE IMAGE. Uneven areas were chosen so that Areas 2 and 5 covered the $\pm 20^\circ$ range suitable for correlation. Approximate scene dimensions are 6250 ft (1905 m) by 4031 ft (1229 m) for channel 5 and 5225 ft (1592 m) by 4031 ft (1229 m) for channels 2 and 4. Each sub-area as well as the total area have been histogrammed. Histogram plots and their respective sub-areas are identified with the following key:

□ Sub-area 1

+ Sub-area 4

○ Sub-area 2

× Sub-area 5

△ Sub-area 3

◇ Sub-area 6

BALTIMORE
SUB-AREA 1

CORRELATION	2	4	
	2	1.000	
	4	-0.157	1.000
CHANNELS	2	4	11
MEAN	2.4955E103	9.3149E+01	2.9940E+02
ST. DEV.	8.0187E102	4.8381E+01	6.2943E+00
TOTAL PTS.	32640.	32640.	40000.

BALTIMORE
SUB-AREA 2

CORRELATION	2	4	
2	1.000		
4	0.174	1.000	
CHANNELS	2	4	11
MEAN	1.9511E+03	1.0001E+02	2.9934E+02
ST. DEV.	7.1298E+02	5.5234E+01	6.3927E+00
TOTAL PTS.	65892.	65892.	80750.

BALTIMORE
SUB-AREA 3

CORRELATION	2	4	
2	1.000		
4	0.263	1.000	
CHANNELS	2	4	11
MEAN	1.5689E+03	7.3852E+01	2.9896E+02
ST. DEV.	5.9838E+02	4.3159E+01	5.2225E+00
TOTAL PTS.	33048.	33048.	40500.

BALTIMORE
SUB-AREA 4

CORRELATION	2	4	5
2	1.000		
4	-0.119	1.000	
5			1.000
CHANNELS	2	4	11
MEAN	2.7111E+03	7.5269E+01	2.0001E+02
ST. DEV.	0.2703E+02	2.8960E+01	4.9329E+00
TOTAL PTS.	34240.	34240.	44000.

BALTIMORE
SUB-AREA 5

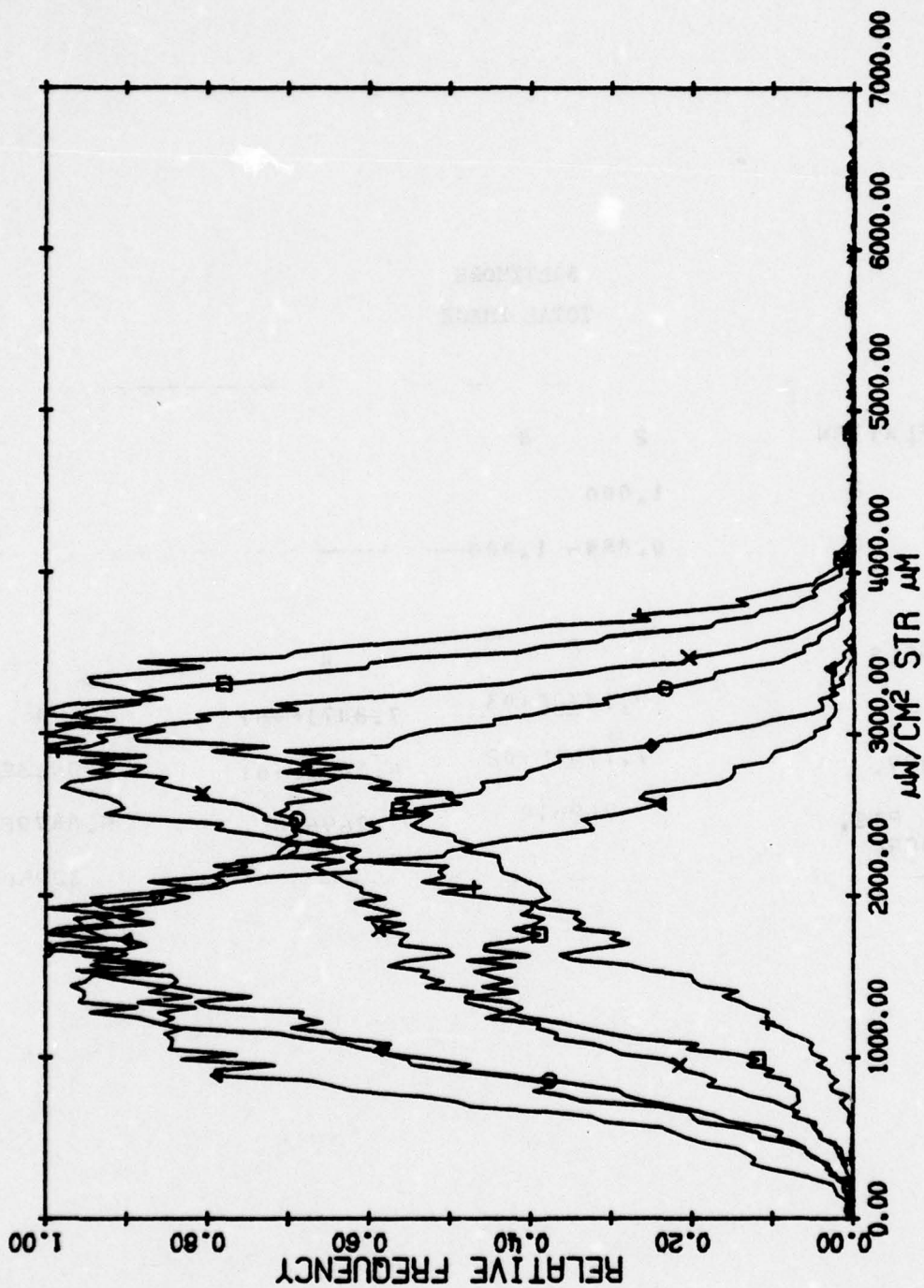
CORRELATION	2	4	11
-2	1.000		
-4	0.075	1.000	
CHANNELS	2	4	11
MEAN	2.2956E+03	6.7554E+01	3.0025E+02
ST. DEV.	7.1763E+02	2.8608E+01	5.7796E+00
TOTAL PTS.	69122.	69122.	80750.

BALTIMORE
SUB-AREA 6

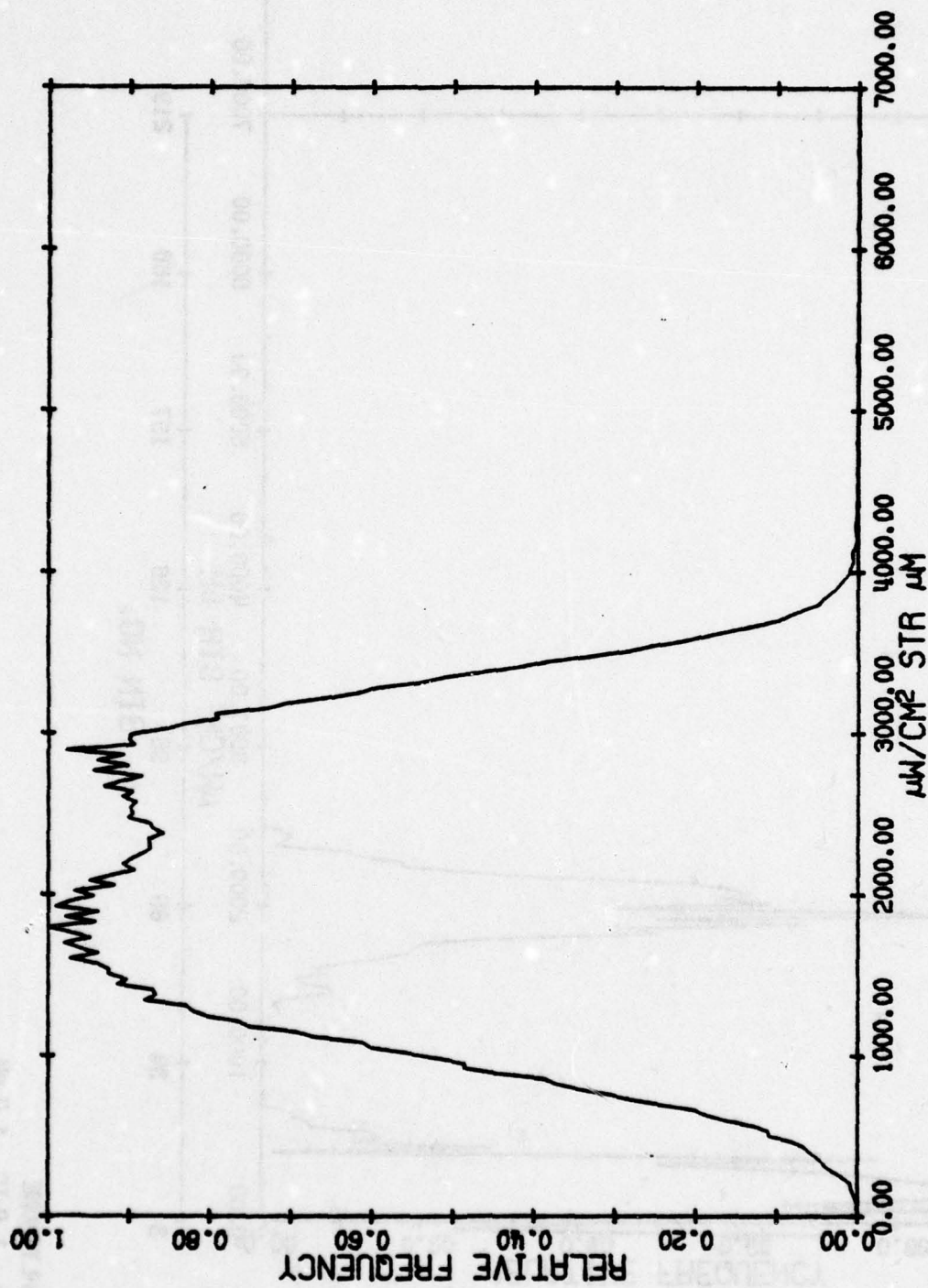
CORRELATION	2	4	
2	1.000		
4	0.235	1.000	
CHANNEL 9-	2	4	11
MEAN	1.7814E+03	5.3057E+01	2.9648E+02
ST. DEV.	6.1299E+02	2.7117E+01	5.2716E+00
TOTAL PTS.	34668.	34668.	40500.

BALTIMORE
TOTAL IMAGE

CORRELATION	2	4	
2	1.000		
4	0.084	1.000	
CHANNELS	2	4	
MEAN -	2.1332E+03	7.8471E+01	11
SI. DEV.	1.7751E+02	4.3876E+01	2.9913E+02
TOTAL PTS. BALTIMORE	269610	269610	5.8879E+00
			322500

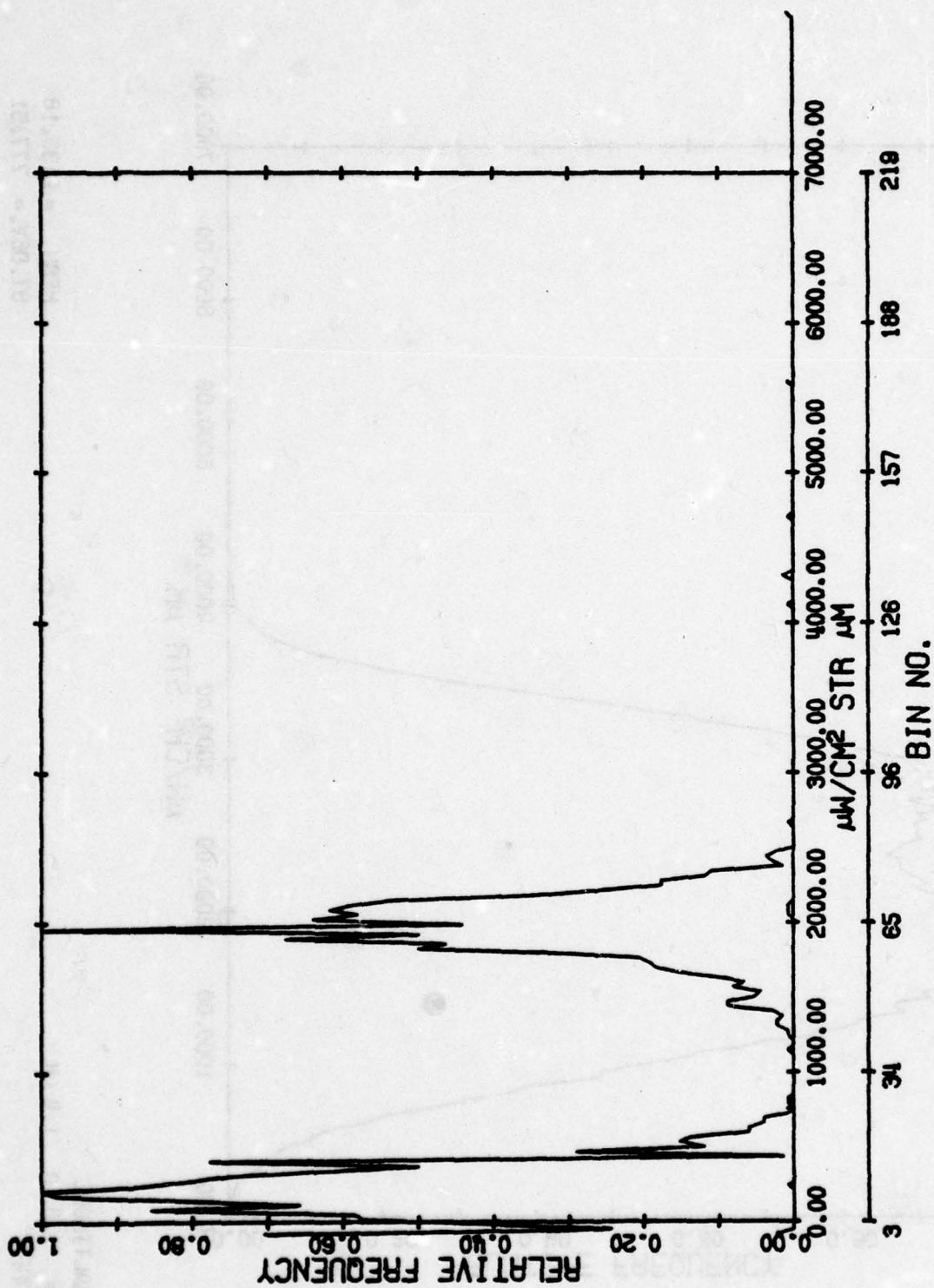


AREA: BALTIMORE
LABOR= 1.0 TO 1.4 μm
SUBPERS

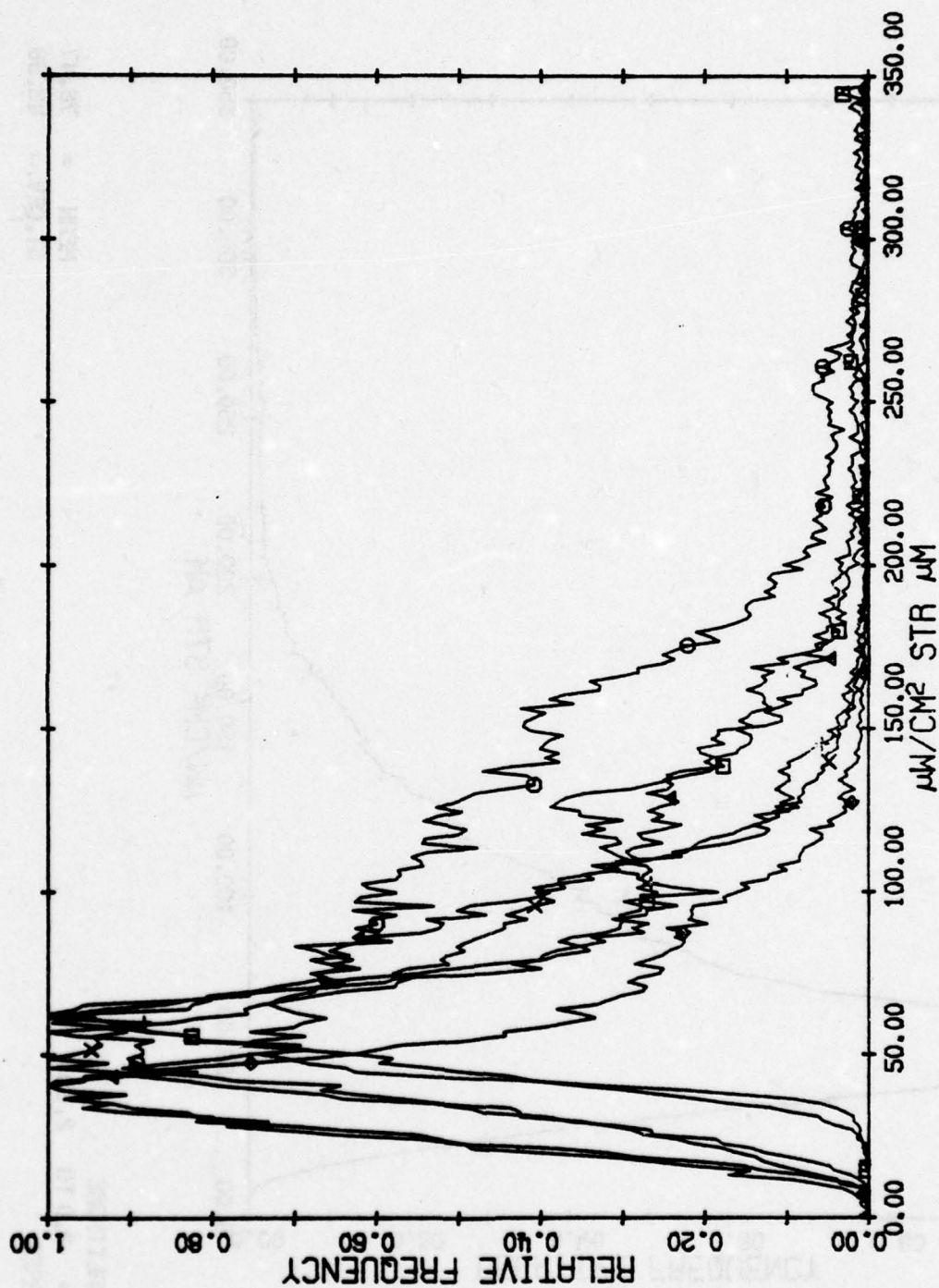


MEAN = 2139.18
ST.DEV. = 777.51

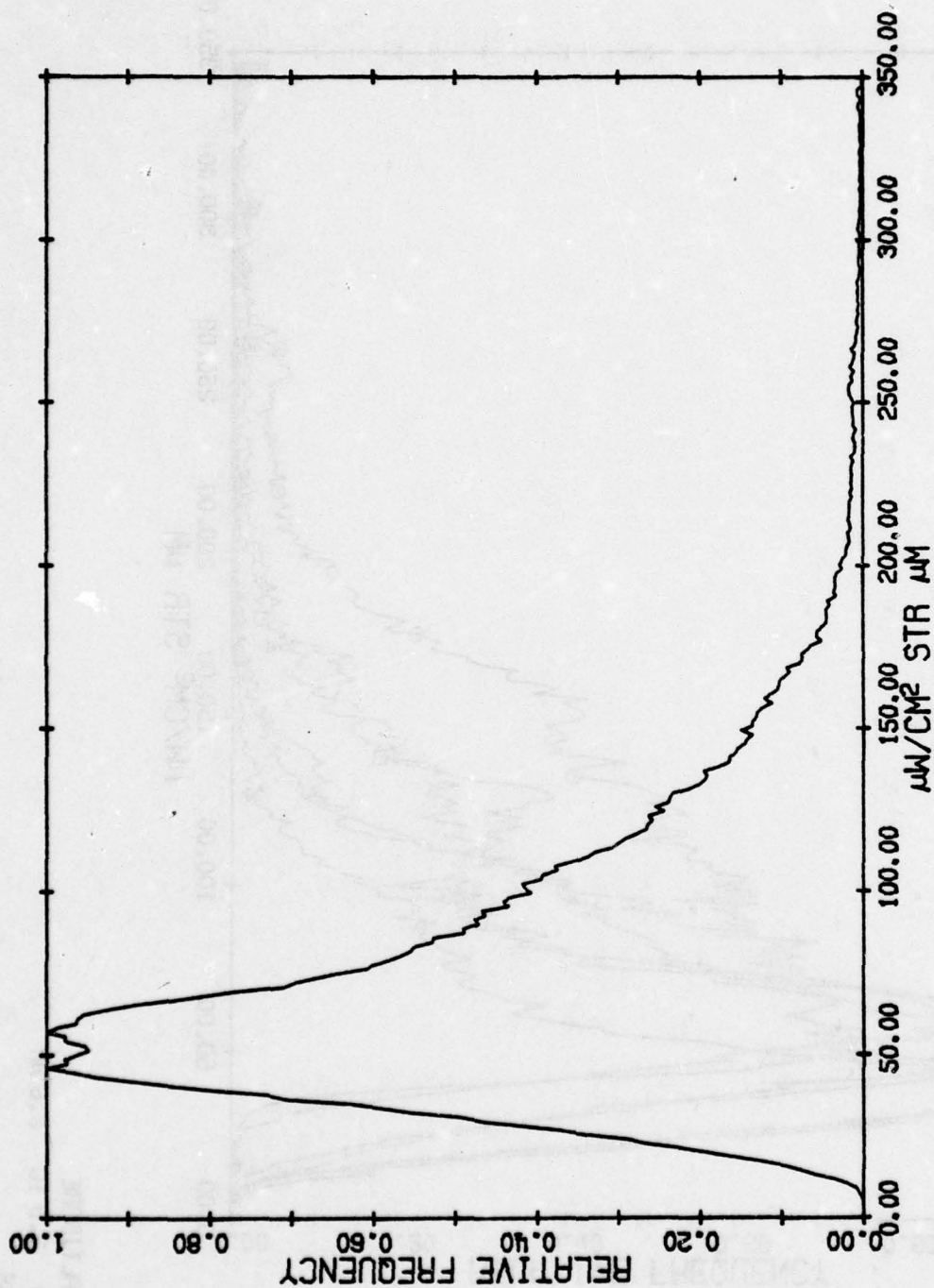
AREA: BALTIMORE
WAVES: 1.0 TO 1.4 μm
TOTAL AREA



AREA: BALTIMORE
 WAVELENGTH: 1.0 TO 1.4 μm
 CALIB. PLATES

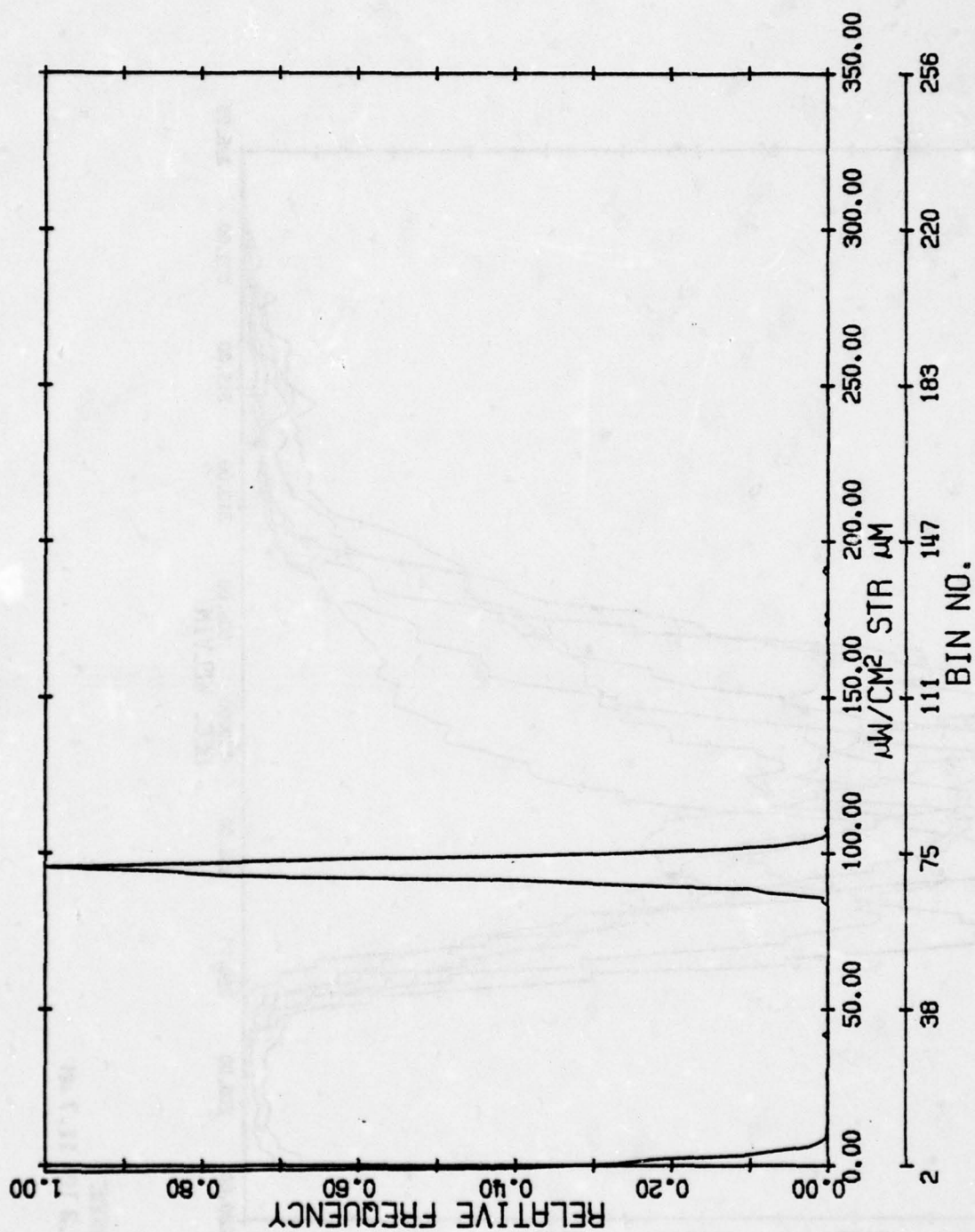


AREA: BALTIMORE
 LAMBDA= 2.0 TO 2.6 μm
 SUBAREAS

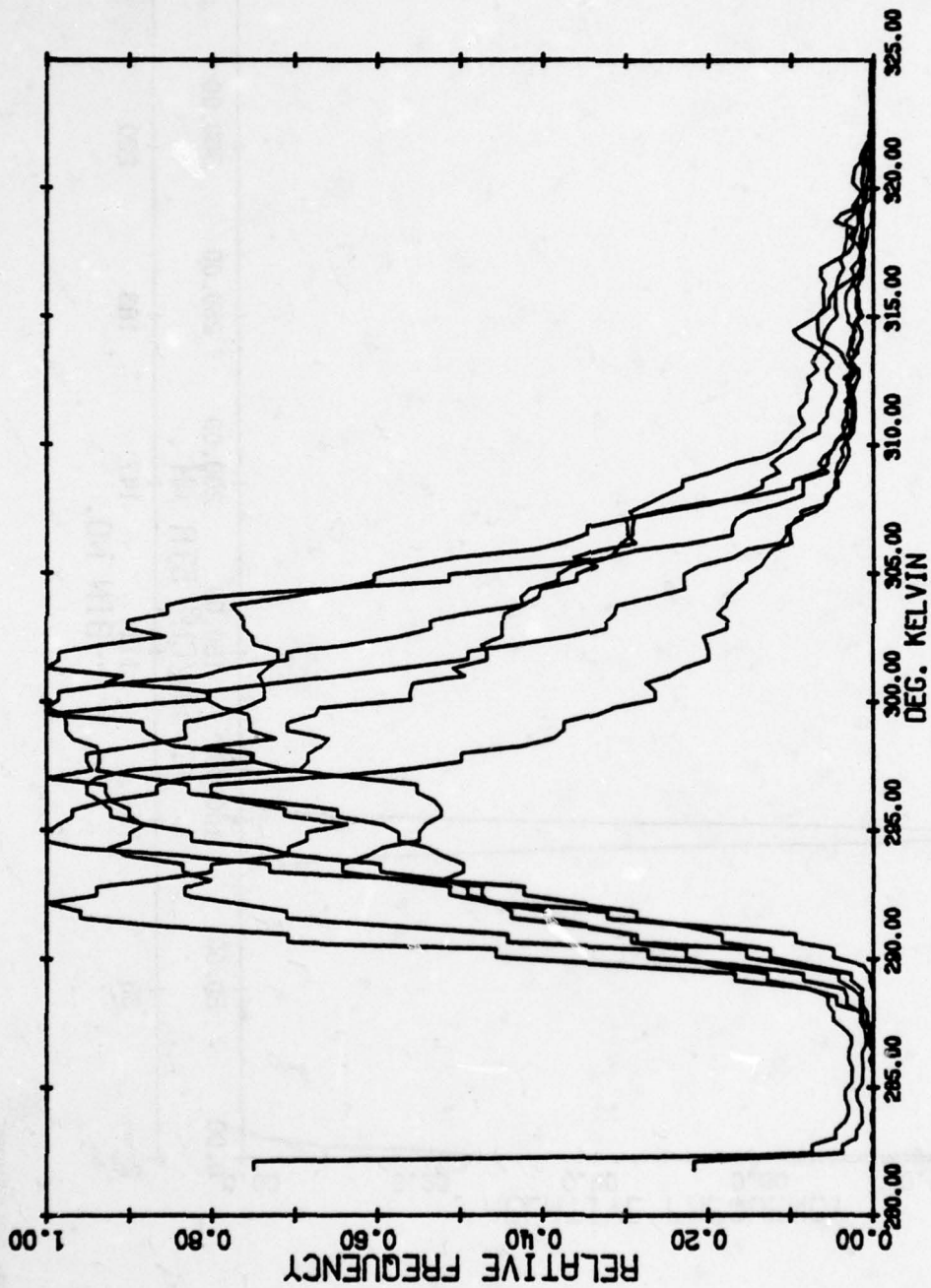


AREA: BALTIMORE
 LAMBDA= 2.0 TO 2.6 μm
 TOTAL AREA

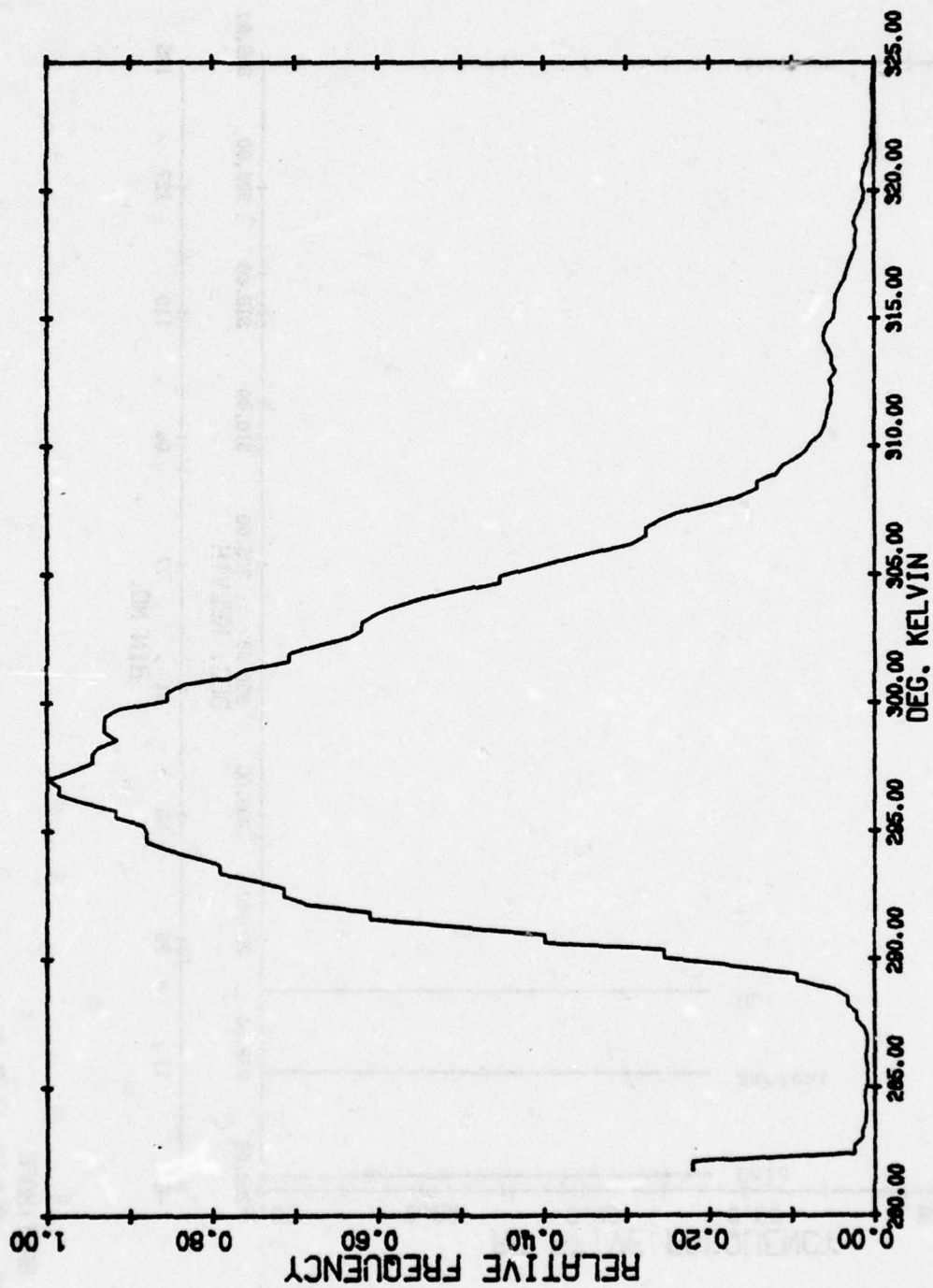
MEAN = 78.47
 ST.DEV.= 43.88



AREA: BALTIMORE
 LAMBDA= 2.0 TO 2.6 μM
 CALIB. PLATES

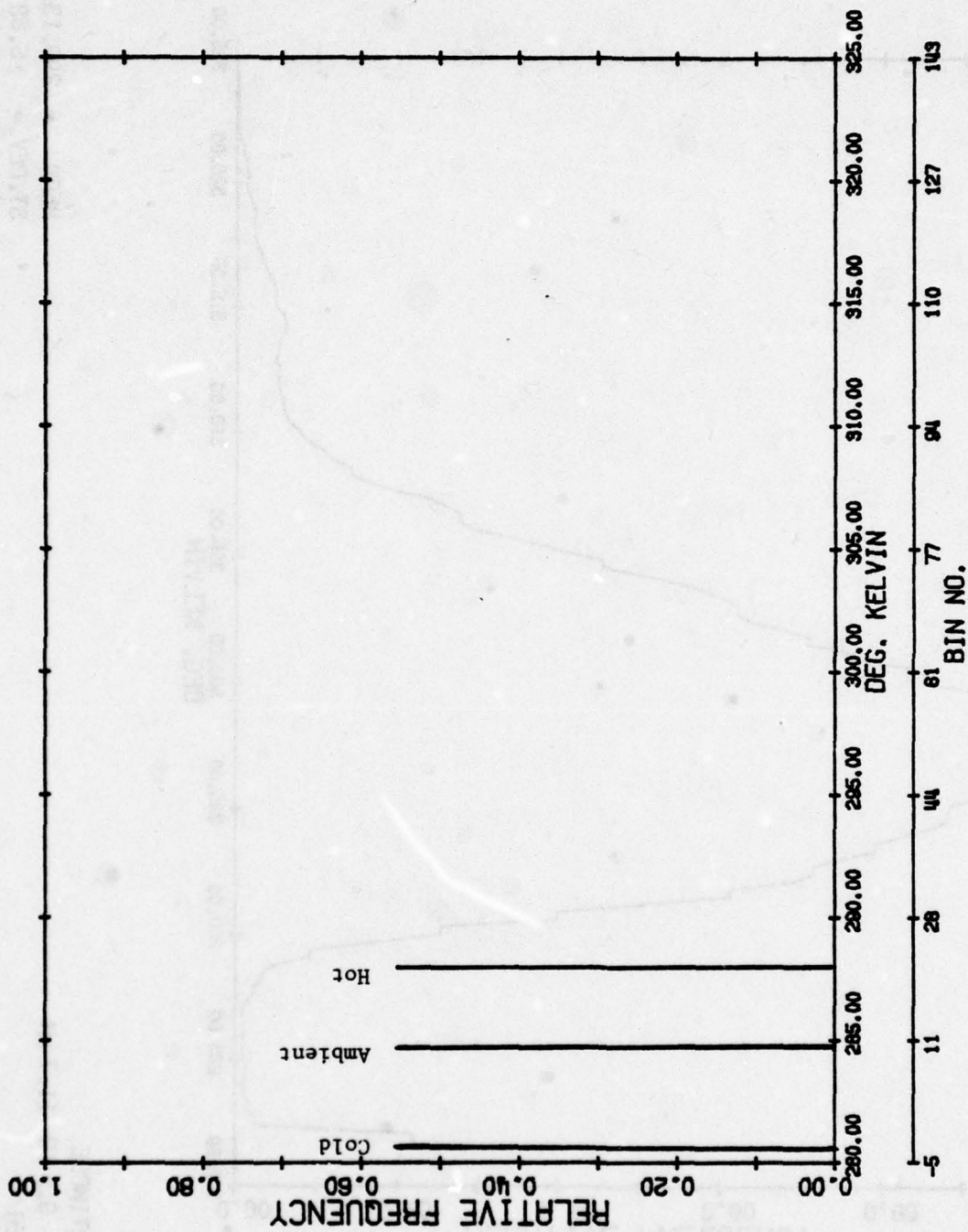


AREA: BALTIMORE
LAMBDA= 9.3 TO 11.7 μ M
SUBAREAS



MEAN = 299.13
ST. DEV. = 5.89

AREA: BALTIMORE
LAMBDA = 9.3 TO 11.7 μ M
TOTAL AREA



AREA: BALTIMORE
 LAMBDA= 9.3 TO 11.7 μ M
 CALIB. PLATES

MILL CREEK*

Scene Type	Mountainous
Date of Flight	30 June 1972
Time of Flight	0733 - 0736
Altitude (Ft)	3000
No. of Sub-Areas	6
No. of Data Points	171,570

Channels	2	3	4	5
Wavelength (m)	1.0-1.4	1.5-1.8	2.0-2.6	9.3-11.7
Resolution (mr)				
In-Track	5.0	5.0	5.0	5.0
Cross-Track	2.5	2.5	2.5	2.9
Nadir Pixel Dimensions (m)				
In-Track	4.572	4.572	4.572	4.572
Cross Track	2.286	2.286	2.286	2.652
Nadir Ground Sample Distance (m)				
In-Track	4.572	4.572	4.572	4.572
Cross-Track	2.286	2.286	2.286	2.286

Line Averaging used for ALL channels.

*These data were obtained with the M-7 scanner. All data are in spatial registration



1.0 - 1.4 μm



1.5 - 1.8 μm

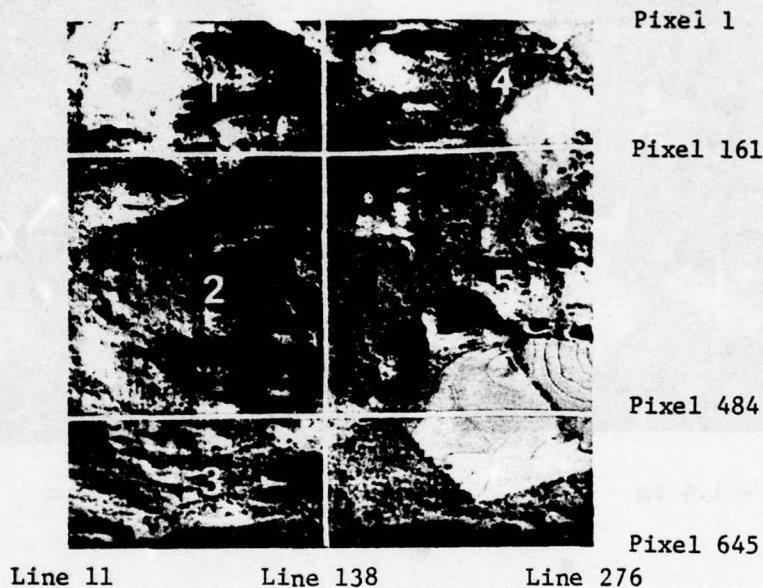


2.0 - 2.6 μm



9.3 - 11.7 μm

LINE SCAN IMAGES PRODUCED FROM THE VARIOUS INFRARED CHANNELS OF MILL CREEK



SUB-AREAS DEFINED FOR STATISTICS GENERATION IN THE MILL CREEK IMAGE. Uneven areas were chosen so that Areas 2 and 5 covered the $\pm 20^\circ$ range suitable for correlation. Approximate scene dimensions are 3990 ft (1216 m) in-track by 4837 ft (1474 m) cross-track. Each sub-area as well as the total area have been histogrammed. Histogram plots and their respective sub-areas are identified with the following key:

- | | |
|--------------|--------------|
| ▣ Sub-area 1 | + Sub-area 4 |
| ○ Sub-area 2 | × Sub-area 5 |
| ▲ Sub-area 3 | ◇ Sub-area 6 |

MILL CREEK
SUB-AREA 1

CIRCULATION	2	3	4	5
2	1.000			
3	0.925	1.000		
4	0.959	0.919	1.000	
5	0.589	0.653	0.634	1.000

CHANFLS	2	3	4	5
MEAN	1.1053E+02	3.9088E+01	5.2601E+00	2.9907E+02
ST. DEV.	8.2802E+01	2.8063E+01	4.4031E+00	1.0911E+00
TOTAL PTS.	20480.	20480.	20480.	20480.

MILL CREEK
SUB-AREA 2

CORRELATION	2	3	4	5
2	1.000			
3	0.812	1.000		
4	0.895	0.834	1.000	
5	0.169	0.361	0.305	1.000

II-88

CHANNELS	2	3	4	5
MEAN	6.3868F+01	2.1860F+01	2.2662E+00	2.9840F+02
ST. DEV.	4.3890F+01	1.4143F+01	1.8549F+00	9.9308F-01
TOTAL PTS.	41344.	41344.	41344.	41344.

MILL CREEK
SUB-AREA 3

CORRELATION	2	3	4	5
2	1.000			
3	0.648	1.000		
4	0.829	0.717	1.000	
5	0.138	0.500	0.345	1.000

CHANNELS	2	3	4	5
MEAN	1.3055F+02	3.7570F+01	4.1033F+00	2.9787E+02
ST. DEV.	5.0883F+01	1.4356F+01	1.6939F+00	8.5154E-01
TOTAL PTS.	20736.	20736.	20736.	20736.

MILL CREEK

SUB-AREA 4

CORRELATION	2	3	4	5
2	1.000			
3	0.749	1.000		
4	0.767	0.863	1.000	
5	0.217	0.405	0.346	1.000

CHANNELS	2	3	4	5
MEAN	1.3146E+02	4.2616E+01	5.0519E+00	2.9781E+02
ST. DEV.	5.7894E+01	2.0884E+01	3.2356E+00	7.8850E-01
TOTAL PTS.	22080.	22080.	22080.	22080.

MILL CREEK
SUB-AREA 5

CORRELATION	2	3	4	5
2	1.000			
3	0.779	1.000		
4	0.668	0.845	1.000	
5	0.094	0.302	0.260	1.000

CHANNELS	2	3	4	5
MEAN	1.1835E+02	3.7550E+01	4.2318E+00	2.9794E+02
ST. DEV.	5.4105E+01	1.7685E+01	2.4486E+00	7.6937E-01
TOTAL PTS.	44574.	44574.	44574.	44574.

MILL CREEK
SUB-AREA 6

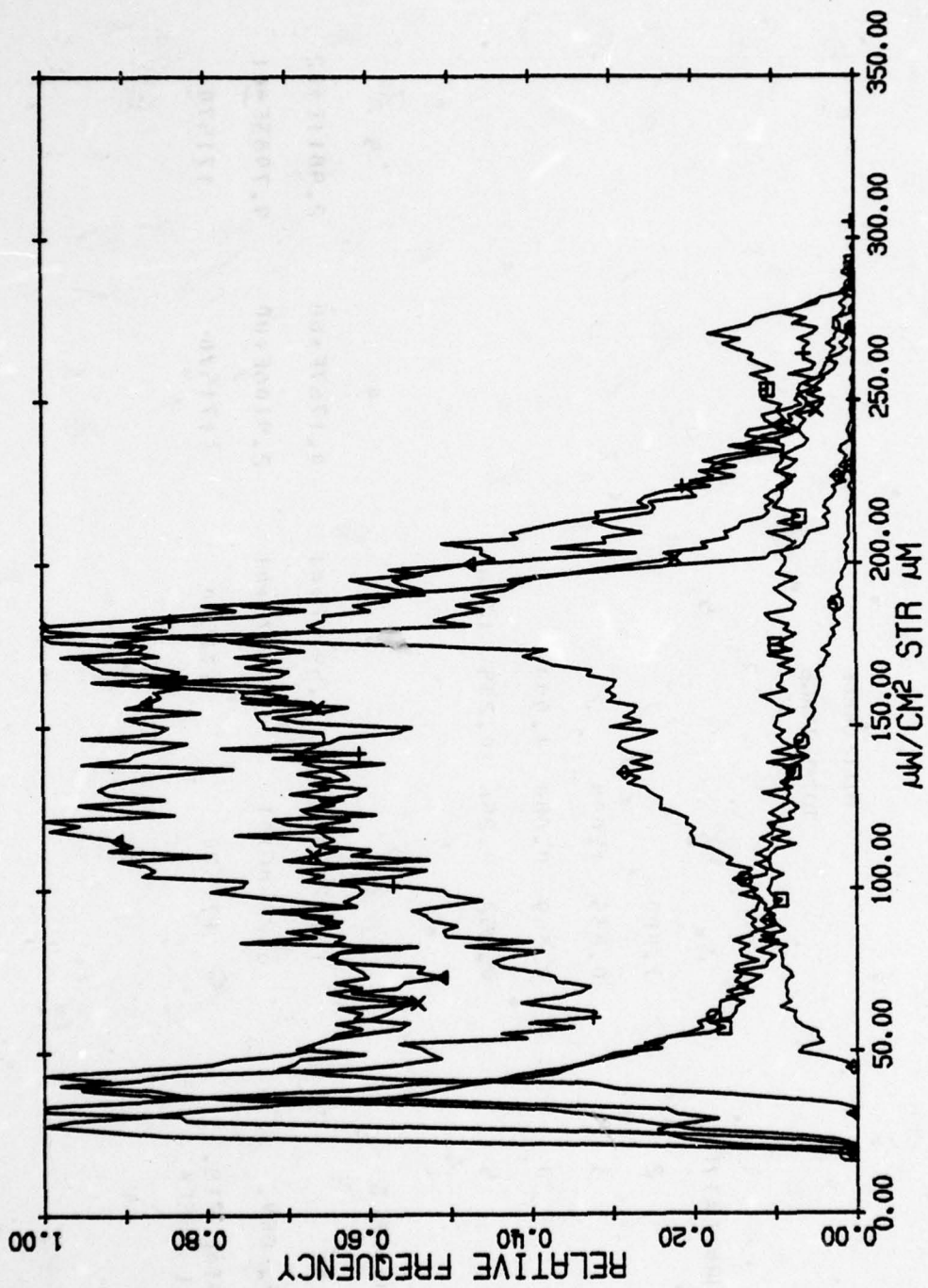
CORRELATION	2	3	4	5
2	1.000			
3	0.702	1.000		
4	0.732	0.859	1.000	
5	0.125	0.424	0.368	1.000

CHANNELS	2	3	4	5
MEAN	1.5479E+02	4.7611E+01	5.8111E+00	2.9752E+02
ST. DEV.	3.8400E+01	1.0965E+01	2.1549E+00	6.5507E-01
TOTAL PTS.	22356.	22356.	22356.	22356.

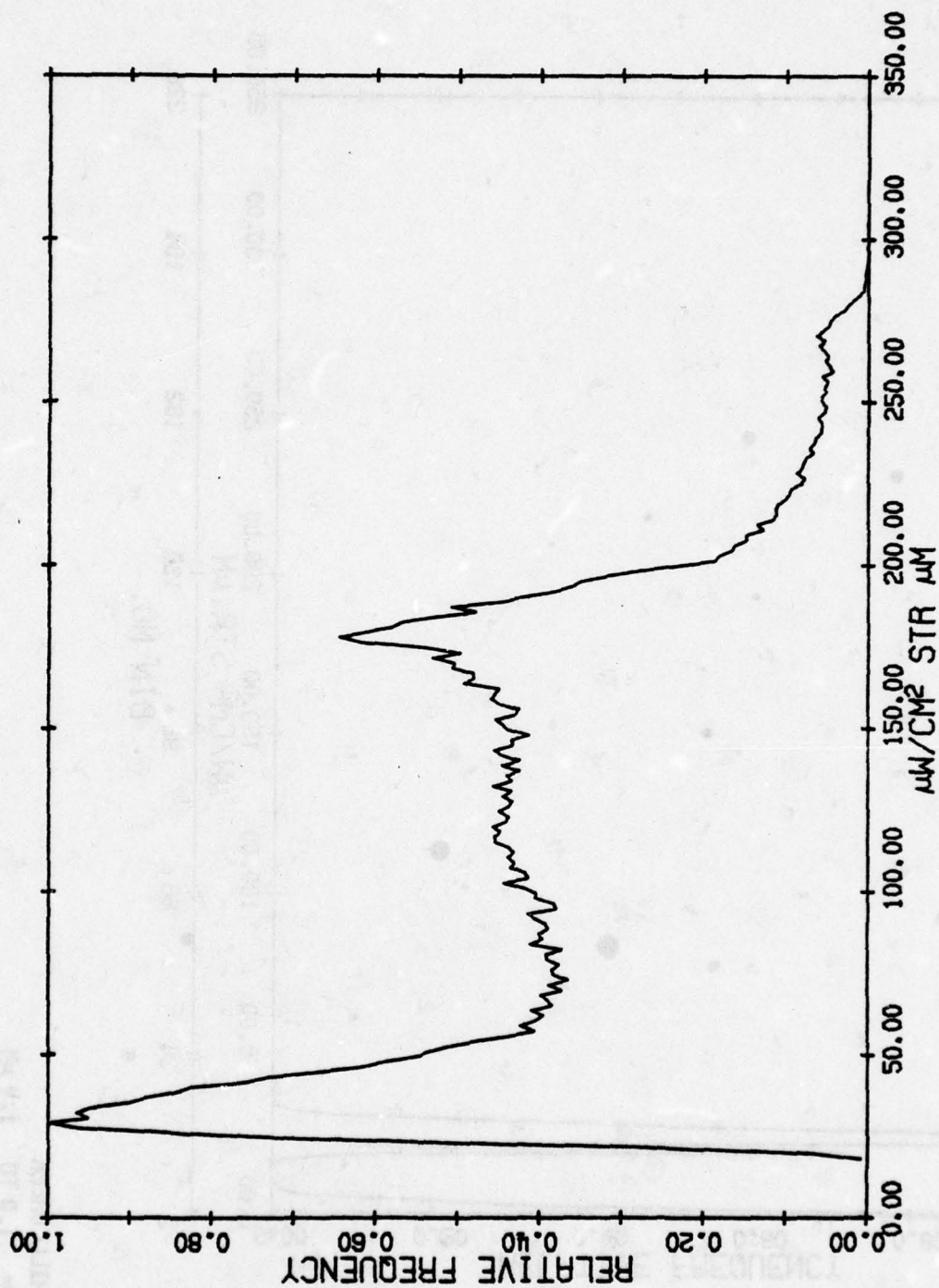
MILL CREEK
TOTAL IMAGE

CORRELATION	2	3	4	5
2	1.000			
3	0.835	1.000		
4	0.860	0.880	1.000	
5	0.052	0.256	0.245	1.000

CHANNELS	2	3	4	5
MEAN	1.1220E+02	3.5919E+01	4.1767E+00	2.9811E+02
ST. DEV.	0.2268E+01	2.0177E+01	2.9106E+00	9.7983E-01
TOTAL PTS. MILL CREEK	171570	171570	171570	171570

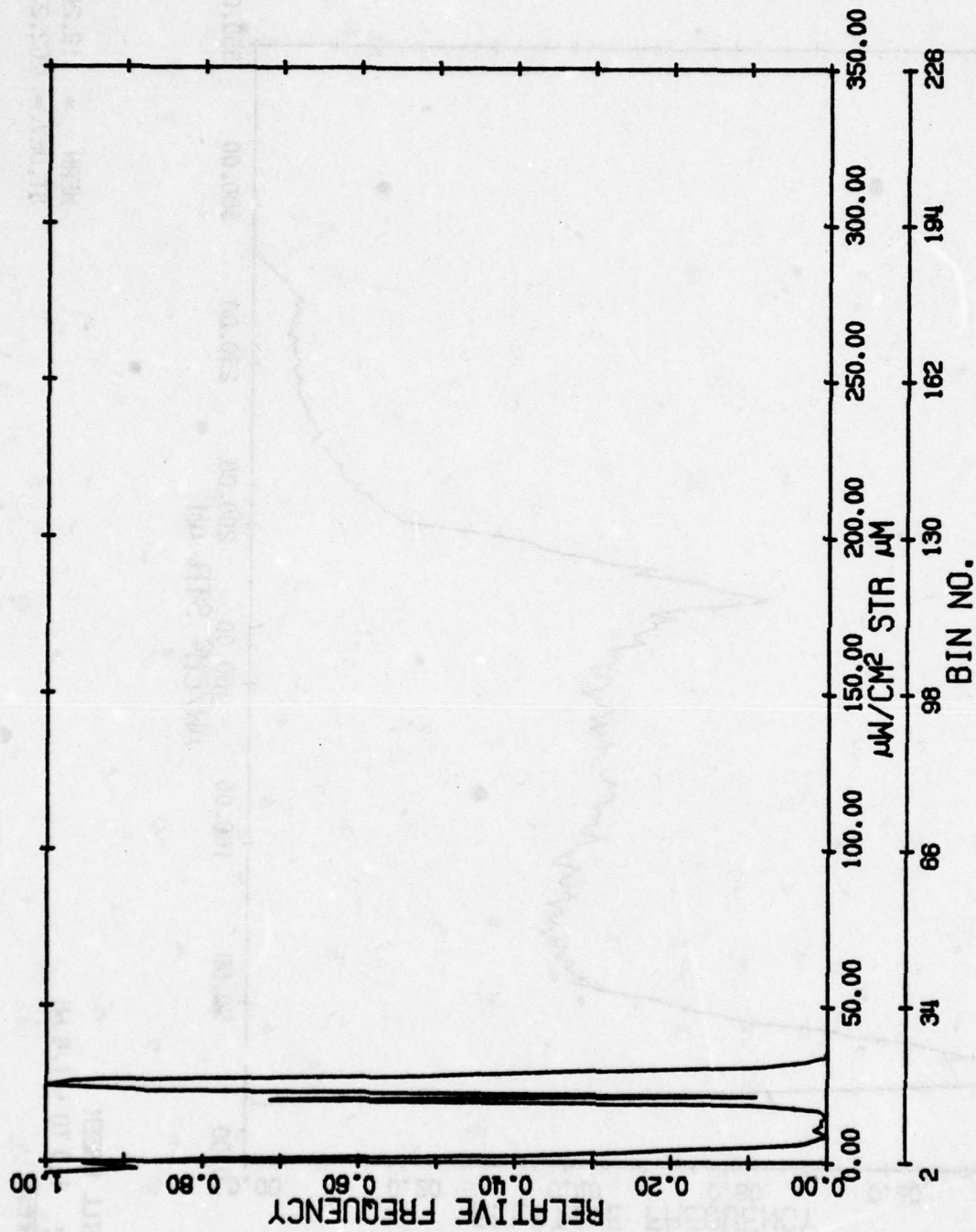


ARERIK MILL CREEK
LAMBDA= 1.0 TO 1.4 μm
SUBPAPERS

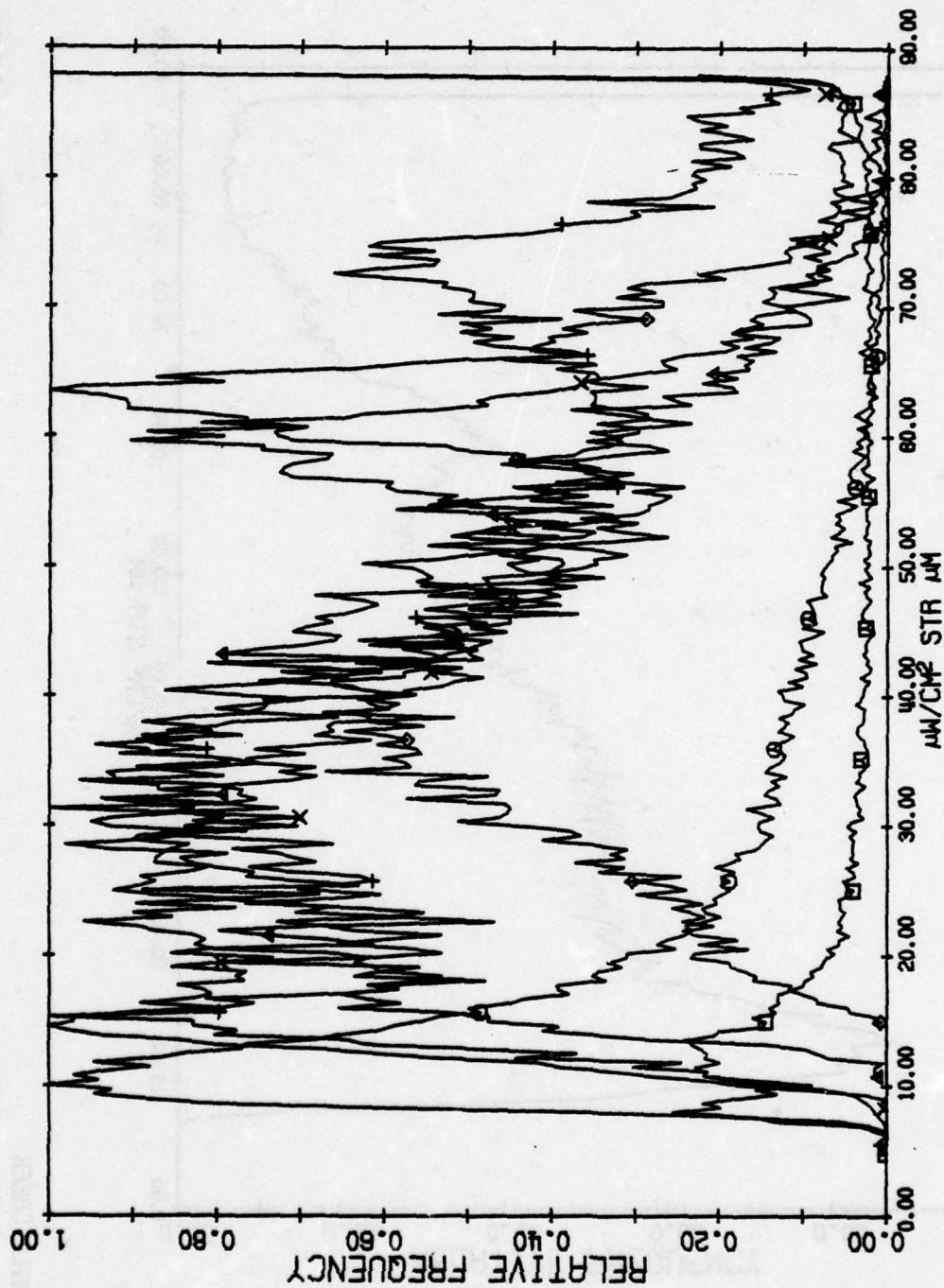


AREA: MILL CREEK
WAVELENGTH= 1.0 TO 1.4 μm
TOTAL AREA

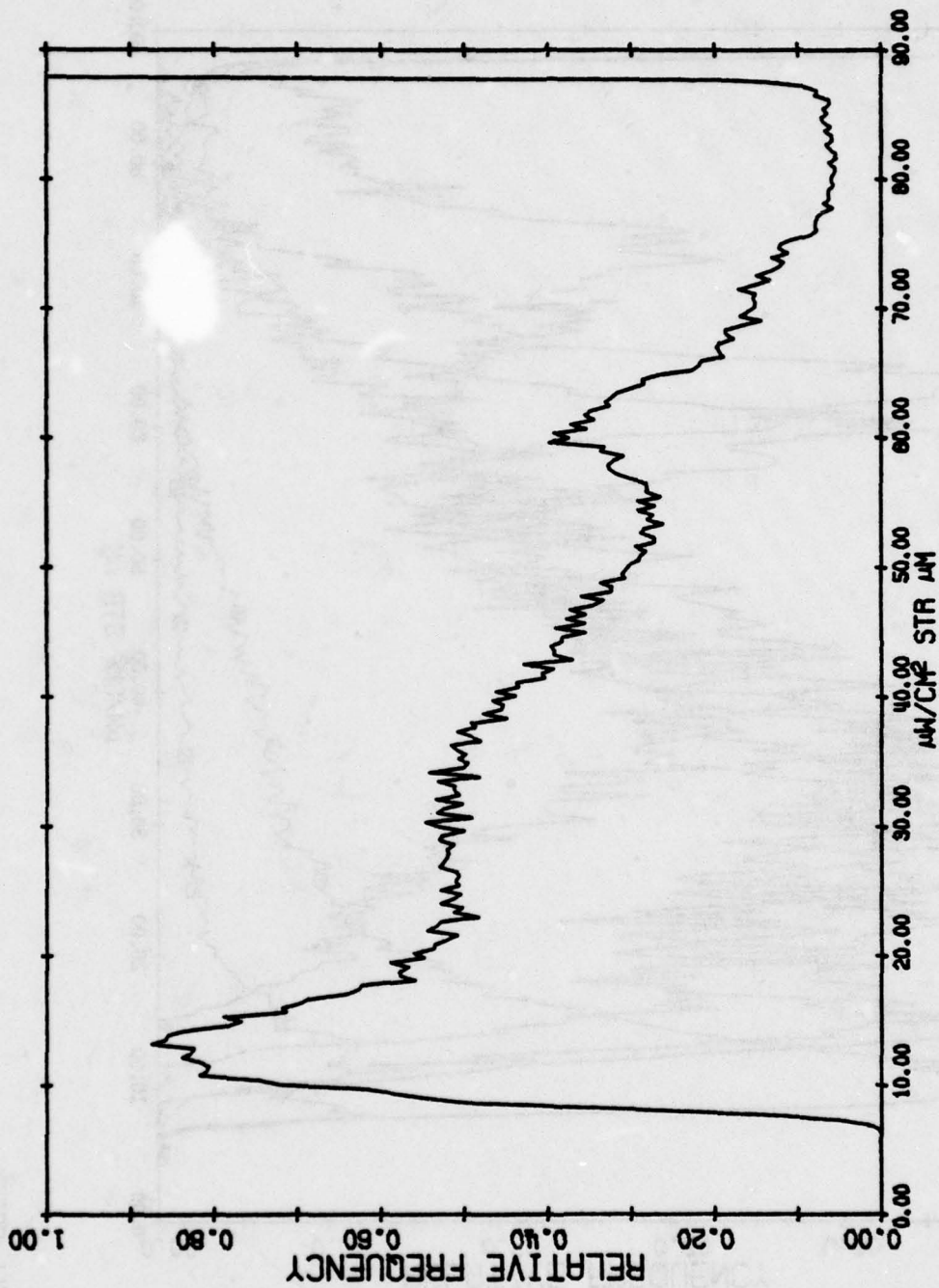
MEAN = 112.20
ST. DEV. = 62.27



AREA: MILL CREEK
WAVELENGTH= 1.0 TO 1.4 μm
CALIB. PLATES

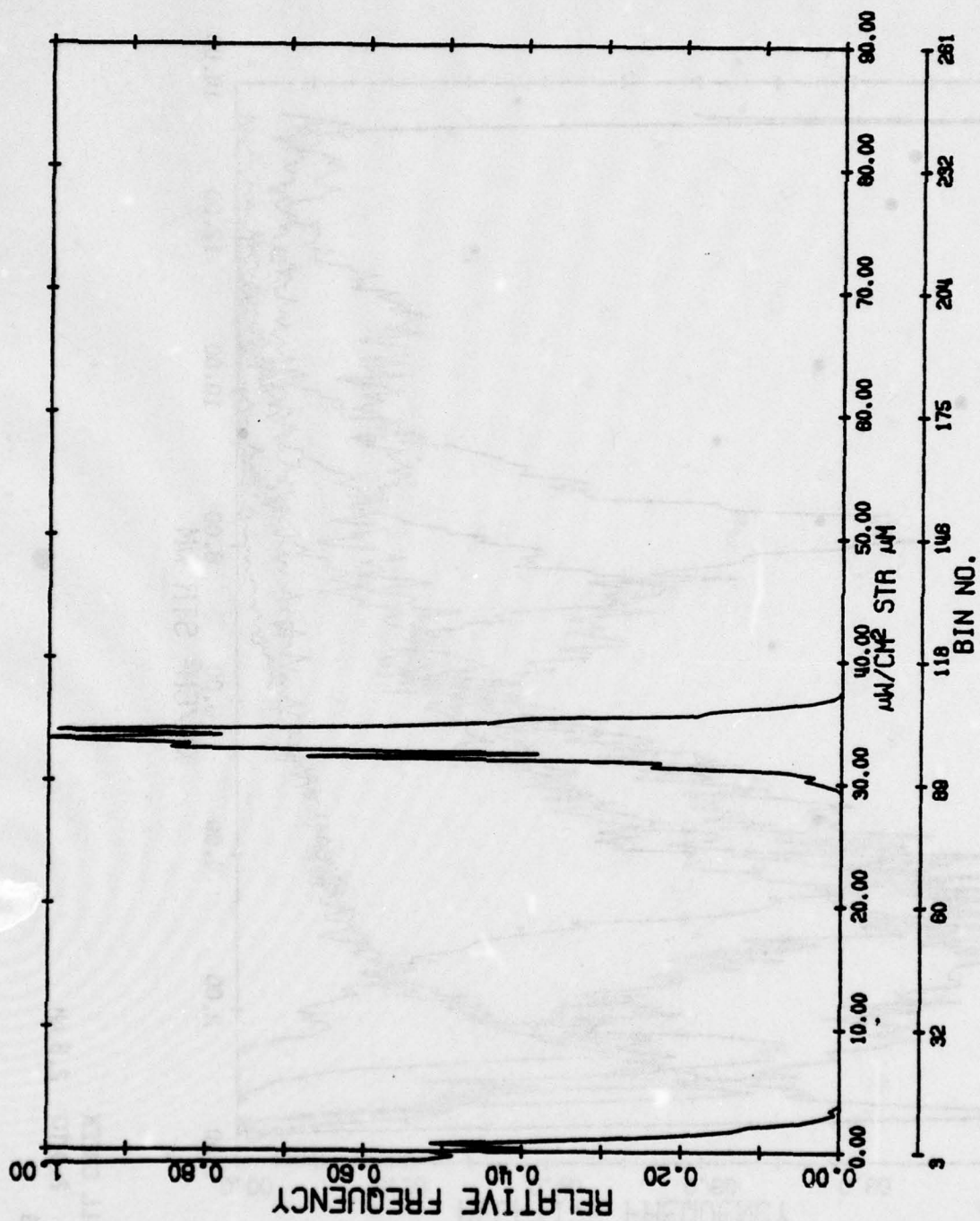


AREA: MILL CREEK
LAMBDA= 1.5 TO 1.8 μm
SUBAREAS

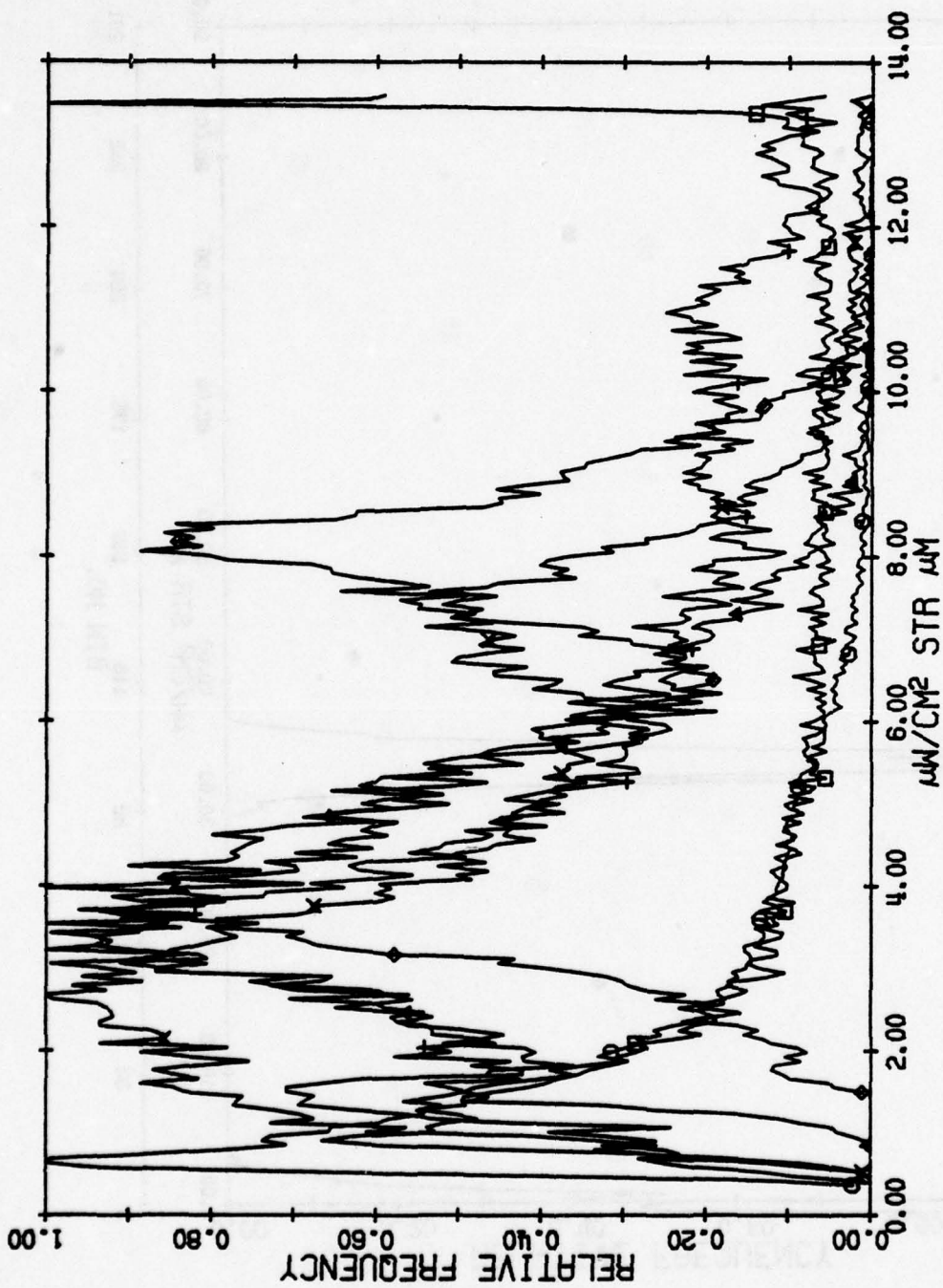


AREA 1 MILL CREEK
 LAMBDA= 1.5 TO 1.8 μm
 TOTAL AREA

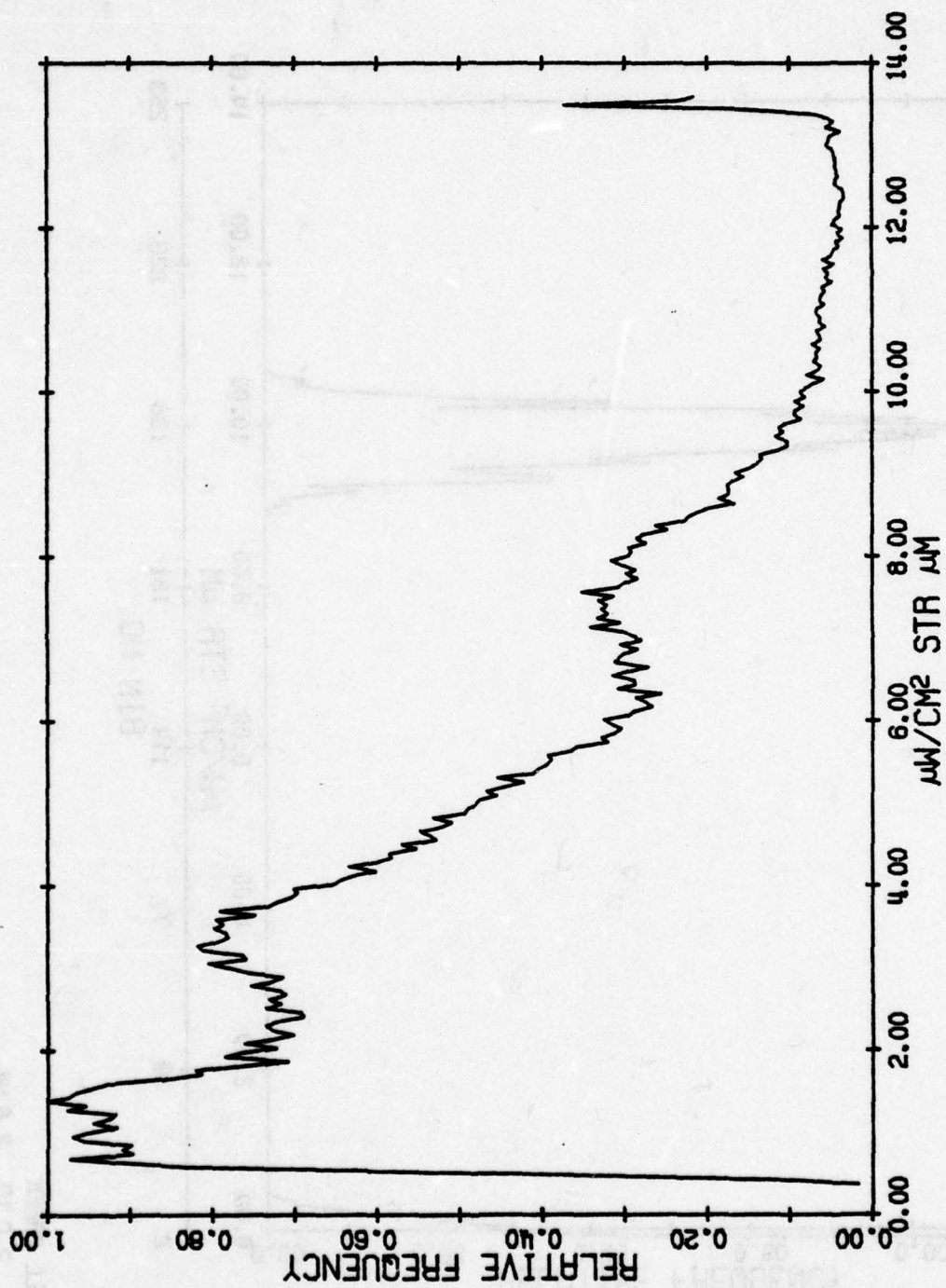
MEAN = 35.92
 ST. DEV. = 20.18



AREA: MILL CREEK
 WAVELENGTH= 1.5 TO 1.8 μm
 CALIB. PLATES

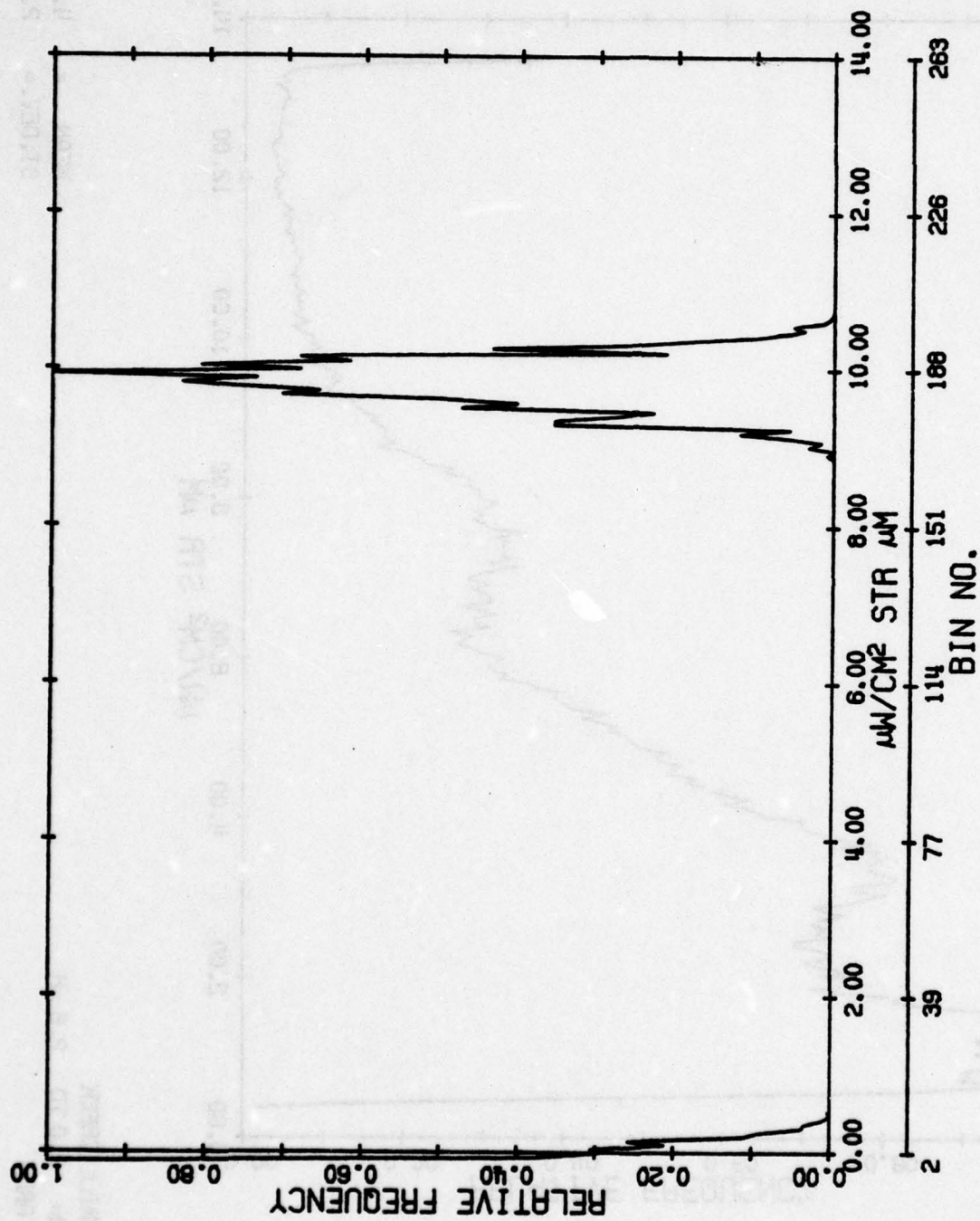


AREA: MILL CREEK
WAVELENGTH 2.0 TO 2.6 μm
SUBPLOTS

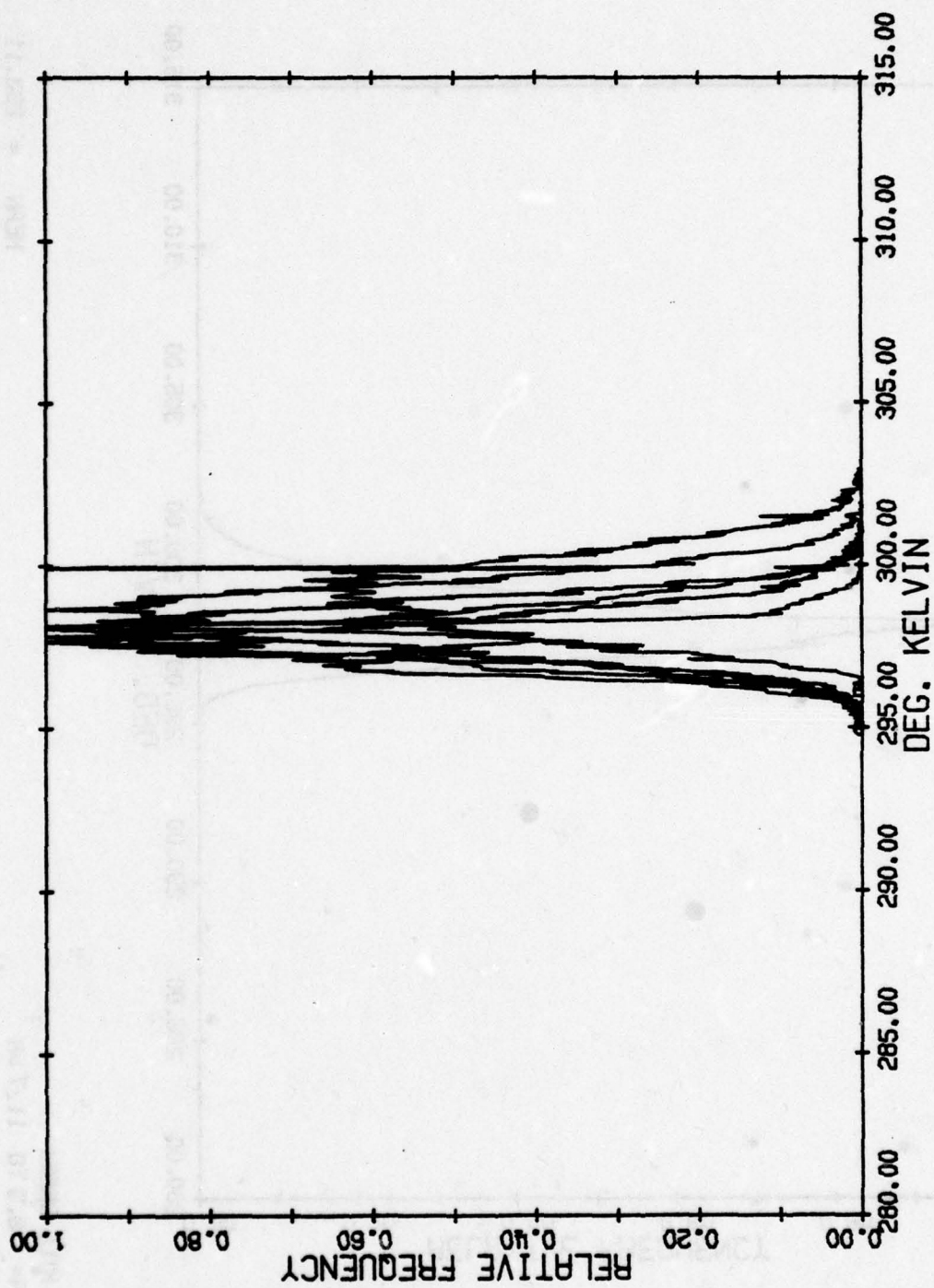


AREA: MILL CREEK
 LAMBDA= 2.0 TO 2.6 μm
 TOTAL AREA

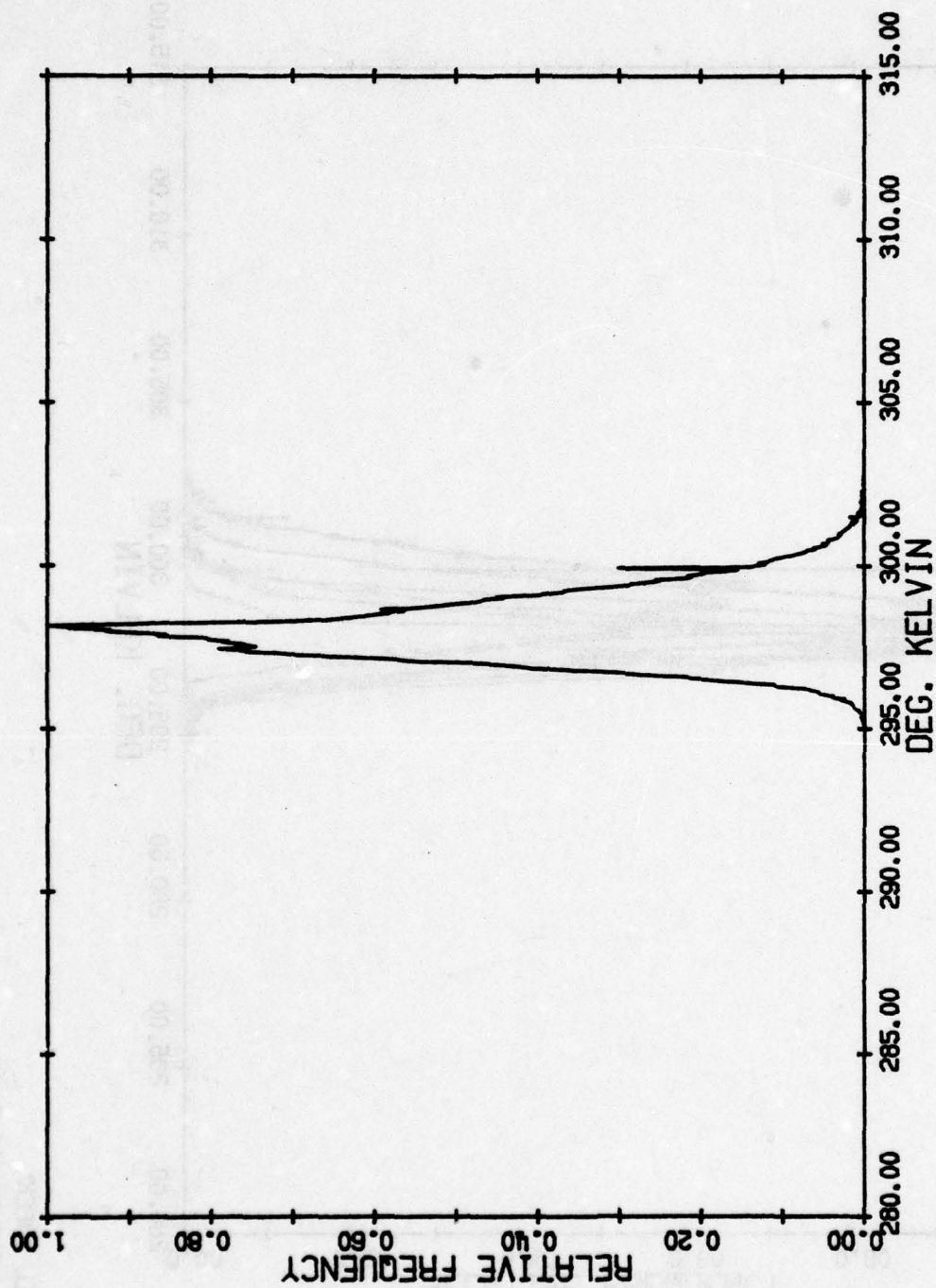
MEAN = 4.18
 ST.DEV.= 2.91



AREA: MILL CREEK
 WAVELENGTH= 2.0 TO 2.6 μm
 CALIB. PLATES

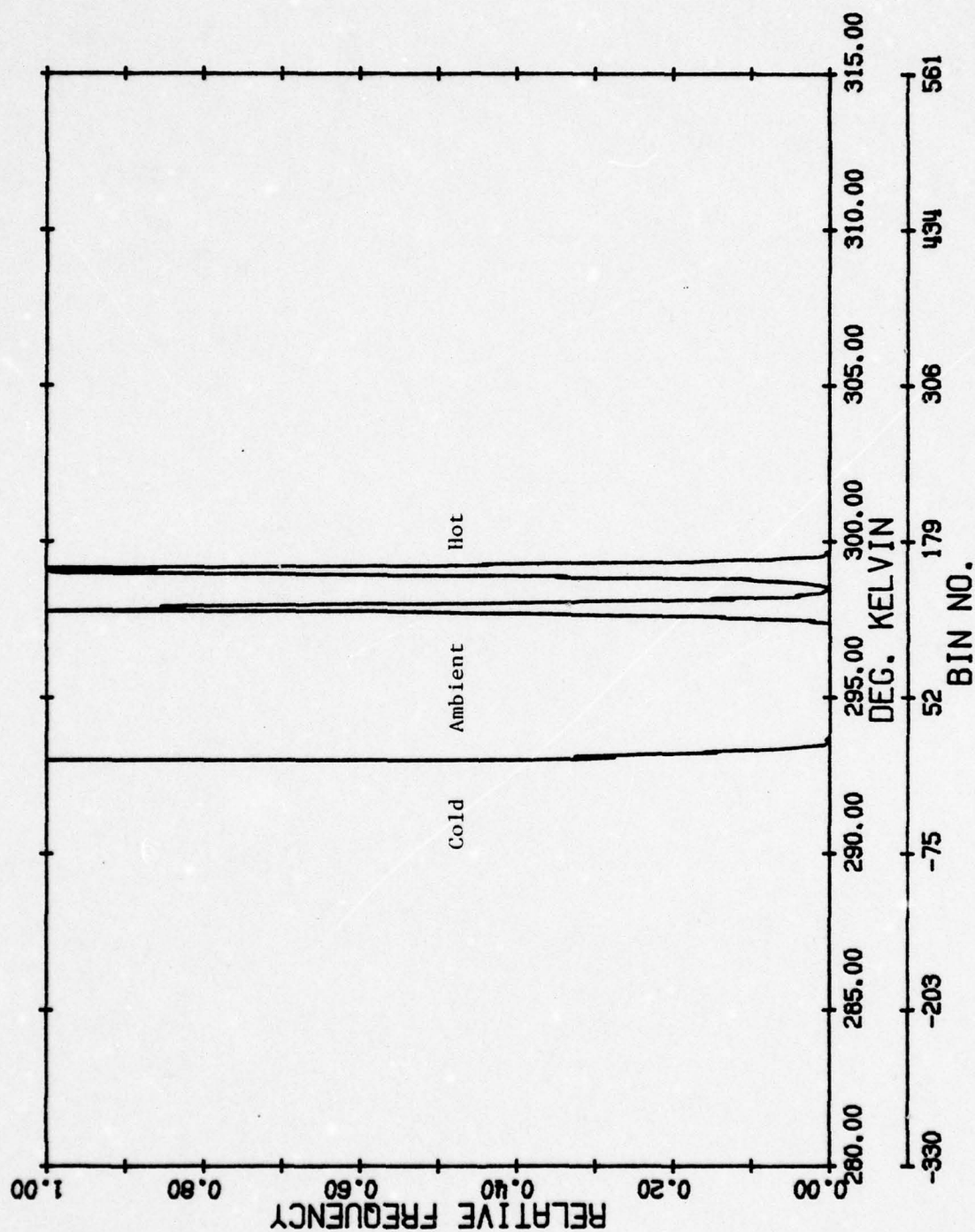


AREA: MILL CREEK
LAMBDA= 9.3 TO 11.7 μ M
SUBAREAS



AREA: MILL CREEK
LAMBDA= 9.3 TO 11.7 μ M
TOTAL AREA

MEAN = 298.11
ST.DEV.= 0.98



AREA: MILL CREEK
 LAMBDA= 9.3 TO 11.7 μ M
 CALIB. PLATES

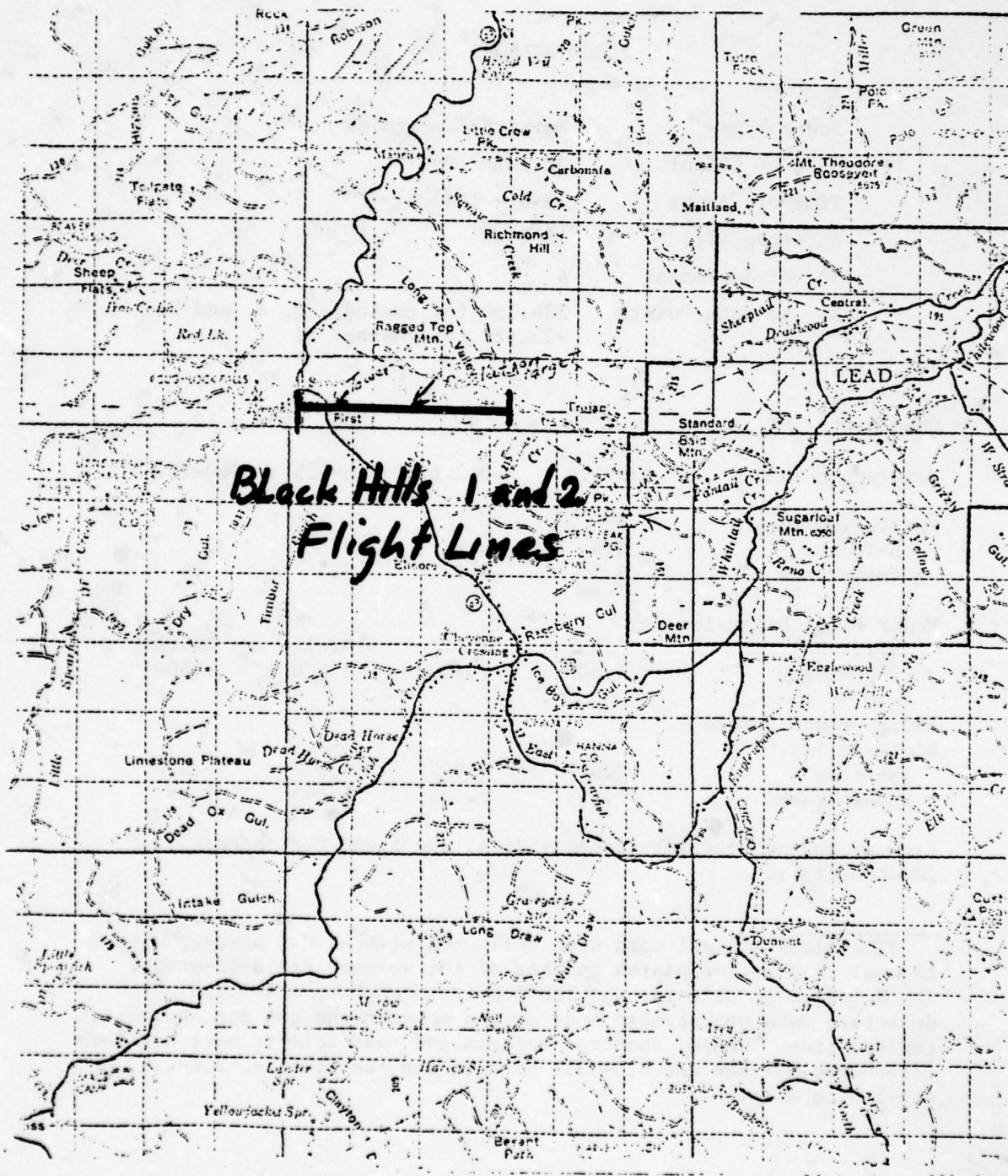
BLACK HILLS-1*

Scene Type	Forested Mountains
Data of Flight	22 July 1969
Time of Flight	1340 - 1342
Altitude (Ft)	1500
No. of Sub-Areas	4
No. of Data Points	224,130 for channels 2, 4, and 5 425,630 for channel 12

Channels	2	4	5	12
Wavelength (μm)	1.0-1.4	2.0-2.6	4.5-5.5	8.0-13.5
Resolution (mr)				
In-Track	6.6	6.6	6.6	3.5
Cross-Track	3.5	3.5	3.5	3.5
Nadir Pixel Dimension (m)				
In-Track	3.017	3.017	3.017	1.600
Cross-Track	1.600	1.600	1.600	1.600
Nadir Ground Sample Distance (m)				
In-Track	3.017	3.017	3.017	1.600
Cross-Track	1.143	1.143	1.143	1.143

Line Averaging used for channels 2, 4, and 5 and for channel 12 independently.

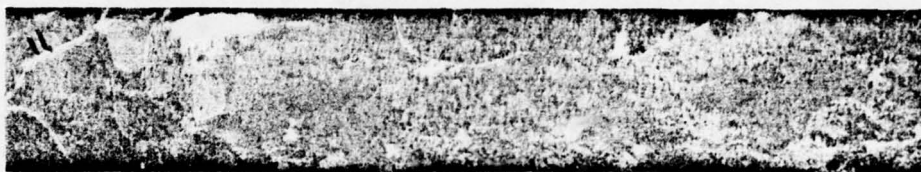
*The Black Hills-1 data were collected with an M-5 scanner with thermal calibration plates in part of the scanner field-of-view. The 8.0-13.5 μm detector and the 1.0-1.4, 2.0-2.6, 4.5-5.5 μm detectors were on opposite ends of the scanner and are not in spatial registration. Hence, spectral correlation coefficients have not been determined between the 8.5-13.5 μm data and the 1.0-1.4, 2.0-2.6, or 4.5-5.5 μm data.



MAP OF BLACK HILLS 1



1.0 - 1.4 μm



2.0 - 2.6 μm



4.5 - 5.5 μm



8.0 - 13.5 μm

LINE SCAN IMAGES PRODUCED FROM THE VARIOUS
INFRARED CHANNELS OF BLACK HILLS-1



Pixel 1

Pixel 311

Line 1	Line 344	Line 689	Line 1034	Line 1374 - channel 12
Line 10	Line 183	Line 369	Line 552	Line 732 - channels 2,4,5

SUB-AREAS DEFINED FOR STATISTICS GENERATION IN BLACK HILLS-1.
 Approximate scene dimensions are 1166 ft (355 m) by 7212 ft
 (2198 m) for channel 12 and 1166 ft (355 m) by 7146 ft (2178 m)
 for channels 2, 4, 5. Each sub-area as well as the total area
 have been histogrammed. Histogram plots and their respective
 sub-areas are identified with the following key:

▣ Sub-area 1	+ Sub-area 4
○ Sub-area 2	× Sub-area 5
▲ Sub-area 3	◇ Sub-area 6

BLACK HILLS-1

SUB-AREA 1

CORRELATION	2	4	5
2	1.000		
4	0.328	1.000	
5	-0.202	0.647	1.000
CHANNELS	2	4	5
MEAN	1.9804F+03	1.2177E+02	2.9485E+02
ST. DEV.	6.6571F+02	6.8058E+01	2.6348F+00
TOTAL PTS.	53940.	53940.	53940.
			106649.

BLACK HILLS-1

SUB-AREA 2

CUPRELATION	2	4	5
2	1.000		
4	0.490	1.000	
5	-0.291	0.370	1.000
CHANNELS	2	4	5
12			
MEAN	1.7373E+03	9.7070E+01	2.7017E+02
ST. DEV.	5.4031E+02	4.3322E+01	2.0097E+00
TOTAL PTS.	57660.	57660.	57660.
			106950.

BLACK HILLS-1
SUB-AREA 3

CORRELATION	2	4	5
2	1.000		
4	0.671	1.000	
5	-0.168	0.298	1.000

CHANNELS	2	4	5	12
MEAN	1.6546E+03	9.8521E+01	2.9468E+02	2.9388E+02
SI, DFV.	5.9506E+02	5.0679E+01	2.2654E+00	2.2431E+00
TOTAL PIS.	56730.	56730.	56730.	106330.

BLACK HILLS-1

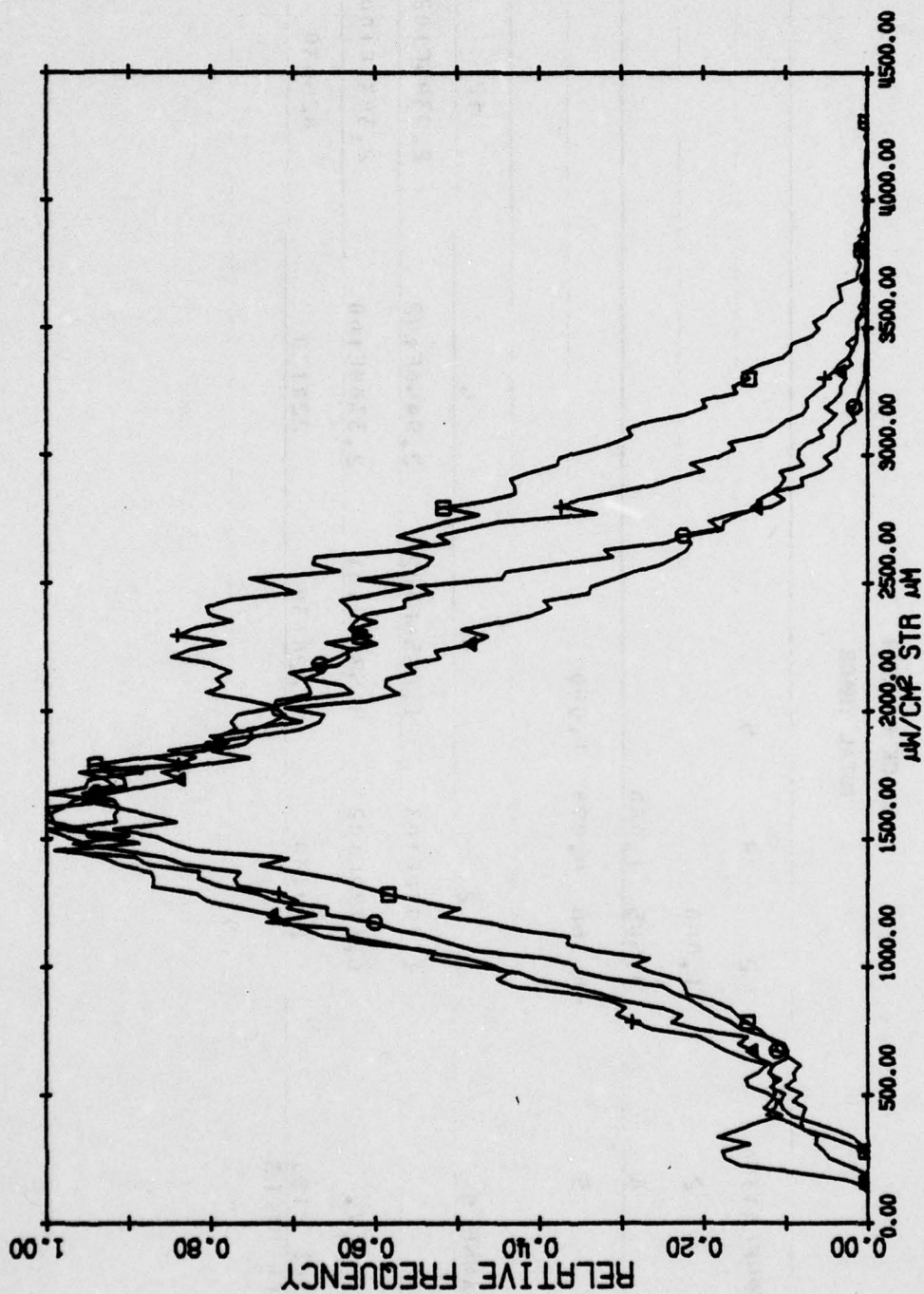
SUB-AREA 4

CORRELATION	2	4	5
2	1.000		
4	0.543	1.000	
5	-0.084	0.559	1.000
CHANNELS	2	4	5
12			
MEAN	1.8304E+03	1.0581E+02	2.9457E+02
ST. DEV.	6.1996E+02	5.3826E+01	2.3698E+00
TOTAL PTS.	55800.	55800.	55800.
			105710.

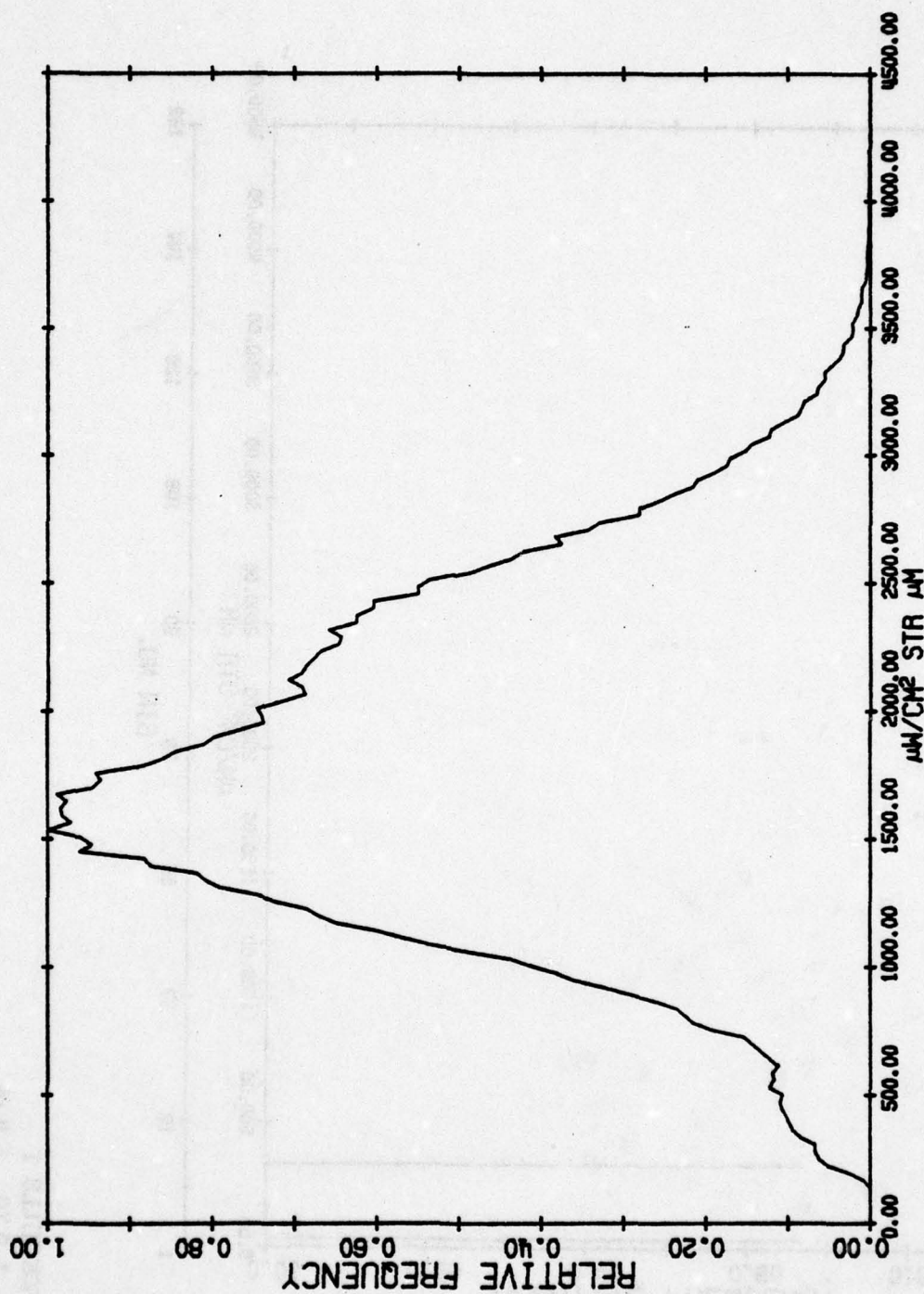
BLACK HILLS-1

TOTAL IMAGE

CORRELATION	2	4	5	
2	1.000			
4	0.505	1.000		
5	-0.166	0.498	1.000	
CHANNELS	2	4	5	12
MEAN	1.7990E+03	1.0556E+02	2.9456E+02	2.9395E+02
ST. DEV.	6.1770E+02	5.5347E+01	2.3389E+00	2.3831E+00
TOTAL PTS.	224130	224130	224130	425630
BLACK HILLS				

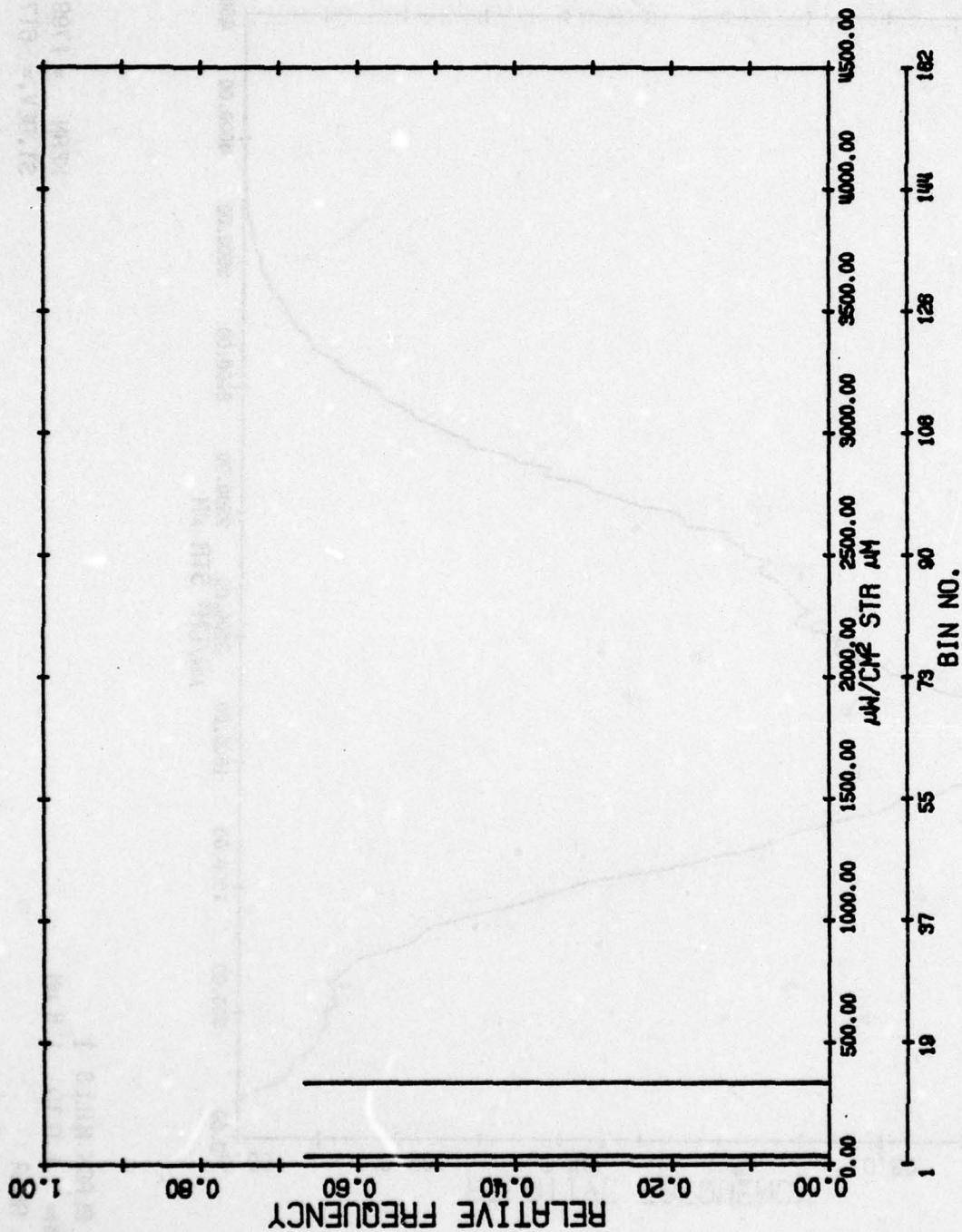


AREA: BLACK HILLS 1
 WAVELENGTH= 1.0 TO 1.4 μm
 SUBPLOTS

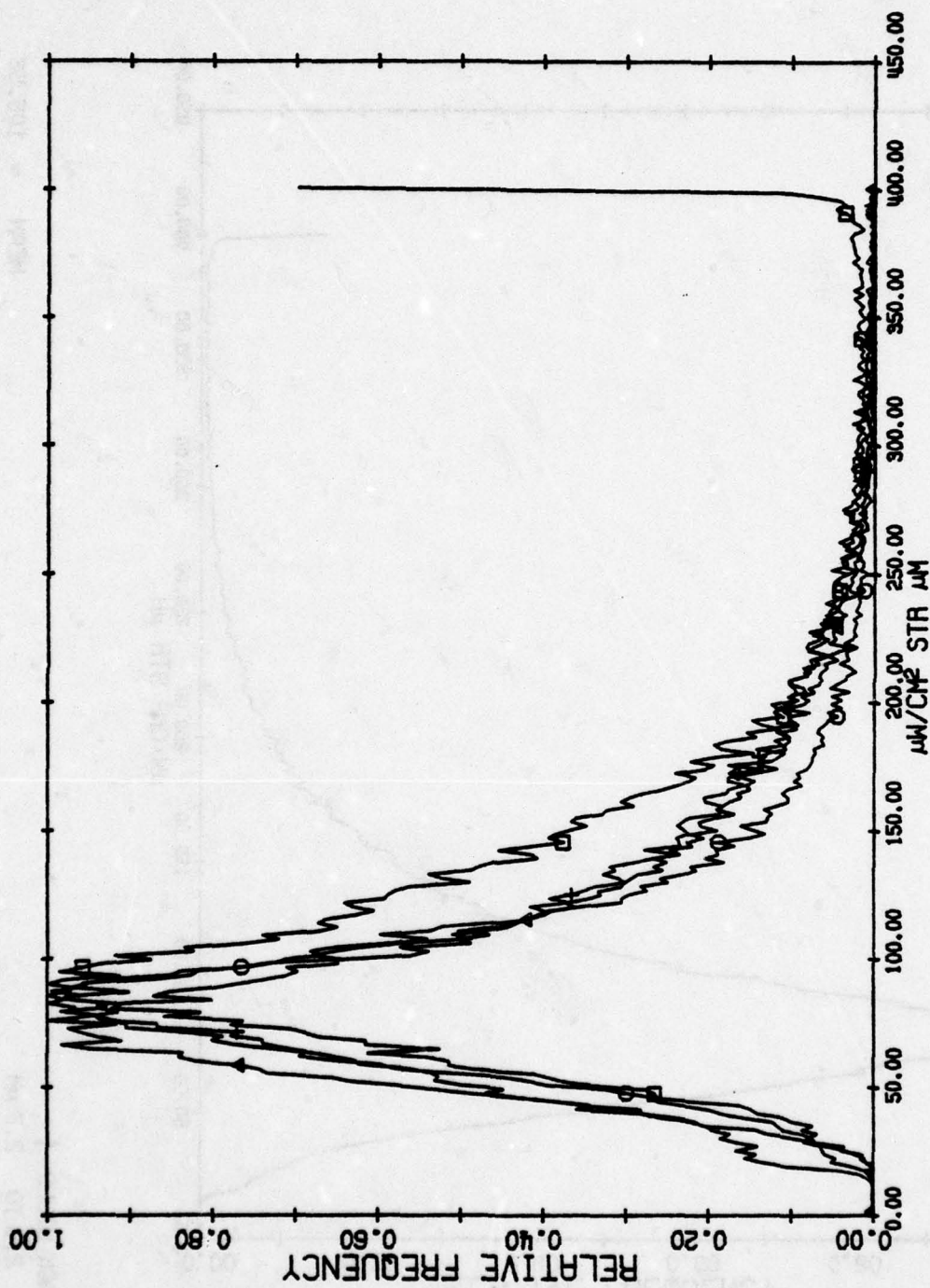


AREA: BLACK HILLS 1
LAMBDA= 1.0 TO 1.4 μm
TOTAL AREA

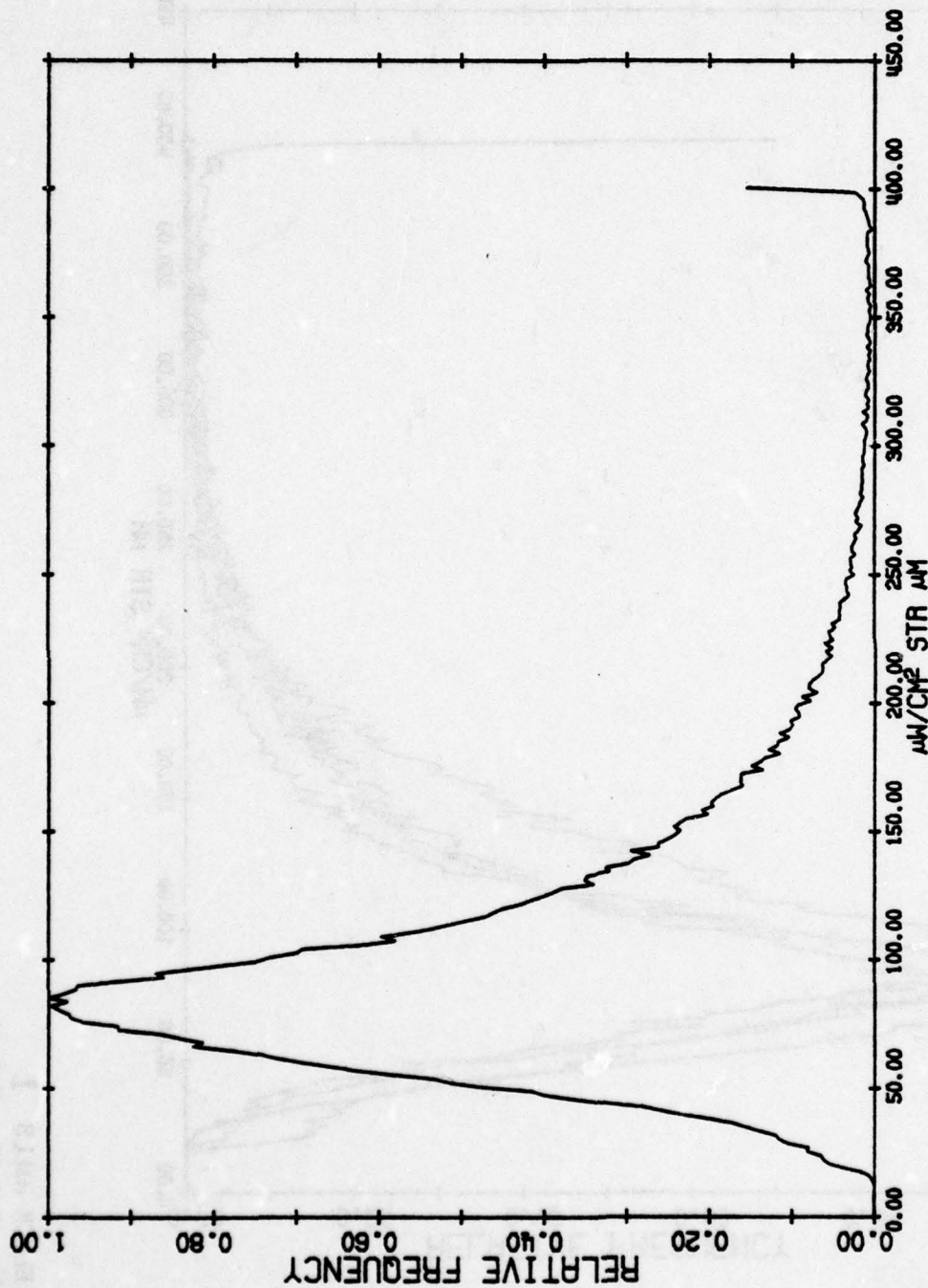
MEAN = 1799.05
ST.DEV. = 617.70



AREA: BLACK HILLS 1
 WAVELENGTH= 1.0 TO 1.4 μm
 CALIB. PLATES

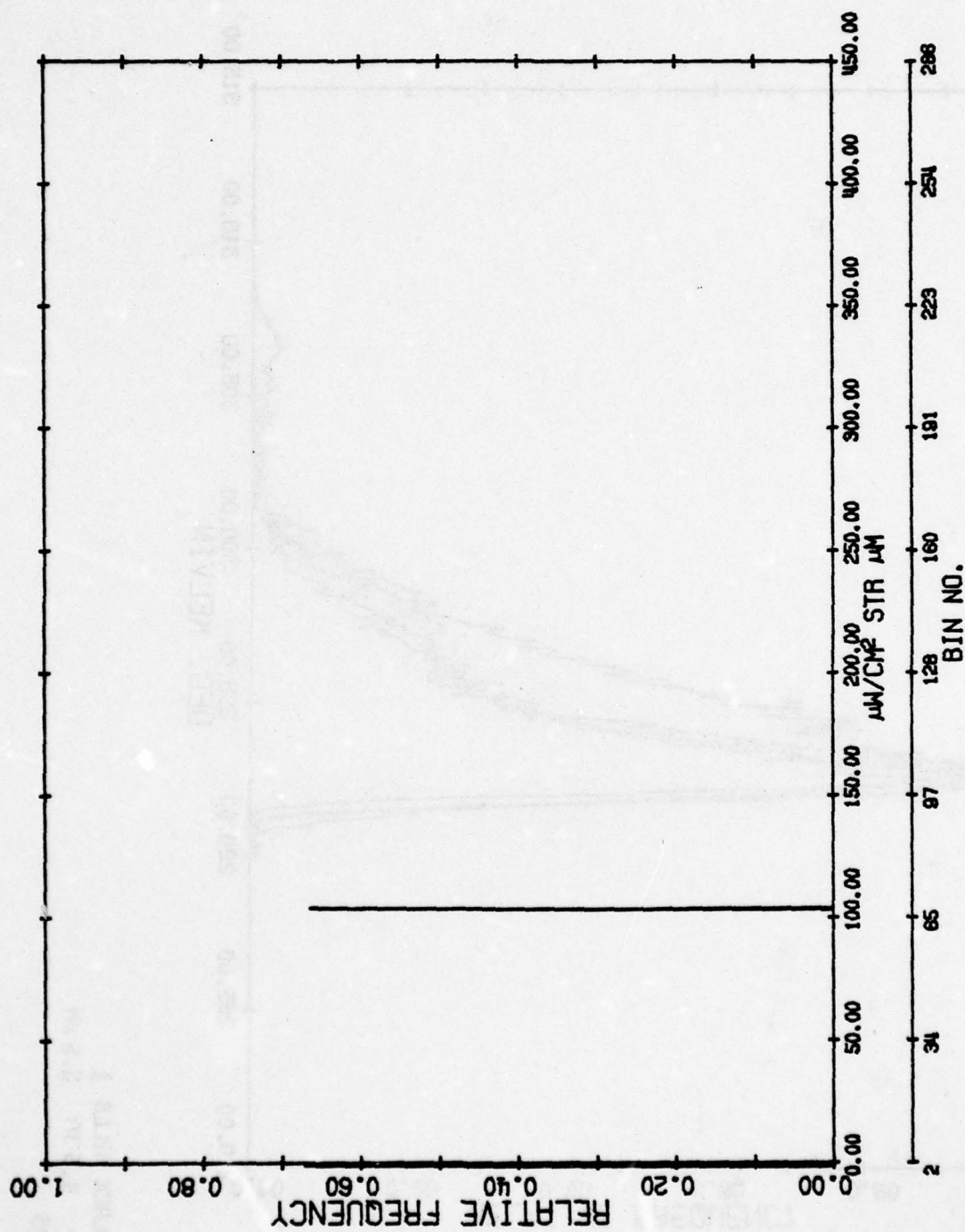


AREA: BLACK HILLS I
 LAMBDA= 2.0 TO 2.6 μm
 SUBPLOTS

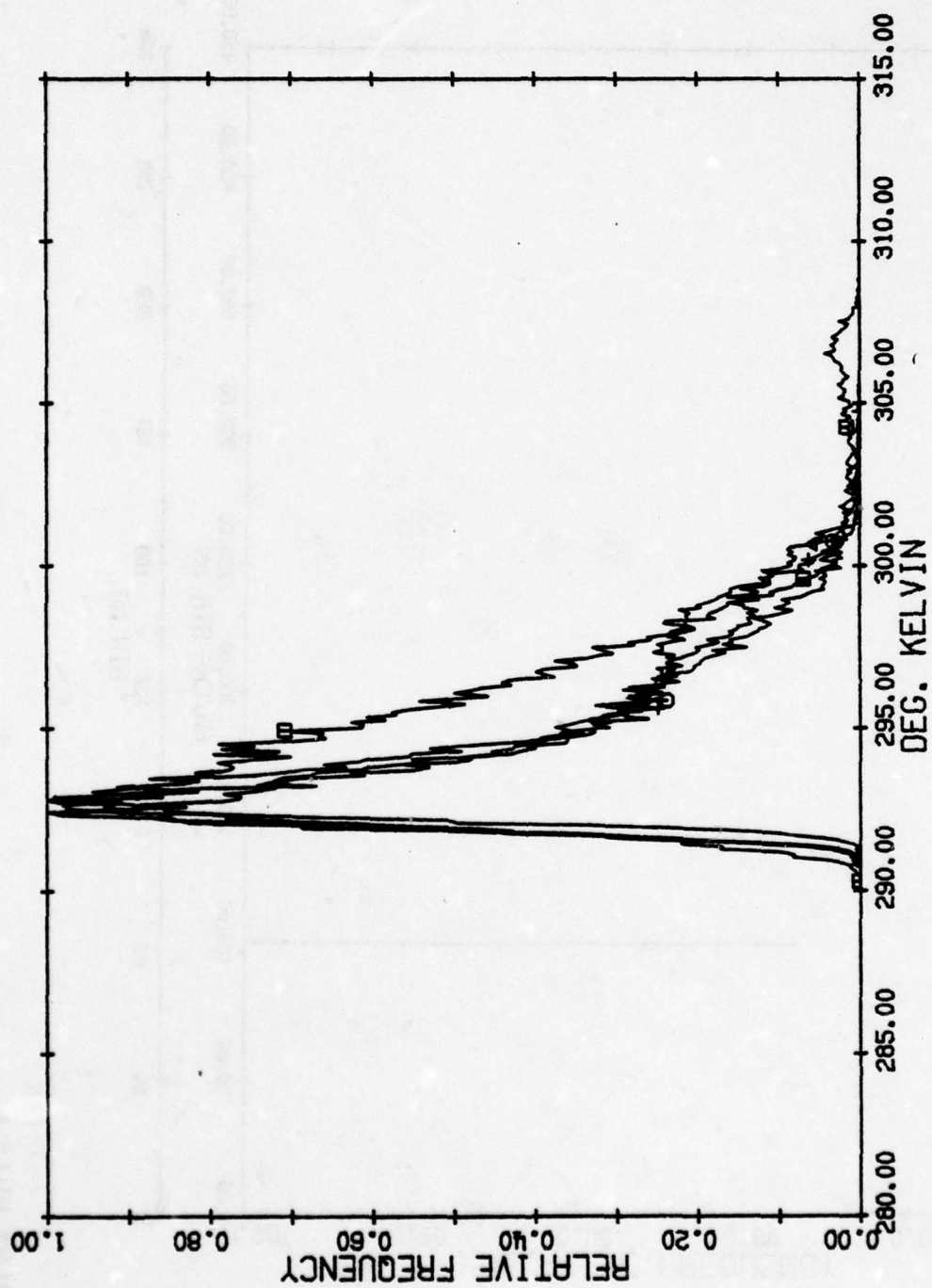


AREA: BLACK HILLS 1
 LAMBDA= 2.0 TO 2.6 μm
 TOTAL AREA

MEAN = 105.56
 ST. DEV. = 55.35



PRER: BLACK HILLS 1
 LAMBDA= 2.0 TO 2.6 μm
 CALIB. PLATES



AREA: BLACK HILLS 1
LAMBDA= 4.5 TO 5.5 μ M
SUBAREAS

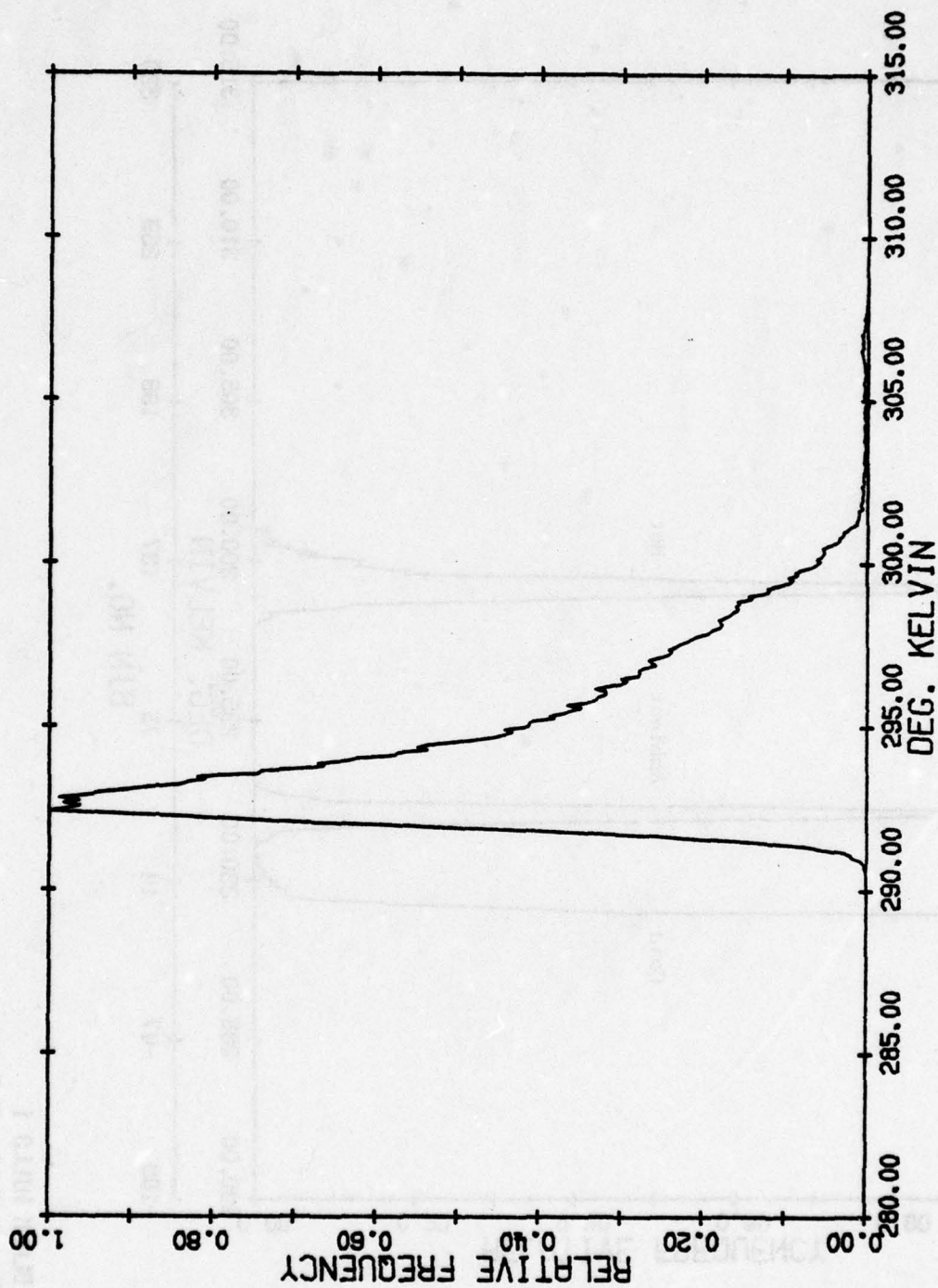
AD-A077 584

ENVIRONMENTAL RESEARCH INST OF MICHIGAN ANN ARBOR IN--ETC F/6 17/5
STATISTICAL ANALYSIS OF TERRAIN BACKGROUND MEASUREMENTS DATA.(U)
MAR 77 R SPELLICY , J BEARD , J R MAXWELL N00123-76-C-0708
ERIM-120500-12-F NL

UNCLASSIFIED

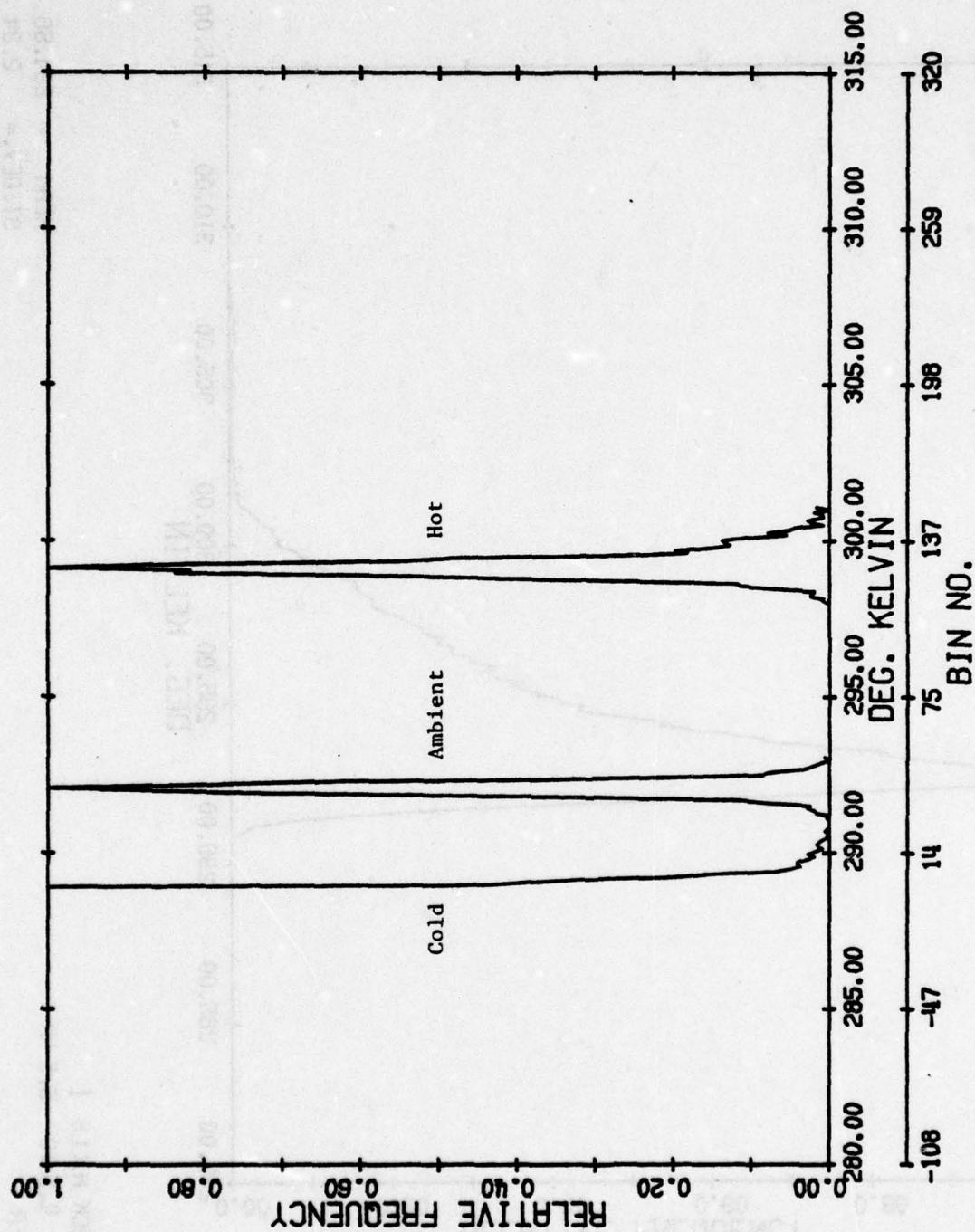
3 OF 4
ADA
077 584



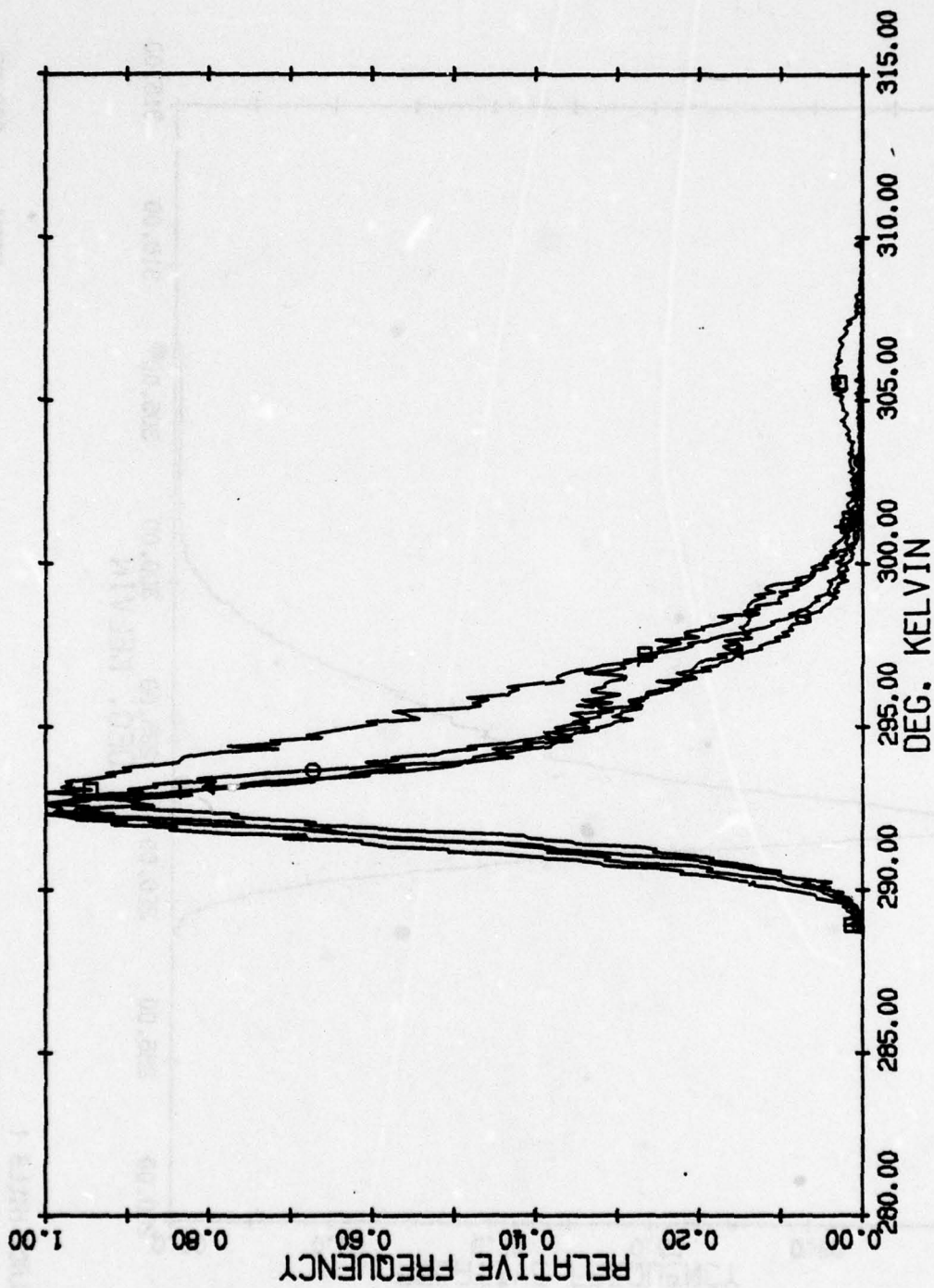


AREA: BLACK HILLS 1
 LAMBDA= 4.5 TO 5.5 μ M
 TOTAL AREA

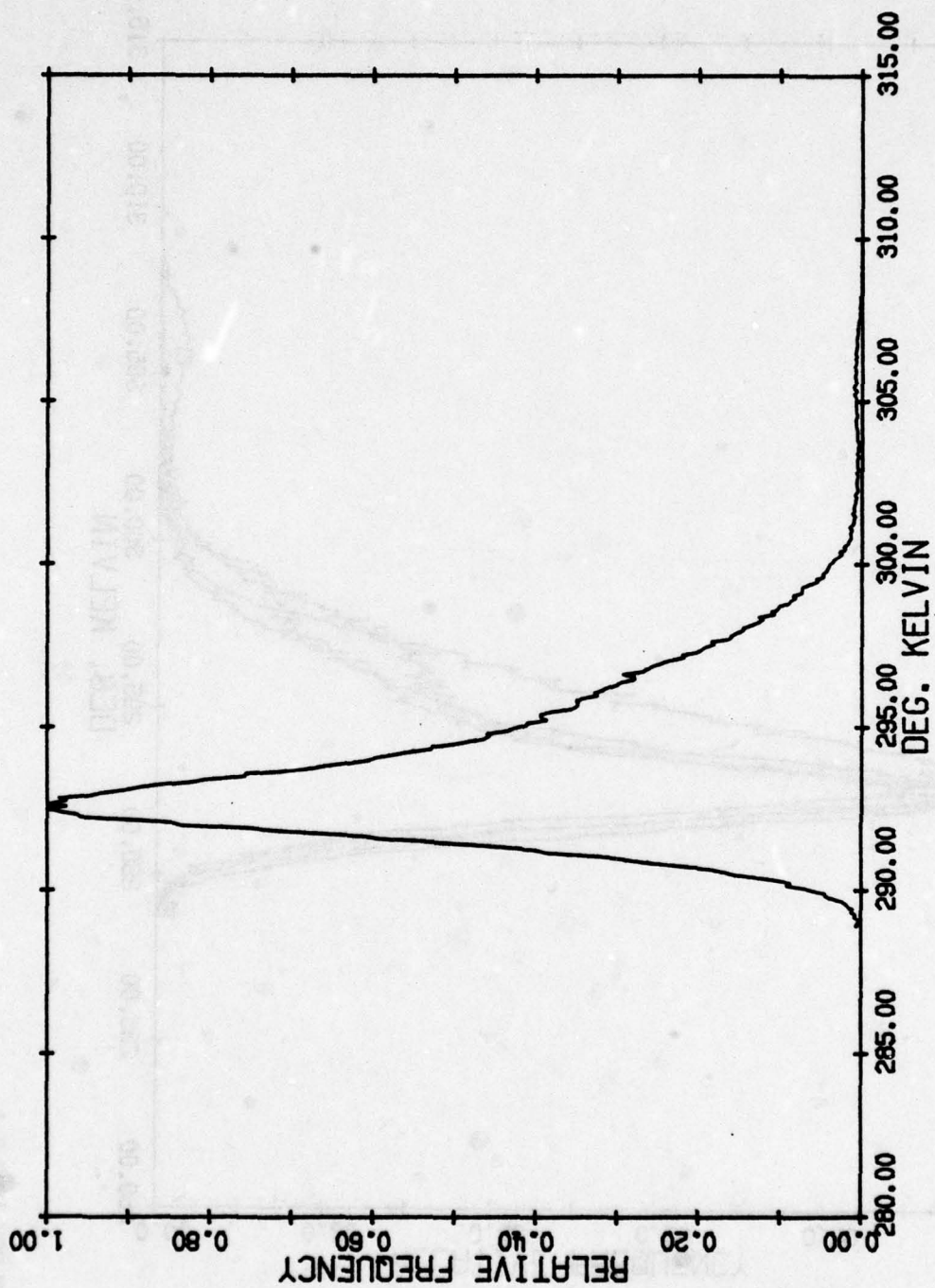
MEAN = 294.56
 ST.DEV.= 2.34



AREA: BLACK HILLS 1
 LAMBDA- 4.5 TO 5.5 μ M
 CALIB. PLATES

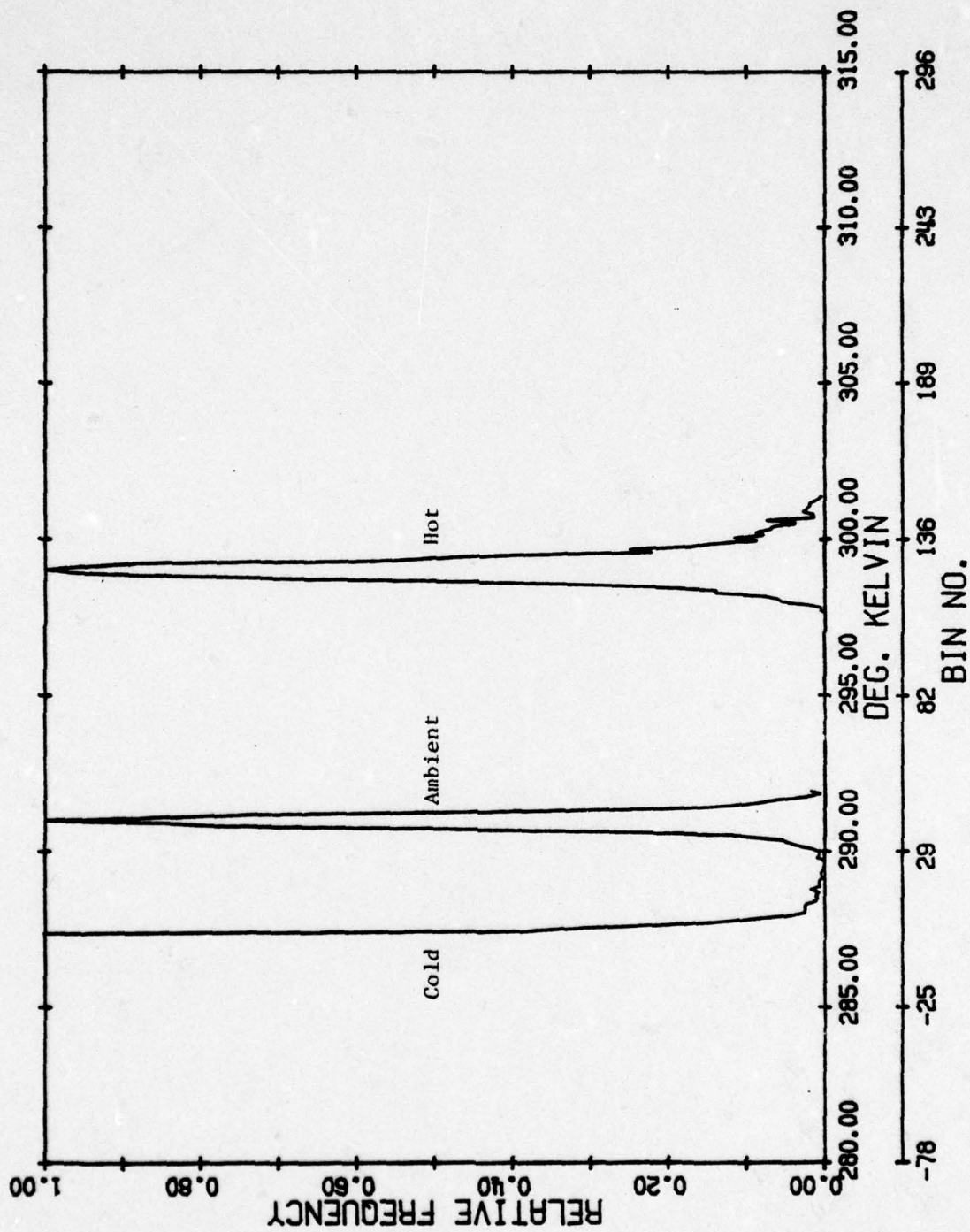


AREA: BLACK HILLS 1
WAVELENGTH= 8.0 TO 13.5 μ M
SUBPLOTS



AREA: BLACK HILLS 1
WAVELENGTH= 8.0 TO 13.5 μ M
TOTAL AREA

MEAN = 293.85
ST. DEV. = 2.38



AREA: BLACK HILLS 1
WAVEL= 8.0 TO 13.5 μ M
CAN 18 PLATES

BLACK HILLS-2*

Scene Type	Forested Mountains		
Date of Flight	22 July 1969		
Time of Flight	1340 - 1342		
Altitude (Ft)	1500		
No. of Sub-Areas	6		
No. of Data Points	468,915		
Channels	5	3	7
Wavelength (μ m)	1.0-1.4	1.5-1.8	2.0-2.6
Resolution (mr)			
In-Track	6.6	6.6	6.6
Cross-Track	3.5	3.5	3.5
Nadir Pixel Dimensions (m)			
In-Track	3.017	3.017	3.017
Cross-Track	1.600	1.600	1.600
Nadir Ground Sample Distance (m)			
In-Track	3.017	3.017	3.017
Cross-Track	1.143	1.143	1.143

Line Averaging used for ALL channels.

*The Black Hills-2 data were collected with an M-5 scanner with calibration reference lamps in the scanner housing. The Black Hills-1 and Black Hills-2 data were collected at the same time with two M-5 scanners in the aircraft.



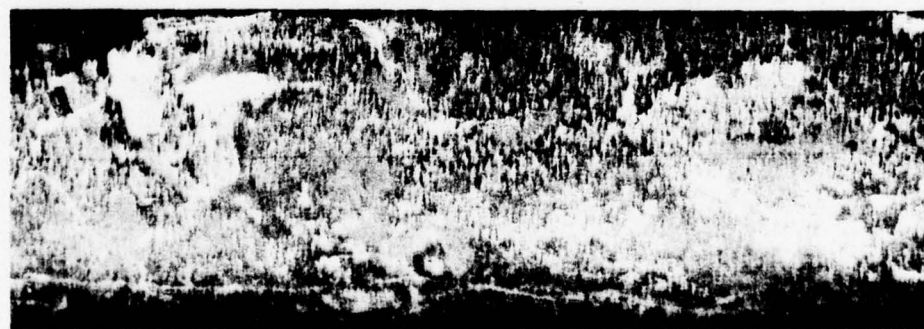
MAP OF BLACK HILLS-2



1.0 - 1.4 μm

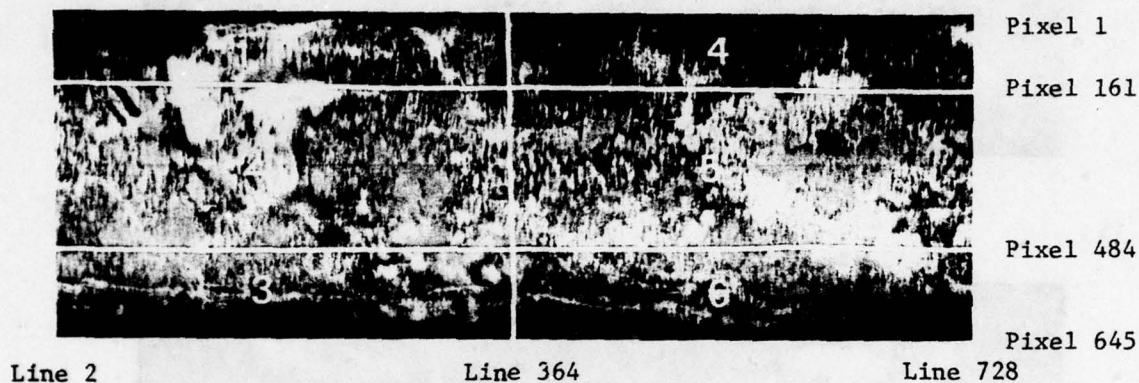


1.5 - 1.8 μm



2.0 - 2.6 μm

LINE SCAN IMAGES PRODUCED FROM THE VARIOUS
INFRARED CHANNELS OF BLACK HILLS-2



SUB-AREAS DEFINED FOR STATISTICS GENERATION IN BLACK HILLS-2 IMAGE. Uneven areas were chosen so that Areas 2 and 5 covered the $\pm 20^\circ$ range suitable for correlation. Approximate scene dimensions are 2418 ft (737 m) by 7206 ft (2196 m). Each sub-area as well as the total area have been histogrammed. Histogram plots and their respective sub-areas are identified with the following key:

- | | |
|--------------|--------------|
| ■ Sub-area 1 | + Sub-area 4 |
| ○ Sub-area 2 | × Sub-area 5 |
| ▲ Sub-area 3 | ◆ Sub-area 6 |

BLACK HILLS-2

SUB-AREA 1

CORRELATION

	3	5	7
3	1.000		
5	0.632	1.000	
7	0.925	0.390	1.000

CHANNELS

	3	5	7
MEAN	4.2957E+02	1.6740E+03	8.5542E+01
ST. DEV.	1.7416E+02	4.7239E+02	5.0259E+01
TOTAL PTS.	58240.	58240.	58240.

BLACK HILLS-2

SUB-AREA 2

CORRELATION	3	5	7
3	1.000		
5	0.562	1.000	
7	0.271	0.205	1.000

CHANNEL'S	3	5	7
MEAN	4.9552E+02	1.7372E+03	1.0016E+02
ST. DEV.	1.2369E+02	4.0619E+02	3.3910E+01
TOTAL PTS.	117572.	117572.	117572.

BLACK HILLS-2
SUB-AREA 3

CORRELATION	3	5	7
3	1.000		
5	0.861	1.000	
7	0.864	0.695	1.000

CHANNELS	3	5	7
MEAN	3.9443E+02	1.4353E+03	8.1228E+01
ST. DEV.	1.3090E+02	4.9175E+02	2.6563E+01
TOTAL PTS.	58968.	58968.	58968.

BLACK HILLS-2

SUB-AREA 4

CORRELATION	3	5	7
3	1.000		
5	0.718	1.000	
7	0.907	0.557	1.000

CHANNELS	3	5	7
MEAN	3.3717E+02	1.2032E+03	6.7338E+01
ST. DEV.	1.1846E+02	3.1479E+02	2.9141E+01
TOTAL PTS.	58080.	58080.	58080.

BLACK HILLS-2
SUB-AREA 5

CORRELATION	3	5	7
3	1.000		
5	0.688	1.000	
7	0.921	0.473	1.000

CHANNELS	3	5	7
MEAN	5.2011E+02	1.7878E+03	1.0507E+02
ST. DEV.	1.5169E+02	4.0022E+02	4.0479E+01
TOTAL PTS.	117249.	117249.	117249.

BLACK HILLS-2
SUB-AREA 6

CORRELATION	3	5	7
3	1.000		
5	0.857	1.000	
7	0.892	0.741	1.000

CHANNELS	3	5	7
MEAN	3.8441E+02	1.4170E+03	7.9316E+01
ST. DEV.	1.3921E+02	4.3637E+02	3.1003E+01
TOTAL PTS:	58806.	58806.	58806.

BLACK HILLS-2
TOTAL IMAGE

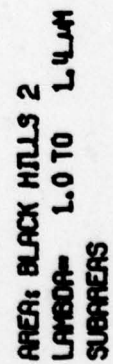
CORRELATION

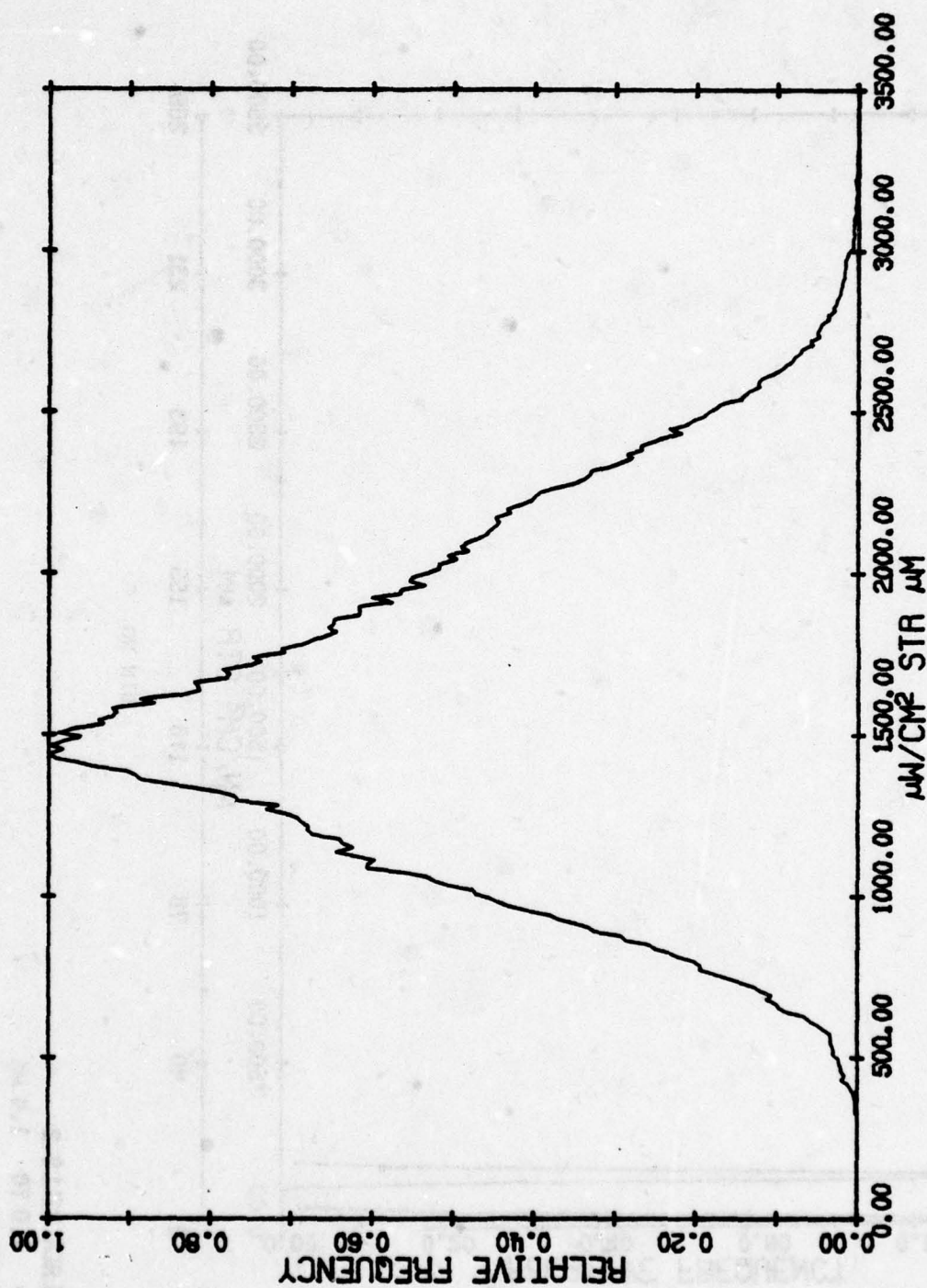
	3	5	7
3	1.000		
5	0.743	1.000	
7	0.908	0.518	1.000

CHANNELS

	3	5	7
MEAN	4.4721E+02	1.6027E+03	9.0510E+01
ST. DEV.	1.5485E+02	4.6380E+02	3.8712E+01

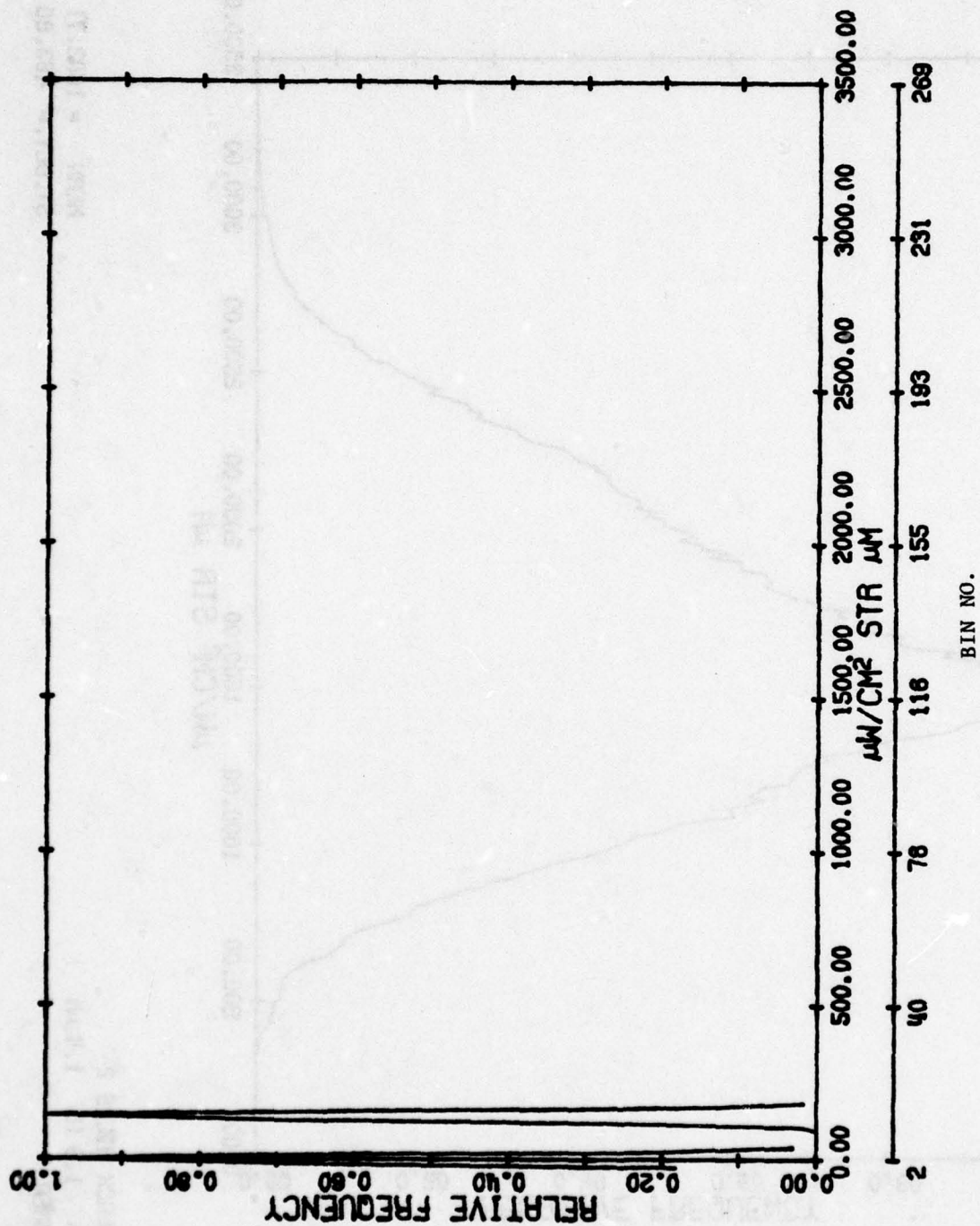
TOTAL PTS.	468915	468915	468915
BLACK HILLS 2			



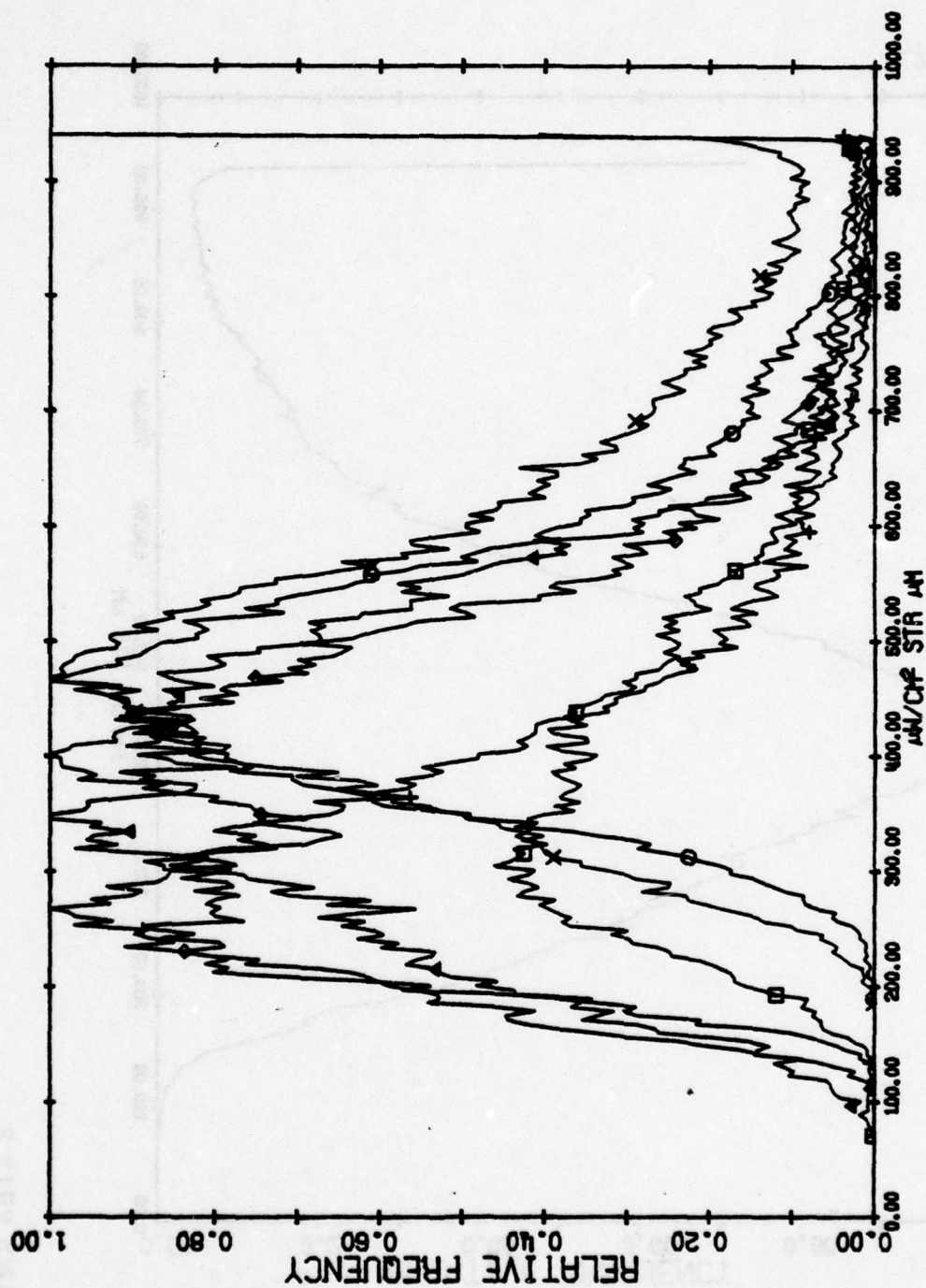


AREA: BLACK HILLS 2
 WAVELENGTH= 1.0 TO 1.4 μm
 TOTAL AREA

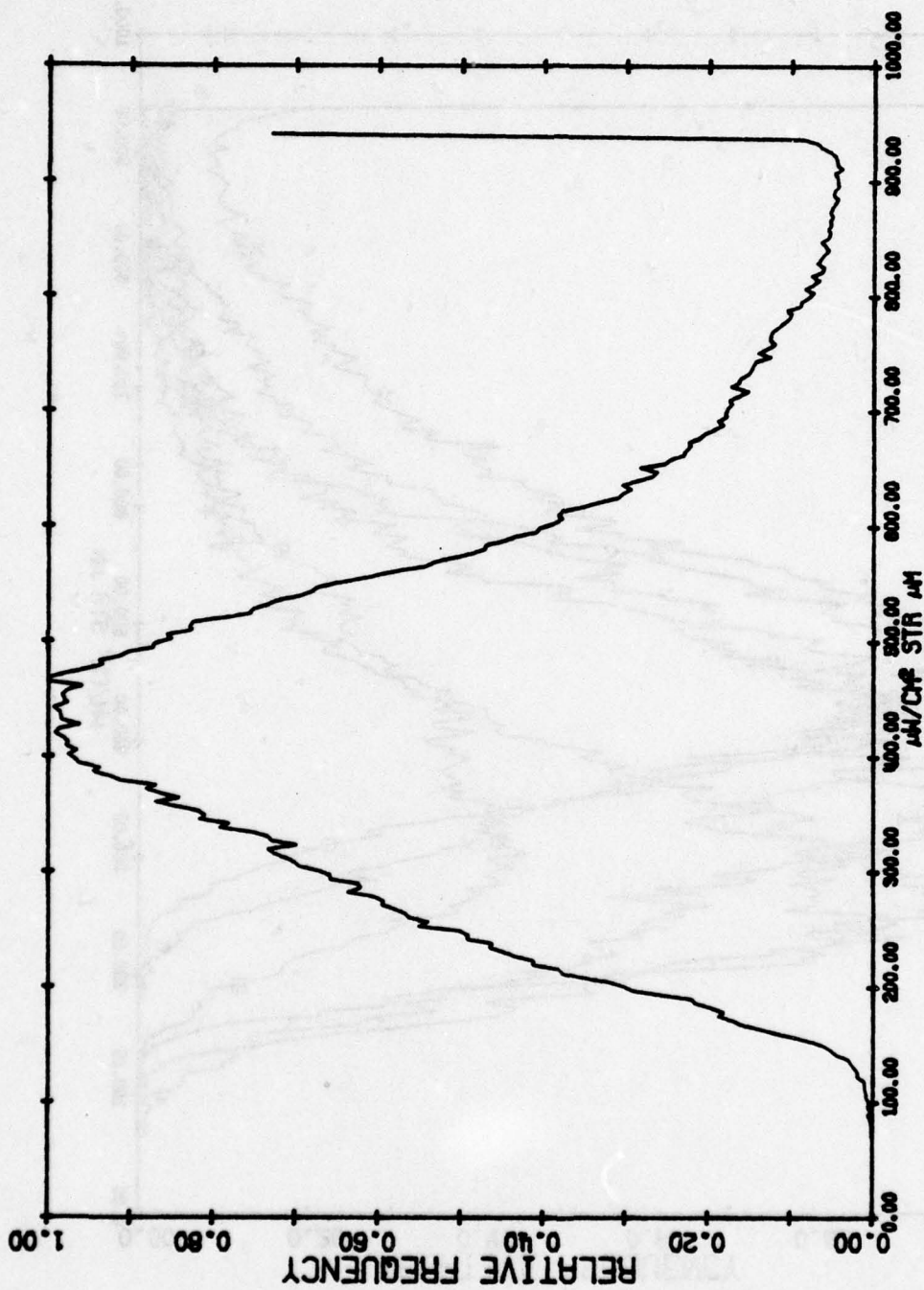
MEAN = 1602.71
 ST. DEV. = 463.80



AREA: BLACK HILLS 2
 WAVELENGTH: 1.0 TO 1.4 μm
 CALIB. PLATES

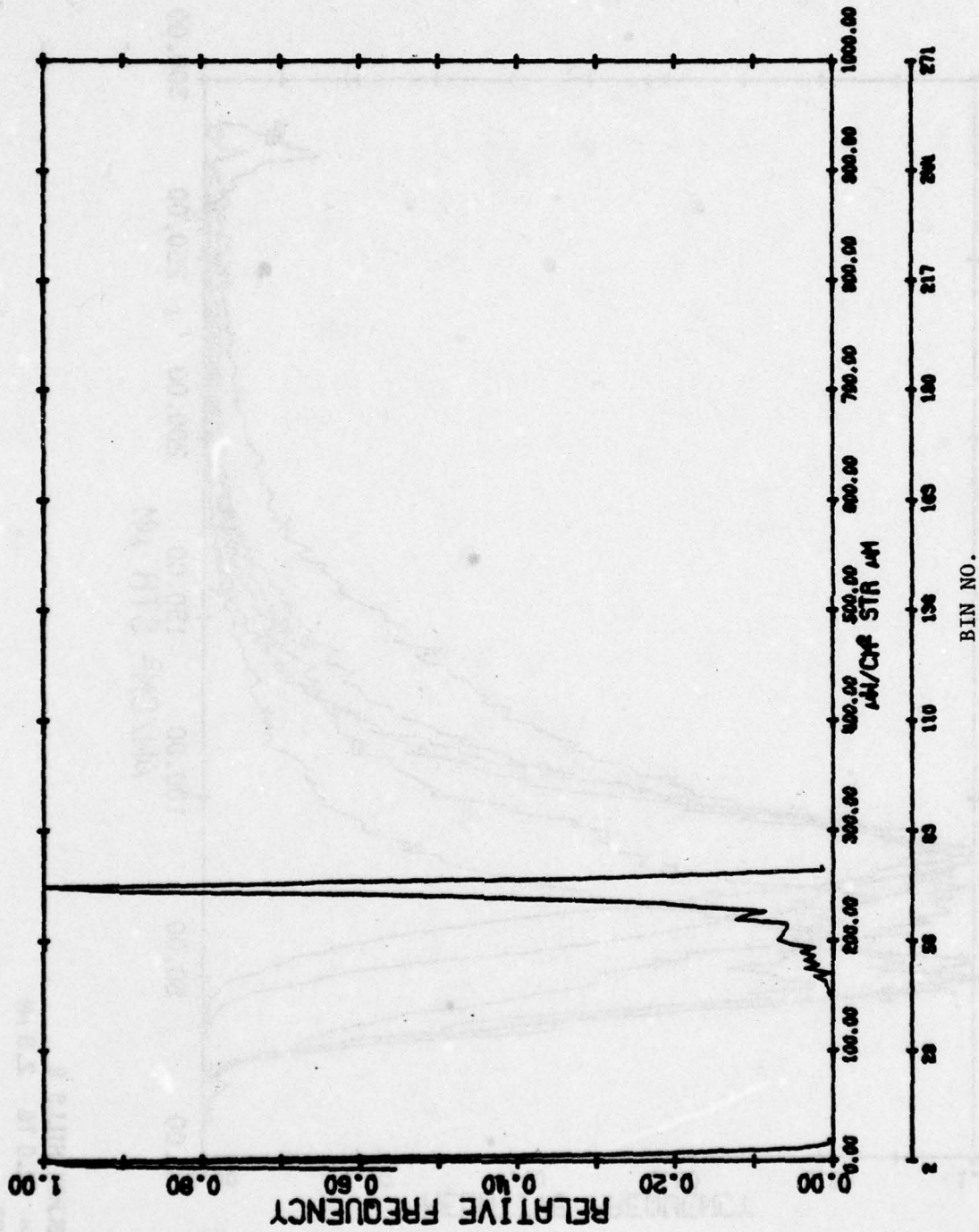


AREA: BLACK HILLS 2
 LAMBDA= 1.570 1.8 μm
 SUBAREAS

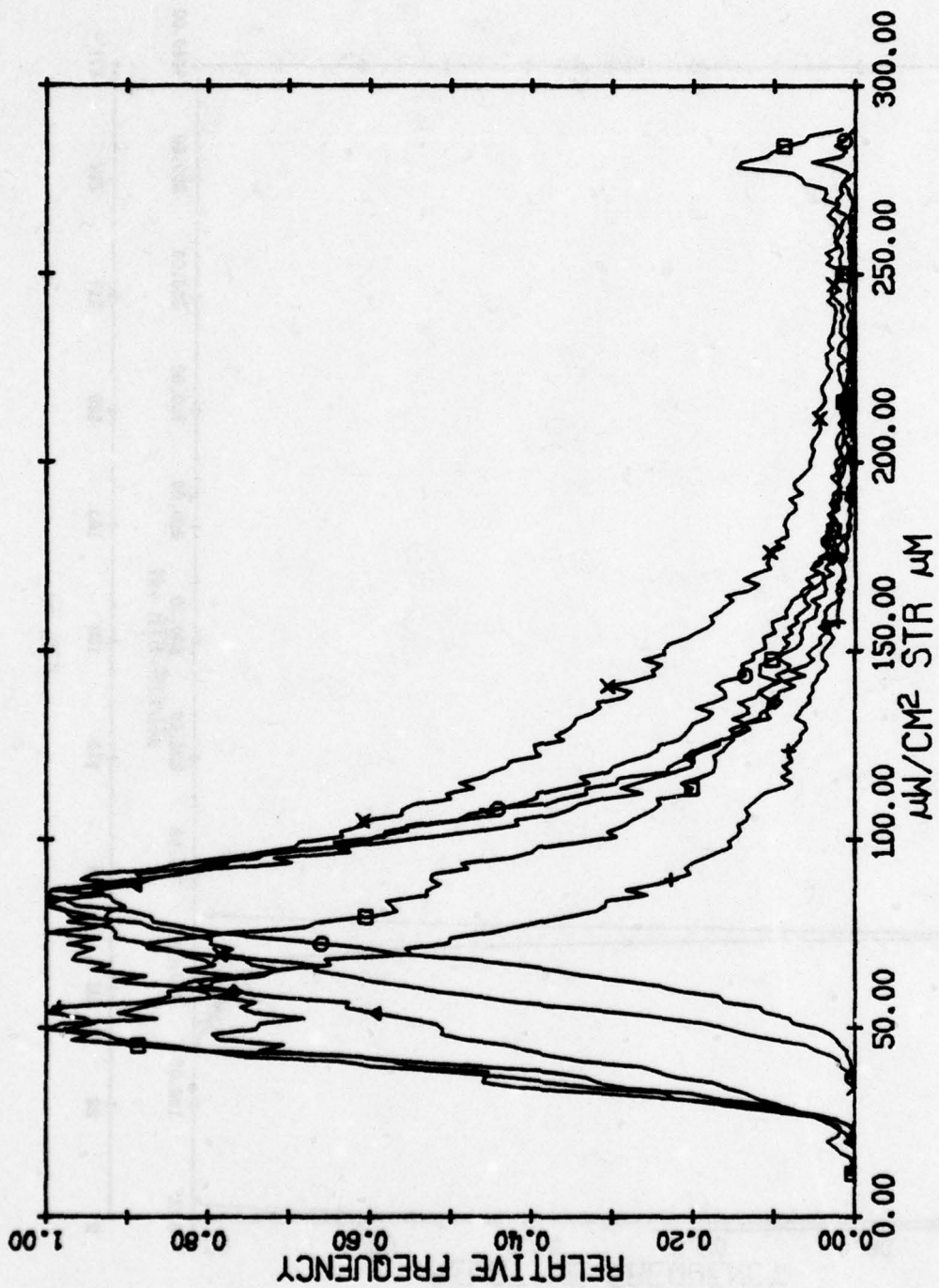


AREA: BLACK HILLS 2
 WAVELENGTH= 1.570 1.8 μM
 TOTAL AREA

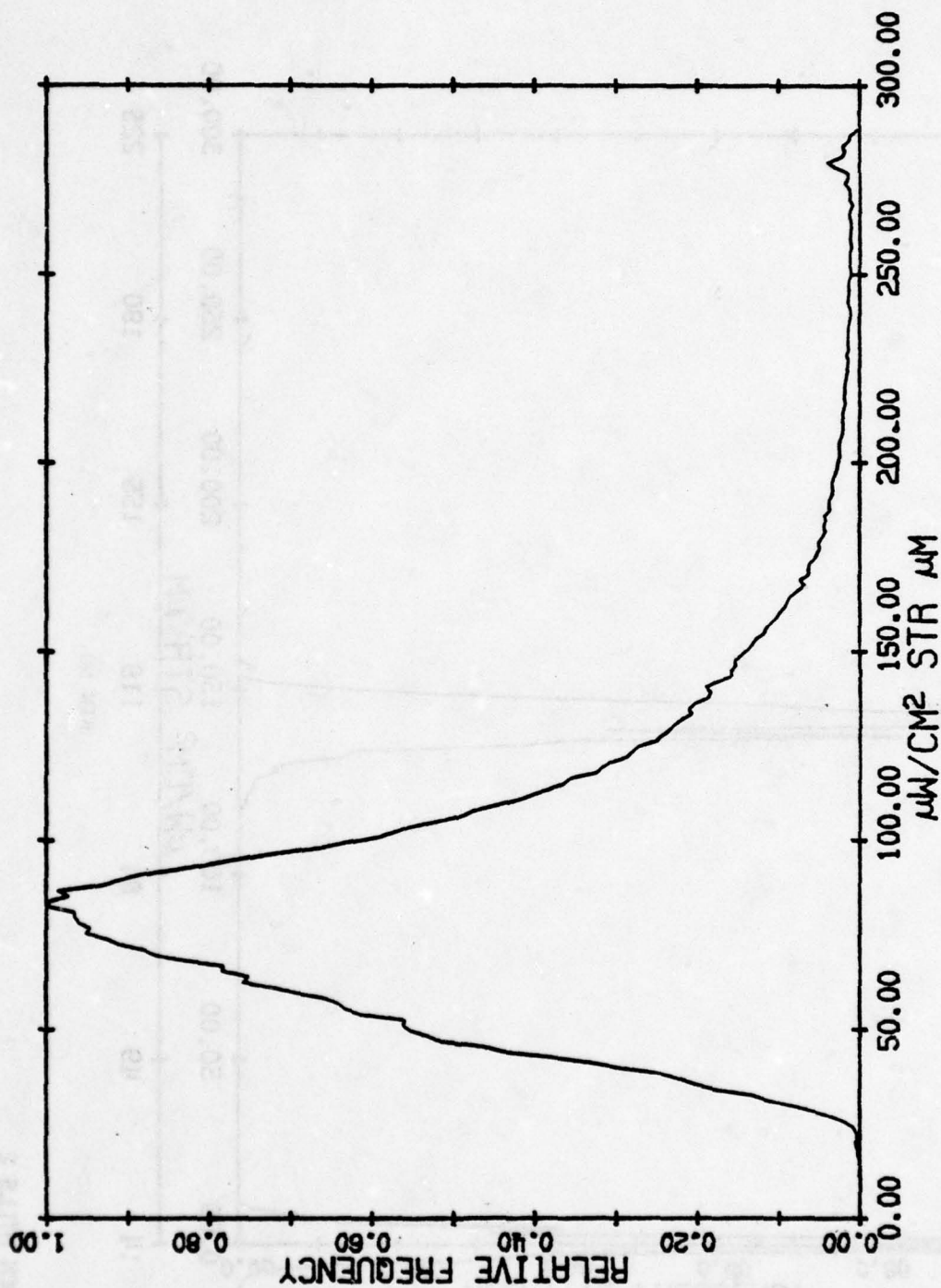
MEAN = 447.21
 ST.DEV. = 154.85



AREA: BLACK HILLS 2
 WAVELENGTH= 1.5 TO 1.8 μm
 CALIB. PLATES

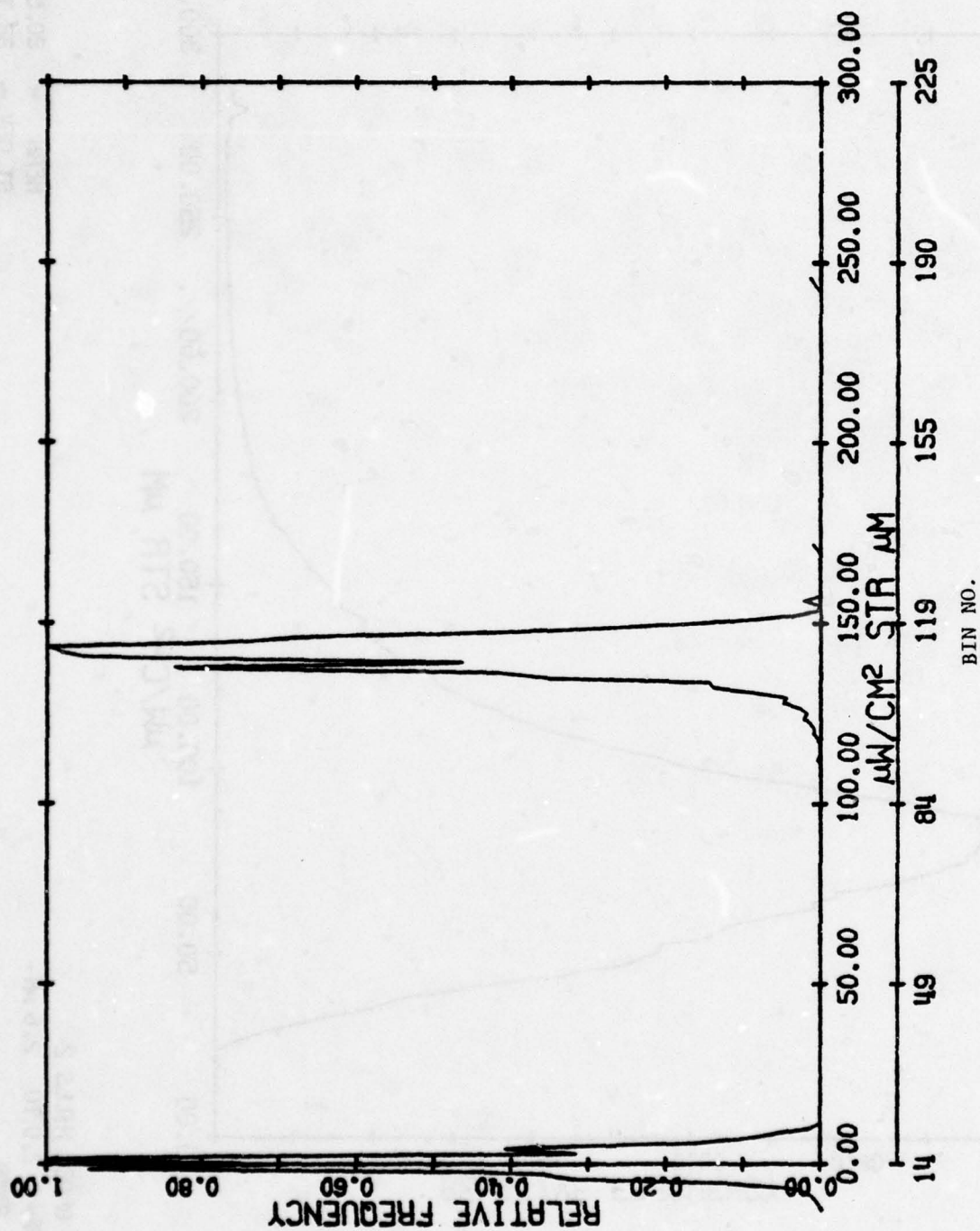


AREA: BLACK HILLS 2
 WAVELENGTH= 2.0 TO 2.6 μm
 SUBAREAS



AREA: BLACK HILLS 2
 LAMBDA= 2.0 TO 2.6 μM
 TOTAL AREA

MEAN = 90.51
 ST.DEV. = 38.71



AREA: BLACK HILLS 2
 WAVELENGTH: 2.0 TO 2.6 μm
 CALIB. PLATES

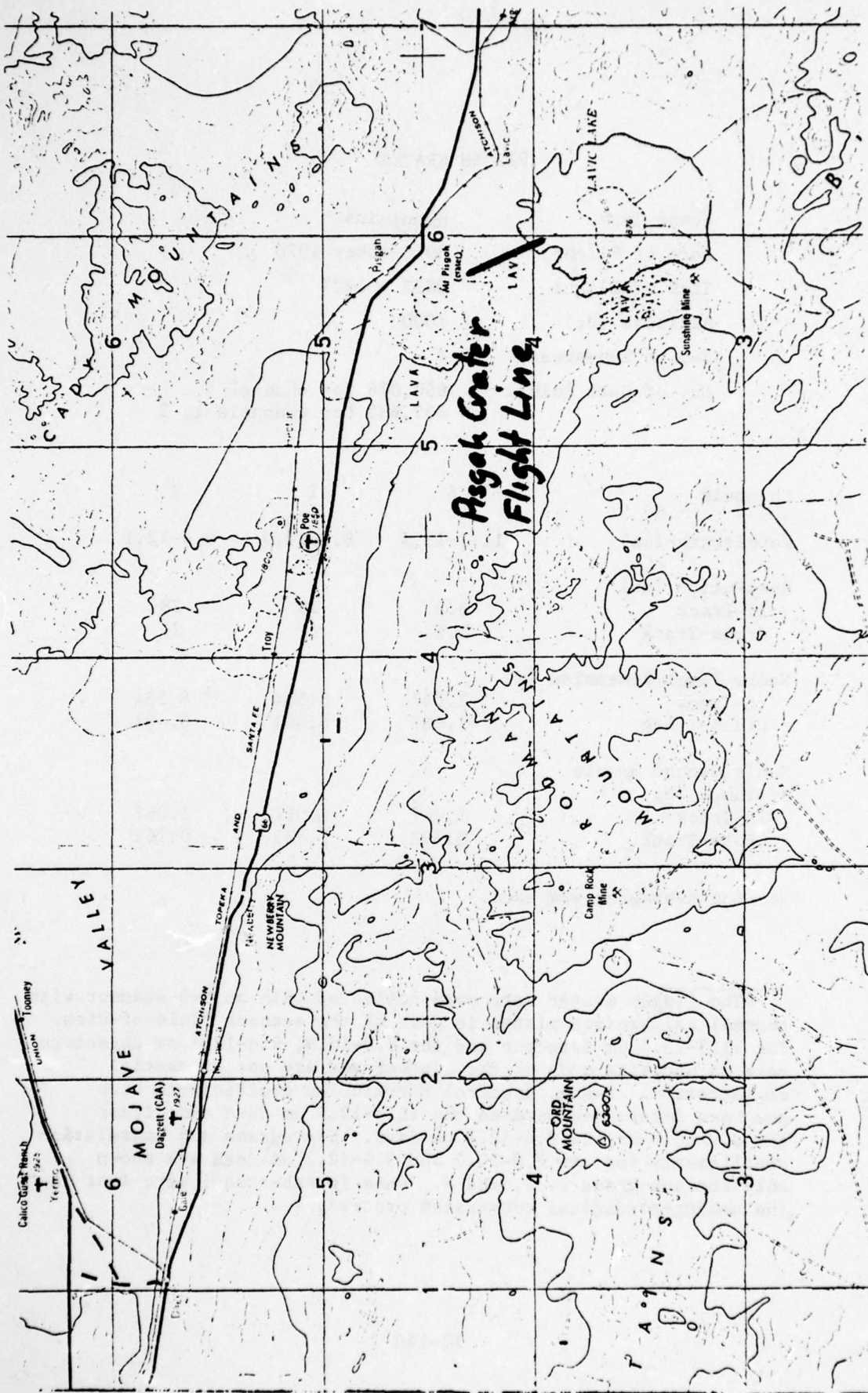
PISGAH CRATER*

Scene Type	Mountains
Date of Flight	30 October 1970
Time of Flight	0822 - 0827
Altitude (Ft)	1000
No. of Sub-Areas	4
No. of Data Points	650,076 for channel 4 637,632 for channels 1, 2

Channels	4	1	2
Wavelength (μ m)	11.3-13.5	8.0-10.9	9.4-12.1
Resolution (mr)			
In-Track	3.5	28	28
Cross-Track	3.5	21	21
Nadir Pixel Dimension (m)			
In-Track	1.067	8.534	8.534
Cross-Track	1.067	6.401	6.401
Nadir Ground Sample Distance (m)			
In-Track	1.067	1.067	1.067
Cross-Track	0.762	0.762	0.762

No Line Averaging was used.

*The Pisgah Crater data were collected with an M-5 scanner with thermal calibration plates in part of the scanner field-of-view. The 11.3-13.5 μ m detector and the 8.0-10.9, 9.4-12.1 μ m detectors were on opposite ends of the scanner and are not in spatial registration. Hence, spectral correlation coefficients have not been determined between the 11.3-13.5 μ m data and either the 8.0-10.9 or the 9.4-12.1 μ m data. Histograms and correlation coefficients for the 8.0-10.9 and 9.4-12.1 μ m data are shown only for sub-areas 2, 3, and 4. Data in sub-area 1 were lost in the analog-to-digital conversion process.



MAP OF PISGAH CRATER AREA



11.3 - 13.5 μm



8.0 - 10.9 μm



9.4 - 12.1 μm

LINE SCAN IMAGES PRODUCED FROM THE VARIOUS INFRARED CHANNELS OF PISCAN CRATER



SUB-AREAS DEFINED FOR STATISTIC GENERATION IN THE PISGAH CRATER IMAGE.
 Approximate scene dimensions are 6805 ft (2074 m) by 820 ft (249 m)
 for channels 1, 2 and 6959 ft (2121 m) by 820 ft (249 m) for channel 4.
 Each sub-area as well as the total area have been histogrammed. Histogram
 plots and their respective sub-areas are identified with the following key.

- Sub-area 1 + Sub-area 4
- Sub-area 2 × Sub-area 5
- ▲ Sub-area 3 ◇ Sub-area 6

PISGAH CRATER

SUB-AREA 1

CHANNELS	4
MEAN	2.9024E+02
ST. DEV.	2.7648E+00
TOTAL PTS.	162519.

PISGAH CRATER
SUB-AREA 2

CORRELATION

	1	2
1	1.000	
2	0.311	1.000

CHANNELS

	1	2	4
MEAN	2.8918E+02	2.8901E+02	2.8911E+02
ST. DEV.	2.5054E+00	2.5412E+00	2.8701E+00
TOTAL PTC.	142899.	142699.	162519.

PISGAH CRATER
SUB-AREA 3

CORRELATION	1	2
1	1.000	
2	0.756	1.000

CHANNELS	1	2	4
MEAN	2.8821E+02	2.8805E+02	2.8870E+02
ST. DEV.	2.3843E+00	2.4706E+00	2.8878E+00
TOTAL PTS.	158922.	158922.	162519.

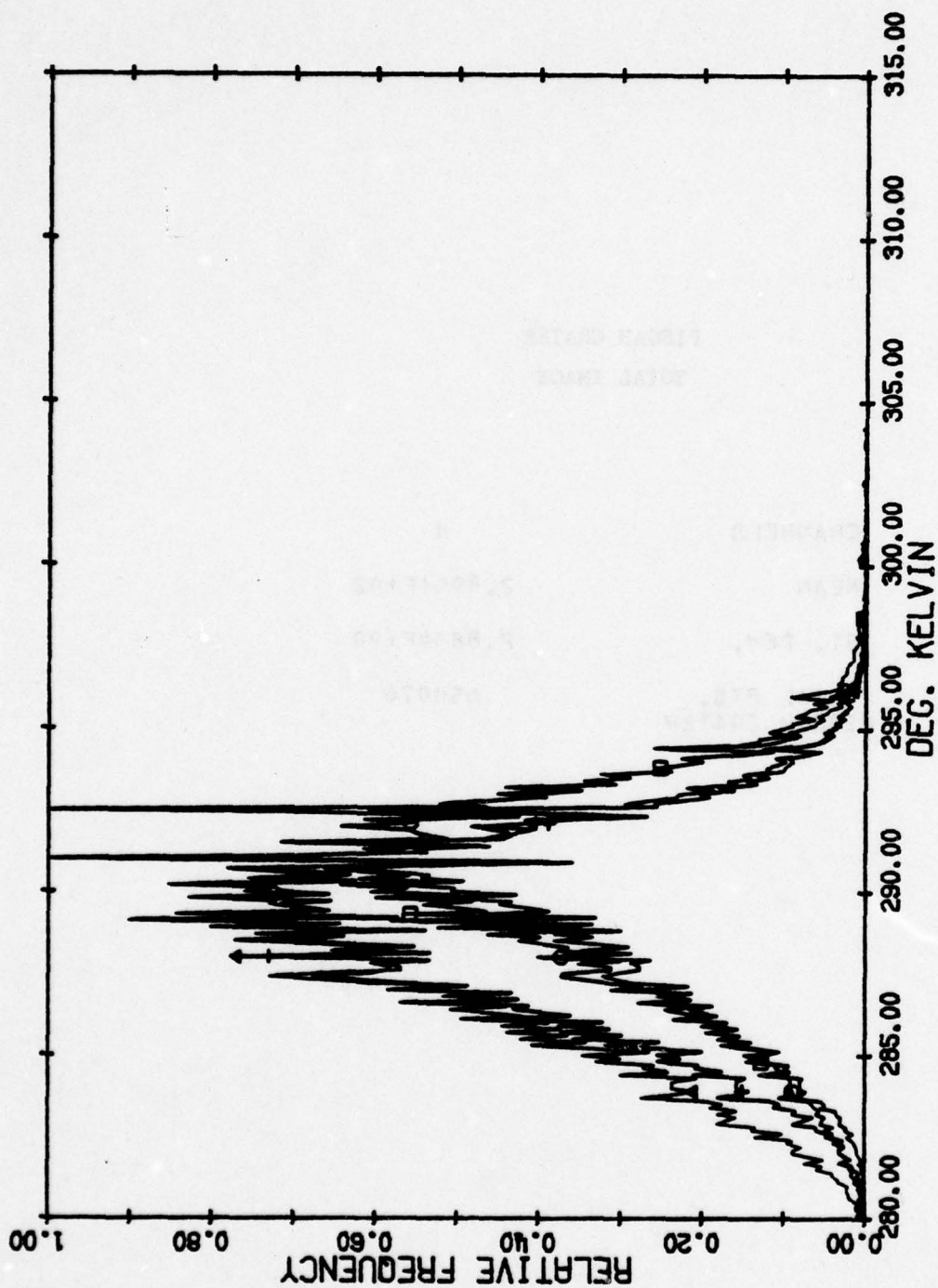
PISGAH CRATER

SUB-AREA 4

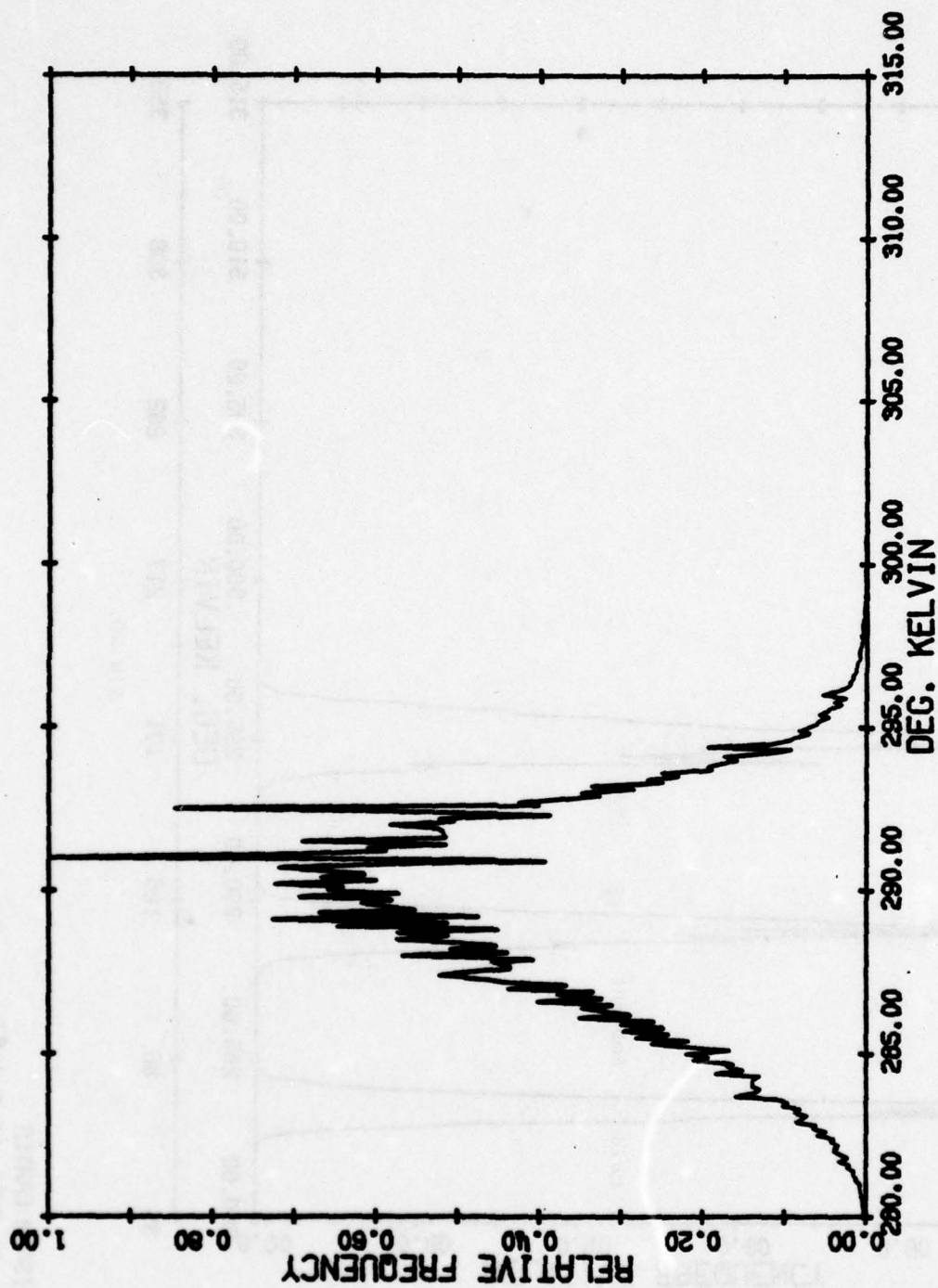
CORRELATION		1	2
1		1.000	
2		0.690	1.000
CHANNELS			
	1	2	4
MEAN	2.9844E+02	2.8924E+02	2.8899E+02
ST. DEV.	2.0618E+00	2.0900E+00	2.7124E+00
TOTAL PTS.	158922.	158922.	162519.

PISGAH CRATER
TOTAL IMAGE

CHANNELS	4
MEAN	2.8951E+02
ST. DEV.	2.8834E+00
TOTAL PTS. PISGAH CRATER	650076

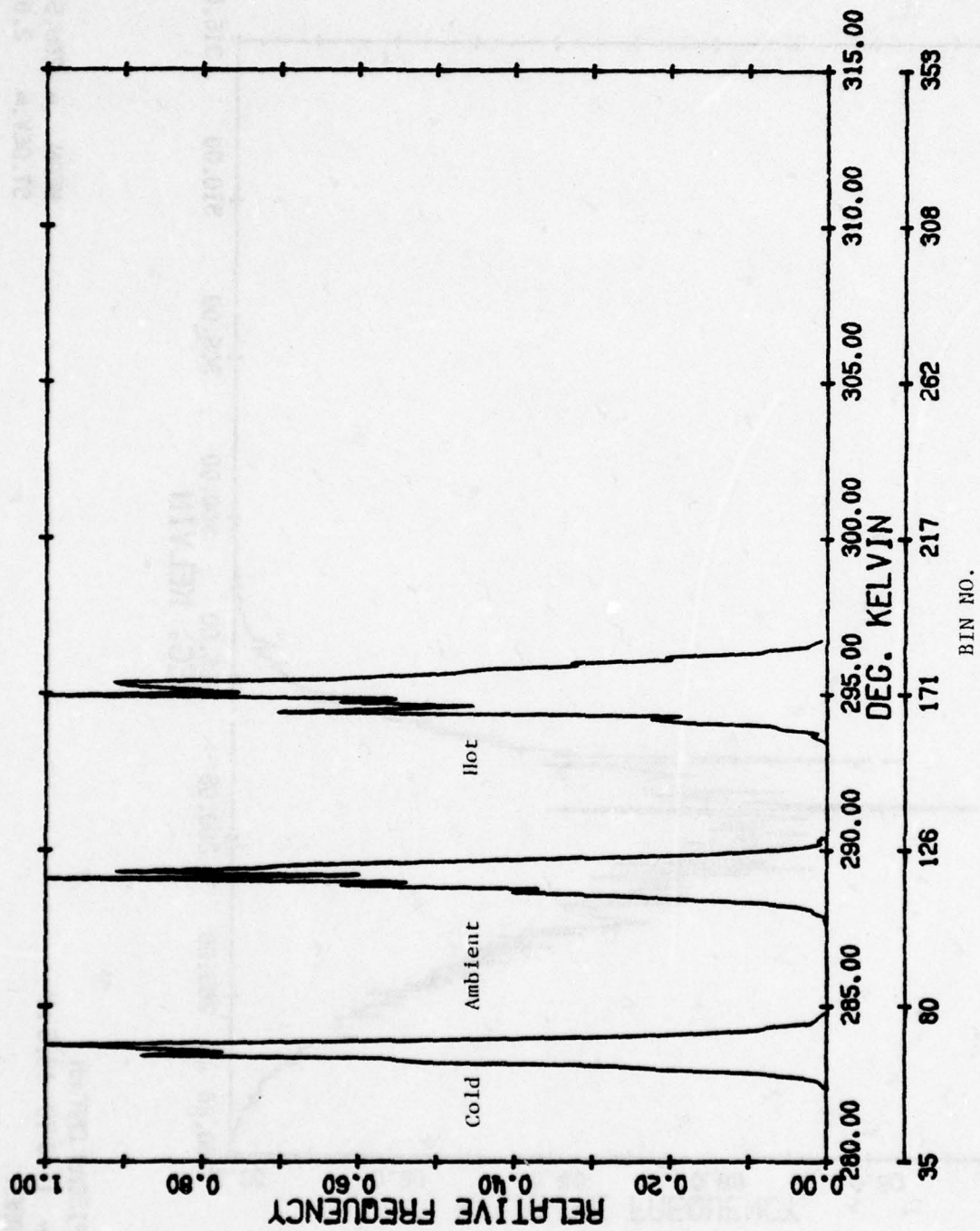


AREA: PISGAM CRATER
 WAVELENGTH 11.3 TO 13.5 μ M
 SUBPLOTS

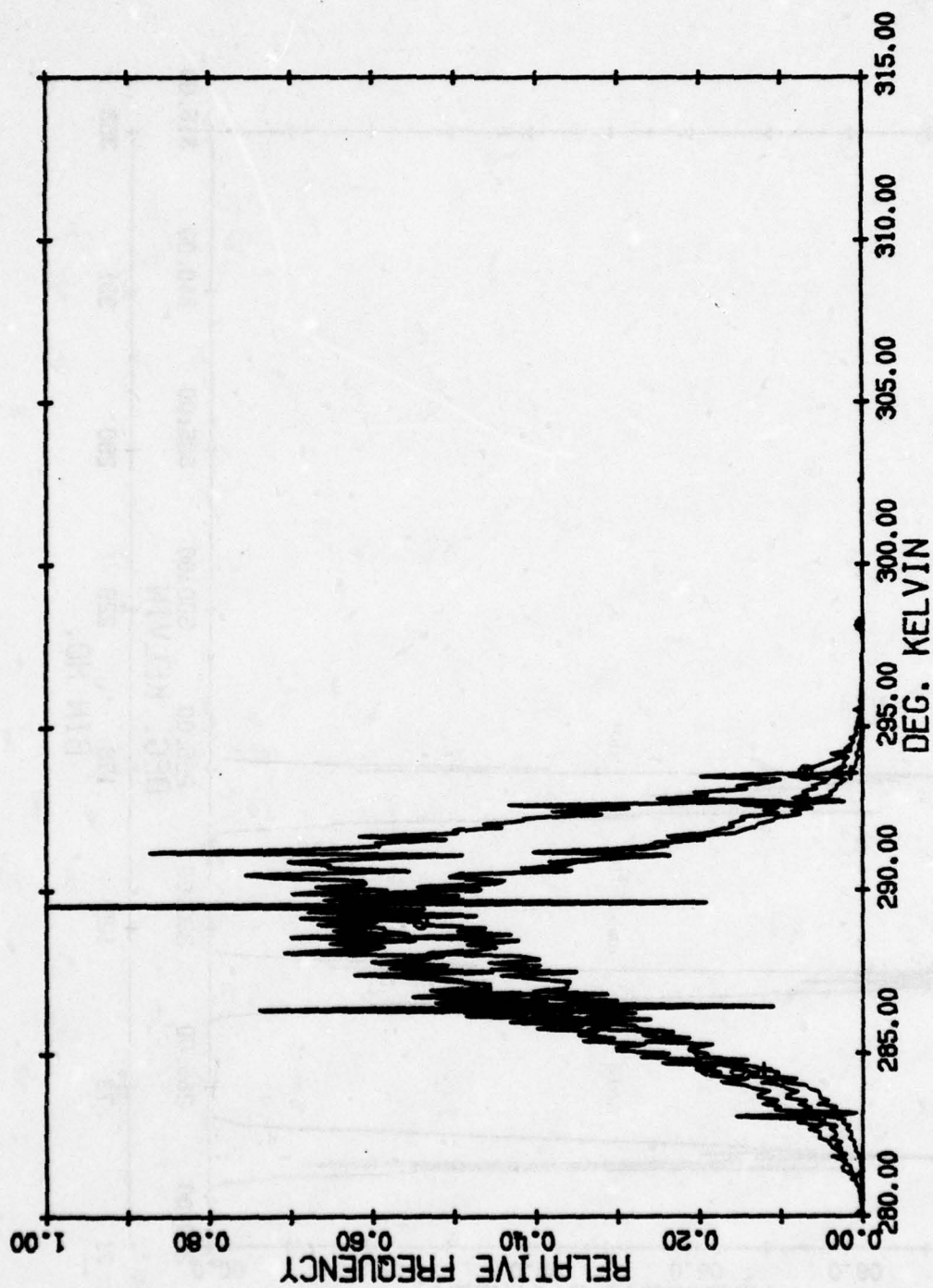


AREA: PISCAN CRATER
WAVELENGTH= 11.3 TO 13.5 μ M
TOTAL AREA

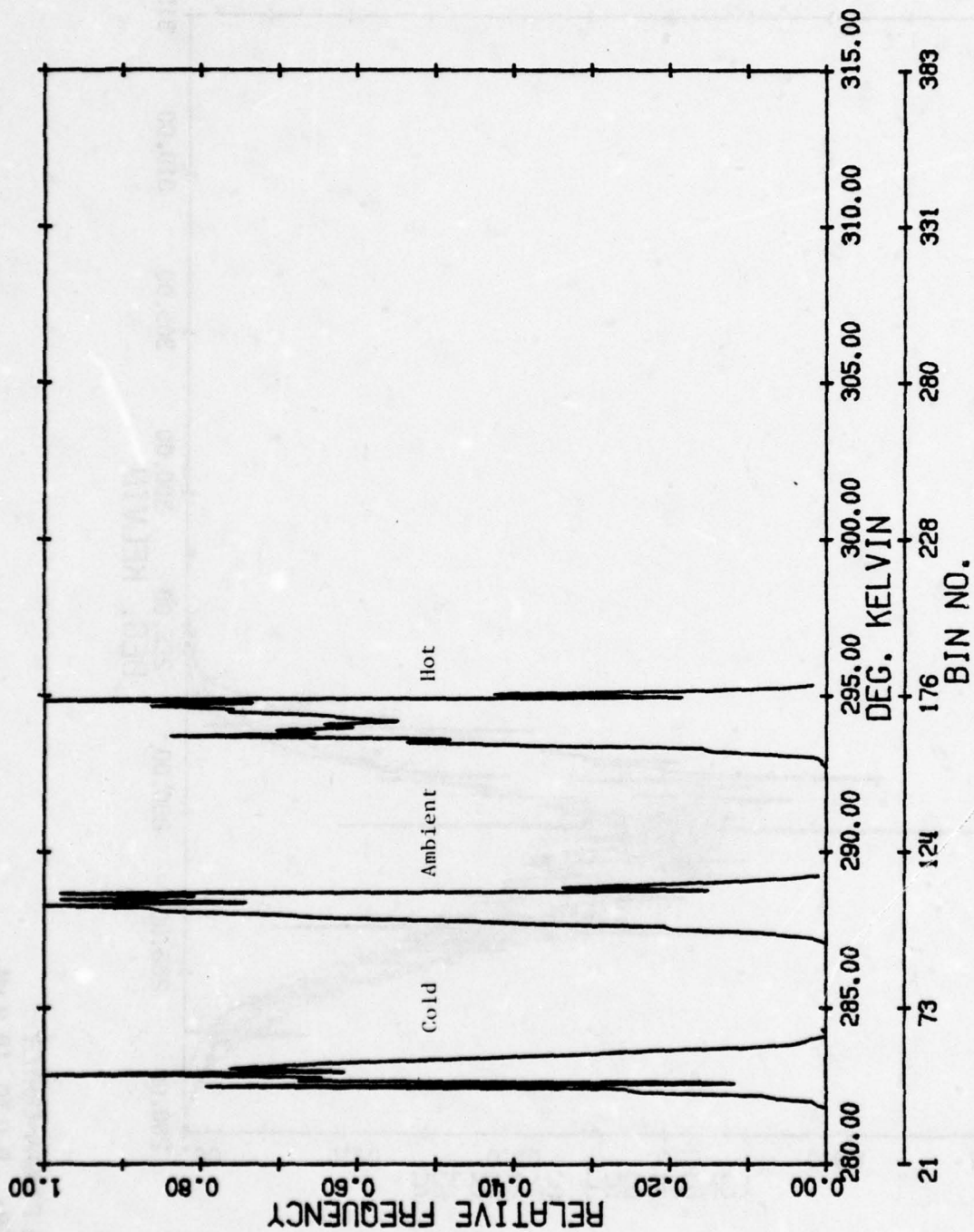
MEAN = 289.51
ST. DEV. = 2.89



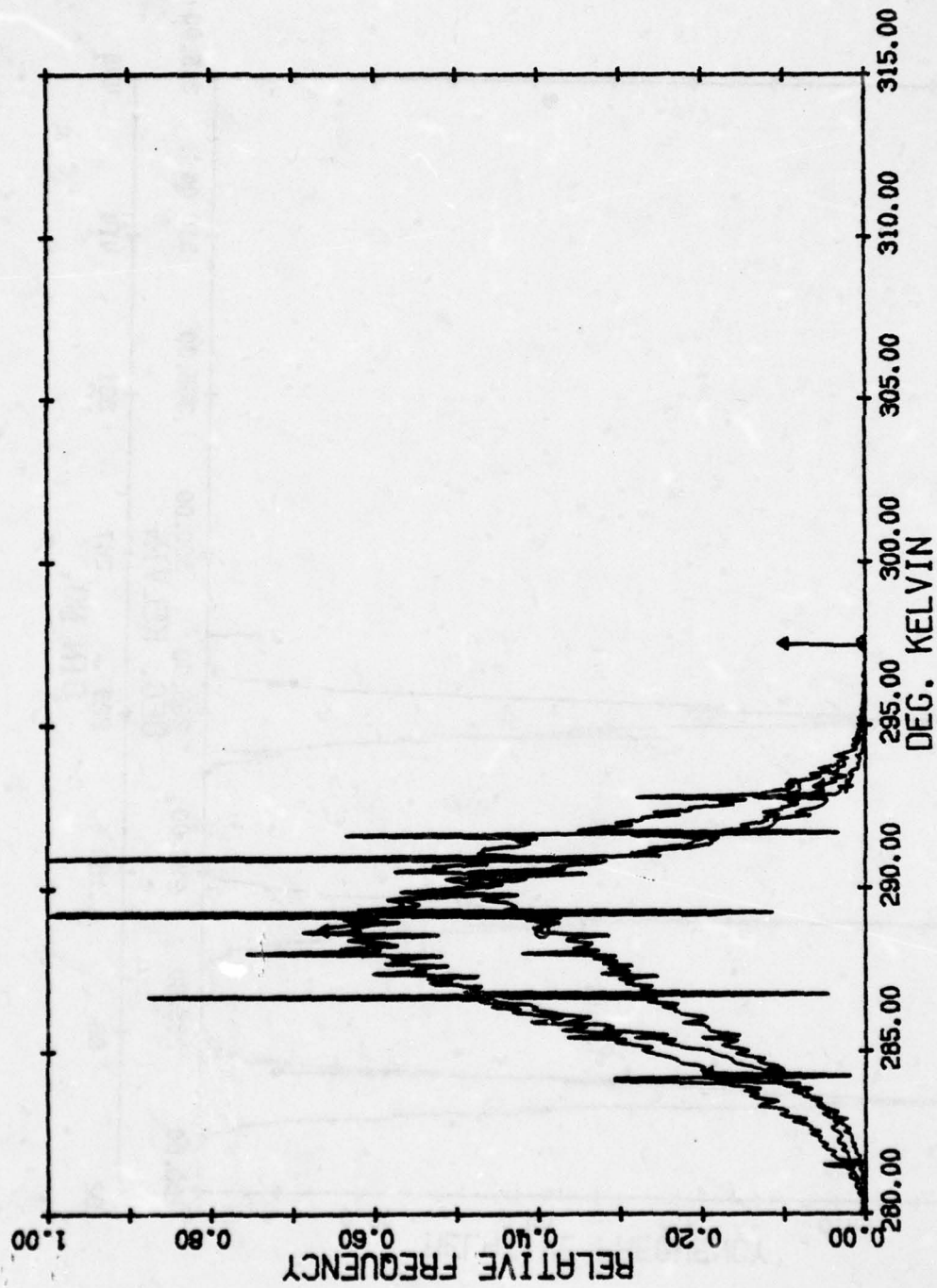
AREA: PISGAM CRATER
 LAMBDA= 11.3 TO 13.5 μ M
 CALIB. PLATES



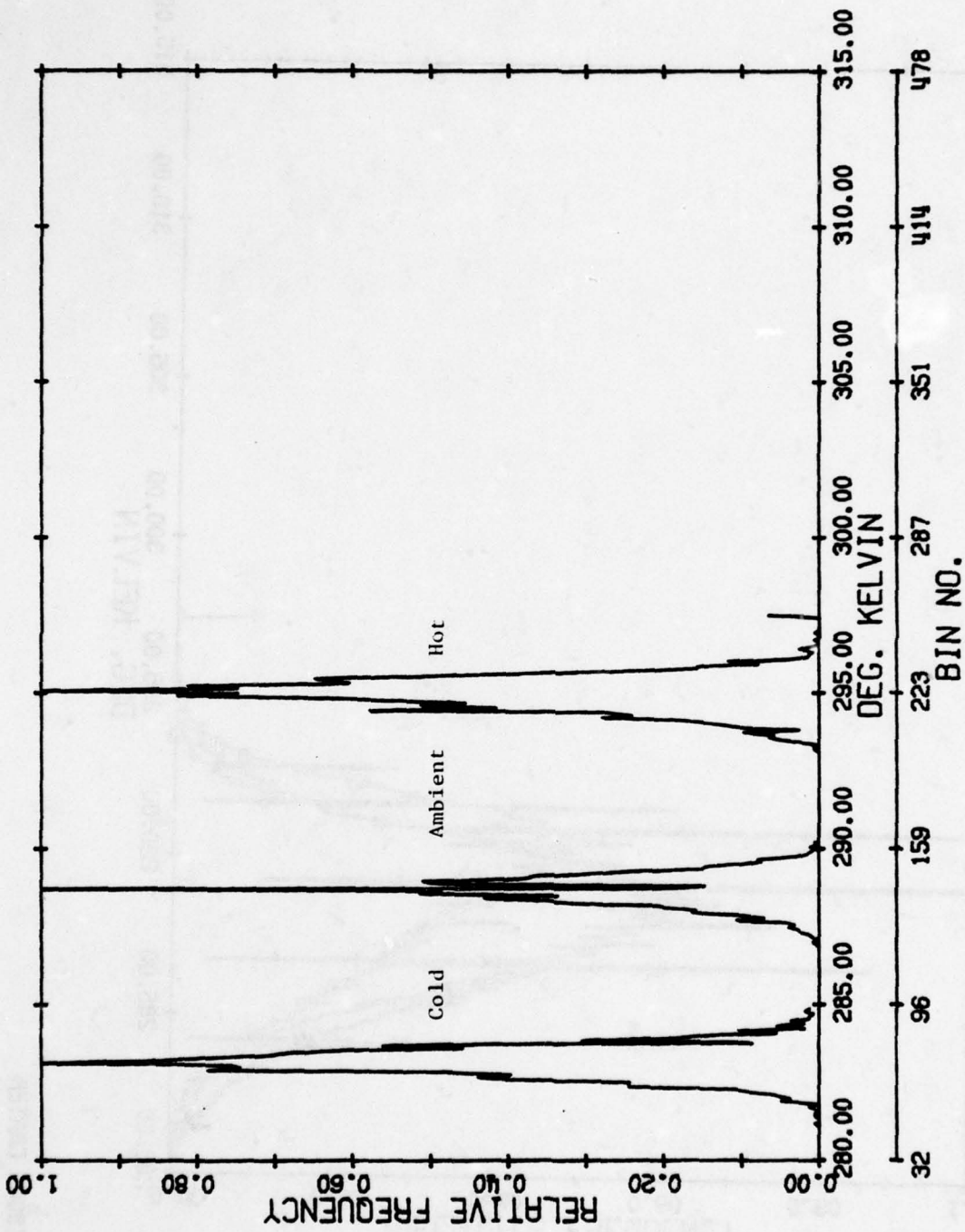
AREA: PISCAN CRATER
WAVELENGTH: 8.0 TO 10.9 μ M
SUBAREAS



AREA: PISGAH CRATER
 LAMBDA= 8.0 TO 10.9 μ M
 CALIB. PLATES



AREA: PISCAN CRATER
 LAMBDA= 9.4 TO 12.1 μ M
 SUBAREAS



AREA: PISGAH CRATER
 LAMBDA= 9.4 TO 12.1 μ M
 CALIB. PLATES

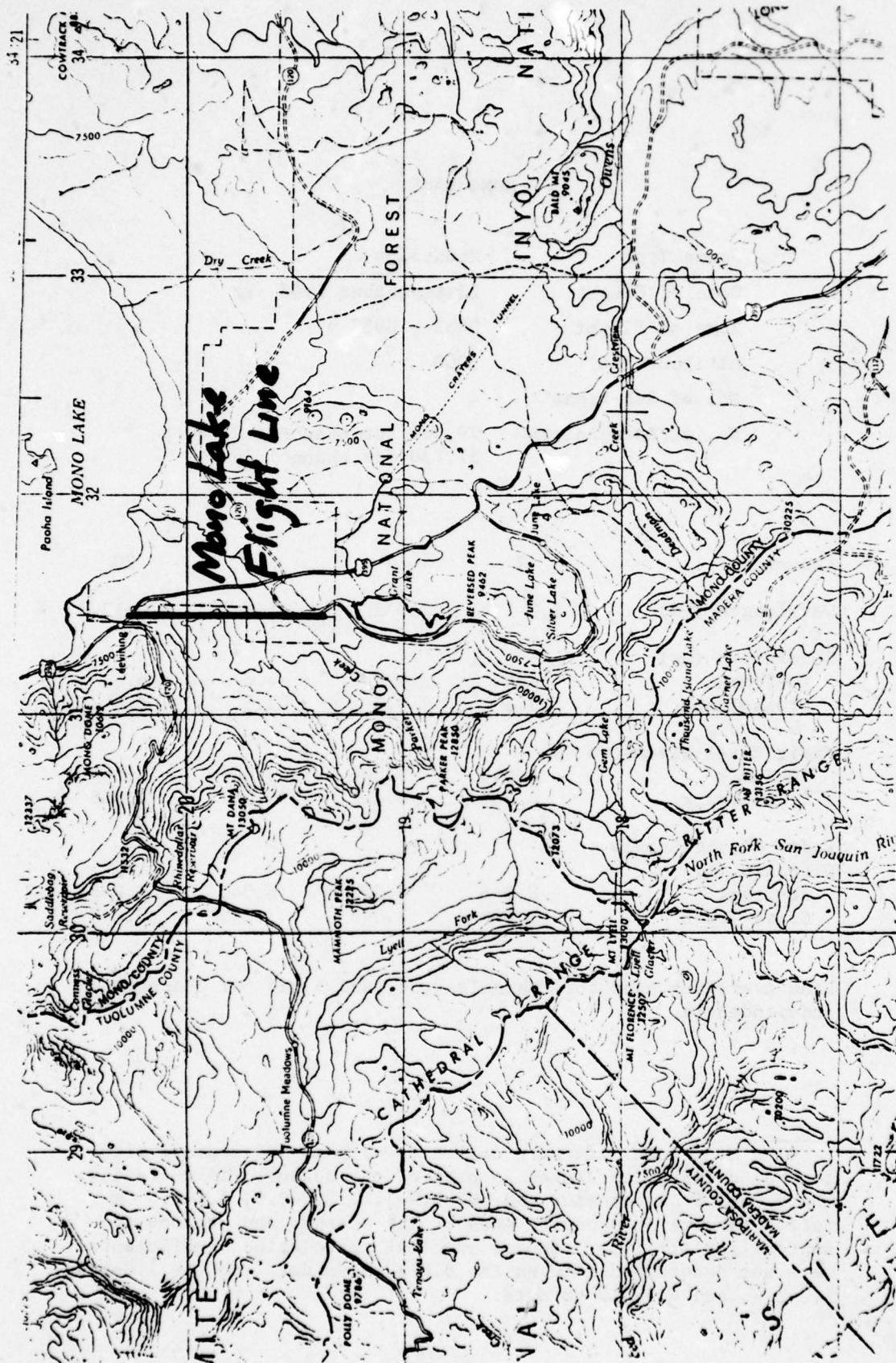
MONO LAKE*

Scene Type	Mountains
Date of Flight	23 September 1968
Time of Flight	0952 - 0957
Altitude (Ft)	4000
No. of Sub-Areas	4
No. of Data Points	79,360 for channels 2, 4, 5 87,730 for channel 20

Channels	2	4	5	20
Wavelength (μm)	1.0-1.4	2.0-2.6	4.5-5.5	8.0-13.5
Resolution (mr)				
In-Track	6.6	6.6	6.6	6.6
Cross-Track	3.5	3.5	3.5	6.6
Nadir Pixel Dimension (m)				
In-Track	8.046	8.046	8.046	8.046
Cross-Track	4.267	4.267	4.267	8.046
Nadir Ground Sample Distance (m)				
In-Track	8.046	8.046	8.046	8.046
Cross-Track	3.048	3.048	3.048	3.048

Line Averaging used for channels 2, 4, and 5 and for channel 20 independently.

*The Mono Lake data were collected with an M-5 scanner with thermal calibration plates in part of the scanner field-of-view. The 8.0-13.5 μm detector and the 1.0-1.4, 2.0-2.6, 4.5-5.5 μm detectors were on opposite ends of the scanner and are not in spatial registration. Hence, spectral correlation coefficients were not determined between the 8.0-13.5 μm data and the 1.0-1.4, 2.0-2.6, and 4.5-5.5 μm data.

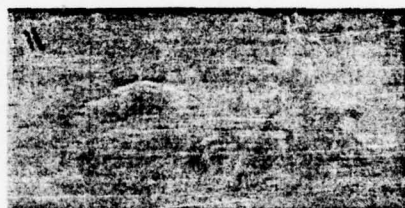




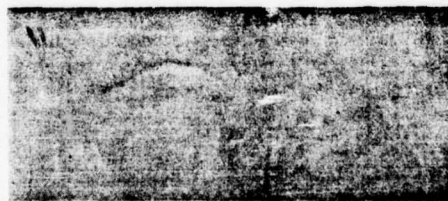
1.0 - 1.4 μm



2.0 - 2.6 μm

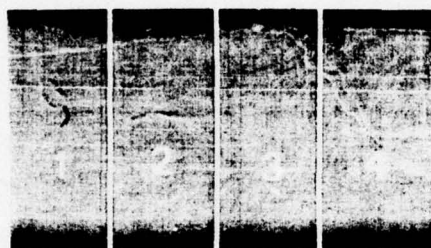


4.5 - 5.5 μm



8.0 - 13.5 μm

LINE SCAN IMAGES PRODUCED FROM THE VARIOUS
INFRARED CHANNELS OF MONO LAKE



Pixel 1

Pixel 311

Line 1	71	142	213	284 - channel 20
Line 11	67	133	199	266 - channels 2,4,5

SUB-AREAS DEFINED FOR STATISTICS GENERATION
IN THE MONO LAKE IMAGE. Approximate scene
dimensions are 7497 ft (2285 m) by 3110 ft
(948 m) for channel 20 and 6758 ft (2059 m)
by 3110 ft (948 m) for channels 2, 4, 5.
Each sub-area as well as the total area have
been histogrammed. Histogram plots and their
respective sub-areas are identified with the
following key:

□ Sub-area 1	+ Sub-area 4
○ Sub-area 2	× Sub-area 5
△ Sub-area 3	◇ Sub-area 6

MONO LAKE

SUB-AREA 1

CORRELATION	2	4	5
2	1.000		
4	0.931	1.000	
5	0.842	0.873	1.000

CHANNELS	2	4	5	20
MEAN	1.9721E+03	9.1899E+01	2.8510E+02	2.8810E+02
ST. DEV.	3.5310E+02	1.8740E+01	1.4328E+00	1.5897E+00
TOTAL PTS.	17980.	17980.	17980.	22010.

MONO LAKE
SUB-AREA 2

CORRELATION	2	4	5
2	1.000		
4	0.901	1.000	
5	0.832	0.845	1.000

CHANNELS	2	4	5	20
MEAN	2.0351E+03	9.3547E+01	2.8533E+02	2.8922E+02
ST. DEV.	3.2655E+02	1.6603E+01	1.0450E+00	1.5805E+00
TOTAL PTS.	20460.	20460.	20460.	22610.

MONO LAKE

SUB-AREA 3

CORRELATION	2				5			
	2				4			
2	1.000							
4	0.874				1.000			
5	0.795				0.758			
					1.000			
CHANNELS	2				4			
	2				5			
MEAN	2.0717E+03				0.4819E+01			
					2.8558E+02			
ST. DEV.	3.1754E+02				1.5014E+01			
					1.0188E+00			
TOTAL PLS.	20460.				20460.			
					22010.			

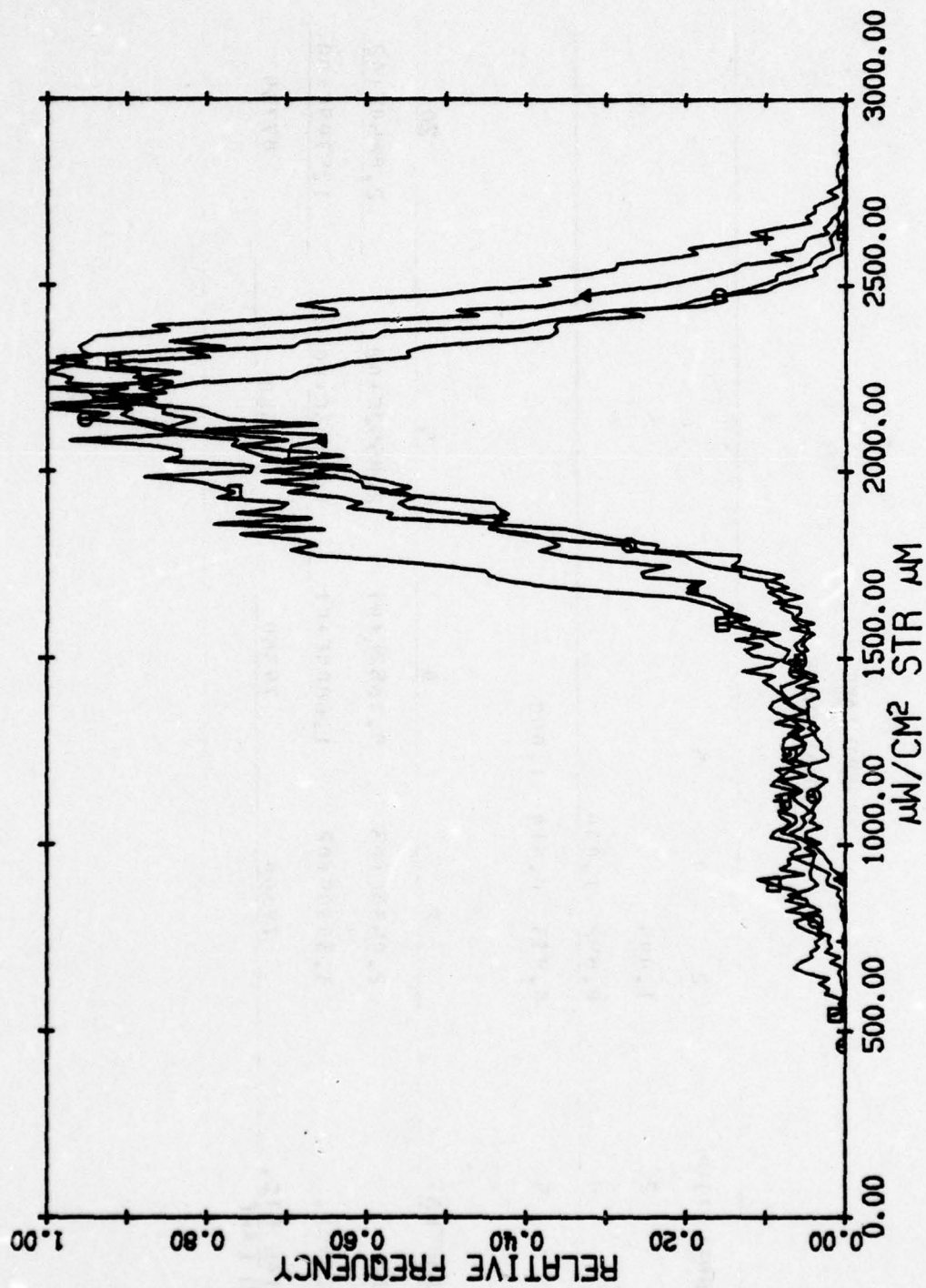
MONO LAKE
SUB-AREA 4

CUMULATION	2	4	5
2	1.000		
4	0.856	1.000	
5	0.802	0.780	1.000

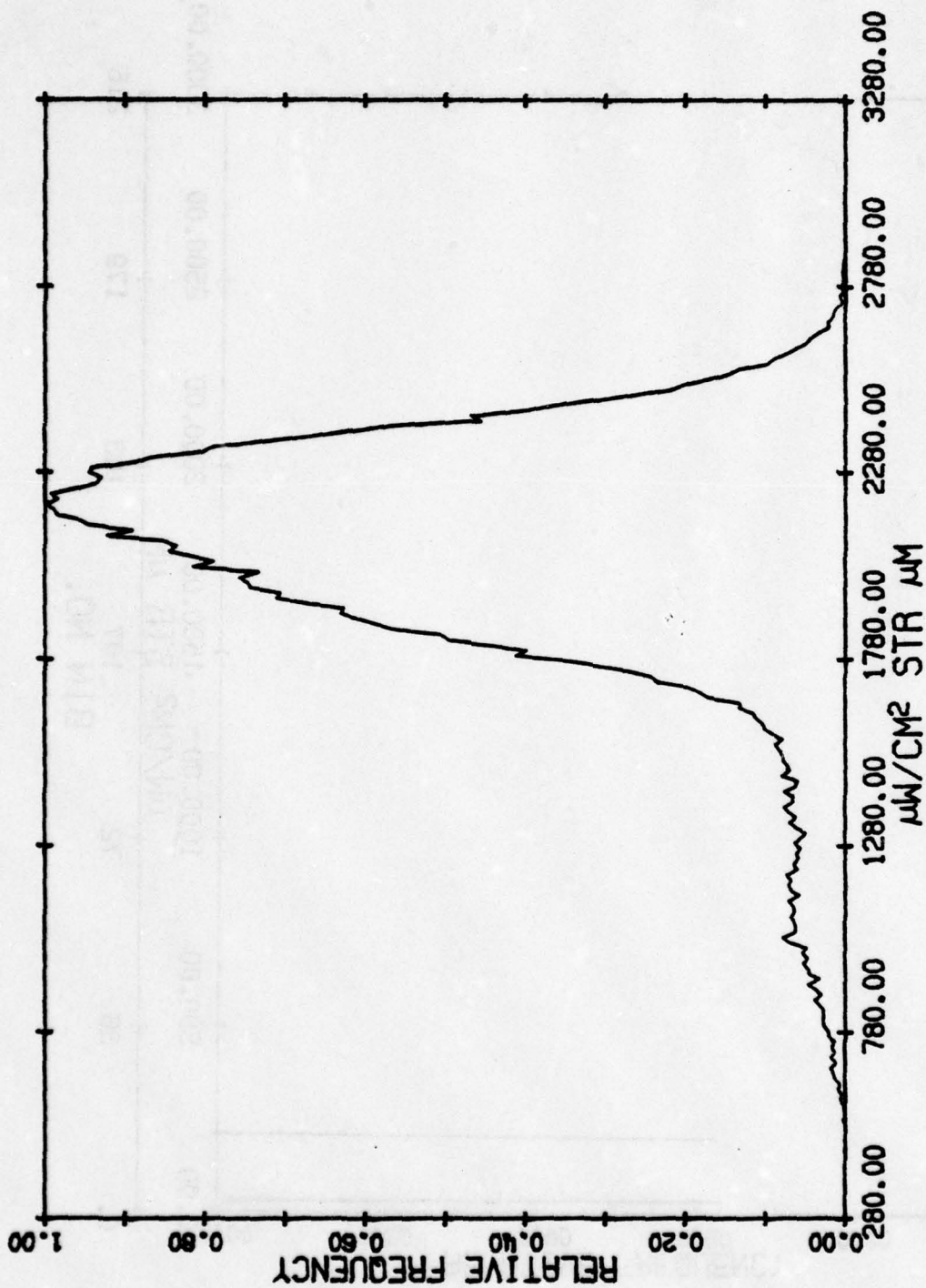
CHANNELS	2	4	5	20
MEAN	2.1248E+03	9.8010E+01	2.8602E+02	2.8911E+02
ST. DEV.	3.2383E+02	1.5330E+01	1.2632E+00	1.6268E+00
TOTAL PLS.	20460.	20460.	20460.	21760.

MONO LAKE
TOTAL IMAGE

CORRELATION	2	4	5
2	1.000		
4	0.892	1.000	
5	0.833	0.814	1.000
CHANNELS	2	4	20
MEAN	2.0534E+03	9.4652E+01	2.8512E+02
ST. DEV.	3.3430E+02	1.6804E+01	1.5789E+00
TOTAL PLS. MONO LAKE	79360	79360	87730

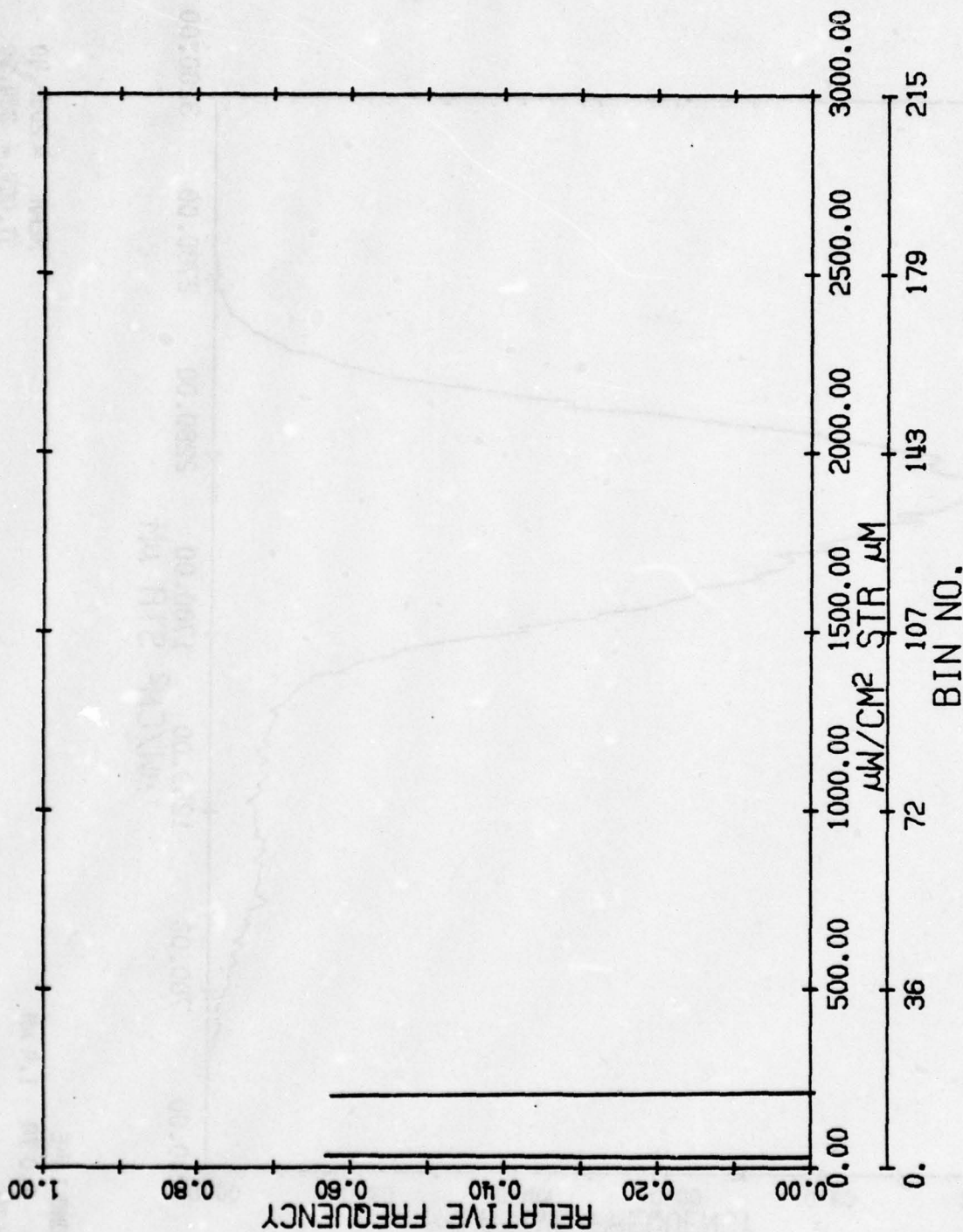


AREA MONO LAKE
WAVELENGTH 1.0 TO 1.4 μm
SUBPLOTS

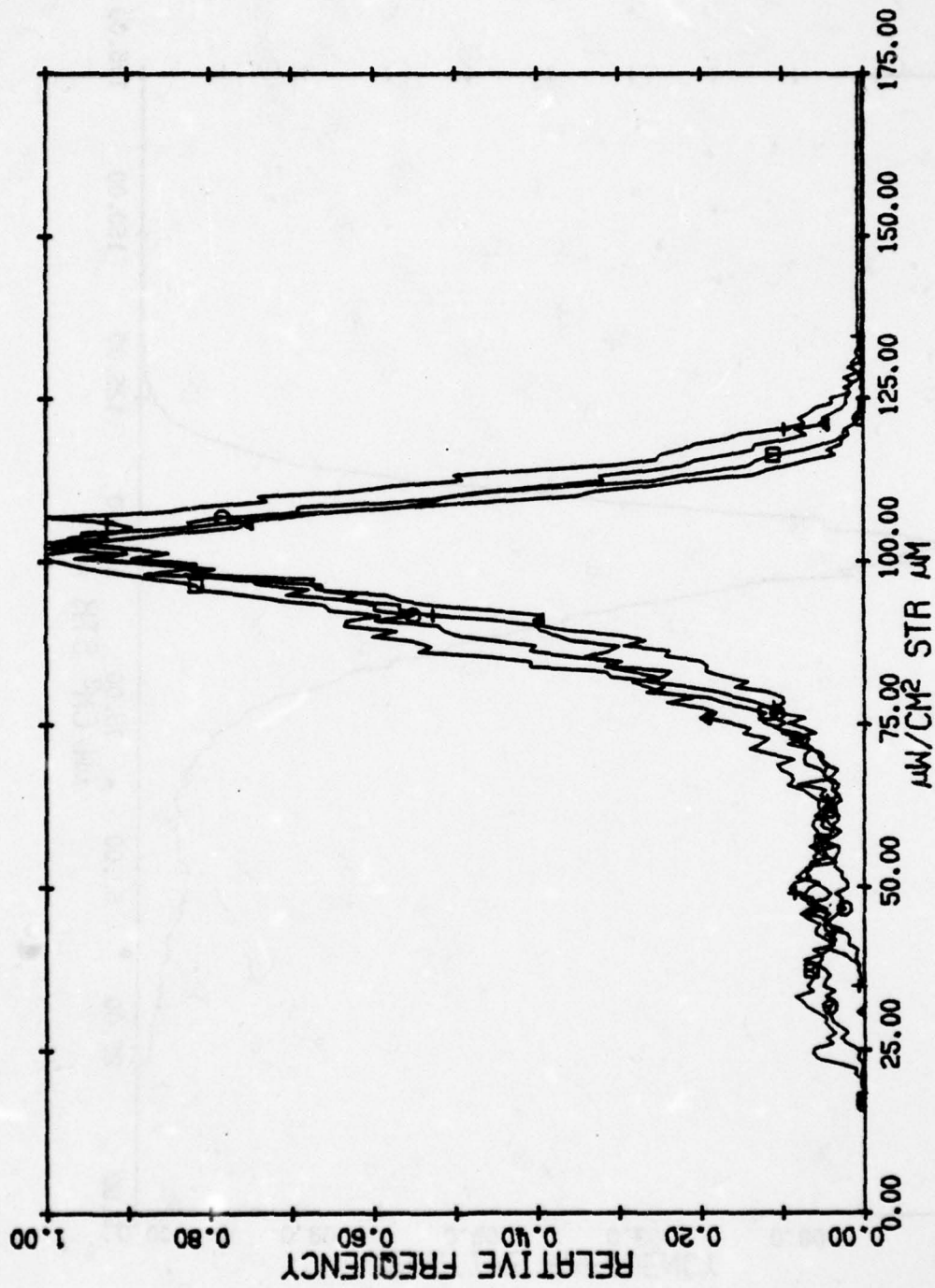


AREA: MONO LAKE
 LAMBDA= 1.0 TO 1.4 μ M
 TOTAL AREA

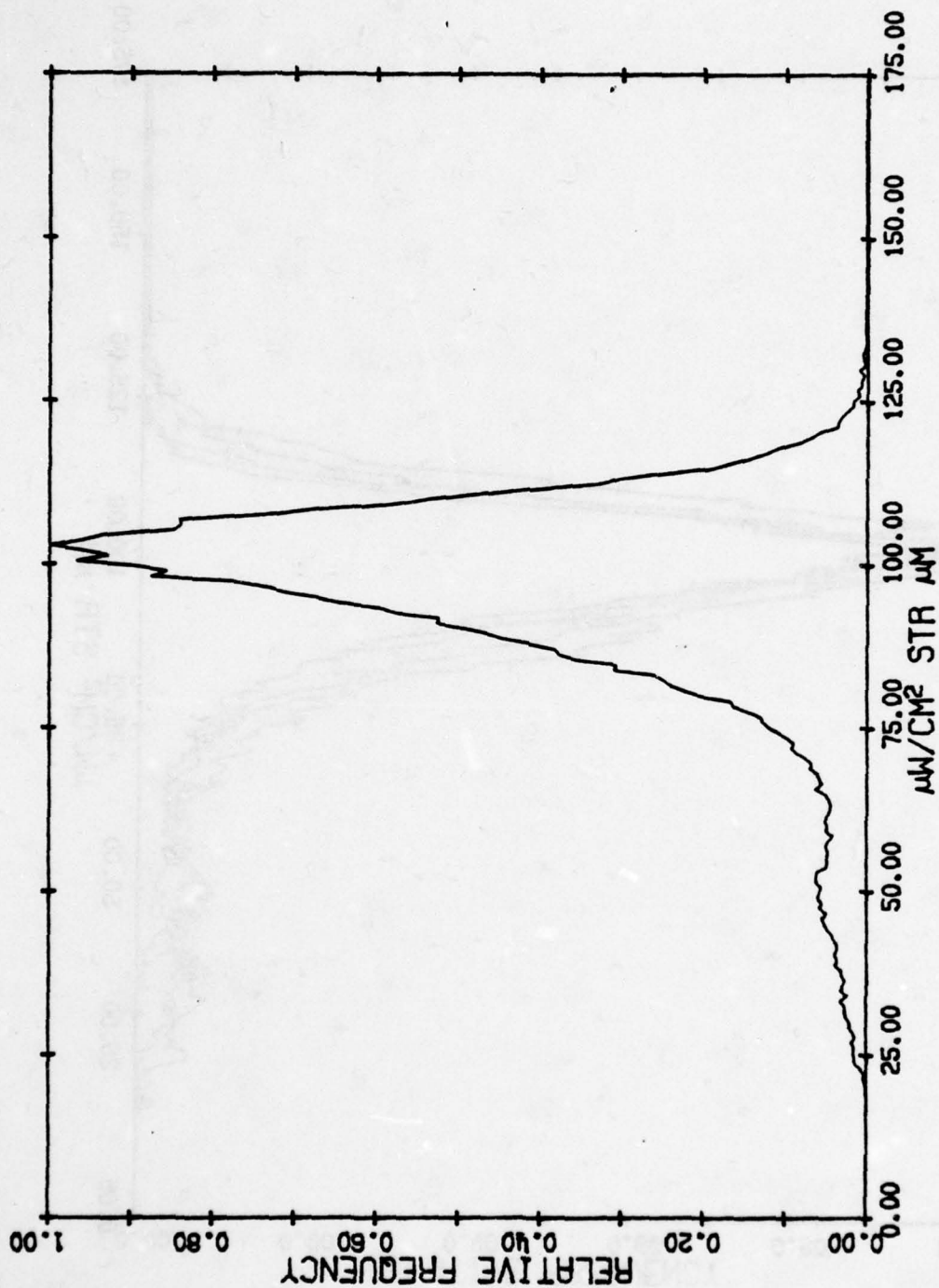
MEAN = 2053.40
 ST.DEV. = 334.30



AREA: MONO LAKE
 LAMBDA= 1.0 TO 1.4 μm
 CALIB. PLATES

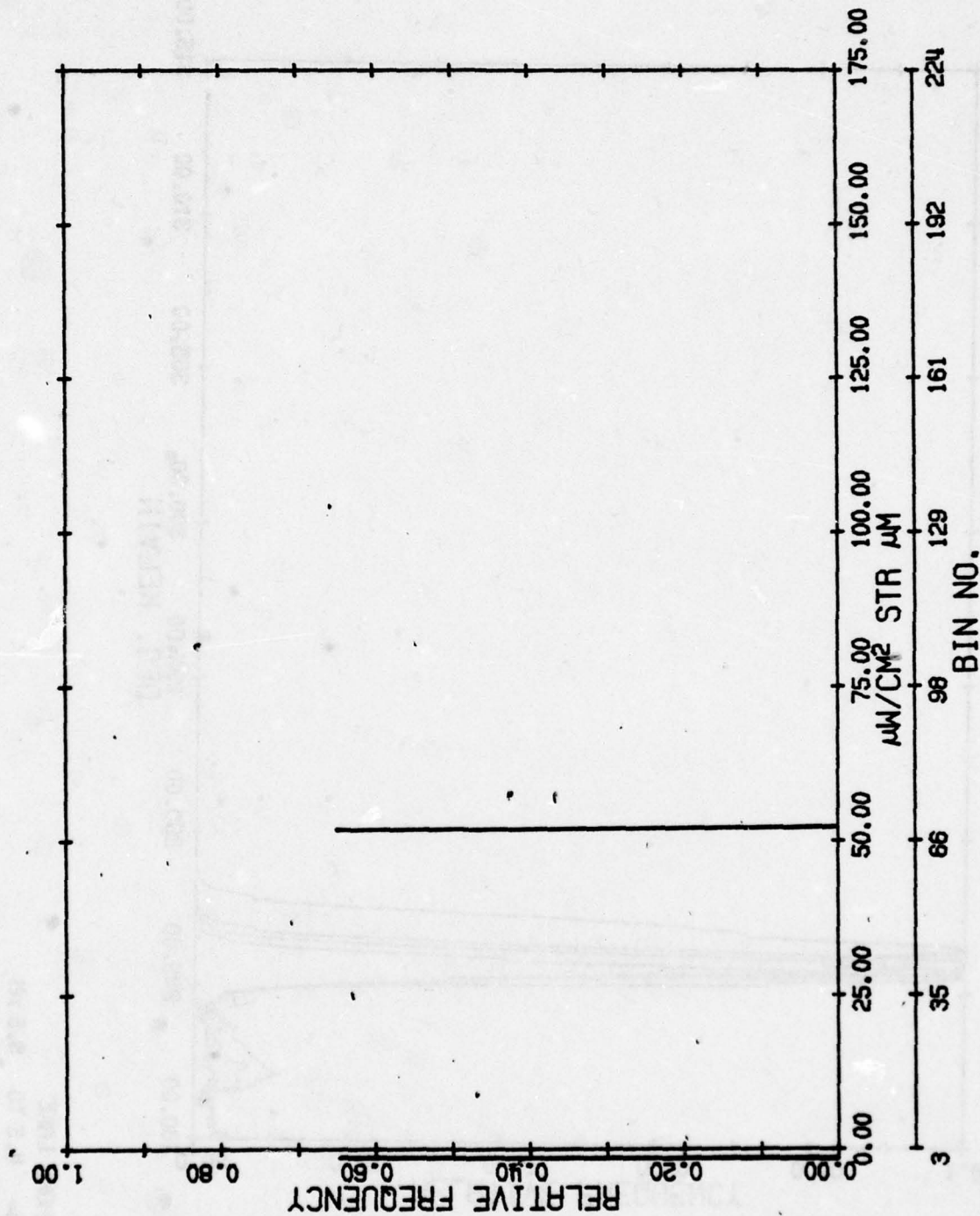


AREA: MONO LAKE
WAVELENGTH= 2.0 TO 2.6 μm
SUBAREAS

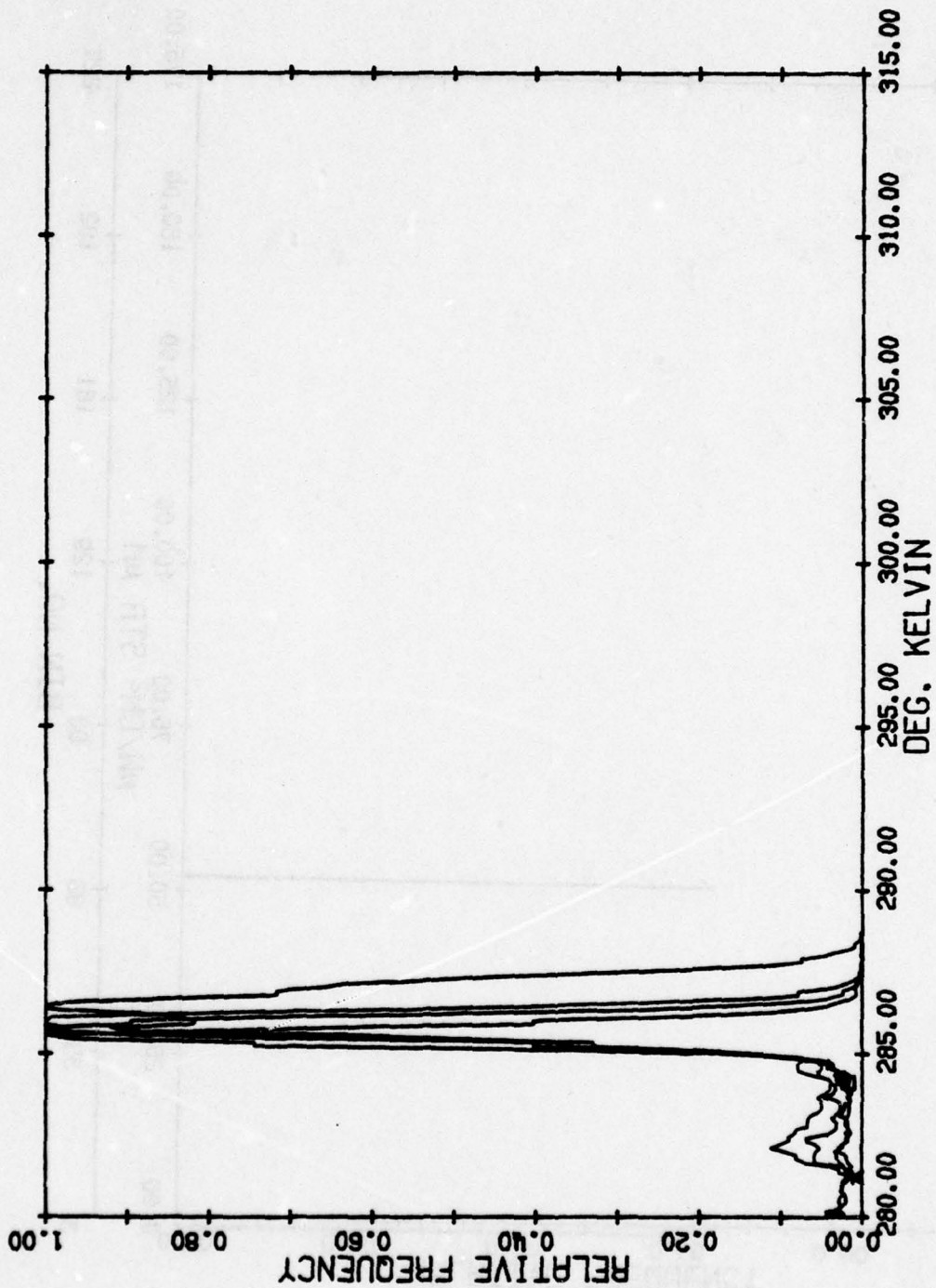


AREA: MONO LAKE
 LAMBDA= 2.0 TO 2.6 μm
 TOTAL AREA

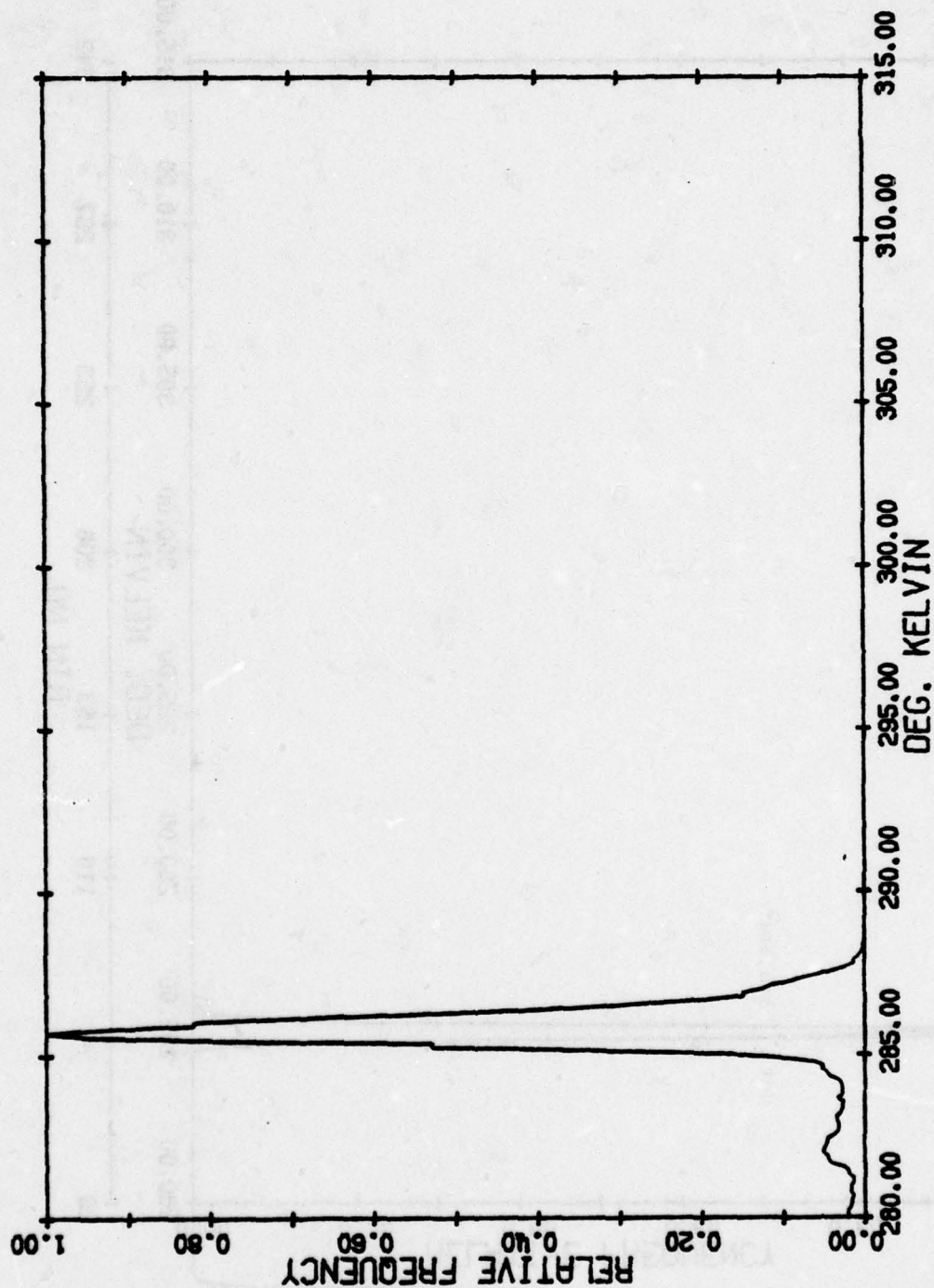
MEAN = 94.65
 ST.DEV. = 16.80



AREA: MONO LAKE
 WAVELENGTH= 2.0 TO 2.6 μm
 CONTINUED

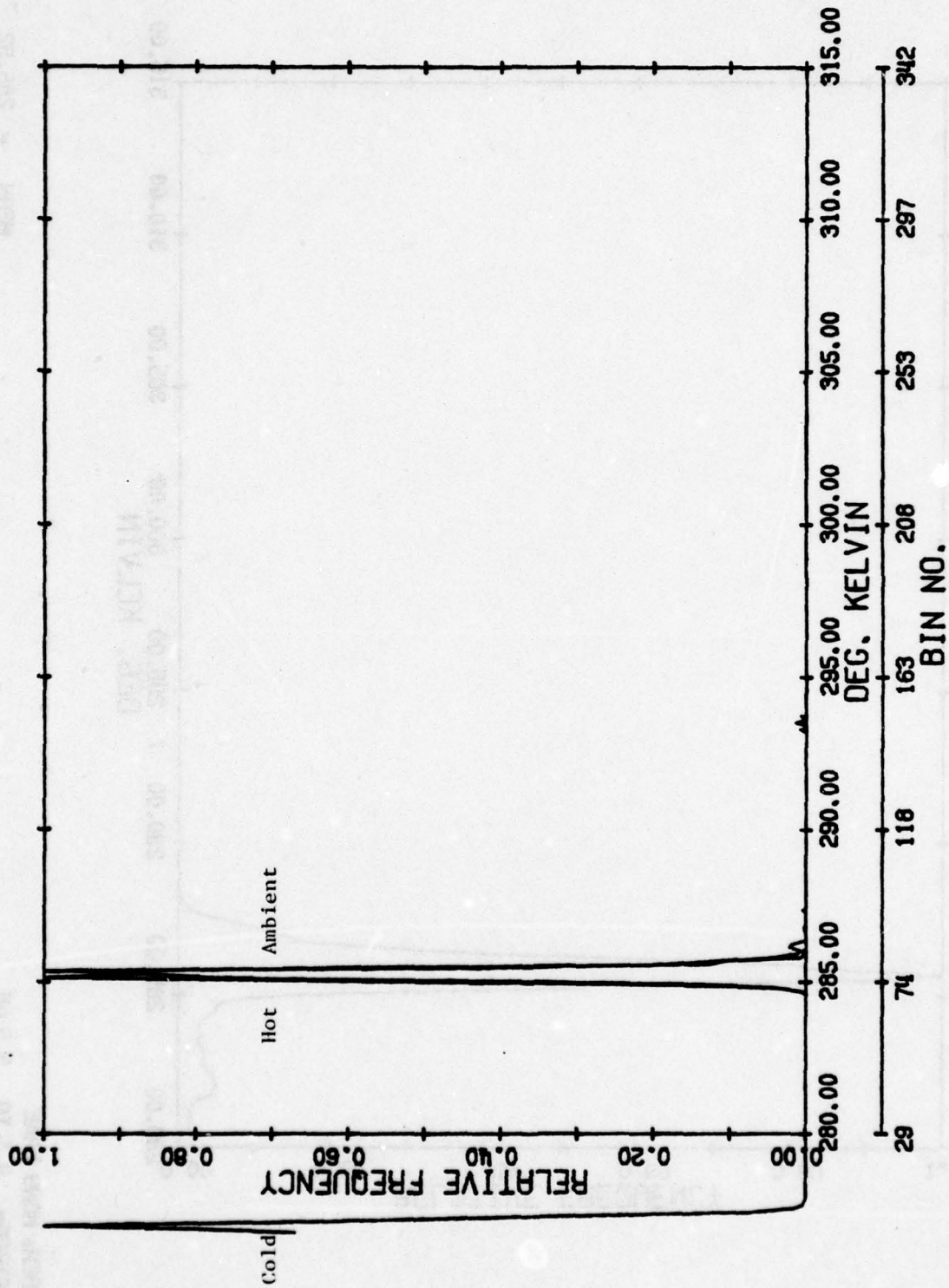


AREA: MONO LAKE
WAVELENGTH: 4.5 TO 5.5 μ M
SUBAREAS

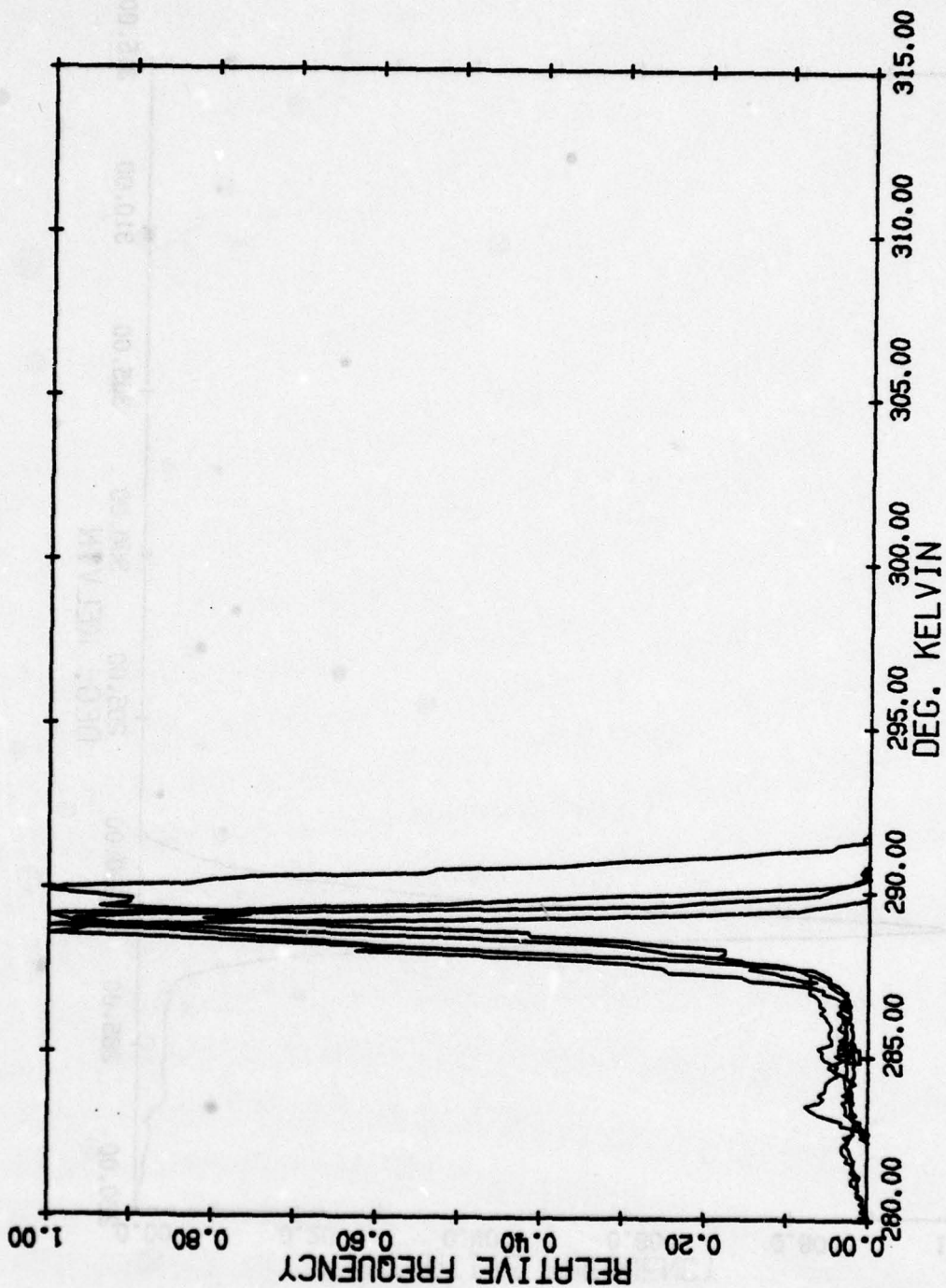


AREA: MONO LAKE
 LAMBDA= 4.5 TO 5.5 μ M
 TOTAL AREA

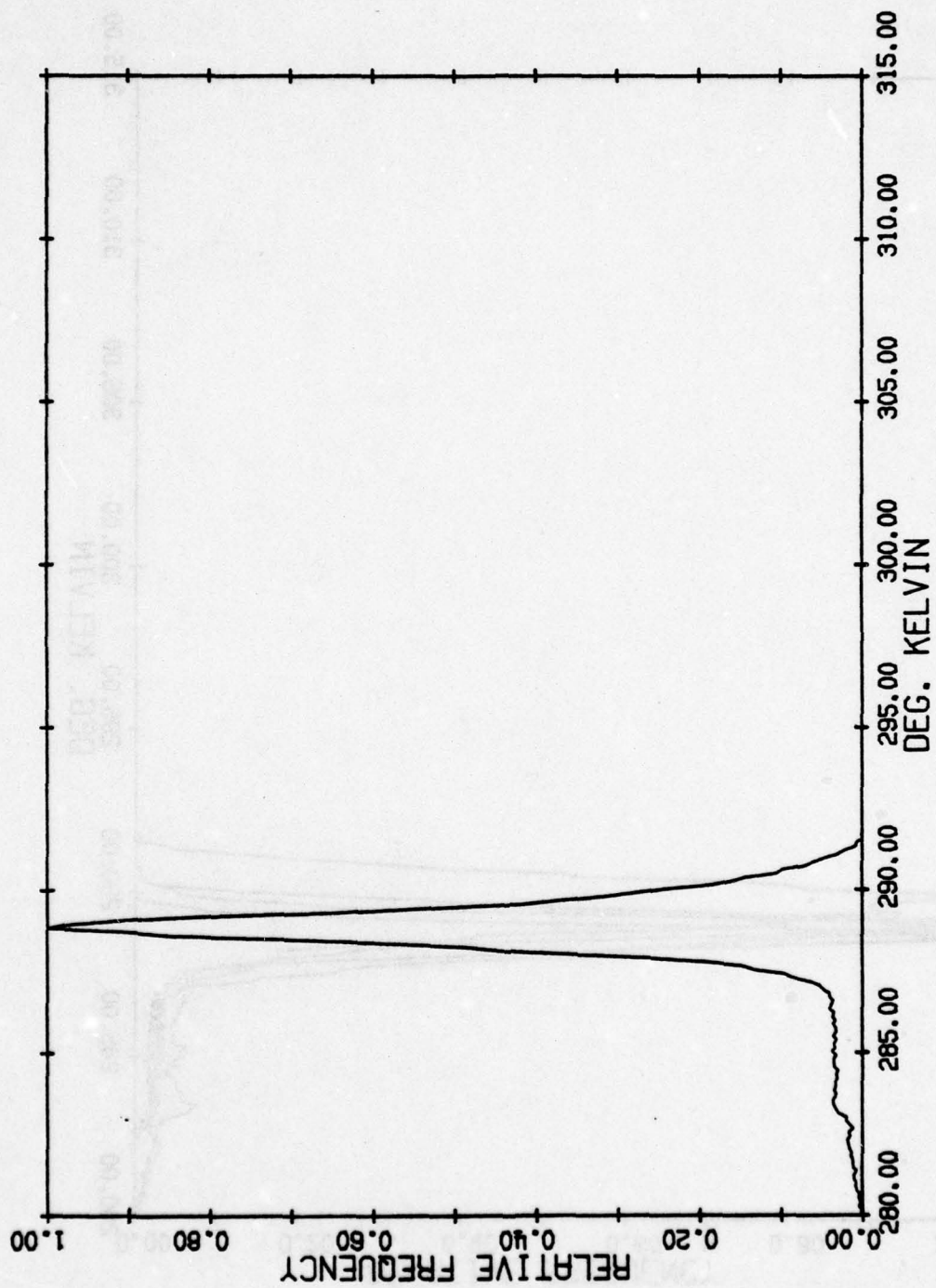
MEAN = 285.52
 ST. DEV. = 1.34



AREA: MONO LAKE
 WAVELENGTH: 4.5 TO 5.5 μ M
 CALIB. PLATES

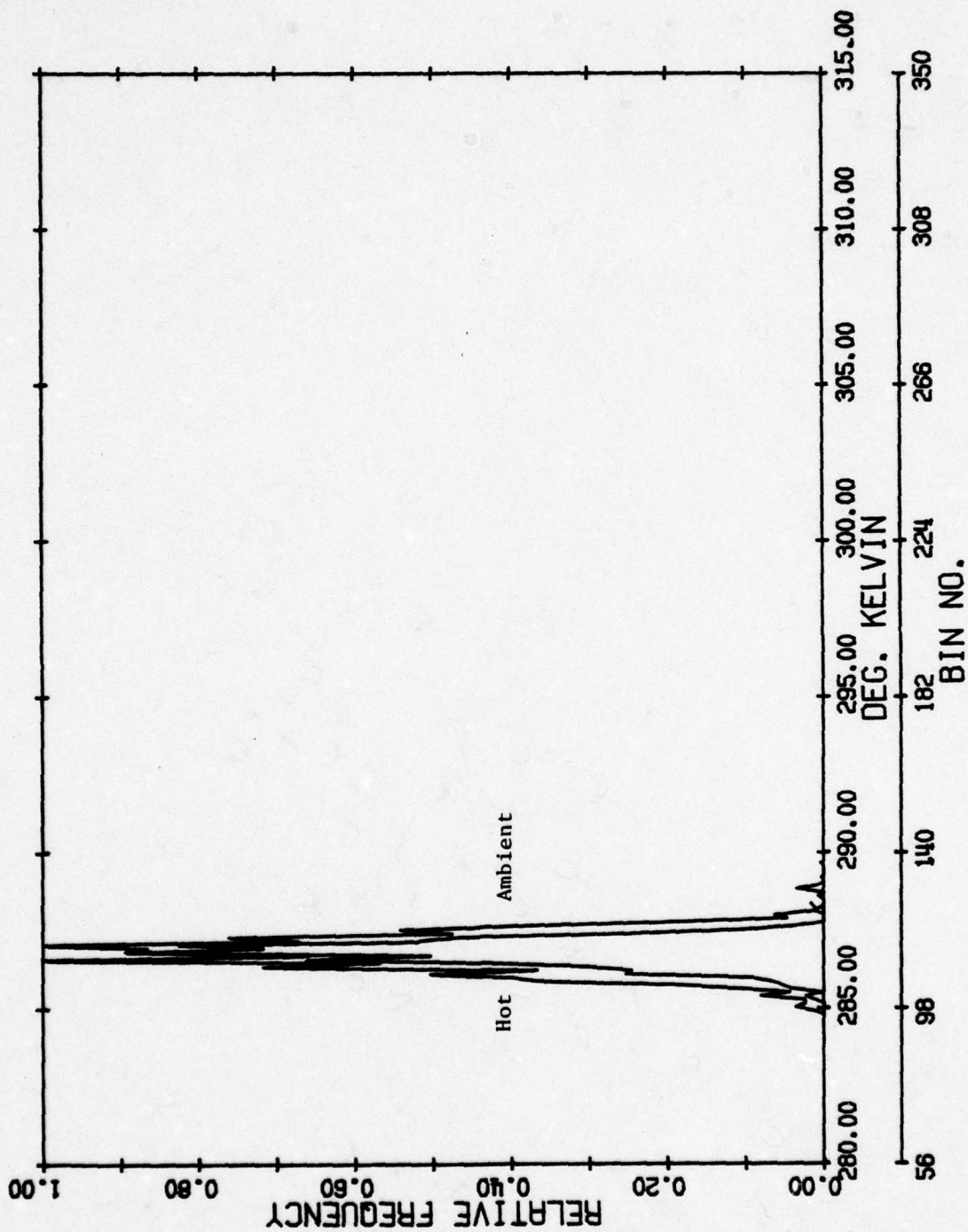


AREA: MONO LAKE
LAMBDA= 8.0 TO 13.5 μ M
SUBPERS



AREA: MONO LAKE
 LAMBDA= 8.0 TO 13.5 μ M
 TOTAL AREA

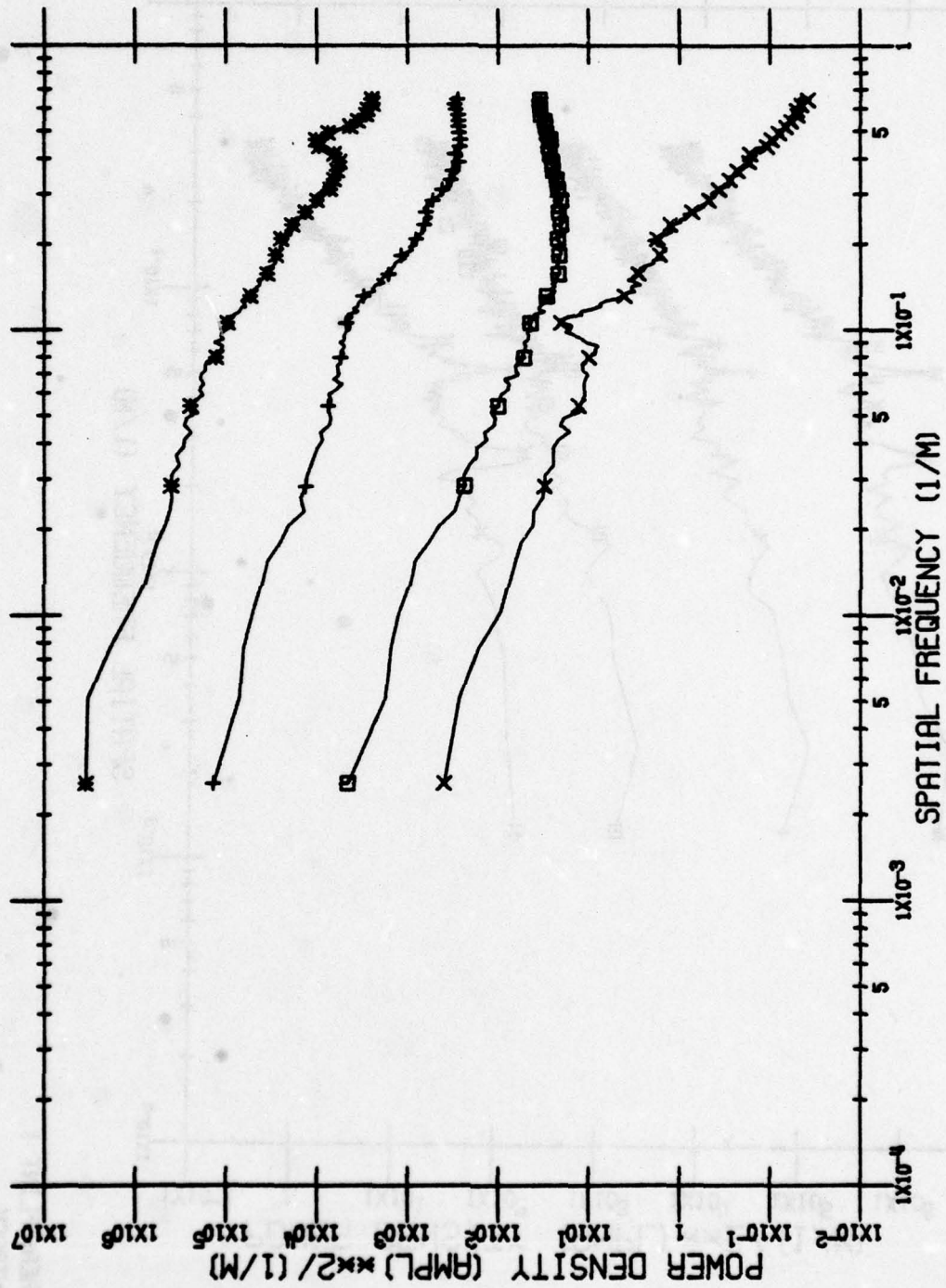
MEAN = 288.50
 ST.DEV. = 1.58



AREA: MONO LAKE
 LAMBDA= 8.0 TO 13.5 μ M
 CALIB. PLATES

PRECEDING PAGE BLANK-NOT FILMED

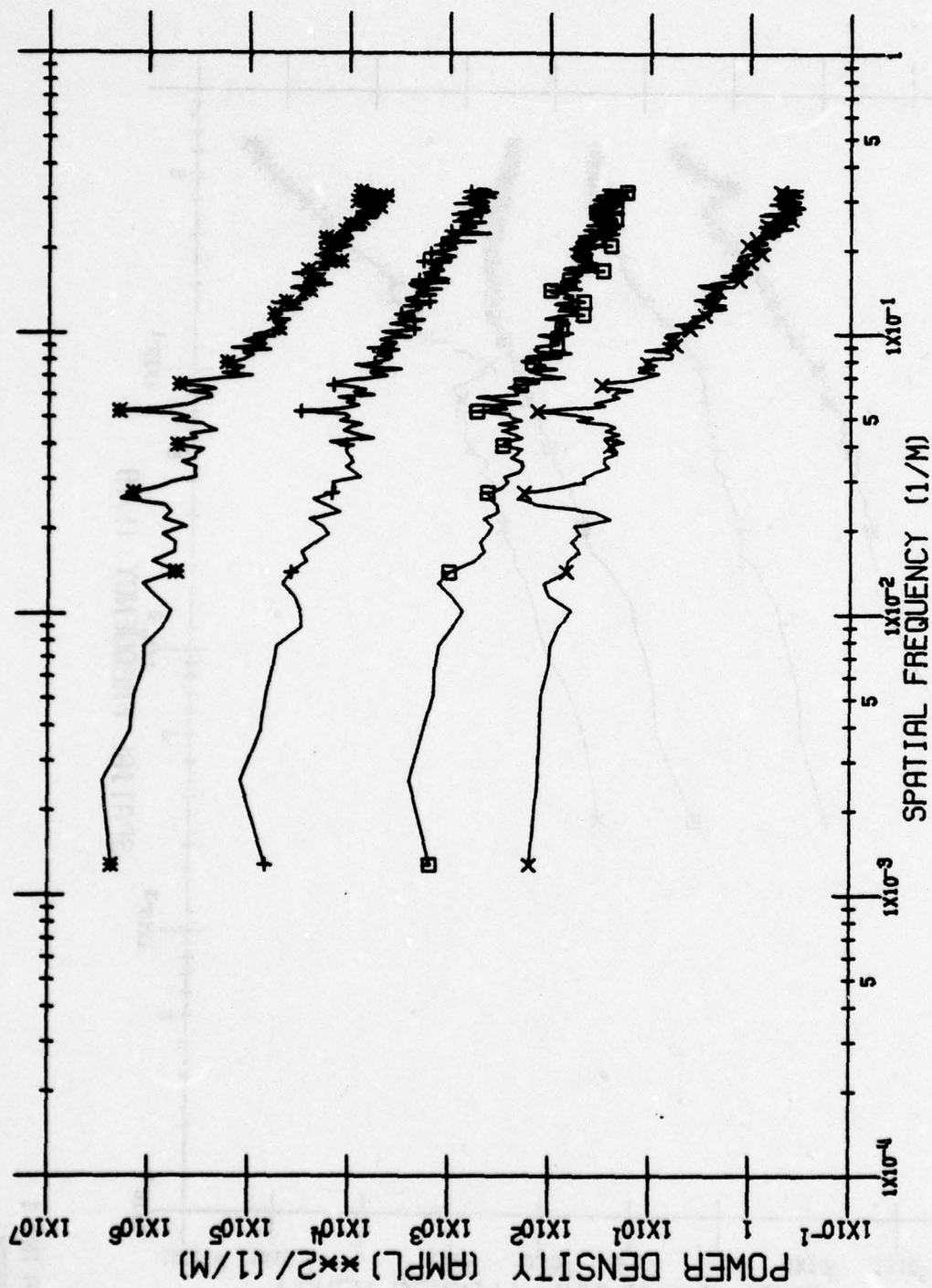
WIENER SPECTRA AND AREA/INTENSITY
STATISTICS FOR FLINT-1 AND MILL CREEK



II-189

AREA: FLINT 1
CROSS-TRACK

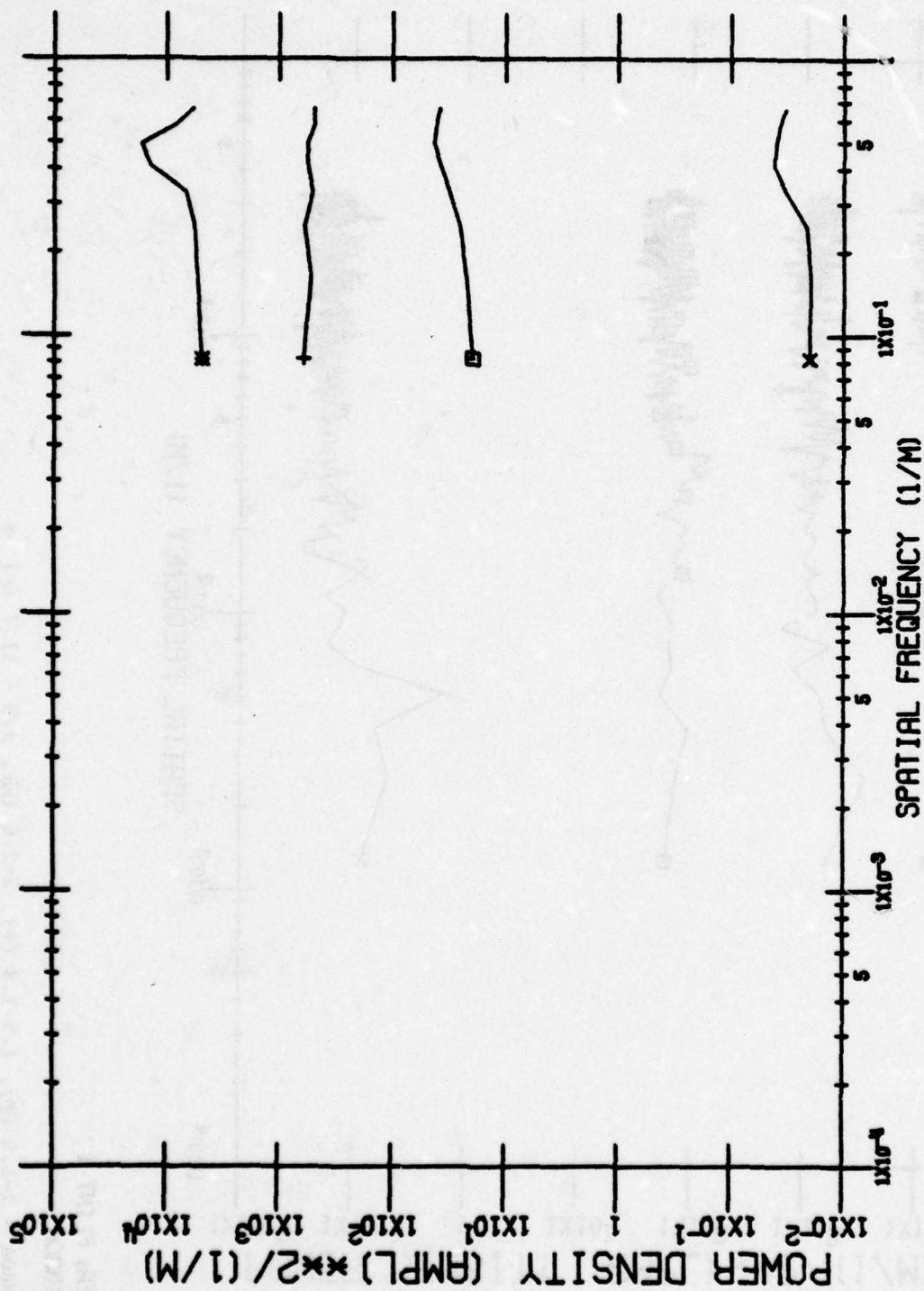
LAMBDA = 1-1.4 (*), 1.5-1.8 (+), 2-2.6 (□), 9.3-11.7 (x) μm



AREA: FLJNT 1

INTRACK

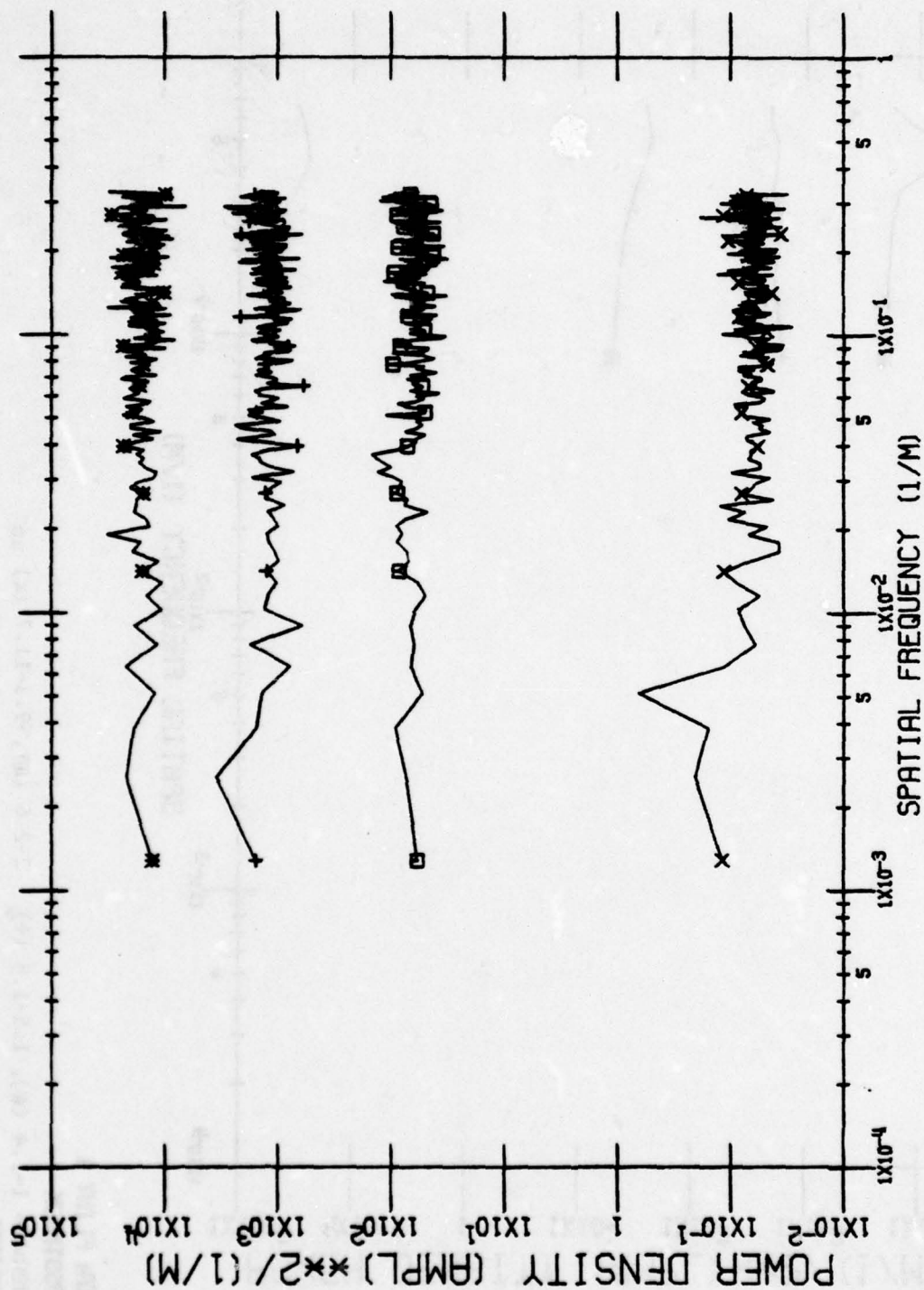
LAMBDA= 1-1.4 (*), 1.5-1.8 (+), 2-2.6 (□), 9.3-11.7 (X) μm



161-191

AREA: FLINT 1
CROSSTRACK

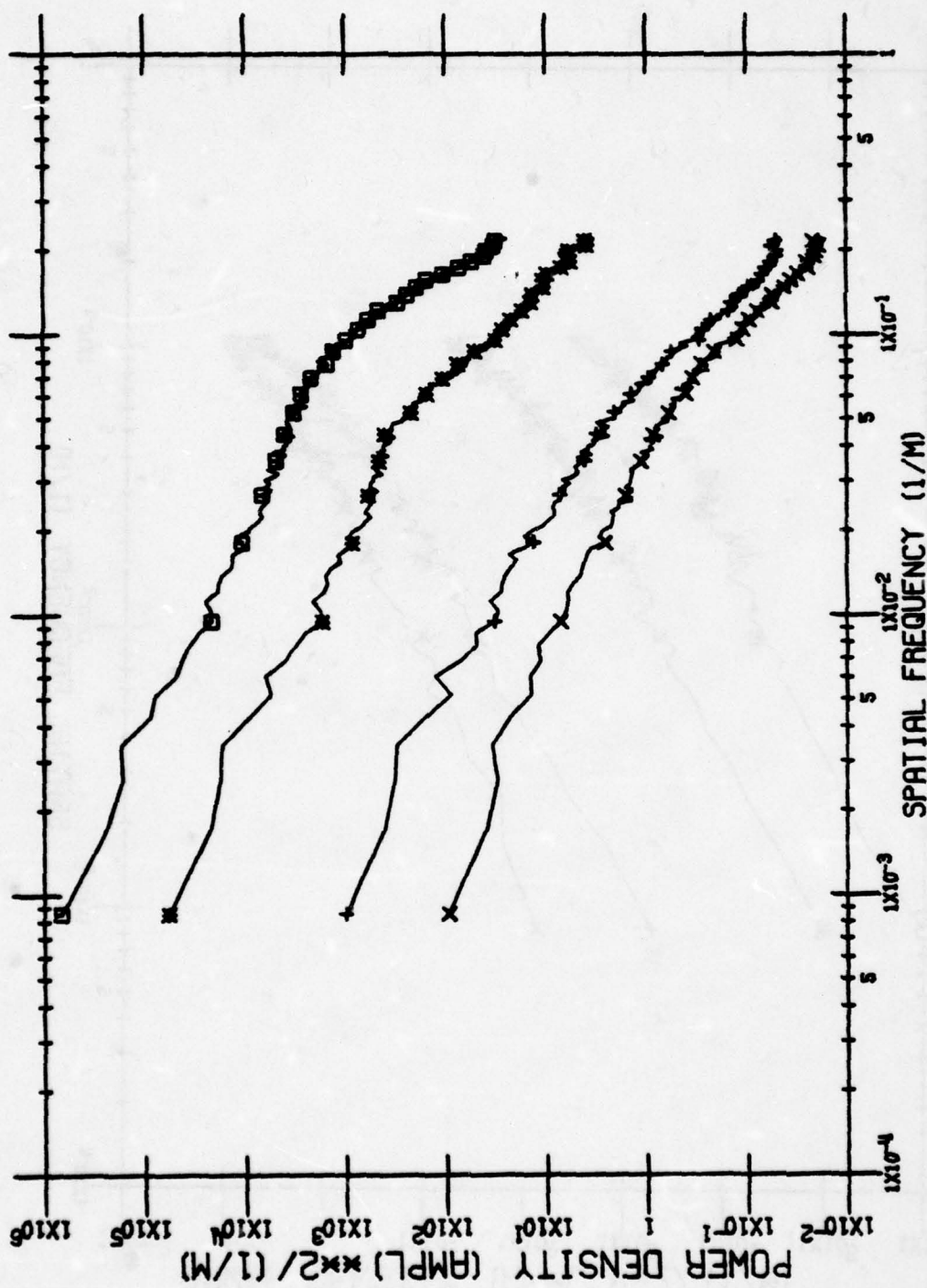
LAMBDA = 1-1.4 (*), 1.5-1.8 (+), 2-2.6 (M), 9.3-11.7 (X) μm
DARKLEVEL



AREA: FLINT 1
INTRACK

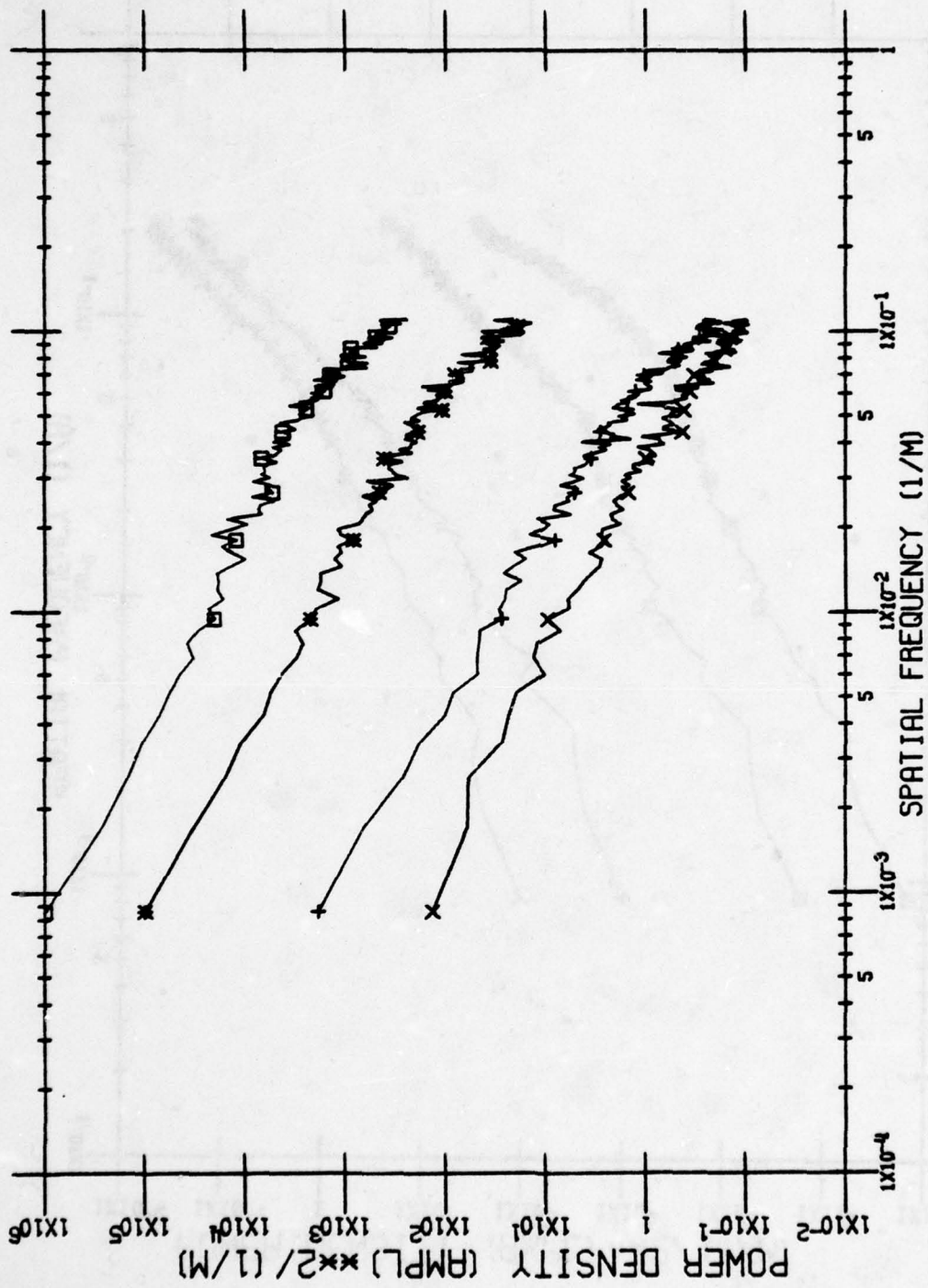
LAMBDA = 1-1.4 (*), 1.5-1.8 (+), 2-2.6 (n), 9.3 - 11.7 (x) μm

DARK LEVEL



AREA: MILL CREEK
CROSSTACK

LAMBDA = 1-1.4 (□), 1.5-1.8 (*), 2-2.6 (+), 9.3-11.7 (x) μm

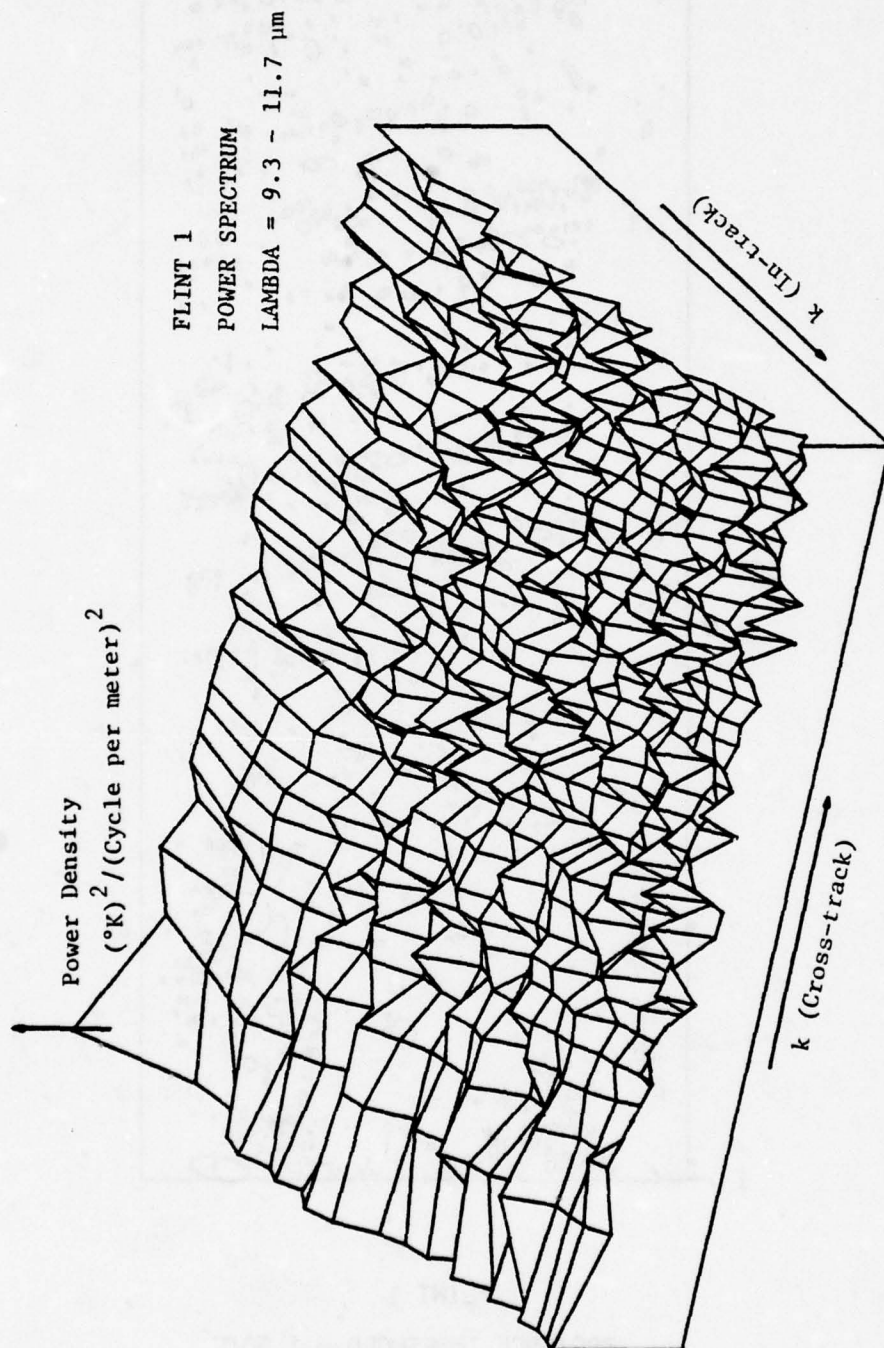


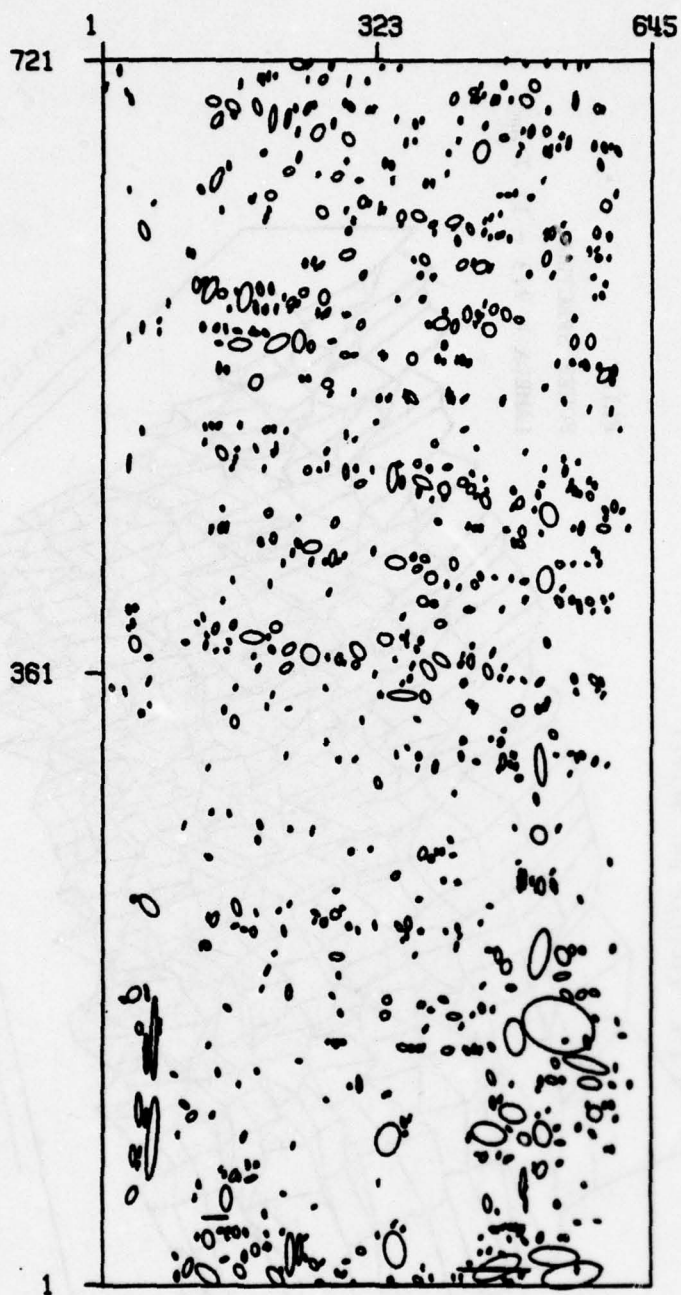
AREA: MILL CREEK

INTRACK

LAMBDA=

1-1.4 (E), 1.5-1.8 (*), 2-2.6 (+), 9.3-11.7 (x) μm





FLINT 1

RADIANCE THRESHOLD = 1.500

LAMBDA= 1.0 TO 1.4 μ M

II-196

FLINT-1

DISTRIBUTION OF RECOGNIZED RADIANCE THRESHOLDS FOR $\sigma = 1.5$

BY AREA

SQUARE METERS	FREQUENCY
0.0 TO 100.0	1012
100.0 TO 200.0	30
200.0 TO 500.0	17
500.0 TO 1000.0	4
1000.0 TO 1500.0	0
1500.0 TO 2000.0	0
2000.0 TO 2500.0	1
2500.0 TO 3000.0	0
3000.0 TO 4000.0	0
4000.0 TO 5000.0	0
5000.0 TO 6000.0	0
6000.0 TO 8000.0	0
8000.0 TO 10000.0	0
10000.0 TO 15000.0	0
15000.0 TO 20000.0	0
20000.0 TO 40000.0	0
40000.0 TO 80000.0	0
80000.0 TO 160000.0	0
OVER 160000.0	0

TOTAL NUMBER OF RADIANCE THR= 1064

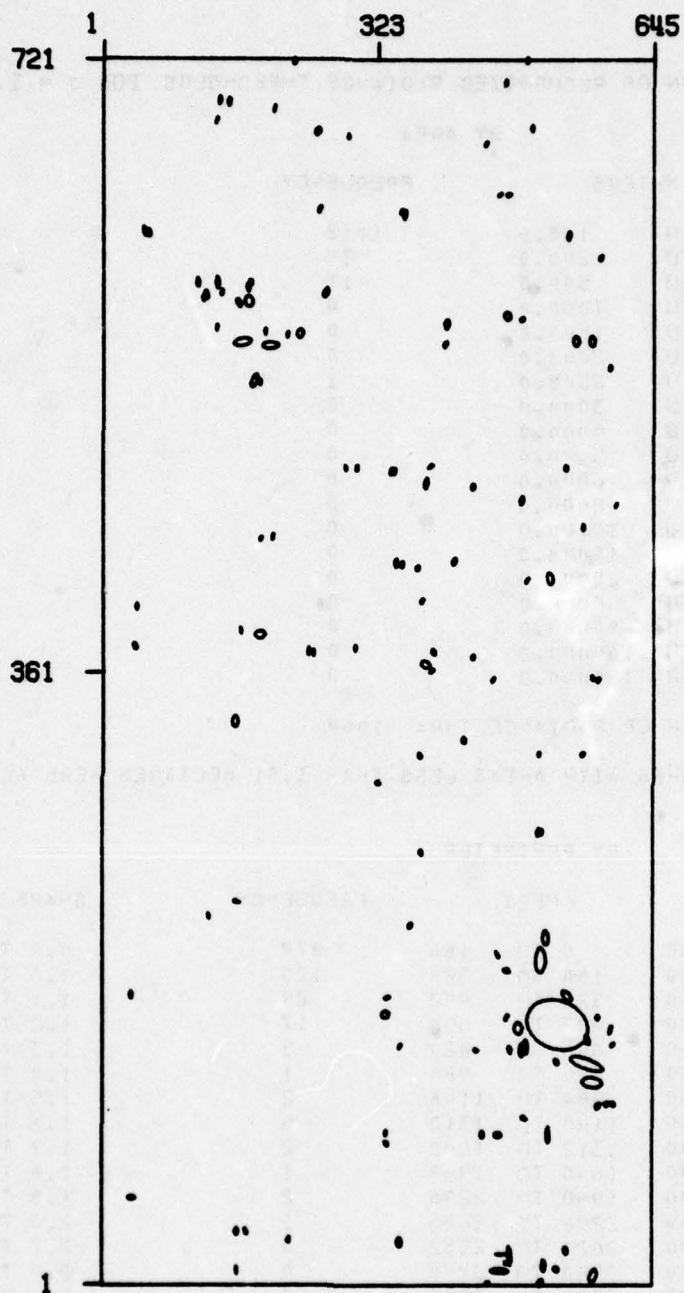
2348 FEATURES WITH AREAS LESS THAN 3.81 HECTARES WERE ALSO RECOGNIZED

BY PERIMETER

METERS	FEET	FREQUENCY
0 TO 50	0 TO 164	879
50 TO 100	164 TO 328	120
100 TO 150	328 TO 492	29
150 TO 200	492 TO 656	17
200 TO 250	656 TO 820	5
250 TO 300	820 TO 984	1
300 TO 350	984 TO 1148	2
350 TO 400	1148 TO 1312	5
400 TO 500	1312 TO 1640	2
500 TO 600	1640 TO 1968	1
600 TO 700	1968 TO 2296	2
700 TO 800	2296 TO 2624	1
800 TO 900	2624 TO 2952	0
900 TO 1000	2952 TO 3280	0
1000 TO 1200	3280 TO 3937	0
1200 TO 1400	3937 TO 4593	0
1400 TO 1600	4593 TO 5249	0
1600 TO 2000	5249 TO 6561	0
OVER 2000	OVER 6561	0

BY SHAPE

SHAPE FACTOR	FREQUENCY
0.0 TO 1.0	2
1.0 TO 1.1	0
1.1 TO 1.2	43
1.2 TO 1.3	41
1.3 TO 1.4	94
1.4 TO 1.5	97
1.5 TO 1.6	87
1.6 TO 1.7	82
1.7 TO 1.8	94
1.8 TO 1.9	53
1.9 TO 2.0	75
2.0 TO 2.2	99
2.2 TO 2.4	66
2.4 TO 2.6	52
2.6 TO 2.8	60
2.8 TO 3.0	25
3.0 TO 3.5	44
3.5 TO 4.0	22
OVER 4.0	28



FLINT 1

RADIANCE THRESHOLD = 2.005

LAMBDA= 1.0 TO 1.4 μ m

FLINT-1

DISTRIBUTION OF RECOGNIZED RADIANCE THRESHOLDS FOR $\sigma = 2.0$

BY AREA

SQUARE METERS	FREQUENCY
0.0 TO 100.0	157
100.0 TO 200.0	2
200.0 TO 500.0	1
500.0 TO 1000.0	0
1000.0 TO 1500.0	0
1500.0 TO 2000.0	1
2000.0 TO 2500.0	0
2500.0 TO 3000.0	0
3000.0 TO 4000.0	0
4000.0 TO 5000.0	0
5000.0 TO 6000.0	0
6000.0 TO 8000.0	0
8000.0 TO 10000.0	0
10000.0 TO 15000.0	0
15000.0 TO 20000.0	0
20000.0 TO 40000.0	0
40000.0 TO 80000.0	0
80000.0 TO 160000.0	0
OVER 160000.0	0

TOTAL NUMBER OF RADIANCE THRE= 191

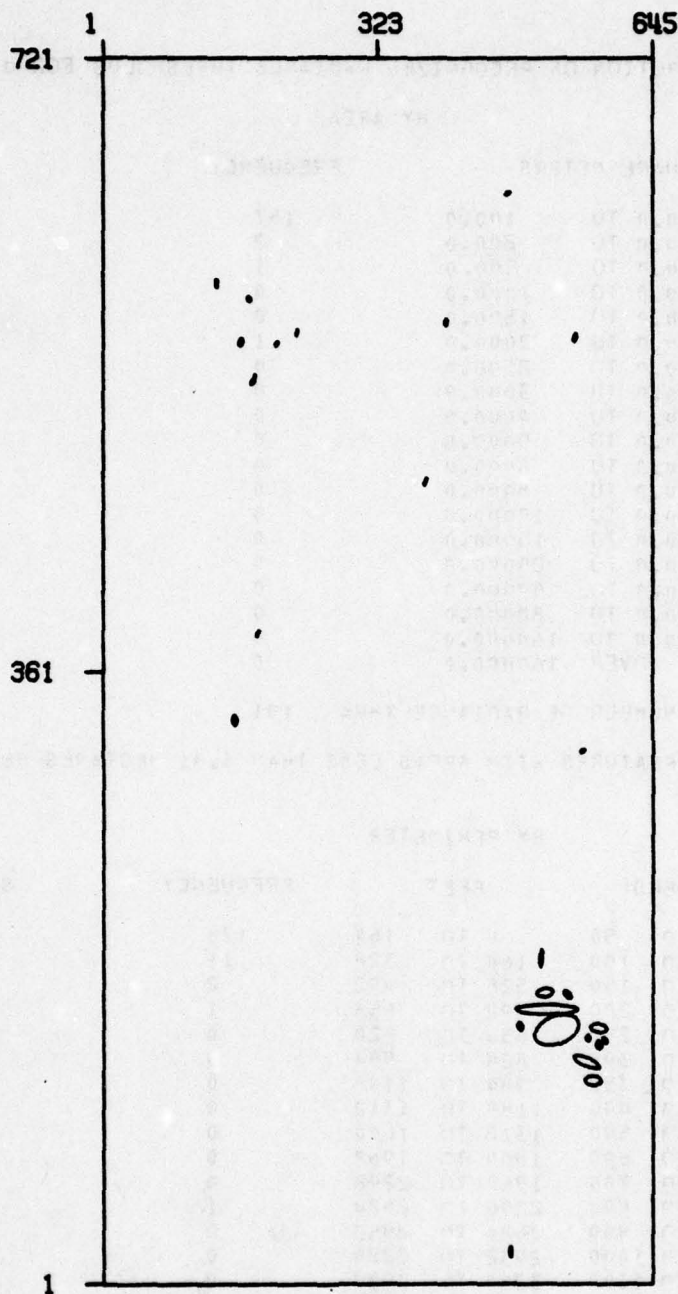
759 FEATURES WITH AREAS LESS THAN 3.81 HECTARES WERE ALSO RECOGNIZED

BY PERIMETER

METERS	FEET	FREQUENCY
0 TO 50	0 TO 164	176
50 TO 100	164 TO 328	11
100 TO 150	328 TO 492	2
150 TO 200	492 TO 656	1
200 TO 250	656 TO 820	0
250 TO 300	820 TO 984	0
300 TO 350	984 TO 1148	0
350 TO 400	1148 TO 1312	0
400 TO 500	1312 TO 1640	0
500 TO 600	1640 TO 1968	0
600 TO 700	1968 TO 2296	0
700 TO 800	2296 TO 2624	1
800 TO 900	2624 TO 2952	0
900 TO 1000	2952 TO 3280	0
1000 TO 1200	3280 TO 3937	0
1200 TO 1400	3937 TO 4593	0
1400 TO 1600	4593 TO 5249	0
1600 TO 2000	5249 TO 6561	0
OVER 2000	OVER 6561	0

BY SHAPE

SHAPE FACTOR	FREQUENCY
0.0 TO 1.0	1
1.0 TO 1.1	0
1.1 TO 1.2	8
1.2 TO 1.3	9
1.3 TO 1.4	24
1.4 TO 1.5	12
1.5 TO 1.6	18
1.6 TO 1.7	17
1.7 TO 1.8	18
1.8 TO 1.9	11
1.9 TO 2.0	22
2.0 TO 2.2	20
2.2 TO 2.4	10
2.4 TO 2.6	8
2.6 TO 2.8	3
2.8 TO 3.0	1
3.0 TO 3.5	2
3.5 TO 4.0	2
OVER 4.0	1



FLINT 1

RADIANCE THRESHOLD = 2.50σ

LAMBDA= 1.0 TO 1.4 μM

FLINT-1

DISTRIBUTION OF RECOGNIZED RADIANCE THRESHOLDS FOR $\sigma = 2.5$

BY AREA

SQUARE METERS	FREQUENCY
0.0 TO 100.0	29
100.0 TO 200.0	1
200.0 TO 500.0	1
500.0 TO 1000.0	1
1000.0 TO 1500.0	0
1500.0 TO 2000.0	0
2000.0 TO 2500.0	0
2500.0 TO 3000.0	0
3000.0 TO 4000.0	0
4000.0 TO 5000.0	0
5000.0 TO 6000.0	0
6000.0 TO 8000.0	0
8000.0 TO 10000.0	0
10000.0 TO 15000.0	0
15000.0 TO 20000.0	0
20000.0 TO 40000.0	0
40000.0 TO 80000.0	0
80000.0 TO 160000.0	0
OVER 160000.0	0

TOTAL NUMBER OF RADIANCE THRE= 32

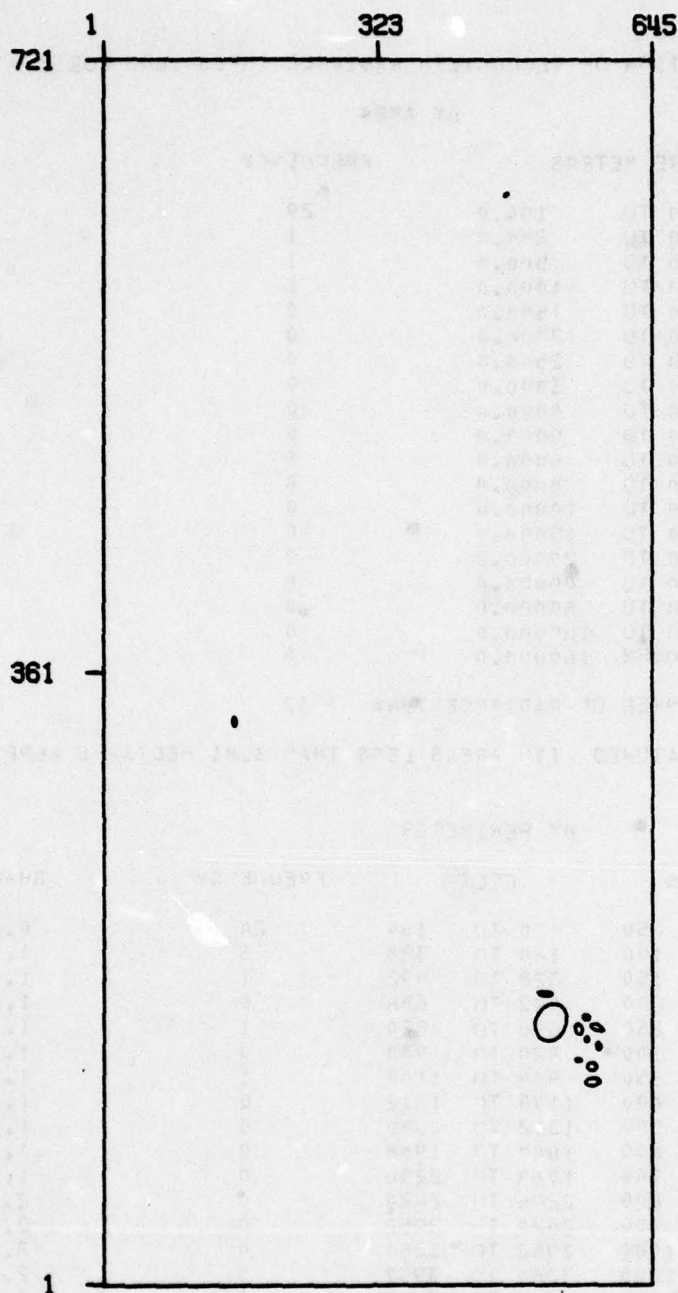
144 FEATURES WITH AREAS LESS THAN 3.81 HECTARES WERE ALSO RECOGNIZED

BY PERIMETER

METERS	FEET	FREQUENCY
0 TO 50	0 TO 164	24
50 TO 100	164 TO 328	5
100 TO 150	328 TO 492	1
150 TO 200	492 TO 656	0
200 TO 250	656 TO 820	1
250 TO 300	820 TO 984	0
300 TO 350	984 TO 1148	1
350 TO 400	1148 TO 1312	0
400 TO 500	1312 TO 1640	0
500 TO 600	1640 TO 1968	0
600 TO 700	1968 TO 2296	0
700 TO 800	2296 TO 2624	0
800 TO 900	2624 TO 2952	0
900 TO 1000	2952 TO 3280	0
1000 TO 1200	3280 TO 3937	0
1200 TO 1400	3937 TO 4593	0
1400 TO 1600	4593 TO 5249	0
1600 TO 2000	5249 TO 6561	0
OVER 2000	OVER 6561	0

BY SHAPE

SHAPE FACTOR	FREQUENCY
0.0 TO 1.0	0
1.0 TO 1.1	0
1.1 TO 1.2	1
1.2 TO 1.3	2
1.3 TO 1.4	2
1.4 TO 1.5	4
1.5 TO 1.6	2
1.6 TO 1.7	1
1.7 TO 1.8	3
1.8 TO 1.9	1
1.9 TO 2.0	4
2.0 TO 2.2	2
2.2 TO 2.4	4
2.4 TO 2.6	0
2.6 TO 2.8	1
2.8 TO 3.0	1
3.0 TO 3.5	3
3.5 TO 4.0	1
OVER 4.0	0



FLINT 1

RADIANCE THRESHOLD = 3.00σ

LAMBDA= 1.0 TO 1.4 μM

II-202

FLINT-1

DISTRIBUTION OF RECOGNIZED RADJANCE THRESHOLDS FOR $\sigma = 3.0$

BY AREA

SQUARE METERS	FREQUENCY
0.0 TO 100.0	16
100.0 TO 200.0	0
200.0 TO 500.0	0
500.0 TO 1000.0	1
1000.0 TO 1500.0	0
1500.0 TO 2000.0	0
2000.0 TO 2500.0	0
2500.0 TO 3000.0	0
3000.0 TO 4000.0	0
4000.0 TO 5000.0	0
5000.0 TO 6000.0	0
6000.0 TO 8000.0	0
8000.0 TO 10000.0	0
10000.0 TO 15000.0	0
15000.0 TO 20000.0	0
20000.0 TO 40000.0	0
40000.0 TO 80000.0	0
80000.0 TO 160000.0	0
OVER 160000.0	0

TOTAL NUMBER OF RADJANCE THRE= 17

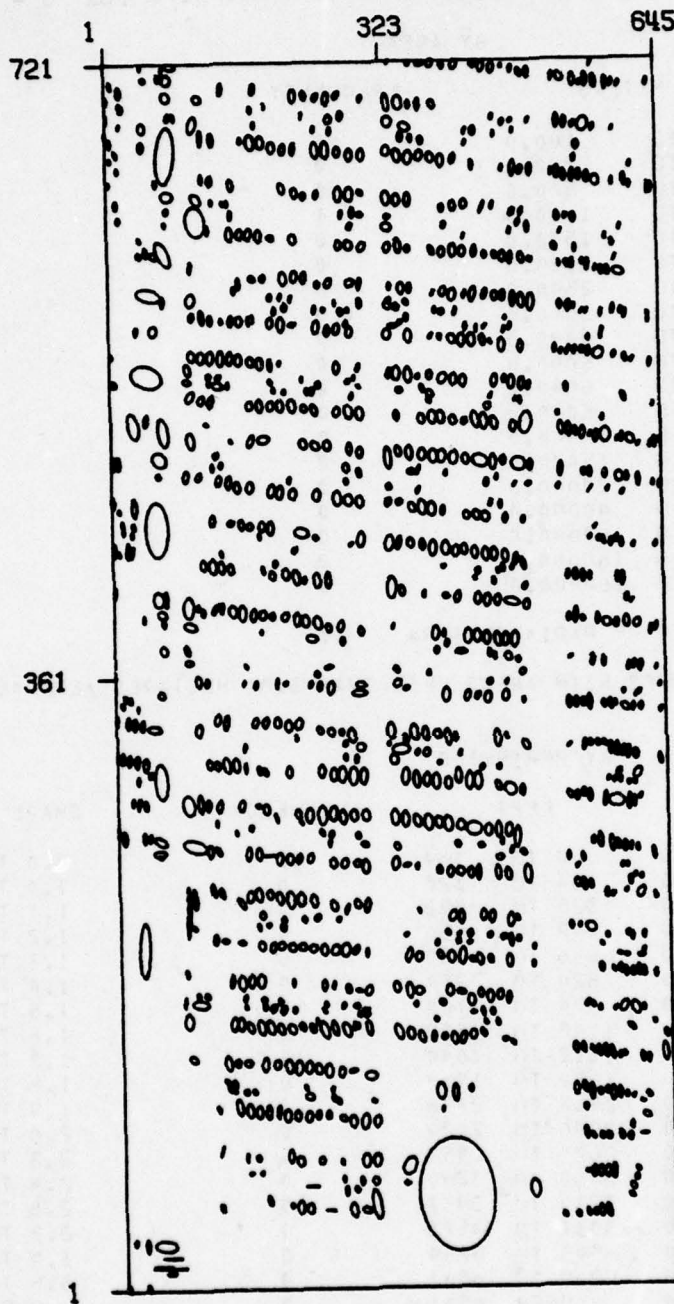
40 FEATURES WITH AREAS LESS THAN 3.81 HECTARES WERE ALSO RECOGNIZED

BY PERIMETER

METERS	FEET	FREQUENCY
0 TO 50	0 TO 164	12
50 TO 100	164 TO 328	4
100 TO 150	328 TO 492	0
150 TO 200	492 TO 656	0
200 TO 250	656 TO 820	0
250 TO 300	820 TO 984	0
300 TO 350	984 TO 1148	0
350 TO 400	1148 TO 1312	0
400 TO 500	1312 TO 1640	1
500 TO 600	1640 TO 1968	0
600 TO 700	1968 TO 2296	0
700 TO 800	2296 TO 2624	0
800 TO 900	2624 TO 2952	0
900 TO 1000	2952 TO 3280	0
1000 TO 1200	3280 TO 3937	0
1200 TO 1400	3937 TO 4593	0
1400 TO 1600	4593 TO 5249	0
1600 TO 2000	5249 TO 6561	0
OVER 2000	OVER 6561	0

BY SHAPE

SHAPE FACTOR	FREQUENCY
0.0 TO 1.0	0
1.0 TO 1.1	0
1.1 TO 1.2	2
1.2 TO 1.3	1
1.3 TO 1.4	3
1.4 TO 1.5	1
1.5 TO 1.6	3
1.6 TO 1.7	0
1.7 TO 1.8	0
1.8 TO 1.9	0
1.9 TO 2.0	1
2.0 TO 2.2	2
2.2 TO 2.4	2
2.4 TO 2.6	0
2.6 TO 2.8	0
2.8 TO 3.0	1
3.0 TO 3.5	0
3.5 TO 4.0	0
OVER 4.0	1



FLINT 1

TEMPERATURE THRESHOLD = 1.50°

LAMBDA= 9.3 TO 11.7 μm

FLINT-1

DISTRIBUTION OF RECOGNIZED TEMP. THRESHOLDS FOR $\sigma = 1.5$

BY AREA

SQUARE METERS	FREQUENCY
0.0 TO 100.0	1278
100.0 TO 200.0	20
200.0 TO 500.0	4
500.0 TO 1000.0	2
1000.0 TO 1500.0	0
1500.0 TO 2000.0	0
2000.0 TO 2500.0	0
2500.0 TO 3000.0	0
3000.0 TO 4000.0	0
4000.0 TO 5000.0	0
5000.0 TO 6000.0	1
6000.0 TO 8000.0	0
8000.0 TO 10000.0	0
10000.0 TO 15000.0	0
15000.0 TO 20000.0	0
20000.0 TO 40000.0	0
40000.0 TO 80000.0	0
80000.0 TO 160000.0	0
OVER 160000.0	0

TOTAL NUMBER OF TEMP. THRE = 1305

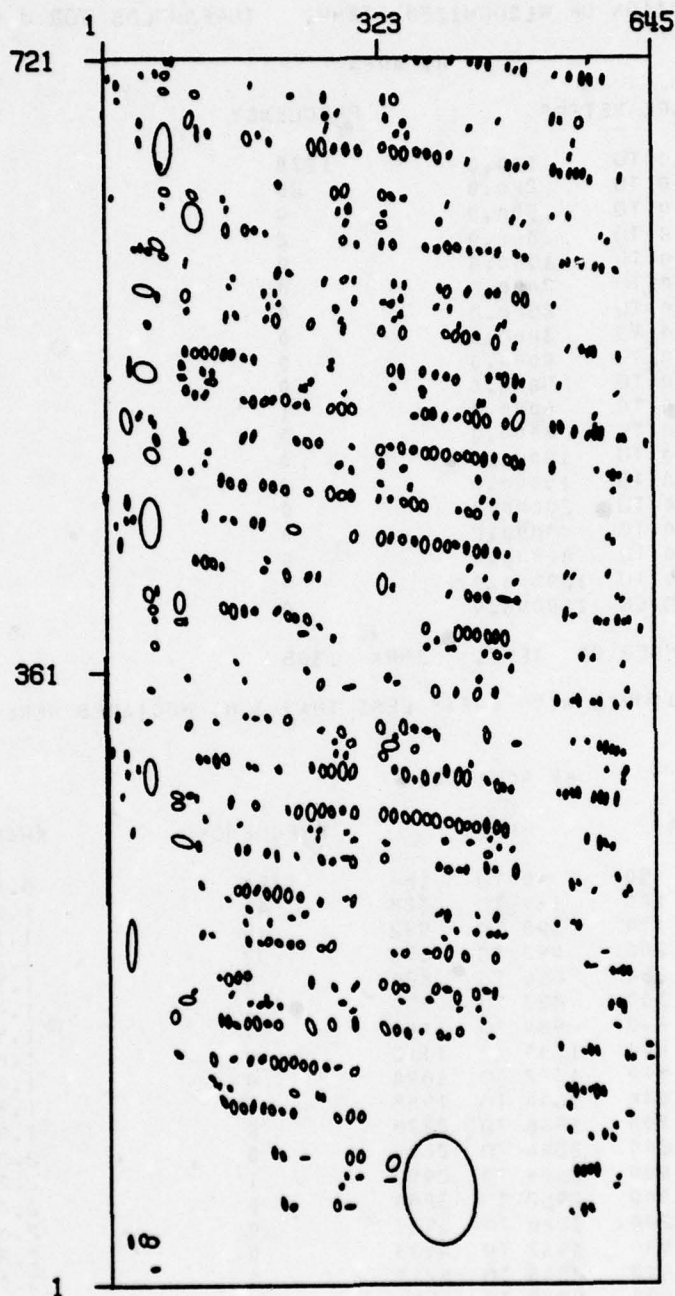
370 FEATURES WITH AREAS LESS THAN 3.81 HECTARES WERE ALSO RECOGNIZED

BY PERIMETER

METERS	FFET	FREQUENCY
0 TO 50	0 TO 164	1254
50 TO 100	164 TO 328	42
100 TO 150	328 TO 492	5
150 TO 200	492 TO 656	2
200 TO 250	656 TO 820	0
250 TO 300	820 TO 984	1
300 TO 350	984 TO 1148	0
350 TO 400	1148 TO 1312	0
400 TO 500	1312 TO 1640	0
500 TO 600	1640 TO 1968	0
600 TO 700	1968 TO 2296	0
700 TO 800	2296 TO 2624	0
800 TO 900	2624 TO 2952	1
900 TO 1000	2952 TO 3280	0
1000 TO 1200	3280 TO 3937	0
1200 TO 1400	3937 TO 4593	0
1400 TO 1600	4593 TO 5249	0
1600 TO 2000	5249 TO 6561	0
OVER 2000	OVER 6561	0

BY SHAPE

SHAPE FACTOR	FREQUENCY
0.0 TO 1.0	3
1.0 TO 1.1	3
1.1 TO 1.2	104
1.2 TO 1.3	186
1.3 TO 1.4	339
1.4 TO 1.5	238
1.5 TO 1.6	167
1.6 TO 1.7	96
1.7 TO 1.8	56
1.8 TO 1.9	31
1.9 TO 2.0	26
2.0 TO 2.2	33
2.2 TO 2.4	10
2.4 TO 2.6	4
2.6 TO 2.8	3
2.8 TO 3.0	4
3.0 TO 3.5	1
3.5 TO 4.0	1
OVER 4.0	0



FLINT 1

TEMPERATURE THRESHOLD = 2.005

LAMBDA= 9.3 TO 11.7 μM

FLINT-1

DISTRIBUTION OF RECOGNIZED TEMP. THRESHOLDS FOR $\sigma = 2.0$

BY AREA

SQUARE METERS	FREQUENCY
0.0 TO 100.0	874
100.0 TO 200.0	8
200.0 TO 500.0	4
500.0 TO 1000.0	2
1000.0 TO 1500.0	0
1500.0 TO 2000.0	0
2000.0 TO 2500.0	0
2500.0 TO 3000.0	0
3000.0 TO 4000.0	0
4000.0 TO 5000.0	1
5000.0 TO 6000.0	0
6000.0 TO 8000.0	0
8000.0 TO 10000.0	0
10000.0 TO 15000.0	0
15000.0 TO 20000.0	0
20000.0 TO 40000.0	0
40000.0 TO 80000.0	0
80000.0 TO 160000.0	0
OVER 160000.0	0

TOTAL NUMBER OF TEMP. THR= 889

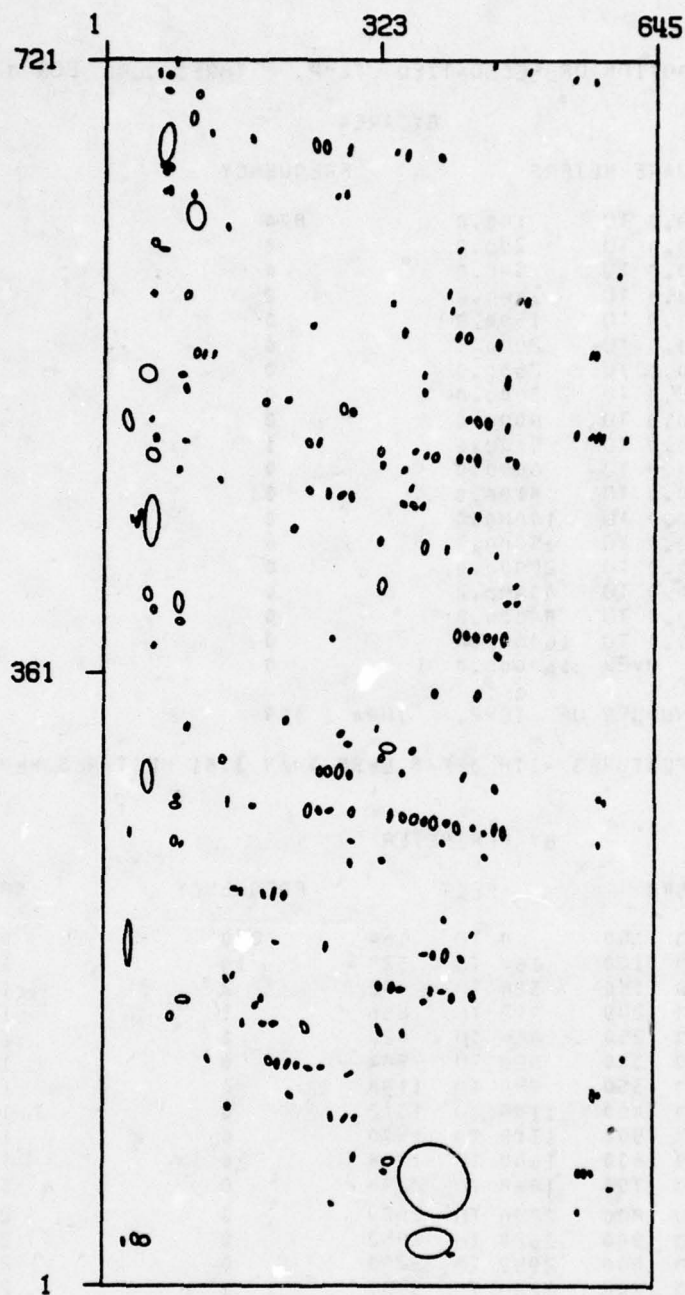
293 FEATURES WITH AREAS LESS THAN 3.81 HECTARES WERE ALSO RECOGNIZED

BY PERIMETER

METERS	FEET	FREQUENCY
0 TO 50	0 TO 164	870
50 TO 100	164 TO 328	14
100 TO 150	328 TO 492	2
150 TO 200	492 TO 656	1
200 TO 250	656 TO 820	1
250 TO 300	820 TO 984	0
300 TO 350	984 TO 1148	0
350 TO 400	1148 TO 1312	0
400 TO 500	1312 TO 1640	0
500 TO 600	1640 TO 1968	0
600 TO 700	1968 TO 2296	0
700 TO 800	2296 TO 2624	0
800 TO 900	2624 TO 2952	0
900 TO 1000	2952 TO 3280	0
1000 TO 1200	3280 TO 3937	1
1200 TO 1400	3937 TO 4593	0
1400 TO 1600	4593 TO 5249	0
1600 TO 2000	5249 TO 6561	0
OVER 2000	OVER 6561	0

BY SHAPE

SHAPE FACTOR	FREQUENCY
0.0 TO 1.0	4
1.0 TO 1.1	1
1.1 TO 1.2	63
1.2 TO 1.3	133
1.3 TO 1.4	172
1.4 TO 1.5	144
1.5 TO 1.6	116
1.6 TO 1.7	93
1.7 TO 1.8	47
1.8 TO 1.9	42
1.9 TO 2.0	37
2.0 TO 2.2	20
2.2 TO 2.4	10
2.4 TO 2.6	3
2.6 TO 2.8	2
2.8 TO 3.0	1
3.0 TO 3.5	0
3.5 TO 4.0	0
OVER 4.0	1



FLINT 1

TEMPERATURE THRESHOLD = 2.50σ

LAMBDA= 9.3 TO 11.7 μM

FLINT-1

DISTRIBUTION OF RECOGNIZED TEMP. THRESHOLDS FOR $\sigma = 2.5$

BY AREA

SQUARE METERS	FREQUENCY
0.0 TO 100.0	271
100.0 TO 200.0	4
200.0 TO 500.0	4
500.0 TO 1000.0	1
1000.0 TO 1500.0	0
1500.0 TO 2000.0	0
2000.0 TO 2500.0	0
2500.0 TO 3000.0	0
3000.0 TO 4000.0	1
4000.0 TO 5000.0	0
5000.0 TO 6000.0	0
6000.0 TO 8000.0	0
8000.0 TO 10000.0	0
10000.0 TO 15000.0	0
15000.0 TO 20000.0	0
20000.0 TO 40000.0	0
40000.0 TO 80000.0	0
80000.0 TO 160000.0	0
OVER 160000.0	0

TOTAL NUMBER OF TEMP. THR= 281

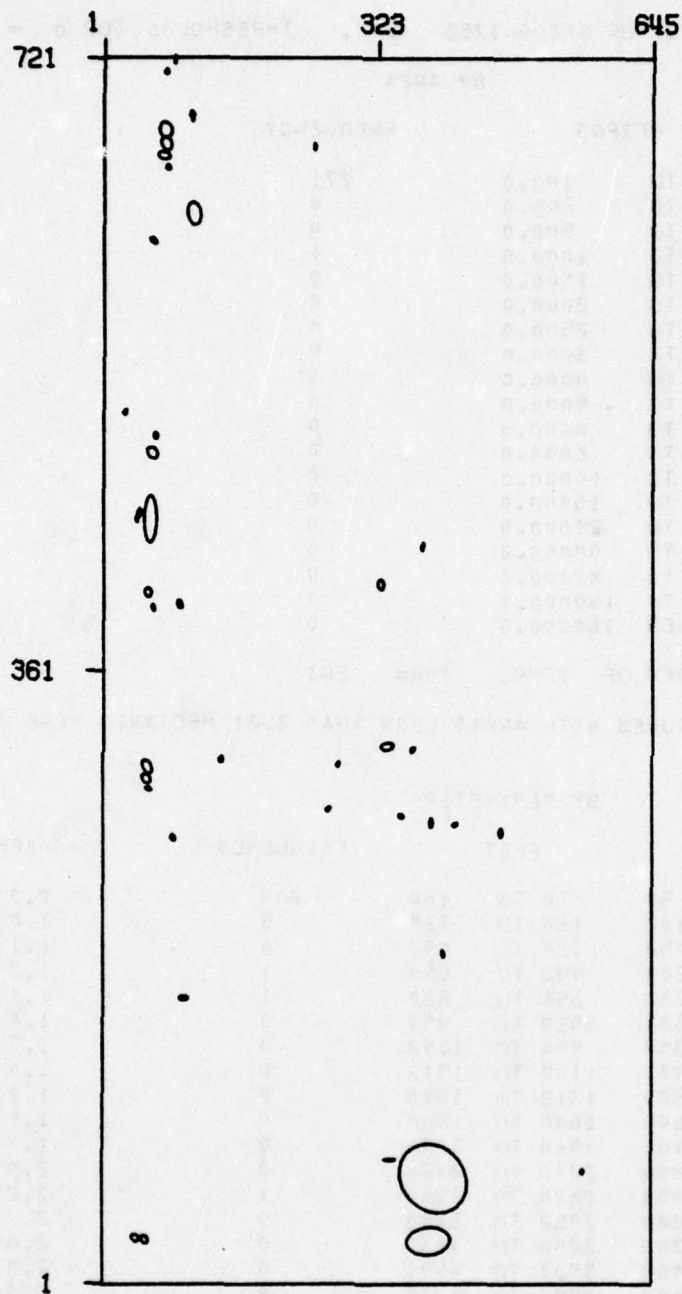
202 FEATURES WITH AREAS LESS THAN 3.81 HECTARES WERE ALSO RECOGNIZED

BY PERIMETER

METERS	FEET	FREQUENCY
0 TO 50	0 TO 164	269
50 TO 100	164 TO 328	5
100 TO 150	328 TO 492	4
150 TO 200	492 TO 656	1
200 TO 250	656 TO 820	1
250 TO 300	820 TO 984	0
300 TO 350	984 TO 1148	0
350 TO 400	1148 TO 1312	0
400 TO 500	1312 TO 1640	0
500 TO 600	1640 TO 1968	0
600 TO 700	1968 TO 2296	0
700 TO 800	2296 TO 2624	0
800 TO 900	2624 TO 2952	1
900 TO 1000	2952 TO 3280	0
1000 TO 1200	3280 TO 3937	0
1200 TO 1400	3937 TO 4593	0
1400 TO 1600	4593 TO 5249	0
1600 TO 2000	5249 TO 6561	0
OVER 2000	OVER 6561	0

BY SHAPE

SHAPE FACTOR	FREQUENCY
0.0 TO 1.0	0
1.0 TO 1.1	1
1.1 TO 1.2	27
1.2 TO 1.3	33
1.3 TO 1.4	44
1.4 TO 1.5	29
1.5 TO 1.6	51
1.6 TO 1.7	27
1.7 TO 1.8	28
1.8 TO 1.9	11
1.9 TO 2.0	11
2.0 TO 2.2	12
2.2 TO 2.4	4
2.4 TO 2.6	0
2.6 TO 2.8	1
2.8 TO 3.0	1
3.0 TO 3.5	0
3.5 TO 4.0	0
OVER 4.0	1



FLINT 1

TEMPERATURE THRESHOLD = 3.00σ

LAMBDA= 9.3 TO 11.7 μM

II-210

FLINT-1

DISTRIBUTION OF RECOGNIZED TEMP. THRESHOLDS FOR $\sigma = 3.0$

BY AREA

SQUARE METERS		FREQUENCY
0.0 TO	100.0	48
100.0 TO	200.0	2
200.0 TO	500.0	1
500.0 TO	1000.0	1
1000.0 TO	1500.0	0
1500.0 TO	2000.0	0
2000.0 TO	2500.0	0
2500.0 TO	3000.0	1
3000.0 TO	4000.0	0
4000.0 TO	5000.0	0
5000.0 TO	6000.0	0
6000.0 TO	8000.0	0
8000.0 TO	10000.0	0
10000.0 TO	15000.0	0
15000.0 TO	20000.0	0
20000.0 TO	40000.0	0
40000.0 TO	80000.0	0
80000.0 TO	160000.0	0
OVER	160000.0	0

TOTAL NUMBER OF TEMP. THR= 53

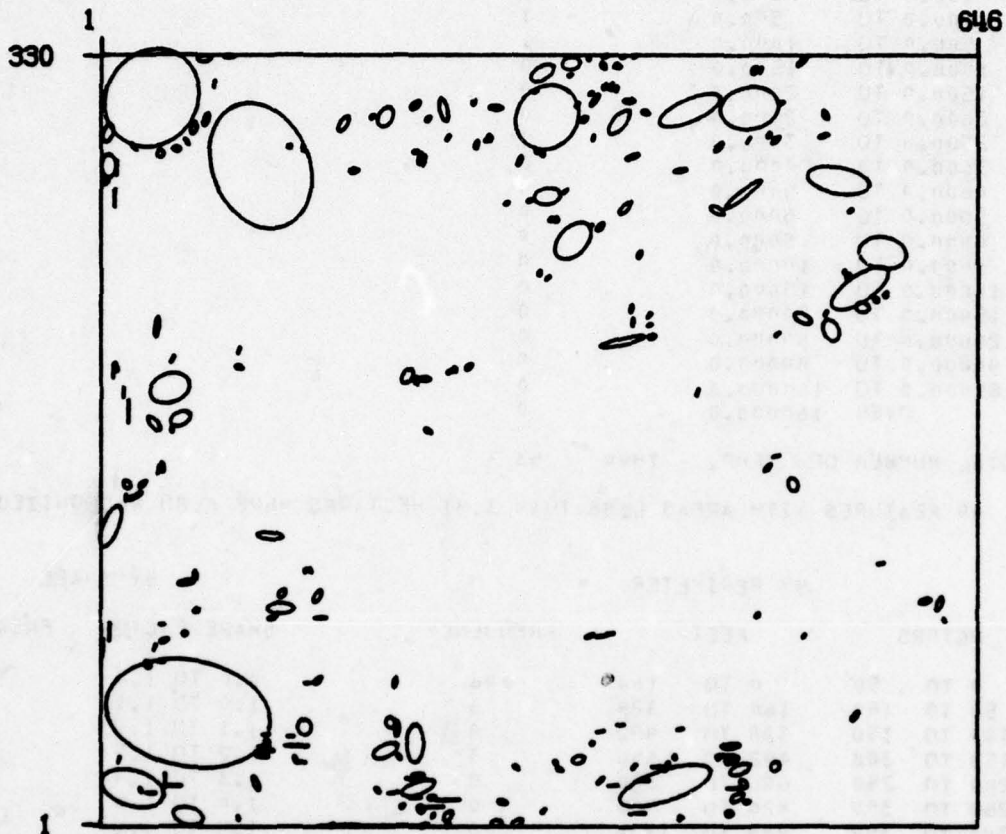
49 FEATURES WITH AREAS LESS THAN 3.41 HECTARES WERE ALSO RECOGNIZED

BY PERIMETER

METERS	FEET	FREQUENCY
0 TO 50	0 TO 164	46
50 TO 100	164 TO 328	3
100 TO 150	328 TO 492	0
150 TO 200	492 TO 656	3
200 TO 250	656 TO 820	0
250 TO 300	820 TO 984	0
300 TO 350	984 TO 1148	0
350 TO 400	1148 TO 1312	0
400 TO 500	1312 TO 1640	0
500 TO 600	1640 TO 1968	0
600 TO 700	1968 TO 2296	0
700 TO 800	2296 TO 2624	0
800 TO 900	2624 TO 2952	1
900 TO 1000	2952 TO 3280	0
1000 TO 1200	3280 TO 3937	0
1200 TO 1400	3937 TO 4593	0
1400 TO 1600	4593 TO 5249	0
1600 TO 2000	5249 TO 6561	0
OVER 2000	OVER 6561	0

BY SHAPE

SHAPE FACTOR	FREQUENCY
0.0 TO 1.0	0
1.0 TO 1.1	1
1.1 TO 1.2	3
1.2 TO 1.3	11
1.3 TO 1.4	9
1.4 TO 1.5	6
1.5 TO 1.6	5
1.6 TO 1.7	6
1.7 TO 1.8	2
1.8 TO 1.9	5
1.9 TO 2.0	0
2.0 TO 2.2	1
2.2 TO 2.4	1
2.4 TO 2.6	1
2.6 TO 2.8	0
2.8 TO 3.0	0
3.0 TO 3.5	1
3.5 TO 4.0	0
OVER 4.0	1



MILLCREEK

RADIANCE THRESHOLD = 1.50σ

LAMBDA= 1.0 TO 1.4 μ M

MILL CREEK

DISTRIBUTION OF RECOGNIZED RADIANCE THRESHOLDS FOR $\sigma = 1.5$

BY AREA

SQUARE METERS		FREQUENCY
0.0 TO	100.0	232
100.0 TO	200.0	45
200.0 TO	500.0	25
500.0 TO	1000.0	14
1000.0 TO	1500.0	5
1500.0 TO	2000.0	3
2000.0 TO	2500.0	0
2500.0 TO	3000.0	0
3000.0 TO	4000.0	2
4000.0 TO	5000.0	3
5000.0 TO	6000.0	1
6000.0 TO	8000.0	2
8000.0 TO	10000.0	1
10000.0 TO	15000.0	1
15000.0 TO	20000.0	0
20000.0 TO	40000.0	2
40000.0 TO	80000.0	1
80000.0 TO	160000.0	0
OVER	160000.0	0

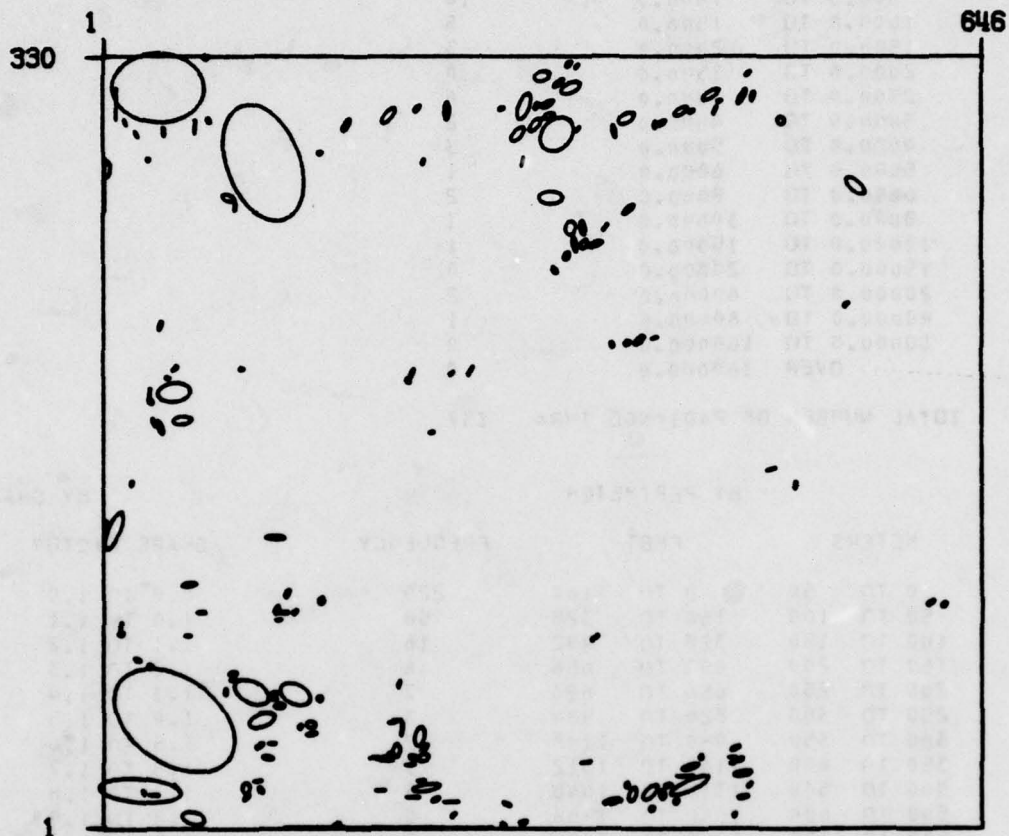
TOTAL NUMBER OF RADIANCE THR= 337

BY PERIMETER

METERS	FEET	FREQUENCY
0 TO 50	0 TO 164	229
50 TO 100	164 TO 328	58
100 TO 150	328 TO 492	16
150 TO 200	492 TO 656	6
200 TO 250	656 TO 820	7
250 TO 300	820 TO 984	3
300 TO 350	984 TO 1148	2
350 TO 400	1148 TO 1312	1
400 TO 500	1312 TO 1640	2
500 TO 600	1640 TO 1968	0
600 TO 700	1968 TO 2296	2
700 TO 800	2296 TO 2624	0
800 TO 900	2624 TO 2952	4
900 TO 1000	2952 TO 3280	0
1000 TO 1200	3280 TO 3937	0
1200 TO 1400	3937 TO 4593	0
1400 TO 1600	4593 TO 5249	2
1600 TO 2000	5249 TO 6561	4
OVER 2000	OVER 6561	1

BY SHAPE

SHAPE FACTOR	FREQUENCY
0.0 TO 1.0	6
1.0 TO 1.1	2
1.1 TO 1.2	145
1.2 TO 1.3	27
1.3 TO 1.4	43
1.4 TO 1.5	14
1.5 TO 1.6	11
1.6 TO 1.7	22
1.7 TO 1.8	15
1.8 TO 1.9	7
1.9 TO 2.0	12
2.0 TO 2.2	9
2.2 TO 2.4	3
2.4 TO 2.6	6
2.6 TO 2.8	2
2.8 TO 3.0	2
3.0 TO 3.5	1
3.5 TO 4.0	3
OVER 4.0	7



MILLCREEK

RADIANCE THRESHOLD = 2.00σ

LAMBDA= 1.0 TO 1.4 μ m

MILL CREEK

DISTRIBUTION OF RECOGNIZED RADIANCE THRESHOLDS FOR $\sigma = 2.0$

BY AREA

SQUARE METERS	FREQUENCY
0.0 TO 100.0	165
100.0 TO 200.0	20
200.0 TO 500.0	26
500.0 TO 1000.0	7
1000.0 TO 1500.0	3
1500.0 TO 2000.0	2
2000.0 TO 2500.0	1
2500.0 TO 3000.0	0
3000.0 TO 4000.0	1
4000.0 TO 5000.0	0
5000.0 TO 6000.0	1
6000.0 TO 8000.0	0
8000.0 TO 10000.0	0
10000.0 TO 15000.0	0
15000.0 TO 20000.0	1
20000.0 TO 40000.0	2
40000.0 TO 80000.0	0
80000.0 TO 160000.0	0
OVER 160000.0	0

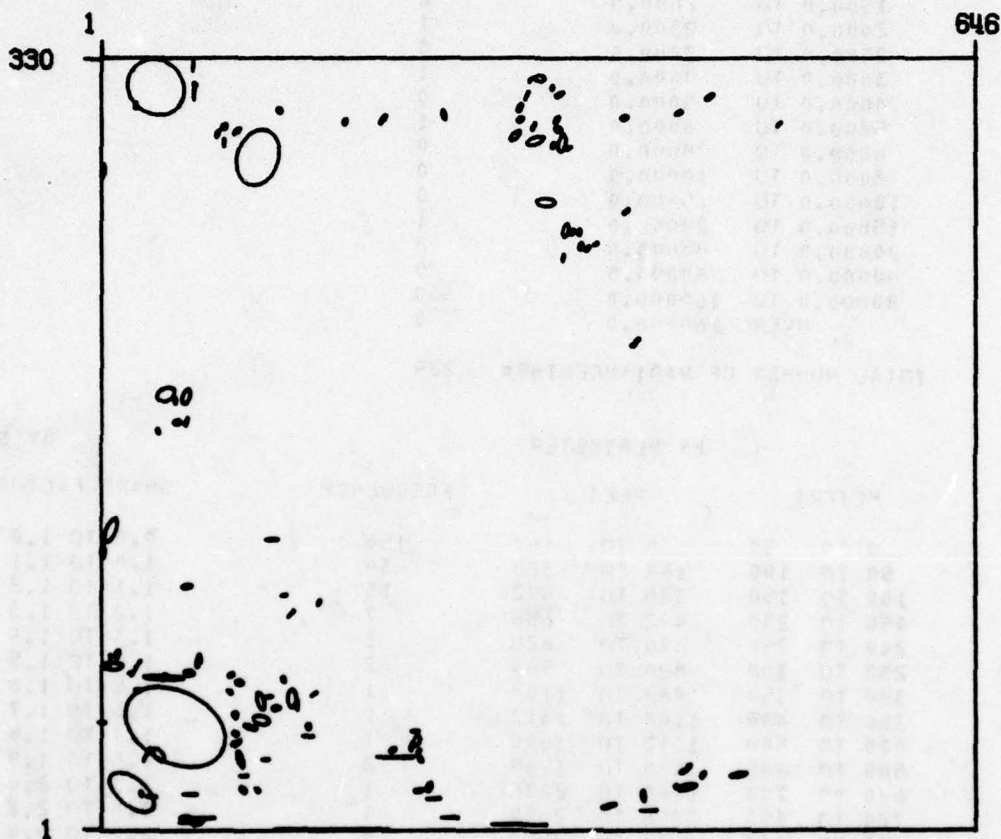
TOTAL NUMBER OF RADIANCE THRESH = 229

BY PERIMETER

METERS	FEET	FREQUENCY
0 TO 50	0 TO 164	156
50 TO 100	164 TO 328	34
100 TO 150	328 TO 492	15
150 TO 200	492 TO 656	7
200 TO 250	656 TO 820	3
250 TO 300	820 TO 984	2
300 TO 350	984 TO 1148	1
350 TO 400	1148 TO 1312	0
400 TO 500	1312 TO 1640	1
500 TO 600	1640 TO 1968	2
600 TO 700	1968 TO 2296	1
700 TO 800	2296 TO 2624	1
800 TO 900	2624 TO 2952	0
900 TO 1000	2952 TO 3280	0
1000 TO 1200	3280 TO 3937	0
1200 TO 1400	3937 TO 4593	0
1400 TO 1600	4593 TO 5249	1
1600 TO 2000	5249 TO 6561	1
OVER 2000	OVER 6561	2

BY SHAPE

SHAPE FACTOR	FREQUENCY
0.0 TO 1.0	1
1.0 TO 1.1	0
1.1 TO 1.2	93
1.2 TO 1.3	13
1.3 TO 1.4	26
1.4 TO 1.5	16
1.5 TO 1.6	15
1.6 TO 1.7	23
1.7 TO 1.8	5
1.8 TO 1.9	4
1.9 TO 2.0	4
2.0 TO 2.2	10
2.2 TO 2.4	4
2.4 TO 2.6	3
2.6 TO 2.8	3
2.8 TO 3.0	0
3.0 TO 3.5	3
3.5 TO 4.0	3
OVER 4.0	3



MILLCREEK

RADIANCE THRESHOLD = 2.50σ

LAMBDA= 1.0 TO 1.4 μ M

MILL CREEK

DISTRIBUTION OF RECOGNIZED RADIANCE THRESHOLDS FOR $\sigma = 2.5$

BY AREA

SQUARE METERS		FREQUENCY
0.0 TO	100.0	138
100.0 TO	200.0	21
200.0 TO	500.0	15
500.0 TO	1000.0	2
1000.0 TO	1500.0	0
1500.0 TO	2000.0	0
2000.0 TO	2500.0	0
2500.0 TO	3000.0	0
3000.0 TO	4000.0	0
4000.0 TO	5000.0	1
5000.0 TO	6000.0	0
6000.0 TO	8000.0	1
8000.0 TO	10000.0	1
10000.0 TO	15000.0	0
15000.0 TO	20000.0	0
20000.0 TO	40000.0	1
40000.0 TO	80000.0	0
80000.0 TO	160000.0	0
OVER	160000.0	0

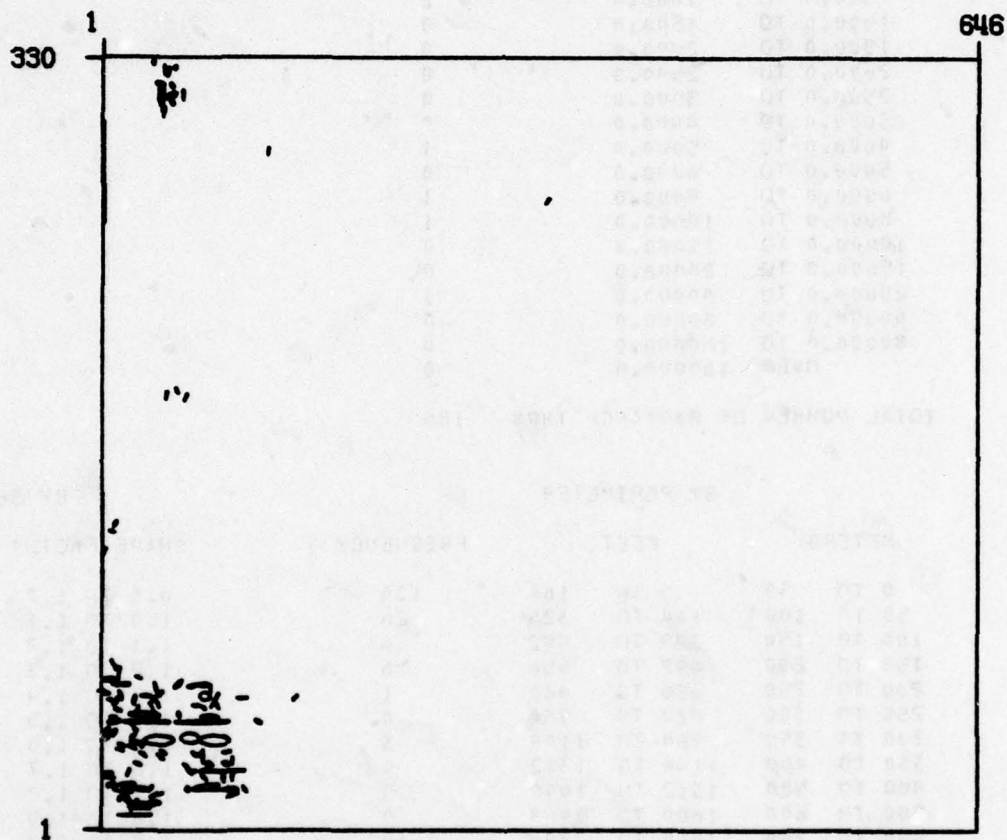
TOTAL NUMBER OF RADIANCE THRE= 180

BY PERIMETER

METERS	FEET	FREQUENCY
0 TO 50	0 TO 164	134
50 TO 100	164 TO 328	26
100 TO 150	328 TO 492	6
150 TO 200	492 TO 656	6
200 TO 250	656 TO 820	1
250 TO 300	820 TO 984	0
300 TO 350	984 TO 1148	3
350 TO 400	1148 TO 1312	0
400 TO 500	1312 TO 1640	0
500 TO 600	1640 TO 1968	0
600 TO 700	1968 TO 2296	0
700 TO 800	2296 TO 2624	0
800 TO 900	2624 TO 2952	0
900 TO 1000	2952 TO 3280	1
1000 TO 1200	3280 TO 3937	0
1200 TO 1400	3937 TO 4593	0
1400 TO 1600	4593 TO 5249	2
1600 TO 2000	5249 TO 6561	0
OVER 2000	OVER 6561	1

BY SHAPE

SHAPE FACTOR	FREQUENCY
0.0 TO 1.0	0
1.0 TO 1.1	0
1.1 TO 1.2	86
1.2 TO 1.3	8
1.3 TO 1.4	20
1.4 TO 1.5	9
1.5 TO 1.6	7
1.6 TO 1.7	11
1.7 TO 1.8	10
1.8 TO 1.9	4
1.9 TO 2.0	4
2.0 TO 2.2	6
2.2 TO 2.4	6
2.4 TO 2.6	0
2.6 TO 2.8	1
2.8 TO 3.0	1
3.0 TO 3.5	2
3.5 TO 4.0	2
OVER 4.0	3



MILLCREEK
 RADIANCE THRESHOLD = 3.00σ
 LAMBDA= 1.0 TO 1.4 μM

MILL CREEK

DISTRIBUTION OF RECOGNIZED RADIANCE THRESHOLDS FOR $\sigma = 3.0$

BY AREA

SQUARE METERS	FREQUENCY
0.0 TO 100.0	173
100.0 TO 200.0	7
200.0 TO 500.0	7
500.0 TO 1000.0	3
1000.0 TO 1500.0	0
1500.0 TO 2000.0	0
2000.0 TO 2500.0	0
2500.0 TO 3000.0	0
3000.0 TO 4000.0	0
4000.0 TO 5000.0	0
5000.0 TO 6000.0	0
6000.0 TO 8000.0	0
8000.0 TO 10000.0	0
10000.0 TO 15000.0	0
15000.0 TO 20000.0	0
20000.0 TO 40000.0	0
40000.0 TO 80000.0	0
80000.0 TO 160000.0	0
OVER 160000.0	0

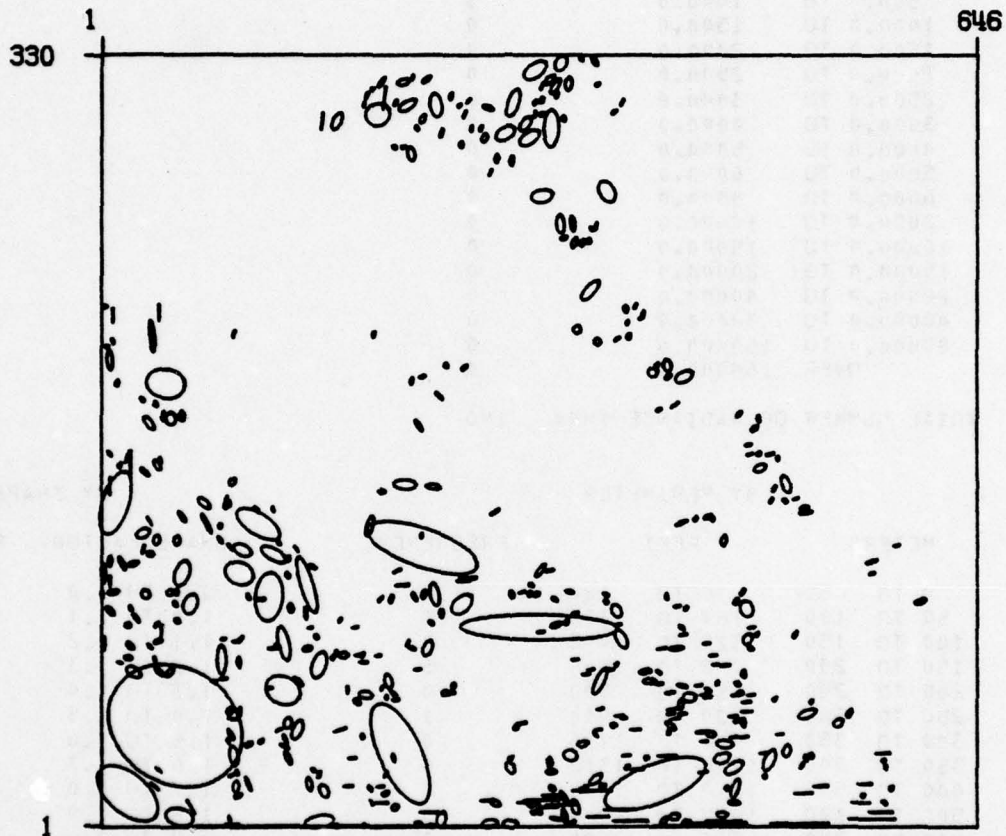
TOTAL NUMBER OF RADIANCE THRE= 190

BY PERIMETER

METERS	FEET	FREQUENCY
0 TO 50	0 TO 164	169
50 TO 100	164 TO 328	11
100 TO 150	328 TO 492	4
150 TO 200	492 TO 656	5
200 TO 250	656 TO 820	0
250 TO 300	820 TO 984	1
300 TO 350	984 TO 1148	0
350 TO 400	1148 TO 1312	0
400 TO 500	1312 TO 1640	0
500 TO 600	1640 TO 1968	0
600 TO 700	1968 TO 2296	0
700 TO 800	2296 TO 2624	0
800 TO 900	2624 TO 2952	0
900 TO 1000	2952 TO 3280	0
1000 TO 1200	3280 TO 3937	0
1200 TO 1400	3937 TO 4593	0
1400 TO 1600	4593 TO 5249	0
1600 TO 2000	5249 TO 6561	0
OVER 2000	OVER 6561	0

BY SHAPE

SHAPE FACTOR	FREQUENCY
0.0 TO 1.0	0
1.0 TO 1.1	0
1.1 TO 1.2	128
1.2 TO 1.3	3
1.3 TO 1.4	14
1.4 TO 1.5	2
1.5 TO 1.6	14
1.6 TO 1.7	14
1.7 TO 1.8	4
1.8 TO 1.9	2
1.9 TO 2.0	1
2.0 TO 2.2	2
2.2 TO 2.4	2
2.4 TO 2.6	0
2.6 TO 2.8	2
2.8 TO 3.0	0
3.0 TO 3.5	2
3.5 TO 4.0	0
OVER 4.0	0



MILL CREEK
TEMPERATURE THRESHOLD = 1.5σ
LAMBDA= 9.3 TO 11.7 μM

MILL CREEK

DISTRIBUTION OF RECOGNIZED TEMP. THRESHOLDS FOR $\sigma = 1.5$

BY AREA

SQUARE METERS	FREQUENCY
0.0 TO 100.0	568
100.0 TO 200.0	70
200.0 TO 500.0	54
500.0 TO 1000.0	21
1000.0 TO 1500.0	8
1500.0 TO 2000.0	3
2000.0 TO 2500.0	1
2500.0 TO 3000.0	0
3000.0 TO 4000.0	4
4000.0 TO 5000.0	0
5000.0 TO 6000.0	1
6000.0 TO 8000.0	0
8000.0 TO 10000.0	1
10000.0 TO 15000.0	4
15000.0 TO 20000.0	0
20000.0 TO 40000.0	0
40000.0 TO 80000.0	1
80000.0 TO 160000.0	0
OVER 160000.0	0

TOTAL NUMBER OF TEMP. THRESH= 736

BY PERIMETER

METERS	FEET	FREQUENCY
0 TO 50	0 TO 164	553
50 TO 100	164 TO 328	91
100 TO 150	328 TO 492	37
150 TO 200	492 TO 656	20
200 TO 250	656 TO 820	10
250 TO 300	820 TO 984	3
300 TO 350	984 TO 1148	4
350 TO 400	1148 TO 1312	3
400 TO 500	1312 TO 1640	3
500 TO 600	1640 TO 1968	1
600 TO 700	1968 TO 2296	2
700 TO 800	2296 TO 2624	3
800 TO 900	2624 TO 2952	1
900 TO 1000	2952 TO 3280	0
1000 TO 1200	3280 TO 3937	0
1200 TO 1400	3937 TO 4593	0
1400 TO 1600	4593 TO 5249	0
1600 TO 2000	5249 TO 6561	0
OVER 2000	OVER 6561	5

BY SHAPE

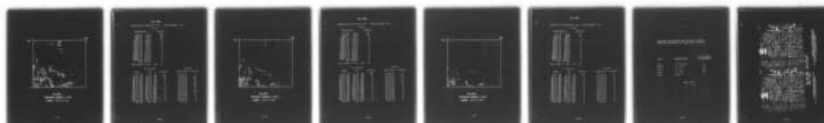
SHAPE FACTOR	FREQUENCY
0.0 TO 1.0	2
1.0 TO 1.1	0
1.1 TO 1.2	378
1.2 TO 1.3	28
1.3 TO 1.4	91
1.4 TO 1.5	29
1.5 TO 1.6	25
1.6 TO 1.7	37
1.7 TO 1.8	31
1.8 TO 1.9	24
1.9 TO 2.0	15
2.0 TO 2.2	28
2.2 TO 2.4	17
2.4 TO 2.6	10
2.6 TO 2.8	2
2.8 TO 3.0	4
3.0 TO 3.5	6
3.5 TO 4.0	4
OVER 4.0	5

AD-A077 584

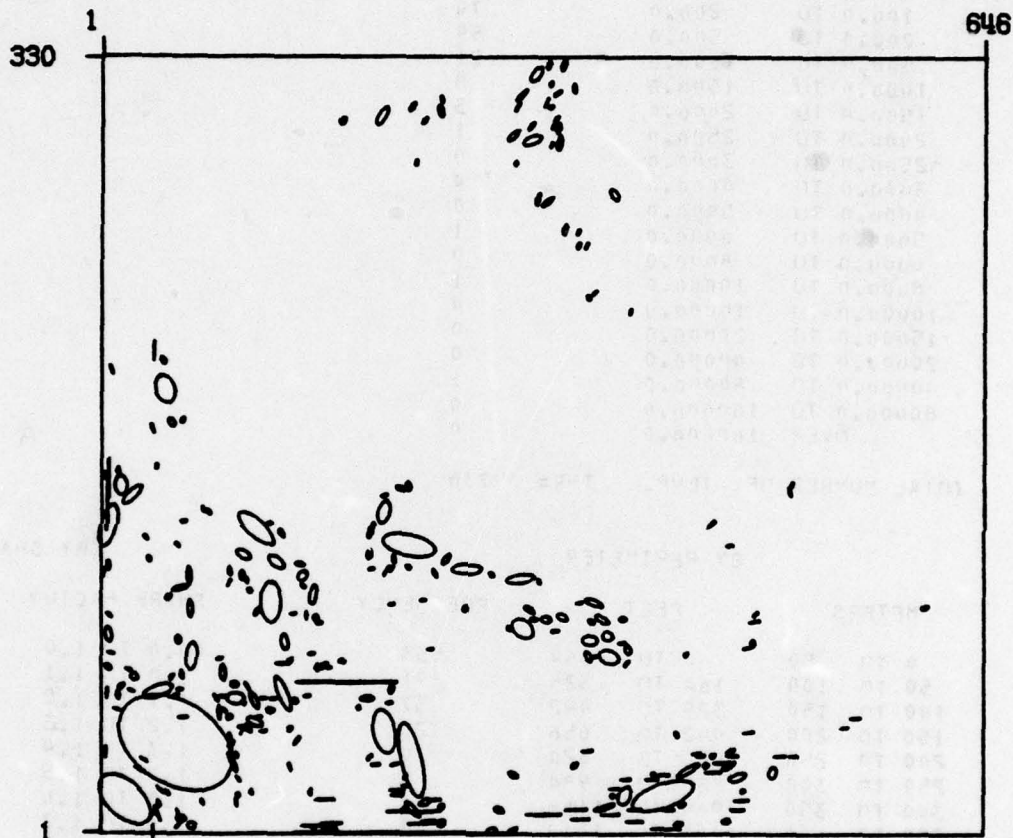
ENVIRONMENTAL RESEARCH INST OF MICHIGAN ANN ARBOR IN--ETC F/G 17/5
STATISTICAL ANALYSIS OF TERRAIN BACKGROUND MEASUREMENTS DATA.(U)
MAR 77 R SPELLICY , J BEARD , J R MAXWELL N00123-76-C-0708
ERIM-120500-12-F NL

UNCLASSIFIED

4 OF 4
ADA
077 584



END
DATE
FILMED
1 -80
DDC



MILLCREEK

TEMPERATURE THRESHOLD = 2.005

LAMBDA= 9.3 TO 11.7 μ M

MILL CREEK

DISTRIBUTION OF RECOGNIZED TEMP. THRESHOLDS FOR $\sigma = 2.0$

BY AREA

SQUARE METERS	FREQUENCY
0.0 TO 100.0	383
100.0 TO 200.0	37
200.0 TO 500.0	28
500.0 TO 1000.0	10
1000.0 TO 1500.0	3
1500.0 TO 2000.0	2
2000.0 TO 2500.0	2
2500.0 TO 3000.0	1
3000.0 TO 4000.0	1
4000.0 TO 5000.0	2
5000.0 TO 6000.0	0
6000.0 TO 8000.0	1
8000.0 TO 10000.0	0
10000.0 TO 15000.0	0
15000.0 TO 20000.0	0
20000.0 TO 40000.0	1
40000.0 TO 80000.0	0
80000.0 TO 160000.0	0
OVER 160000.0	0

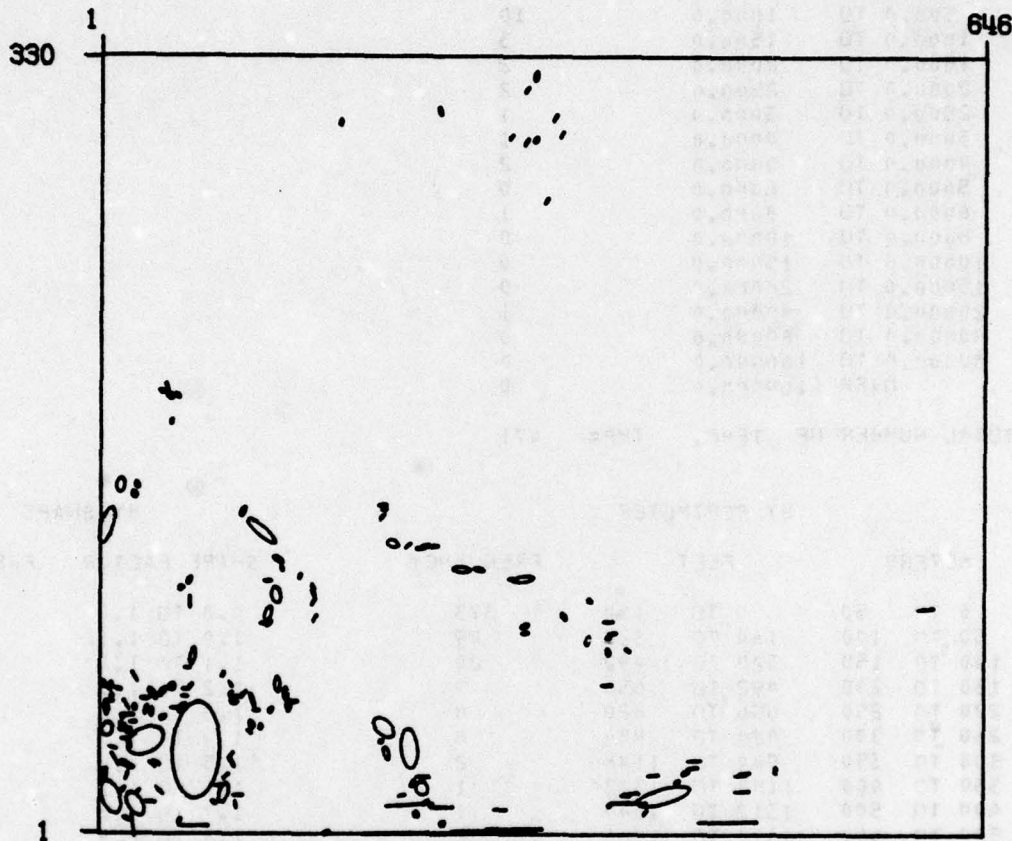
TOTAL NUMBER OF TEMP. THRS 471

BY PERIMETER

METERS	FEET	FREQUENCY
0 TO 50	0 TO 164	373
50 TO 100	164 TO 328	49
100 TO 150	328 TO 492	20
150 TO 200	492 TO 656	9
200 TO 250	656 TO 820	4
250 TO 300	820 TO 984	4
300 TO 350	984 TO 1148	2
350 TO 400	1148 TO 1312	1
400 TO 500	1312 TO 1640	1
500 TO 600	1640 TO 1968	2
600 TO 700	1968 TO 2296	2
700 TO 800	2296 TO 2624	0
800 TO 900	2624 TO 2952	2
900 TO 1000	2952 TO 3280	1
1000 TO 1200	3280 TO 3937	0
1200 TO 1400	3937 TO 4593	0
1400 TO 1600	4593 TO 5249	0
1600 TO 2000	5249 TO 6561	0
OVER 2000	OVER 6561	1

BY SHAPE

SHAPE FACTOR	FREQUENCY
0.0 TO 1.0	0
1.0 TO 1.1	0
1.1 TO 1.2	255
1.2 TO 1.3	19
1.3 TO 1.4	51
1.4 TO 1.5	14
1.5 TO 1.6	20
1.6 TO 1.7	29
1.7 TO 1.8	18
1.8 TO 1.9	12
1.9 TO 2.0	8
2.0 TO 2.2	12
2.2 TO 2.4	10
2.4 TO 2.6	8
2.6 TO 2.8	3
2.8 TO 3.0	5
3.0 TO 3.5	2
3.5 TO 4.0	2
OVER 4.0	3



MILLCREEK
 TEMPERATURE THRESHOLD = 2.505
 LAMBDA= 9.3 TO 11.7 μ M

MILL CREEK

DISTRIBUTION OF RECOGNIZED TEMP. THRESHOLDS FOR $\sigma = 2.5$

BY AREA

SQUARE METERS	FREQUENCY
0.0 TO 100.0	229
100.0 TO 200.0	16
200.0 TO 500.0	11
500.0 TO 1000.0	2
1000.0 TO 1500.0	3
1500.0 TO 2000.0	2
2000.0 TO 2500.0	1
2500.0 TO 3000.0	1
3000.0 TO 4000.0	0
4000.0 TO 5000.0	0
5000.0 TO 6000.0	0
6000.0 TO 8000.0	0
8000.0 TO 10000.0	0
10000.0 TO 15000.0	1
15000.0 TO 20000.0	0
20000.0 TO 40000.0	0
40000.0 TO 80000.0	0
80000.0 TO 160000.0	0
OVER 160000.0	0

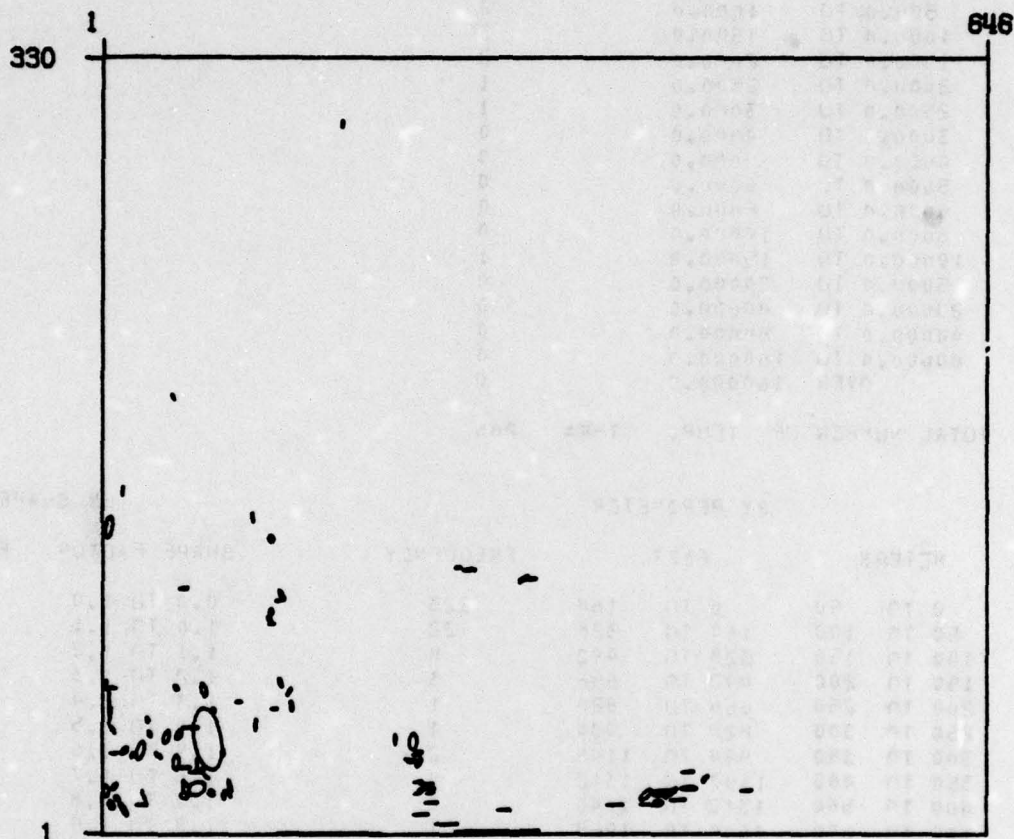
TOTAL NUMBER OF TEMP. THRS 266

BY PERIMETER

METERS	FEET	FREQUENCY
0 TO 50	0 TO 164	223
50 TO 100	164 TO 328	22
100 TO 150	328 TO 492	8
150 TO 200	492 TO 656	3
200 TO 250	656 TO 820	1
250 TO 300	820 TO 984	1
300 TO 350	984 TO 1148	2
350 TO 400	1148 TO 1312	0
400 TO 500	1312 TO 1640	2
500 TO 600	1640 TO 1968	1
600 TO 700	1968 TO 2296	1
700 TO 800	2296 TO 2624	0
800 TO 900	2624 TO 2952	0
900 TO 1000	2952 TO 3280	1
1000 TO 1200	3280 TO 3937	0
1200 TO 1400	3937 TO 4593	0
1400 TO 1600	4593 TO 5249	0
1600 TO 2000	5249 TO 6561	0
OVER 2000	OVER 6561	1

BY SHAPE

SHAPE FACTOR	FREQUENCY
0.0 TO 1.0	0
1.0 TO 1.1	0
1.1 TO 1.2	161
1.2 TO 1.3	9
1.3 TO 1.4	27
1.4 TO 1.5	10
1.5 TO 1.6	11
1.6 TO 1.7	15
1.7 TO 1.8	6
1.8 TO 1.9	2
1.9 TO 2.0	6
2.0 TO 2.2	5
2.2 TO 2.4	3
2.4 TO 2.6	2
2.6 TO 2.8	2
2.8 TO 3.0	2
3.0 TO 3.5	0
3.5 TO 4.0	3
OVER 4.0	2



MILLCREEK

TEMPERATURE THRESHOLD = 3.00°C

LAMBDA= 9.3 TO 11.7 μm

MILL CREEK

DISTRIBUTION OF RECOGNIZED TEMP. THRESHOLDS FOR $\sigma = 3.0$

BY AREA

SQUARE METERS	FREQUENCY
0.0 TO 100.0	112
100.0 TO 200.0	12
200.0 TO 500.0	7
500.0 TO 1000.0	1
1000.0 TO 1500.0	0
1500.0 TO 2000.0	0
2000.0 TO 2500.0	0
2500.0 TO 3000.0	0
3000.0 TO 4000.0	0
4000.0 TO 5000.0	1
5000.0 TO 6000.0	0
6000.0 TO 8000.0	0
8000.0 TO 10000.0	0
10000.0 TO 15000.0	0
15000.0 TO 20000.0	0
20000.0 TO 40000.0	0
40000.0 TO 80000.0	0
80000.0 TO 160000.0	0
OVER 160000.0	0

TOTAL NUMBER OF TEMP. THRESH= 133

BY PERIMETER

METERS	FEET	FREQUENCY
0 TO 50	0 TO 164	106
50 TO 100	164 TO 328	17
100 TO 150	328 TO 492	5
150 TO 200	492 TO 656	2
200 TO 250	656 TO 820	2
250 TO 300	820 TO 984	0
300 TO 350	984 TO 1148	0
350 TO 400	1148 TO 1312	0
400 TO 500	1312 TO 1640	0
500 TO 600	1640 TO 1968	0
600 TO 700	1968 TO 2296	0
700 TO 800	2296 TO 2624	0
800 TO 900	2624 TO 2952	0
900 TO 1000	2952 TO 3280	0
1000 TO 1200	3280 TO 3937	0
1200 TO 1400	3937 TO 4593	1
1400 TO 1600	4593 TO 5249	0
1600 TO 2000	5249 TO 6561	0
OVER 2000	OVER 6561	0

BY SHAPE

SHAPE FACTOR	FREQUENCY
0.0 TO 1.0	0
1.0 TO 1.1	0
1.1 TO 1.2	77
1.2 TO 1.3	4
1.3 TO 1.4	15
1.4 TO 1.5	4
1.5 TO 1.6	6
1.6 TO 1.7	3
1.7 TO 1.8	4
1.8 TO 1.9	4
1.9 TO 2.0	4
2.0 TO 2.2	3
2.2 TO 2.4	1
2.4 TO 2.6	5
2.6 TO 2.8	1
2.8 TO 3.0	1
3.0 TO 3.5	0
3.5 TO 4.0	0
OVER 4.0	1

ARTIFICIAL COLOR COMPOSITE IMAGE FOR FLINT-1 AND THE
PSEUDO-IMAGE GENERATED USING AREA/INTENSITY STATISTICS

<u>Color</u>	<u>Intensity Range</u>	<u>No. of Ellipses In Pseudo-Image</u>
Red	4σ and Above	9
Yellow	3σ to 4σ	102
Green	2σ to 3σ	1127
Blue	1σ to 2σ	2163
Brown	Below 1σ	-

Mean = 294 K

σ = 3.1 K



Blue = 293 - 303°K Yellow = 304 - 307°K
 Green = 301 - 304°K Red = 307 - 310°K
 Brown = <293°K

ARTIFICIAL COLOR REPRESENTATION
 OF THE PSEUDO-IMAGE GENERATED FROM THE
 9.3 - 11.7 μ m CHANNEL OF FLINT-1.

ARTIFICIAL COLOR IMAGE OF THE
 9.3 - 11.7 μ m CHANNEL OF FLINT-1.